

Improving Recording and Interpretation of Fossil Tracks

Ashleigh Louise Ann Wiseman

A thesis submitted in partial fulfilment of the requirements of Liverpool John Moores
University for the degree of Doctor of Philosophy

February 2019

Abstract

Hominin fossilised trackways are commonly used to reconstruct locomotory behaviour and to characterise track-maker biometrics. They are the most direct representation of hominin locomotion available, yet the recording and measurement of the tracks and the subsequent interpretation to characterise the track-maker is problematic. The fossil sites are susceptible to extreme cases of erosion, often resulting in the destruction of the fossil beds. In this project, a series of experiments using non-invasive methods tested the applicability of Unmanned Aerial Vehicle (UAV) technology to rapidly and accurately record footprints before further damage to the fossil interface occurred. Various flight paths, UAVs and camera types were incorporated to test the accuracy in minute depth reconstruction and subsequent 3D mesh creation. Data from the UAV was compared to traditional handheld methods of 3D modelling. Results indicated that a handheld DSLR camera following a circular path should be deployed to record fossil footprints.

After successfully identifying the best practise for creating 3D reconstructions of footprints, this study sought to determine if the track-maker was identifiable from print shapes. An experimental study that combined morphological assessments with that of 3D motion capture systems to record modern human movement across different substrates at several speeds examined the variability in footprint shapes and investigated if these shapes can be used to infer biometric and/or biomechanical information about the track-maker. Numerous patterns of morphology were recognised, such as the changing prominence of the midfoot impression associated with limb posture, and a ridge-like impression that extends across the forefoot associated with an effective toe-off on a looser sediment. The latter was identified in a number of fossilised footprints. Although the internal morphology of tracks was sensitive to changes in shape concurrent with a range of variables (substrate typology and kinematics), track outlines were much more consistent within an individual. Outlines were statistically compared between tracks from nine different fossil localities, ranging from the Pliocene to the Holocene. It was established that all prints belonging to *Homo* species are statistically similar in outline shape, but disparate from prints associated with australopithecines.

The main conclusion of this thesis as a whole is that functional morphology can be inferred from fossil tracks. Track morphologies are sensitive to substrate and speed, which need to be considered and approximated for accurate identification of the track-maker. The reconstruction of biometrics, however, needs to be refined by further analytical methods.

Acknowledgements

I would like to first thank my director of studies, Isabelle De Groote, for the opportunity to work on this project and for all her help and guidance during the last three years. Additionally, I would like to thank my second supervisor, Thomas O'Brien, for his help and advice on the biomechanics aspect of this project, and my third supervisor, Frederic Bezombes, for his help on implementing the UAV technology section of this project.

Liverpool John Moores University funded all aspects of this research, with the DigiArt EU Horizon 2020 Fund generously providing free access to photogrammetry software, and I am extremely grateful to both for their assistance. The LJMU Graduate School, the European Society for Human Evolution and the British Federation for Women Graduates are all additionally thanked for providing funding to attend numerous conferences.

The ability to collect fossil footprint data during fieldwork at Formby Point, UK would not have been possible without the cooperation of the National Trust, UK. I am additionally grateful for the generous invite of Dominique Cliquet and Jeremy Dureau to join the excavation team at Le Rozel, France. I would especially like to thank Dominique for his hospitality during my stay at Le Rozel.

I would particularly like to thank students of Liverpool John Moores University (2016-2017) and The University of Manchester (summer 2016) for assisting in the excavations at Formby Point, UK.

Other fossil footprint data was kindly provided by Professor Matthew Bennett, Dr. Kevin Hatala, and my collaborators from Happisburgh, UK: Dr. Nick Ashton and Professor Christopher Stringer. I am grateful to all of these individuals for not only permitting access to fossil data, but also for their insightful discussions on the fossil material which aided the production of our manuscript, currently in revision. I would also like to thank Professor Bogdan Onac for access to the Vârtope, Romania footprint and Masao and colleagues (2016) for making the Site S footprints available online for further research. Additionally, the National Museum of Kenya, the Iziko Museums of South Africa, and the Terra Amata Museum, France all kindly provided photographs of fossil footprints.

I am especially grateful to the 100 people who volunteered their time and energy to be participants in this project. Without them, Chapter Three would not have been possible. Deborah Vicari, Megan Quick, Wazir Ahmed and George Dallow all very kindly helped

me construct/deconstruct my experimental trackways – which involved moving 500 Kg of sand, 45+ litres of water and the construction of timber walkways, followed by a very big clean-up job! These experiments would not have been possible without their help. On that note, I also thank the staff and students of the biomechanics lab for allowing me to take over their lab with my experimental trackways, and for their patience during my two month data collection.

Raihana Sharir and Natasha Francksen are thanked for teaching me how to operate the 3D motion capture system. Ian Poole is thanked for his guidance on the 3D motion camera set-up. Alex Moore kindly taught me how to use photogrammetry software, and also assisted in the set-up of the experimental trackways discussed in Chapter Two. Additionally, I also thank Dr. Peter Falkingham for further help with photogrammetry and for help with software.

I am grateful to Alessio Veneziano for helping me to understand the basics of R during the early stages of my PhD journey. Additionally, I would like to thank Giada Giacomini for her discussions over the past few years on computing statistical modelling in R. Megan Quick is thanked for proofreading my thesis. Finally, Dr. Zewdi Tsegai is thanked for helping me understand complex statistical modelling, and for inviting me to undertake a research placement at the Department of Human Evolution, MPI-EVA – the knowledge gained during my stay gave me a much more rounded view on the interpretations of the results of this thesis.

I am extremely thankful to my family for all their support and encouragement ever since I first began my undergraduate studies.

Table of Contents

Abstract	ii
Acknowledgements	iii
Table of Contents	v
List of Figures	xi
List of Tables	xiii
Glossary	xv

CHAPTER ONE: Introduction 1

<i>Terminology</i>	1
1.1 Structure of thesis	2
1.2 Justification of thesis	2
1.3 Anatomy and function of the human foot	3
1.4 Functional interpretations of fossilised footprints	5
<i>Laetoli (Site G and Site S), Tanzania</i>	5
<i>Koobi Fora Formation, East Turkana, Kenya</i>	9
<i>Gombore II-2, Ethiopia</i>	12
<i>Langebaan, South Africa</i>	13
<i>Happisburgh, UK</i>	14
<i>Neanderthal sites</i>	15
<i>Formby Point, Sefton Coast, UK</i>	17
<i>Walvis Bay, Namibia</i>	18
1.5 Uncertainties in footprint studies.....	19
1.6 Aims of thesis	20
1.7 Research Questions	21

CHAPTER TWO: Identifying the optimal recording method for fragile, *in situ*

tracks	24
2.1.0 Introduction	27
2.1.1 Aims and objectives	28
2.2.0 The effects of erosion on track morphology and preservation	28
2.2.1 Aims	30
2.2.2 Geological and archaeological context	30
2.2.3 Experimental design	32

2.2.4 Holocene track data collection	34
2.2.5 Methodology	34
2.2.5 Results	39
<i>Morphological change prior to fossilisation</i>	39
<i>Morphological change after exposure/excavation</i>	42
<i>Morphological change in the Holocene animal tracks</i>	46
2.2.6 Discussion	47
<i>Taphonomic changes to track morphology prior to diagenesis</i>	47
<i>Morphological changes to a human track after exposure/excavation</i> ...	48
<i>Morphological changes to animal tracks after exposure/excavation</i>	51
2.2.7 Remarks on the effects of diagenesis in track morphology	52
2.3.0 The need for non-invasive recording methods: The applicability of UAV technology for recording fragile fossils <i>in situ</i>	52
2.3.1 Aims	55
2.3.2 Experimental design	56
2.3.3 Methodology	57
2.3.4 Model creation	61
<i>Point cloud production</i>	61
<i>Mesh creation</i>	61
2.3.5 Analyses	62
<i>Point cloud density</i>	62
<i>Point cloud comparisons</i>	63
<i>Assessing shape/size distortion in the 3D mesh analyses</i>	63
2.3.6 Results	65
<i>Model reconstruction</i>	65
2.3.7 Model quality	67
<i>Close-range photogrammetry or aerial photogrammetry?</i>	69
2.3.8 Comparing point cloud entities	73
<i>Camera stills versus video recording</i>	73
<i>Camera type</i>	77
<i>Close range photogrammetry versus aerial photogrammetry</i>	78
<i>The Panasonic Lumix DMC-GH4 DSLR at various heights</i>	80
2.3.9 Shape variability in model reconstruction	84
<i>Shape variability determined during the first set of experiments</i>	85
<i>Shape variability determined during the second set of experiments</i>	85

2.3.10 Size variability in model reconstruction	89
2.3.11 Discussion	92
2.3.12 Limitations of the study	93

CHAPTER THREE: Investigating the relationship between lower limb kinematics, biometrics and track morphology across various types of substrates and speeds . 97

3.1.0 Introduction	100
3.1.1 Aims and objectives	103
3.2.1 Study protocol	103
3.2.2 Experimental design	105
3.2.3 Photogrammetry	107
3.2.4 Statistical analyses of tracks	107
<i>Correcting discrepancies in track dimensions</i>	108
3.2.5 Biometric predictions	109
<i>Stature predictions</i>	109
<i>Age and sex predictions</i>	109
<i>Mass predictions</i>	109
<i>Hip height</i>	110
3.2.6 3D motion capture	110
<i>Calibrated volume and QTM camera settings</i>	111
<i>Static/calibration trials</i>	112
<i>Motion trials</i>	113
<i>Identified issues with the BHBK trials</i>	113
3.2.7 Data processing and extraction	115
3.2.8 Statistical analyses	116
3.2.9 ‘Averaged’ track creation	116
<i>Identifying the influence of kinematics on track production</i>	118
<i>Hallucal abduction angles</i>	119
3.3.0 Results	120
3.3.1 Measurement repeatability	120
3.3.2 Variations in linear measurements	123
<i>Total track length</i>	126
<i>Long axis of the foot</i>	126
<i>Hallux length</i>	126
<i>Forefoot width</i>	131

<i>Heel width</i>	131
<i>Walking with a flexed limb (BHBK)</i>	132
<i>Corrected track measurements</i>	134
3.3.3 Biometric Predictions	135
<i>Stature prediction</i>	135
<i>Stature prediction based on tracks produced on the firm substrate when walking</i>	136
<i>Stature prediction based on tracks produced on the firm substrate when fast walking</i>	137
<i>Stature prediction based on tracks produced on the firm substrate when jogging</i>	138
<i>Stature prediction based on tracks produced on the loose substrate when walking</i>	138
<i>Stature prediction based on tracks produced on the loose substrate when fast walking</i>	139
<i>Stature prediction based on tracks produced on the loose substrate when jogging</i>	139
<i>Age and sex predictions</i>	143
<i>Mass predictions</i>	143
<i>Hip height</i>	145
3.3.4 Lower limb kinematics	150
<i>Kinematics of the hip</i>	150
<i>Kinematics of the knee</i>	151
<i>Kinematics of the ankle</i>	151
3.3.5 Locomotory behaviour reflected in track morphology	157
<i>Morphological disparity between tracks during several speeds</i>	162
<i>Morphological disparity on the same substrates at different speeds</i> ...	162
<i>Morphological disparity on the same substrates with different limb postures</i>	162
<i>Associations between activity and track morphology</i>	164
3.3.6 The influence of a flexed limb posture on track morphology	164
3.3.7 Variation in hallucal abduction across different substrates	165
3.4.0 Discussion	166
3.4.1 Can biometric information be accurately extracted from track dimensions? ..	167
3.4.2 Establishing shape patterns associated with kinematics in track morphology .	168

<i>The range of motion in the hip in fossil hominins</i>	169
<i>The range of motion in the knee in fossil hominins</i>	169
<i>The range of motion in the ankle in fossil hominins</i>	171
3.4.3 Revisiting the BHBK hypothesis	174
3.4.4 Revisiting the BHBK hypothesis: the dynamic movement of the foot	177
3.5.0 Limitations and future directions	179
CHAPTER FOUR: Exploring patterns of shape affinities between fossil tracks	181
4.1.0 Introduction	184
4.1.1 Chapter aims and objectives	185
4.2.1 Protocol and experimental design	185
<i>Conditions included in assessments</i>	186
4.2.2 Geometric morphometric analyses of the tracks	187
<i>2D and 3D landmark selection</i>	187
<i>Statistical analyses</i>	189
4.3.1 Results	190
<i>3D landmark configurations</i>	191
<i>2D landmark configurations</i>	194
4.3.2 Applicability of using 2D landmark configurations to quantify track shape ..	195
4.4.0 The morphological affinity of the early Pleistocene tracks from Happisburgh, England with other tracks of Pliocene, Pleistocene and Holocene age	196
4.4.1 Data acquisition	198
4.4.2 Geometric morphometric analyses	202
<i>The effect of speed on track outline</i>	205
<i>Adult track variation</i>	205
<i>Substrate controls</i>	206
4.4.3 Comparing linear track metrics	206
4.4.4 Results	207
<i>Track shape results</i>	207
<i>The influence of speed on track shape</i>	210
<i>Adult track variation</i>	211
<i>The effect of substrate on track outline in fossil samples</i>	213
<i>Comparing linear track measurements</i>	215
<i>Foot proportions</i>	223
4.5.1 Discussion	224

<i>Disparities and affinities in hominin track shapes</i>	225
<i>Trends in foot functional morphology inferred from comparative analyses</i>	226
<i>The morphological affinity of the Happisburgh tracks</i>	228
<i>Limitations of substrate</i>	229
4.5.2 Concluding remarks.....	230
CHAPTER FIVE: General discussion	231
5.1 Considerations for the functional interpretations of tracks	233
5.2 From discovery to archive	236
CHAPTER SIX: Conclusions	238
6.1 Addressing thesis objectives	238
6.2 Overall conclusions	243
6.3 Future directions	244
References	246
Appendix A	271
Appendix B	281
Appendix C	282
Appendix D	283
Appendix E	285
Appendix F	291
Appendix G	297

List of Figures

Figure 1.1 Schematic diagram of foot anatomy	4
Figure 2.1 Diagram explaining the destructive nature of the high tide	32
Figure 2.2 Set-up of the experimental footprints	33
Figure 2.3 Photographic examples of the destructive nature of the high tide	35
Figure 2.4 Landmark datasets for the human prints and animal prints	37
Figure 2.5 PCA results of shape change in the experimental footprints	40
Figure 2.6 Regression of shape to size in the experimental footprints	42
Figure 2.7 PCA results of shape change in the Holocene human footprints	44
Figure 2.8 PCA results of shape change in the Holocene animal footprints	46
Figure 2.9 Erosion of footprints from Happisburgh, UK and Formby Point, UK	50
Figure 2.10 Diagram explaining the effects of occlusion during photogrammetry	55
Figure 2.11 Experimental set-up of the flight tests	56
Figure 2.12 Diagram explaining the effect of camera offset angle	59
Figure 2.13 Flight paths designed for the experiments	61
Figure 2.14 3D mesh production in different software	62
Figure 2.15 Landmark datasets for each object tested during flight deployment	64
Figure 2.16 An example of camera motion blur during the UAV flight tests	66
Figure 2.17 Examples of poor model reconstruction	67
Figure 2.18 The point cloud density of all models	72
Figure 2.19 Point cloud comparisons of camera stills versus video recording	75
Figure 2.20 Point cloud comparisons of camera type	79
Figure 2.21 Point cloud comparisons from testing the effect of action camera height on point cloud resolution	81
Figure 2.22 Point cloud comparisons from testing the effect of camera height on point cloud resolution	83
Figure 2.23 Example of a 3D mesh with the sub-division of each object	84
Figure 2.24 PCA plots of shape change	88
Figure 3.1 Diagram providing an overview of the workflow process	104
Figure 3.2 Photograph of laboratory set-up	106
Figure 3.3 Linear dimensions measured in this study	108
Figure 3.4 Diagram of laboratory set-up and position of each camera	111
Figure 3.5 The LJMU Lower Limb and Trunk Model used in the study	112
Figure 3.6 Examples of movement across the firm substrate	114

Figure 3.7 Example of the rigid-track registration method employed in this study ...	118
Figure 3.8 Calculation of hallux angle for each registered track	119
Figure 3.9 Regression of track length measurements from each substrate	129
Figure 3.10 Regression of track width measurements from each substrate	132
Figure 3.11 Regression of stature to total foot length	135
Figure 3.12 Bland-Altman graphs displaying the differences of mean stature prediction on the firm substrate	141
Figure 3.13 Bland-Altman graphs displaying the differences of mean stature prediction on the loose substrate	142
Figure 3.14. Regression of foot length with body mass.....	144
Figure 3.15 Regression of all linear measurements with body mass	146
Figure 3.16 Regression of stature to hip height and foot length to hip height	147
Figure 3.17 Graphs of joint angles across different substrates	152
Figure 3.18 Graphs of joint angles across different substrates with a flexed limb	153
Figure 3.19 Track depth maps between the two different substrates	158
Figure 3.20 Boxplot of arch height measured from footprints.....	159
Figure 3.21 Mesh comparisons of tracks produced across a range of variables	163
Figure 3.22 Track depth maps between the different substrates with a BHBK.....	165
Figure 3.23 Graphs of the association between hallucal abduction with joint angles .	166
Figure 3.24 Examples of the ridge-like appearance in fossil footprints.....	173
Figure 3.25 Comparison of the experimental tracks with the Laetoli tracks	175
Figure 3.26 Comparison between the experimental tracks and the Langebaan track .	176
Figure 4.1 2D and 3D landmark configurations.....	189
Figure 4.2 Histogram of the frequency of Procrustes distances	191
Figure 4.3 PCA graph of shape change between participants	193
Figure 4.4 Poor resolution 3D models from Happisburgh, UK	197
Figure 4.5 Examples of photographs of fossil tracks used in the study	200
Figure 4.6 Landmarks used within the current study	204
Figure 4.7 Four linear dimensions of each footprint used in this study	207
Figure 4.8 PCA graphs with shape deformation grids	209
Figure 4.9 PCA graphs with shape deformation grids	210
Figure 4.10 PCA graphs grouped according to track depth	214
Figure 4.11 Variability in dimensions between various fossil localities	221
Figure 4.12 Boxplot of the angle of hallux abduction in fossil footprints	222
Figure 4.13 Boxplots of the variability in foot proportions in fossil footprints	224

List of Tables

Table 2.1	Experimental footprint length measurements and predicted stature values ...	41
Table 2.2	Holocene footprint length measurements and predicted stature values	43
Table 2.3	The depth of the Holocene human tracks	45
Table 2.4	Camera specifications for the cameras used during the study	57
Table 2.5	The effect of camera angle on the captured area	60
Table 2.6	Number of points per point cloud of each model	70
Table 2.7	Results of the Student's <i>t</i> -test of point cloud densities	71
Table 2.8	Descriptive statistics for point cloud density	73
Table 2.9	The number of points per cloud to cloud comparisons	76
Table 2.10	ANOVA results of intra group variability	85
Table 2.11	One-way ANOVA computed on the landmark configurations	87
Table 2.12	Results of the Student's <i>t</i> -test of object measurements	91
Table 2.13	Data capture time for each flight test and recording method	95
Table 3.1	Observer-error for extracting linear measurements from tracks	121
Table 3.2	Intra-track variability of track dimensions	122
Table 3.3	Results of the Student's <i>t</i> -test for disparity in track dimensions	124
Table 3.4	The reported percentage change in track length dimensions	130
Table 3.5	The reported percentage change in track width dimensions	133
Table 3.6	Correction factor to predict actual foot length	134
Table 3.7	Percentage errors of the predicted stature ranges	140
Table 3.8	Results of the Pearson's correlation between mass and track dimensions...	144
Table 3.9	Results of the Pearson's correlation between hip height and foot length	147
Table 3.10	Percentage errors of the predicted hip height prediction ranges	149
Table 3.11	One-way ANOVA computed on joint angles on different substrates	154
Table 3.12	One-way ANOVA computed on joint angles on different substrates	156
Table 3.13	Descriptive statistics for arch height	160
Table 3.14	Student's <i>t</i> -test for arch height between different substrates	160
Table 4.1	MANOVA computed on intra-trackway shape differences	194
Table 4.2	List of fossilised footprints used in this study	201
Table 4.3	Nested MANOVA of shape differences to test the influence of trackway ..	209
Table 4.4	MANOVA of shape scores to test the influence of speed	211
Table 4.5	MANOVA of shape scores to test the influence of speed (adult tracks)	212
Table 4.6	Mean measurements and mean predicted stature of each fossil track	216

Table 4.7 One-way ANOVA and Games-Howell Post-Hoc test on dimensions	217
Table 4.8 One-way ANOVA and Games-Howell Post-Hoc tests for hallux angle.....	222
Table 4.9 Changing proportions of the hallux to track length in fossil tracks	223
Table 4.10 Changing proportions of the 2 nd digit to track length in fossil tracks	224

Glossary

Ma: Millions of years ago

Ka: Thousands of years ago

AMH: Anatomically modern human

BHBK: Bent-hip bent-knee

EHEK: Erect-hip erect-knee

WHO: World Health Organisation

GM: Geometric morphometrics

MIS: Marine Isotope Stage

CS: Centroid Size

MLA: Medial longitudinal arch

Chapter One

Introduction

Hominin fossilised trackways are commonly used to reconstruct the locomotory behaviour of hominins and to characterise track-maker biometrics. These interpretations are reliant upon accurately reconstructed three-dimensional (3D) models, yet the recording and measurement of the tracks and the subsequent interpretation to characterise the track-maker is problematic. In this project, methods of recording fossil track material will be explored, with the aim of identifying recording methods that can effectively remove the excavator from site thus minimising damage to the fossil interface. With precise 3D reconstructions of fossil trackways, the ability to identify the track-makers' biometric information, such as stature, sex and body mass, and locomotory behaviour will be explored by examining modern human movement across several types of substrates and speeds. This experimental approach will examine the dependence of track characteristics and substrate mechanics, and the relationship between the resulting track morphologies and lower limb kinematics and biometrics.

Terminology

Terminology of all footprints (experimental and fossil) in this thesis follows standard labelling approaches by Marty et al. (2009). A singular print is referred to as a 'track'. A collection of prints following a consecutive path created by the same person is referred to as a 'trackway'.

Most tracks used in this study are not fossilised. Only the poorly preserved Langebaan, South Africa trackway is fully lithified. The Laetoli, Tanzania and the Ileret, Kenya trackways are partially lithified. All other fossil data (Engare Sero, Ethiopia; Happisburgh, UK; Terra Amata, France; Le Rozel, France; Formby Point, UK; Walvis Bay, Namibia) are found in soft, unlithified sediments. However, the term 'fossilised footprints' is colloquially used in the literature to refer to prehistoric trackways, particularly those which are non-modern human (Bennett and Morse 2014). The term 'fossilised footprints' is used within this thesis to differentiate prehistoric track material from that of experimental data, following standard conventions of labelling.

1.1 Structure of thesis

In the succeeding chapters, a multi-disciplinary approach to the assessment of hominin trackways will be presented, followed by an overall discussion. Chapter One will provide an overview of previous research on fossil material to provide a framework for the subsequent chapters. Chapter Two will identify the optimal recording methods for fragile, *in situ* trackways which are susceptible to imminent damage/erosion. Chapter Three will explore methods of 3D track analysis by characterising modern human movement across three different substrates at several speeds and limb postures, and will investigate the association between limb movement and substrate mechanics with the resulting footprint shapes. The interpretive approaches reached in Chapter Three will provide an insight into the comparative assessment of fossil tracks from the Pliocene, Pleistocene and Holocene, as presented in Chapter Four. Finally, Chapter Five will provide an overall discussion of the key findings of this project and will offer recommendations on the best practises, as identified in the presented studies, for recording fossil material through to methods of analysis. Through an exploration of analytical methods, this project will address the validity of using fossil trackways to identify the biometric information and the locomotory behaviour of the track-maker; inferences which are contentiously debated in the contemporaneous fossil skeletal record (e.g., Aiello and Dean 2002).

1.2 Justification of thesis

In this multi-disciplinary project, the effect of erosion on prehistoric human trackways was recorded for the first time, thus stressing the need to identify the best practise for recording *in situ* fossil material quickly and efficiently (Chapter Two). The results offered interesting insights into applied methods for 3D modelling of fossil trackways. Importantly, issues in accurate depth reconstruction were recognised, indicating that issues in biometric predictions and biomechanical inferences will be prevalent if certain recording methods are employed. Only after the correct 3D reconstruction of trackways can information about the track-maker then be characterised (Chapters Three and Four).

Additionally, the relationship between substrate mechanics, lower limb kinematics and biometrics with that of print morphology is poorly understood, despite many recent and novel techniques to address this issue. By applying 3D motion capture systems this project directly explored this relationship, providing a greater comprehension into print formation (Chapter Three). The exploration of this relationship permitted the comparative assessment of numerous fossil trackways belonging to at least six hominin species

(Chapter Four). A brief outline on the significance of this research for assessing print morphology in hominin species is outlined below.

1.3 Anatomy and function of the human foot

Human bipedal locomotion is characterised by an extended limb posture at both the hip and knee joints. The human gait cycle is characterised by repetitive events that allow the human body to traverse efficiently, which consists of alternating phases of single and double-limb support known as the swing and stance phases (Levine et al. 2012). During each of these phases only the foot comes into contact with the ground (i.e., the underlying substrate), and if sediment conditions are optimal (i.e., water saturation and particle composition) then a footprint is created (Bennett and Morse 2014). It is the trace-fossil record of a footprint that offers palaeoanthropologists a direct representation of hominin bipedal behaviour.

Specifically, a footprint is a representation of the human foot. The foot is believed to be a highly specialized form which is unique amongst apes for efficient, bipedal movement (Ker et al. 1987; Aiello and Dean 2002). Within the foot there exists a complex structure of hard and soft tissues, comprising of the derived plantar aponeurosis of the foot, and the compliant medial and longitudinal arches of the midfoot region (Elftman and Manter 1935; Harcourt-Smith and Aiello 2004) (Figure 1.1a). These highly derived structures are efficient in energy production, acting as a spring to regulate the production of elastic energy in the foot to permit low energy costs during walking (Ker et al. 1987; Carvaggi et al. 2010). Importantly, these structures permit an effective propulsion in the forefoot during the toe-off phase of the gait cycle (Levine et al. 2012), which is enhanced by anatomical specifications of the foot (the tarsals, metatarsals and phalanges).

The foot is characterized by short pedal phalanges (Latimer and Lovejoy 1990; Harcourt-Smith et al. 2015; Trinkaus and Patel 2016), shorter, robust and less curved metatarsals than other extant apes to reduce torsion (Ward et al. 2011; Vereecke et al. 2003; Lovejoy et al. 2009; Fernandez et al. 2018), and a specified form of the ankle joint (hindfoot anatomy) to permit the leg to move efficiently over the base of support during walking (Aiello and Dean 2002). Together these anatomies, alongside a shorter forefoot relative to the total foot length, permit an effective toe-off propulsion for walking (Aiello and Dean 2002) (Figure 1.1b). Generally, it is these morphological specifications in fossil hominin foot bones that are used to reconstruct functional morphology and to identify

bipedal behaviour (e.g., Holowka et al. 2017; DeSilva et al. 2018; Holowka and Liebermann 2018; Farris et al. 2019).

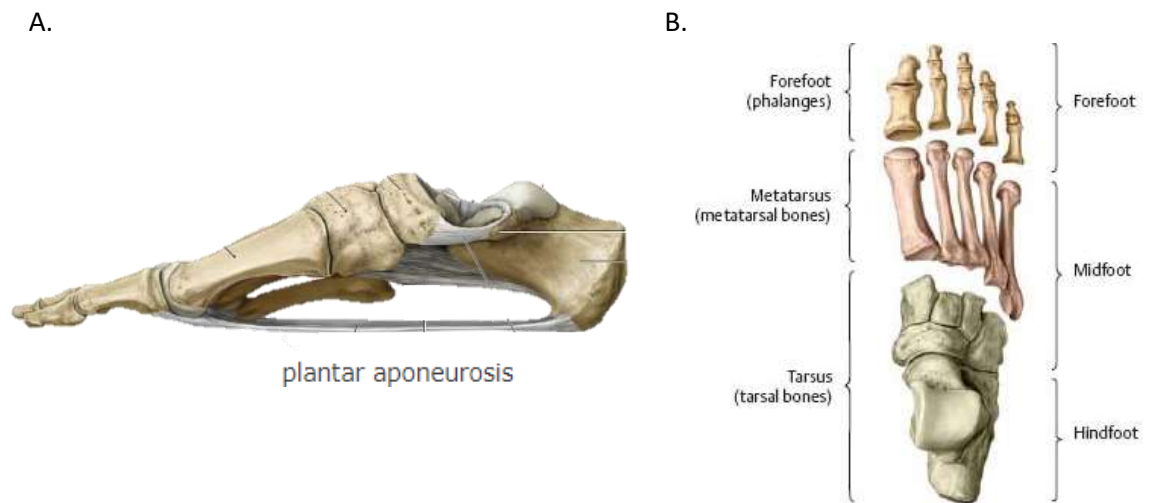


Figure 1.1. (A) A stylised version of the medial view of the human foot with the plantar aponeurosis labelled. The midfoot foot arches are visible above the plantar aponeurosis. (B) Anatomical representation of the modern human foot, divided into the forefoot, midfoot and hindfoot. Image credits: <https://doctorlib.info/medical/anatomy/28.html> [accessed 02/05/2019].

Whilst it is generally agreed that *Homo* species (e.g., *Homo erectus*, *Homo antecessor*, *Homo heidelbergensis*, *Homo neanderthalensis* and *Homo sapiens*) are obligate bipeds based upon the morphology of the foot bones (Trinkaus 1983; Aiello and Dean 1990; Lorenzo et al. 1999), the locomotory behaviour of early hominins (australopiths and paranthropines) is contentious. For example, *Australopithecus afarensis* pedal remains from Hadar, Ethiopia dated to c.3.0–3.4 Ma display a mosaic of anatomical features, with some researchers arguing that these remains are consistent with obligate bipedalism (Latimer and Lovejoy 1982; Latimer and Lovejoy 1989). Other researchers are more hesitant to claim full bipedal locomotion and instead argue these pedal remains, alongside other post-cranial remains, are indicative of a range of locomotory behaviours (Susman and Stern 1982; Stern and Susman 1983; Susman 1983; Lovejoy et al. 2002).

Whilst it is a reasonable assumption to postulate that early hominins (e.g., australopithecines) would have been capable of short bouts of bipedal motion similar to

extant non-human great apes, it remains contentious if bipedal locomotion was habitually employed in these groups due to a mosaic of primitive and derived anatomical features.

A direct source of locomotory evidence can instead be found in trace-fossils of the foot (tracks). Tracks are a direct representation of hominin bipedalism, and it is the morphological patterns within tracks that can be used to reconstruct function much more efficiently than from skeletal material.

1.4 Functional interpretations of fossilised footprints

Numerous fossilised trackways have been discovered, belonging to a range of hominin species from a wide geographical and temporal range, potentially dating as early as ~5.7 Ma (Leakey and Hay 1979; Day 1991; Roberts et al. 1996; Roberts and Berger 1997; Kim and Kim 2004; Onac et al. 2005; Evans 2007; Avanzini et al. 2008; Bennett et al. 2009; Nakamura 2009; Morse et al. 2013; Ashton et al. 2014; Masao et al. 2016; Stoetzel et al. 2016; Gierlinski et al. 2017; Altamura et al. 2018; Bustos et al. 2018; McLaren et al. 2018). Biometric information about the track-maker can be inferred from track dimensions, while internal shape patterns can be used to characterise functional morphology and locomotion (Lockley et al. 2008; Bennett and Morse 2014). Trackway discoveries which are included in analyses for this thesis are discussed below. A more comprehensive review of the literature pertinent to each component of this project can be found at the beginning of each chapter.

Laetoli (Site G and Site S), Tanzania

The Laetoli, Tanzania trackways are the oldest known non-disputable hominin footprints (Bennett et al. 2016a), dating to 3.66 Ma (Leakey and Hay 1979). There are two known footprint-bearing beds at Laetoli: Site G (Leakey and Hay 1979) and the newly discovered Site S (Masao et al. 2016). The trackways have been assigned to *Australopithecus afarensis* (Leakey and Hay 1979), which is the generally accepted consensus, with few exceptions (Tuttle et al. 1991).

The Site G footprints represent a minimum of three individuals across two superimposed trackways. The G1 trackway (n=38 prints) is most commonly assessed for functional variance owing to clear shape outlines. The G2/3 trackways (n=31 prints) are often overlooked in analytical assessments due to superimposition of the prints, resulting in these trackways being much less informative for any biomechanical or biometric assessments (Bennett et al. 2016b).

In 2016, a new methodology was reported by Bennett et al. (2016b) that permitted the G3 trackway to be ‘extracted’ from the superimposed G2/3 composite trackways. Using track registration, a method which generates the mean shape of a track within a trackway (Pataky and Goulermas 2008), Bennett et al. (2016b) designed a user-friendly, automated method based on user-defined landmarks for track registration. This method made it possible for the mean G3 track topology to be produced.

The G3 trackway was determined to have a greater predicted stature of the track-maker compared to previous estimates of the superimposed prints (Tuttle et al. 1990) and also had more clearly defined digits (Bennett et al. 2016b). However, a few distinct morphologies were identified: the heel shape and depth, and the angle of hallux abduction were disparate between the G1 and G3 trackways. All of these morphologies would suggest slight variations in movement during trackway creation (Bennett et al. 2016b). Bennett et al. (2016) offered possible explanations for the morphological disparity between the G1 and G3 trackways: (1) the trackways could have been made by different bipedal hominin species, (2) sexual dimorphism in the track-makers, or (3) disparity in substrate material properties. The latter is a prevalent issue in ichnological studies as differences in substrate typology are well-documented to affect the shape of a print (e.g., D’Août et al. 2010; Morse et al. 2013). Regardless of the topographical differences, the method of track registration is a promising new avenue for analysing track shapes (Belvedere et al. 2018), which will be applied in this project (Chapter Three).

The Laetoli trackways have been the focus of much scholarly debate since the first discovery in the 1970s (Leakey and Hay 1979; Clarke 1979; Day and Wickens 1980; White 1980; Leakey and Harris 1987). Researchers have argued over the functional morphology and gait of the track-makers in the past 40 years, leading to the so-called bent-hip bent-knee (BHBK) hypothesis (Tuttle et al. 1990; Berge et al. 2006; Tuttle 2008; Raichlen et al. 2010; Meldrum et al. 2011; Crompton et al. 2012).

Reconstructions of the Laetoli track-makers’ kinematics have been contentiously debated, with some arguing for a BHBK and others postulating that the Laetoli track-maker likely walked with an erect limb (Bennett and Morse 2014). This is concurrent with debates regarding the function in contemporaneous skeletal remains belonging to the assumed track-maker (e.g., Latimer and Lovejoy 1982; Stern and Susman 1983), highlighting the issues in inferring functional morphology of track shapes.

While some studies argue for a relatively stiff arch in the midfoot impression (Ward et al. 2011), corresponding to modern human-like gait characteristics (Raichlen et al. 2010; Crompton et al. 2012), other studies have argued that the Laetoli footprints exhibit morphology consistent with slightly flexed lower limb kinematics (Hatala et al. 2016a; 2016b). Hatala et al. (2016a) compared footprint pressure points with those of chimpanzees and determined that proportional toe depth could not be distinguished between modern humans and chimpanzees, in contrast to the work of Raichlen et al. (2010) and Crompton et al. (2012). Evidently, there are issues in using footprint depths to postulate limb kinematics, and that other morphological avenues must be explored.

Prior to the extraction of the G3 trackway (Bennett et al. 2016b), only the G1 trackway was available for kinematic investigations (although, to date no study has yet used the extracted G3 trackway in assessments). With only one trackway available, interpretations were limited. The discovery of the new Site S was fundamental in advancing locomotory interpretations of australopiths by adding more prints to the fossil database. The three new trackways (n=14 prints) from Site S are likely contemporaneous with the Site G footprints (Masao et al. 2016). 3D models of the new trackways were immediately made publically available, permitting other researchers to examine the trackways thus enhancing functional interpretations into australopithecine locomotory behaviour.

Raichlen and Gordon (2017) assessed the functional morphology of the Site S trackways to determine their affinity to the Site G trackways, but to also predict the limb posture (erect or flexed) of the Laetoli track-maker. It was assumed that the Laetoli track-maker would have walked with an erect limb. A modern human comparative sample-set was used, alongside the G1 trackway. Proportional toe depths (the product of forefoot depth and heel depth) were determined to be more variable in the Site S trackways than those from Site G, likely explained by differences in substrate material properties (Raichlen et al. 2010). No differences were found in proportional toe depths between experimental trials employing different gaits with various ranges of motion (Raichlen and Gordon 2017). Raichlen and Gordon (2017) concluded that the hominin(s) responsible for the Site S and G footprints likely walked with an extended limb rather than a BHBK gait.

However, Raichlen and Gordon's (2017) study was unable to test the nuanced differences in gait characteristics (e.g., dorsiflexion of the ankle) determined by Hatala et al. (2016a), whereby it was argued that footprint morphology corresponds to joint angles in the hip, knee and ankle. Hatala et al. (2016a) assumed that the Laetoli track-maker would have walked with a more flexed limb, which was fully supported by testing toe depth patterns.

These assumptions and results were further corroborated by more recent experimental designs which explored the dynamic movement of the foot during trackway creation (Hatala et al. 2018). Both of these studies used the same methodology by measuring proportional toe depths, yet reached contrasting conclusions regarding limb posture reconstructions (Hatala et al. 2016a; Raichlen and Gordon 2017). Evidently, there are methodological issues with correlating footprint depths with function, suggesting that other methods must be employed to characterise the relationship between form and function. Future experimental studies would benefit from a larger modern sample size exploring a range of joint angles and limb postures in conjunction with footprint morphology. By utilising a larger population size, morphological patterns can be explored in greater detail.

The functional significance debate of the Laetoli track-maker has resulted in these trackways being incorporated into a range of comparative footprint assessments. Some of these studies have explored changing footprint morphologies (Bennett et al. 2009; Morse et al. 2013), whilst others have used the Laetoli tracks to validate other trackway discoveries as ‘hominin’ (Bennett et al. 2010; Gierlinksi et al. 2017).

The latter scenario was employed to recently published prints from Crete. Possible hominin footprints were reported from Trachilos, Crete (Gierlinski et al. 2017) dated to ~5.6 Ma (vans Hinsbergen and Meulenkamp 2006). The assignment of the footprints to the ichnotaxon ‘hominin’ is equivocal due to the lack of any contemporaneous fossil material and, further, due to Crete’s island status hindering early hominin ranges, although the presence of a late Miocene land bridge has been argued (Poulakakis et al. 2005). The morphology of the prints was contended to be consistent with that of a bipedal track-maker, supported by reviews of the paper (Crompton 2017).

Gierlinski et al. (2017) utilised a landmark-based geometric morphometric approach using modern unshod individuals, the Laetoli G1 trackway (these are the temporally closest prints, assuming that both fossil trackways belong to *Praehominipes*) and mixed extant non-human primate prints to test the theory that the Miocene trackways were created by a bipedal Homininae/basal hominin. Based upon morphological affinities between the Trachilos trackways and known hominin trackways, two potential track-makers were tentatively identified: (1) a basal member of the clade Hominini or (2) the tracks belong to a yet unidentified extinct non-hominin primate. Gierlinski et al. (2017)

favour an early hominin as the culprit based upon biogeographic reconstructions of the Messian period.

Unfortunately, 3D models of the tracks have not been made publicly available, nor have another research team had the opportunity to analyse the prints. One such review of the Trachilos tracks does highlight numerous errors in the original report; such as a lack of scalebars in published photographs, confusing statements on shape/size variation, and a lack of clear identification of anatomical features, resulting in other researchers claiming that the Trachilos trackways were not made by a primitive hominin (Meldrum and Sarmento 2018). Until a further, comprehensive assessment of the footprints can be made then these tracks can only be contentiously accepted as potentially hominin (Crompton 2017; Bennett, 2019, pers. comm.).

Regardless of the debated ichnotaxon assignment of the Trachilos prints, the ability to apply geometric morphometrics to explore track shapes is an exciting and promising research avenue. Footprints lack the anatomically-defined landmarks that are necessitated and utilised in a range of shape-space assessments (e.g., Bookstein 1990; Dryden and Mardia 1998; Zelditch et al. 2012). Yet, landmark-based assessments of fossil footprints using geometrically-defined landmarks (Bookstein 1990) permitted the identification of shape patterns within track impressions (Berge et al. 2006; Bennett et al. 2009; Bennett et al. 2010; Lallensack et al. 2016), signifying that shape-space methods can be successfully utilised to explore shape patterns in a range of fossil footprints. These methods will be employed in Chapter Four to investigate shape patterns of fossil tracks, but to also confirm the ichnology of the Happisburgh, UK prints (Ashton et al. 2014).

Koobi Fora Formation, East Turkana

A few years after the discovery of the first hominin trackways at Laetoli, Tanzania, further hominin tracks were discovered at the Koobi Fora Formation, East Turkana, Kenya (Behrensmeyer and Laporte 1981). Unfortunately, only singular prints were discovered, inhibiting a comprehensive assessment into the locomotion of the track-maker, and even preventing ichnotaxon assignment to the prints. It was not until nearly 30 years later were complete trackways discovered in the East Turkana Basin. In 2007 the first set of hominin trackways at the Okote Member of the Koobi Fora Formation were discovered at the locality FwJj14E, with the surrounding region being extensively excavated over the following two years (Bennett et al. 2009; Hatala et al. 2017). Due to the proximity to the

local village of Ileret, the tracks are commonly known as the Ileret footprints (Bennett et al. 2009).

Twenty hominin trackways in total intermixed with a large assortment of animal tracks were uncovered during the 2007-2010 excavation seasons (Hatala et al. 2017). During 2010-2014, the excavations at FwJj14E were expanded to investigate further stratigraphic sequences and revealed a further 53 hominin tracks – 48 of these tracks were discovered on the UFS (Upper Footprint Surface), three tracks were found on the LFS (Lower Footprint Surface), and two were found on an intermediate layer (Dingwall et al. 2013; Richmond et al. 2013; Hatala et al. 2017). All tracks have been ascribed to *Homo erectus* based upon comparative body size estimates (Bennett et al. 2009). Additionally, the prints display derived features of the foot: an adducted hallux and a clear midfoot impression (Hatala et al. 2016a). These footprint morphologies fit well with anatomical specifications of *Homo erectus* remains (Harcourt-Smith and Aiello 2004), strengthening the taxonomic assignment of the tracks.

The Okote Member of the Koobi Fora Formation was fully excavated in 2013. The Koobi Fora sediments are largely uniform between each locality: the sediment layer is composed of laminated silts with intervening layers of fine-grained, stratified silts and sands (Bennett et al. 2009; Hatala et al. 2017), covered by fine silty sands, a process which was thought to have occurred quickly after trackway production (Roach et al. 2016; Hatala et al. 2017). Evidence of repeated sediment deposition in the surrounding lake margin offered a unique opportunity to assess repeated visits to the lake shore over a period spanning ~20,000 years by hominin groups (Roach et al. 2016), evident by the Ileret Tuff Complex (ITC) (Hatala et al. 2017).

The ITC has been dated to 1.15-1.52 Ma, with the underlying sediment bed dated to 1.5 Ma (Brown et al. 2006; McDougall and Brown 2006). The Ileret Tuff containing the hominin prints has been dated to 1.52 Ma (Bennett et al. 2009).

All Turkana Basin tracks were measured in the field prior to 3D data capture (Hatala et al. 2017). These measurements were directly compared with those of modern, contemporaneous unshod individuals of the Daasanach people from Ileret (Hatala et al. 2016b) and with modern, captive chimpanzees (Hatala et al. 2016a). Published linear measurements from other fossil footprint sites were also collected and compared directly with the Turkana Basin track dimensions (Hatala et al. 2017): Roccamonfina, Italy (Avanzini et al. 2008); Happisburgh, UK (Ashton et al. 2014); and Laetoli, Tanzania

(Bennett et al. 2016b; Hatala et al. 2016a; Masao et al. 2016). The Turkana Basin tracks were found to be comparatively similar to those made by contemporaneous extant individuals (Hatala et al. 2016b) and to the Roccamonfina tracks (Hatala et al. 2017). Taking simple linear measurements has thus permitted track metrics to be comparatively compared between fossil sites.

Track dimensions have been previously used to infer biometrics of the track-makers, such as using foot length to calculate stature (Martin 1914; Robbin 1984), footprint area to calculate body mass (Dingwall et al. 2013), or a linear regression of foot length and width to predict body mass (Domjanic et al. 2015). The relationship between track dimensions and body mass was explored within the group from Daasanach, Kenya (Dingwall et al. 2013; Hatala et al. 2016b). Footprint area (calculated as the product of forefoot breadth to foot length) was used to provide mass predictions for each individual in this group. This method was extrapolated to the Ileret prints. Body mass estimates (\bar{x} =50.0 Kg) were found to be similar between these two groups and were found to be broadly consistent with skeletal estimates of *Homo erectus*, and inconsistent with *Paranthropus boisei* (Grabowski et al. 2015), strengthening the claim that *Homo erectus* was likely the Ileret track-maker (Hatala et al. 2016c).

Assuming that footprint dimensions are an accurate representation of body mass in hominins, overall body mass in the Ileret track-maker has been consistently predicted to be greater than that of the Laetoli track-maker (Hatala et al. 2016c; Hatala et al. 2017). Body mass predictions of the Laetoli footprints correspond to mass predictions from skeletal material belonging to *Australopithecus afarensis* (Grabowski et al. 2015), the hominin attributed to making the trackways (Tuttle et al. 1991; Masao et al. 2016).

Body mass estimates derived from track dimensions were also used to estimate sex of the track-makers (Hatala et al. 2016c). The majority of the tracks were likely created by males. Assuming the prediction that social groupings existed within the Ileret hominins, it is probable that these early hominins had multi-male social interactions (Hatala et al. 2017). Hence, trackways are not only indicative of the track-maker's biometrics and lower limb biomechanics, but are also a reflection of social behaviour in early hominin groups (Hatala et al. 2016c; Roach et al. 2016; Hatala et al. 2017), which would be otherwise unknown from fossilised skeletal material.

Although multiple methods of biological profiling have been presented (e.g., Dingwall et al. 2013; Domjanic et al. 2015), few of these studies have developed methods using

experimental footprints created in a range of different substrates. To date, no study has explored the variability of print dimensions when created at several speeds across substrates of varying compliancy. The variability in track dimensions will be directly quantified in Chapter Three. By understanding the dependence of track dimensions and substrate deformity during footprint creation, the ability to accurately predict the biometrics of the track-maker will be improved.

Although the Ileret tracks are not yet publicly available, 3D reconstructions of the prints have been created (Hatala et al. 2017). All footprint-bearing surfaces in the Turkana Basin were recorded using photogrammetry to create high quality 3D models for the digital preservation of the prints (Falkingham 2012; Falkingham et al. 2018), which are preserved in an unconsolidated sediment, thought to be at a substantial risk of damage through natural erosion processes (Roach et al. 2013; Bennett et al. 2013; Zimmer et al. 2018). Immediately after excavation and digital recording, the trackways were reburied to aid long-term preservation (Hatala et al. 2017).

Gombore II-2, Ethiopia

Excavations in 2013-2015 at Gombore II-2, Ethiopia yielded an inter-mixed selection of hominin and other animal trackways (bovids, equids, suids, hippopotamuses, birds and a selection of unidentifiable tracks) alongside a collection of archaeological material (lithic assemblages and faunal material) which were discovered in a trampled sandy silt sediment (Altamura et al. 2018). Whilst the surface containing the prints was not dated directly, the overlaying and underlying stratigraphic sequences were dated to $^{40}\text{Ar}/^{39}\text{Ar}$ 0.875 ± 0.010 Ma and $^{40}\text{Ar}/^{39}\text{Ar}$ 0.709 ± 0.013 Ma (Altamura et al. 2018), with a chronological constraint of ~ 0.78 Ma determined by a Matuyama/Brunhes magnetostratigraphic boundary (Tamrat et al. 2014).

The trackways were formed in a sandy-silt and were infilled with sand lenses of $\sim 0.1\text{m}$ thick. The absence of pedogenetic processes, breccia and/or desiccation cracks on the surface layer indicates that the sediment was only exposed for a brief time before the area was covered by overlaying sediments (Altamura et al. 2018). Excavations have yielded numerous thin layers of accumulated sand lenses, with superimposed trackway layers located next to palaeo-channels, suggesting the area was frequented by both hominins and other animals (Altamura et al. 2018).

The trackways have been tentatively assigned to *Homo heidelbergensis* via the discovery of fossilised skeletal material belonging to this taxon from the underlying stratigraphic layer (Altamura et al. 2018). Eleven hominin tracks were tentatively identified (Altamura et al. 2018), using the characterisation protocol proposed by Morse et al. (2013). Only one of the tracks displayed key morphological features that assigned the footprint to a hominin taxon (Altamura et al. 2018). Other prints were unfortunately trampled by overlaying trackways, leading to superimposition of the material.

Due to the success of other studies that employed geometric morphometric methods to characterise shape affinities between fossil hominin tracks (Berge et al. 2006; Bennett et al. 2009; Bennett et al. 2010), a geometric morphometric assessment of the Gombore II-2 prints was conducted using the juvenile prints from Walvis Bay, Namibia (Bennett et al. 2014) as a comparative sample due to the small dimensions of the Gombore II-2 prints (Altamura et al. 2018). This study assumed that the prints were made by *Homo* species and that shapes of the footprints would be similar between these two groups despite eco-geographical and temporal differences. An overlay of the resulting Procrustes scores from the Principal Components Analysis identified that the Gombore II-2 tracks belong to young children, perhaps as young as six months old (Altamura et al. 2018), supported by further comparative data from the World Health Organisation (WHO) (de Onis 2006). The Gombore II-2 prints thus offer the earliest insight into infant/young juvenile behaviour and movement of Early Pleistocene hominins.

Furthermore, track morphology was consistent with *Homo* tracks from other African and Eurasian sites (Bennett et al. 2009; Morse et al. 2010; Ashton et al. 2014; Bennett et al. 2014; Roach et al. 2016). These footprints have not yet been made publicly available for further assessment by other research teams.

Langebaan, South Africa

A poorly preserved trackway containing just two prints was discovered in Langebaan, South Africa (Roberts and Berger 1997; Helm et al. 2018), dated to ~120 Ka BP (Roberts 2008; Jacobs and Roberts 2009). The prints are preserved in calcareous aeolianites – the only such hominin trackway to be lithified, and thus fully fossilised (Bennett and Morse 2014). The tracks were declared hominin due to a rim-like structure surrounding the prints (Roberts 2008). Comparative track-creation experiments combined with the Late Pleistocene age of the trackway ascribed the prints to archaic modern humans (Roberts 2008), although recently *Homo naledi* has been proposed as the potential track-maker

(Helm et al. 2018; Helm et al. 2019). However, due to the poor topographical morphology of the trackway (Roberts 2008), some researchers have questioned if they are indeed human (Bennett and Morse 2014). The questionable ichnology of the trackway combined with its small size (n=2 prints) has excluded these trackways from comparative fossil track assessments since their discovery, despite the curators' of the Iziko Museums, South Africa willingness to share the material.

Happisburgh, UK

Coastal erosion in 2013 at Happisburgh, UK exposed a sediment bed composed of laminated silts which contained a large selection of potentially hominin tracks (Ashton et al. 2014). In total, 152 small (c.50 mm-320 mm) hollows were discovered, 49 of which were identified as potentially hominin tracks. Of these, only 12 were included in the original analyses when the discovery was first announced due to the severe erosion of many of the prints (Ashton et al. 2014). No tracks could be associated as belonging to a singular trackway; rather, the sediment bed is a mixture of singular prints.

By association with other dated evidence, the age of the bed was estimated at around 950 Ka or 850 Ka via combination of palaeo-magnetism of the sediments and biostratigraphy (Ashton et al. 2014). Contemporaneous skeletal material in Western Europe during this period has been ascribed to *Homo antecessor* (Carbonell et al. 2005; Carbonell et al. 2008). Inferences of body size made from the Happisburgh tracks by Ashton et al. (2014) are consistent with estimated body sizes for *Homo antecessor* (Pablos et al. 2012) and, consequently, the tracks have been tentatively ascribed to this species.

Most of the tracks were determined to belong to juveniles (Ashton et al. 2014), based upon track length sizes as derived from the WHO (de Onis 2006). The larger tracks at Happisburgh were determined to be comparable in size to those from Ileret, Kenya (Hatala et al. 2017).

Unfortunately, the footprints were destroyed by marine erosion a few weeks after exposure. High quality 3D data was, regrettably, not captured prior to the loss of the tracks (Ashton et al. 2014), resulting in modelled tracks with unreliable depth dimensionality. From the available data, the prints exhibit little anatomical detail, which have so far precluded any comprehensive functional interpretation of the track-makers. This has led to the necessary exclusion of the Happisburgh tracks from many of the recent comparative analyses of hominin footprints (e.g., Hatala et al. 2016b; Bennett et al. 2016a). Even if

detailed mapping of the footprints had been conducted, the nature of the very soft sediments may impact the dimensions of the tracks and the subsequent interpretations of the track-makers. A comprehensive assessment of the metrics and shape of experimental prints created in a range of substrates will be conducted in Chapter Three, which will provide inferences of the Happisburgh track-makers in Chapter Four.

Neanderthal sites

Until very recently, the available data for Neanderthal (*Homo neanderthalensis*) trackways was limited to just two singular footprints from two cave sites: Vârtop Cave, Romania dated to >62 Ka (Onac et al. 2005) and Terra Amata, France dated to 380 Ka (DeLumley 1966); although, the latter has been argued to potentially belong to *Homo erectus* or *Homo heidelbergensis* (Bennett and Morse 2014). Although both of these prints had distinct anatomical features (e.g., an adducted hallux and a prominent midfoot impression) and were undeniably hominin, there were too few prints belonging to this species for these tracks to be included in any comparative assessments with other hominin footprints. To date, no comprehensive assessment of Late Pleistocene hominin track morphology has been conducted due to a lack of adequate data – with the exception of the terminal Pleistocene anatomically modern human (AMH) footprints from Willandra Lakes, Australia (Webb et al. 2006). Fortunately, recent excavations have uncovered a large selection of Neanderthal trackways.

A series of extensive investigations began in 2012 at Le Rozel, Manche, France to expose a Mousterian lithic assemblage at the Le Rozel rock-shelter site, which also uncovered a large collection of hominin trackways (Cliquet, 2018, pers. comm). The site was first exposed via coastal erosion in the 1960s (Stoetzel et al. 2016). The site is characterised by a long and complex stratigraphic sequence as part of a sand dune formation spanning the Upper Pleistocene region (Stoetzel et al. 2016; Mercier et al. 2017), yielding a rich abundance of Mousterian lithic assemblages and faunal remains (Scuvee and Verague 1984; Cliquet 2016; Mercier et al. 2017). The lower part of the sequence has been dated to Marine Isotope Stage (MIS) 5 (Folz 2000; Van Vliet-Lanoë et al. 2006), with the micro-faunal remains typical of the Late Pleistocene and of a temperate environment (Stoetzel et al. 2016). Sedimentary analysis has suggested that the site was occupied at least twice (Van Vliet-Lanoë et al. 2006), although recent investigations in 2017-2018 would suggest more frequent occupations (Cliquet, 2018, pers. comm.).

Due to the abundance of archaeological material discovered in recent years at Le Rozel (currently this is the largest selection of Palaeolithic footprints discovered in Europe), new sediment samples were collected for the site to be re-dated using single-grain luminescence (OSL) dating techniques (Preusser et al. 2008) on both quartz samples and feldspars data. Both materials yielded significantly variable dates of the site: the quartz produced dates of 70 ± 10 Ka to 86 ± 9 Ka; whereas the feldspar data produced dates ranging from 114 ± 11 Ka to 126 ± 12 Ka (Mercier et al. 2017). Laboratory error during sample preparation likely caused this large discrepancy between dates. However, the data does support the theory of high sedimentation rates of the dune creation, which ultimately led to footprint preservation (Cliquet, 2018, pers. comm). Despite errors in dating methods, all methods indicate that Le Rozel was occupied during MIS 5 (Mercier et al. 2017).

To date, ~800 tracks intermixed with a small number of lithics and faunal bones (Cliquet 2016; Mercier et al. 2017) have been uncovered within a series of micro-layers (Cliquet, 2018, pers. comm). These tracks are a mixture of singular prints and complete trackways. A few handprints have also been uncovered at the site, which are quite rare in the fossil record having only been uncovered at one other site: Roccamonfina, Italy which has been dated to $^{40}\text{Ar}/^{39}\text{Ar}$ 345 ± 6 Ka BP and ascribed to *Homo heidelbergensis* (Avanzini et al. 2008; Panarello et al. 2018). The new phase of excavations directly exploring the footprint assemblage at Le Rozel have produced lithic assemblages typical of the Middle Palaeolithic which are commonly ascribed to *Homo neanderthalensis* (Mercier et al. 2017), strengthening the claim of *Homo neanderthalensis* as the track-maker (Cliquet, 2018, pers. comm.).

The trackways predominantly belong to infants and juveniles, with only a small number of adult trackways uncovered (Duveau et al. in review). Typically, only very short trackways ($n\leq 4$ prints) are discovered, with much trampling and superimposition of the trackways. The excavation season in 2018 yielded two long trackways (the longest was composed of nine prints) belonging to juveniles within the same micro-layer, travelling in the same direction. These trackways offer the rare opportunity at Le Rozel to examine the lower limb kinematics of the Neanderthal juvenile (Duveau et al. in review), which will surely be aided by further discoveries at Le Rozel in future excavation seasons.

Unfortunately, the footprints are formed in easily deformable materials: sandy and sandy-silts (Mercier et al. 2017). Consequently, soon after exposure the prints are destroyed by natural weathering; even small wind speeds can be damaging to the sediment, as noted during excavations in 2018. The prints are manually solidified using a resin material and

removed from the excavation immediately after exposure and 3D model creation for curation. Future research into these prints will offer an exciting insight into the ontogenetic kinematics of Neanderthals.

Formby Point, Sefton Coast, UK

Numerous Holocene human and animal tracks have been identified along the Sefton Coast, UK (Cowell et al. 1993; Roberts et al. 1996; Gonzalez et al. 1997; Huddart et al. 1999; Roberts 2009). Two names are interchangeably used for these trackways: Sefton Coast and Formby Point. The trackways have been specifically uncovered (and are continuing to do so) at Formby Point, a 4 km stretch of the Sefton Coastline. As such, the trackways will be referred to as the Formby Point trackways within this thesis following naming conventions by Huddart et al. (1999).

Formby Point is characterised by silty, fine-grained sands and peat sediments and overlaying sand dunes (Roberts et al. 1996), preserved in unlithified soft-sediments (Roberts 2009; Bennett and Morse 2014). Encroaching coastlines have led to the exposure of numerous ancient sediments since the 1970s, many of which contain Holocene human and animal tracks (Huddart et al. 1999; Roberts 2009). By 2014, 145 human trackways had been documented (Bennett et al 2014). Further trackways have been recorded since 2014 (Burns, 2016, pers. comm), with ~30 trackways documented as part of this thesis.

Carbon and OSL dating of the previously excavated sediments have yielded dates from 6650 ± 700 OSL BP $\sim 3575 \pm 45$ ^{14}C BP (Roberts 2009). The latter date was obtained by dating roots that overlay the fossilised beds, indicating a *terminus ante quem* for the beds (Roberts et al. 1996; Huddart et al. 1999; Roberts 2009), confirming a Mesolithic age. The fossilised beds offer an interesting insight into human activity of the Late Mesolithic-Early Neolithic transition along the Sefton Coast.

The geological age of the trackways and the morphology of the prints have been cumulatively used to assign AMHs as the track-maker (Roberts 1996). The trackways belong to infants, juveniles and adults. Such a diverse collection of prehistoric, AMH, unshod individuals does not currently exist elsewhere (Bennett and Morse 2014), highlighting the archaeological importance of these fragile impressions. This unique sample of prehistoric human prints has been previously used to investigate changing hominin footprint shapes (e.g., Lockley et al. 2008; Bennett et al. 2009; Bennett et al. 2010; Morse et al. 2010), thus circumventing the need to collect contemporaneous data

from extant unshod groups (e.g., Dingwall et al. 2013) which can be logistically costly. Due to the ease of access to the Formby Point trackways, the prints will be used as a modern comparative sample-set in Chapters Two and Four.

Although the trackways are rapidly lost to marine erosion soon after exposure (Bennett et al. 2010; Wiseman and De Groote 2018), the prevalence of the sediment beds that are continually appearing with the tide suggests that further footprints will be uncovered in the future to add to the ever-growing database of the Formby Point trackways.

Walvis Bay, Namibia

A selection of modern human trackways at Walvis Bay, Namibia dated to the Holocene was first documented in 1996 (Kinahan 1996), with further appearances of the trackways over the past decade, concurrent with sand dune movement (Morse et al. 2013; Bennett et al. 2014). A series of mudflats and sand/silt filled inter-dune channels were exposed by a combination of moving sand dunes and flood drainage from the nearby river estuary (Bennett et al. 2014). These sediment beds contain a mixture of human (juvenile and adult) and animal (domestic cattle, elephant, giraffe, sheep and bird) trackways (Kinahan 1996; Morse et al. 2013; Bennett et al. 2014). The sediments were dated to 1.5 Ka^{-1} using OSL dating of quartz grains within the substrate (Bennett et al. 2014).

Perhaps the most important discovery at Walvis Bay was the identification of a trackway belonging to just one individual (Morse et al. 2013). Within this trackway there exists significant variability in topographical morphology owing to the trackway spanning four different substrate typologies ranging from soft to firm, with the track shapes corresponding to these differences in typology by varying in length and width, thus over- and/or under-estimating the biometrics of the track-maker (Morse et al. 2013). Body mass predictions ranged from severely obese to critically underweight in this individual, as the direct consequence of changes in substrate mechanics. Consequently, track dimensions and the subsequent biometric predictions are significantly influenced by substrate material properties.

Although the relationship between substrate mechanics and footprint shapes had been previously well-documented prior to this discovery (e.g., Gatesy et al. 1999; Milán 2006; D'Août et al. 2010; Raichlen et al. 2010; Bates et al. 2013b), this was the first occurrence of substrate influencing footprint shapes so drastically within a singular human trackway (Morse et al. 2013). New, experimental methods were designed to directly investigate the

influence of substrate mechanics on track shape by assuming that nuanced differences in substrate can significantly affect footprint formation (e.g., Falkingham and Gatesy 2014; Falkingham et al. 2014). More recent experiments have included a consideration of biometrics with that of lower limb movement and substrate deformation, which all cumulatively influence trackway production (Gatesy and Falkingham 2017; Hatala et al. 2018). It is only with the application of new, novel experimental designs which incorporate a range of controlled variables, such as substrate and joint movements, has this dynamic relationship began to be understood in human footprint formation (Hatala et al. 2018), although a comprehensive investigatory approach incorporating a wider selection of controlled variables (e.g., different speeds and substrates) is still required. With a greater comprehension of this relationship, the validity of biometric and biomechanical inferences of fossil trackways can be improved.

3D models of the Walvis Bay tracks are publicly available to other research teams to utilise. Combined with the selection of the Formby Point footprints, a vast range of anatomically modern trackways belonging to unshod individuals of various ages are available for comparative assessments of fossilised hominin trackways. By incorporating these two prehistoric groups into any analyses then footprint studies will be advanced.

1.5 Uncertainties in footprint studies

Despite a wealth of fossilised hominin footprints extending from a wide temporal and geographical range, the circumstances leading to footprint creation remains contentious (D'Août et al. 2010; Morse et al. 2013; Falkingham et al. 2014). The relationship between lower limb movement, substrate mechanics, biometrics, and footprint morphology are mostly unknown (e.g., Bennett and Morse 2014; Gatesy and Falkingham 2017). This relationship is continuing to be explored (e.g., Falkingham and Gatesy 2014; Hatala et al. 2018), with recent studies offering a greater comprehension into assessing fossil tracks. Via the application of new methods that combine 3D real-time kinematics with that of footprint morphology, the comprehension of the relationship between form and function is somewhat improved, but requires further exploration. Within this project, 3D motion capture systems will be employed to directly address these uncertainties.

Once a greater comprehension of footprint morphology is achieved, it will be possible to statistically compare track shapes between different fossil localities by applying methods such as geometric morphometrics (e.g., Berge et al. 2006; Bennett et al. 2009; Gierlinski

et al. 2017). Importantly, a greater comprehension of the events which lead to footprint creation (e.g., limb kinematics, biometrics and substrate deformity) will permit the Happisburgh, UK tracks to be compared with other fossil tracks for the first time.

1.6 Aims of thesis

The overall aim of this thesis is to improve the recording and analyses of fossil trackways. To achieve this, methods of recording will be refined, and a series of biomechanical experiments will be conducted to investigate the association between substrate mechanics, lower limb kinematics and footprint morphologies.

This is an exploratory project given that this was the first study to directly quantify the effects of erosion on track morphology, as published in the *Journal of Archaeological Science: Reports* 2018, which has since generated debate regarding the accuracy of biometric and biomechanical inferences from tracks (De Silva et al. 2018) and, additionally, has offered interesting insights into the degradation of other fossil trackways (Zimmer et al. 2018). Because significant degradation can occur to a footprint thus affecting size and shape, the first aim of this project was to identify the best practise(s) for creating 3D models of prints (Chapter Two).

It is particularly pertinent to create accurate 3D models for the digital preservation of fossil footprints for sites where the fossils are at immediate risk of destruction after exposure, such as the Le Rozel trackways. Immediately after excavation, these tracks are susceptible to damage (even in low wind speeds), highlighting the need for rapid methods of digital recording to be deployed. As the excavations at Le Rozel are still ongoing and, additionally, the Formby Point trackways are continuously appearing concurrent with coastal erosion, the identification of rapid, non-invasive recording methods is paramount. Especially because these methods could be used with immediate effect at numerous fossil footprint localities if successful. Different recording methods, including the applicability of non-invasive methods (Unmanned Aerial Vehicles), will be tested in Chapter Two.

After the successful and accurate construction of a 3D modelled footprint, the second aim of this project was to determine if a track can be used to identify the biometrics and locomotory behaviour of the track-maker (Chapter Three). If the track-maker can be accurately identified regardless of speed and/or substrate mechanics, this will permit the comparative assessment of fossil tracks. Previous studies have only included fossil tracks which belong to similar speeds/substrate materials to avoid the issue of variable speeds

and/or substrates introducing additional error in to shape assessments (e.g., Bennett and Morse 2014). This is the first study to include numerous hominin fossil tracks inclusive of a range of substrate typologies in one comparative assessment (Chapter Four).

To address these aims, this project analysed a collection of fossilised trackways and experimentally generated trackways. Prehistoric track material was collected during fieldwork at Formby Point, Merseyside, UK in 2016-2017 with the permission of the National Trust, UK. Excavation was aided by students from Liverpool John Moores University (2016-2017) and The University of Manchester (summer 2016). The sample comprises of AMH trackways and a diverse selection of animal trackways, such as roe deer and auroch. This material was documented daily before its destruction by coastal erosion.

Trackways from Le Rozel, France were documented during fieldwork in summer 2018. Fossil trackway material from Laetoli, Tanzania; Ileret, Kenya; Happisburgh, UK; Terra Amata, France; Vârtope Cave, Romania; Langebaan, South Africa; and Walvis Bay, Namibia were also included in analyses.

Experimental trackway material belonging to modern humans was collected in the Biomechanics Laboratory, Tom Reilly Building, Liverpool John Moores University, UK. Ethical approval was granted by the Liverpool John Moores University Research Ethics Committee (REC: 16/NSP/041).

1.7 Research Questions

As this project is multi-disciplinary, several research questions will be addressed. Overall, this research hopes to build upon previous studies which have investigated the relationship between print morphology with that of substrate mechanics, biometrics and lower limb movement (e.g., D'Août et al. 2010; Raichlen et al. 2010; Hatala et al. 2018). A combination of analytical methods will be adopted to explore this relationship, including an incorporation of a wider range of controlled variables. It was only possible to explore this relationship by first identifying the best practises for the successful reconstruction of 3D modelled trackways.

Research questions are briefly described here.

Chapter Two: A combination of fossil footprints and experimental trackways were recorded daily to quantify the daily degradation/erosion of trackways via the application

of 3D geometric morphometric techniques. The results addressed the following research questions:

- 1) Does degradation affect footprint morphology prior to fossilisation?
- 2) To what extent will erosional processes alter the shape and size of a footprint after exposure?
- 3) Will predicted changes in shape and size as the direct consequence of either degradation and/or erosion alter biometric predictions of the track-maker?

Because erosion was found to significantly affect the shape and size of footprints after erosion, the second part of this study was to identify a rapid recording method(s) for trackways by deploying a range of UAVs and camera types, following different flight paths and recording via different methods of photograph capture. These experiments addressed the final research question of this chapter:

- 4) Can UAV technology be deployed to reconstruct fossil footprints via photogrammetry? And are the produced models of high enough resolution to allow reconstructions usable in ichnological studies?

Chapter Three: Further experiments were designed in which modern humans were recruited to move across different types of substrates at several speeds and limb postures. 3D motion capture systems were used to capture kinematic variables, which were compared to track shape production to determine if kinematics and biometrics are reflected in foot impressions. The results addressed the following research questions:

- 1) Are track dimensions of a single individual consistent when created in several types of substrates at different speeds and limb postures?
- 2) Can track dimensions be used to accurately identify the track-maker's biometrics?
- 3) Are lower limb kinematics reflected in track shapes?
- 4) Can limb posture be reconstructed from track shapes in a range of substrates?

Chapter Four: 2D geometric morphometric methods were applied to fossilised footprints collected from nine different sites. Importantly, this was the first study to investigate the functional morphology of the Happisburgh, UK tracks within a wide comparative context. Landmarks were selected to synthesise only the outline shape of the prints to provide a comparative assessment of changing track shapes between Pliocene, Pleistocene and Holocene fossils. This comparative assessment addressed the following questions:

- 1) Can 2D geometric morphometrics be used to synthesise the functional morphology of tracks?
- 2) Can the outline shape (a representation of anatomy and biometrics) of fossil tracks be captured and statistically compared?
- 3) If so, do the Happisburgh tracks share any shape affinities with other Pliocene, Pleistocene and/or Holocene tracks?

Cumulatively, the designed experiments and methods employed here will address the global research question of this thesis:

Can a footprint be used to identify the biometric information and the locomotory behaviour of the track-maker?

The presented multi-disciplinary approach to analysing fossil trackways will hopefully address this research question, but it will only be possible to do so after refining methods of track analysis. This ranges from fossil discovery to functional interpretations.

Chapter Two

Identifying the optimal recording method for fragile, *in situ* tracks

In this chapter, two studies are presented which identify the issues in extracting reliable information from track dimensions and morphology. The first study quantifies the daily degradation of prehistoric and experimental tracks using shape analysis to determine how erosion may affect the shape and size of a track thereby producing unreliable biometric predictions of the track-maker and influencing inferences regarding locomotion. The results from this study determined the need for the rapid recording of tracks, which would otherwise be destroyed by environmental erosion, and/or trampling, and were published in the Journal of Archaeological Science: Reports, 2018. The second study tested the applicability of using non-destructive Unmanned Aerial Vehicles to rapidly record tracks. Various Unmanned Aerial Vehicles, flight paths, camera types, and heights were incorporated in this study to identify the accuracy in minute depth reconstruction and subsequent 3D mesh creation. Results have indicated that currently Unmanned Aerial Vehicle technology does not record fossil track data to the standards required by palaeoanthropologists.

This chapter formed the basis of one publication available in Appendix A:

Wiseman, A. L. A. & De Groote, I. 2018. A three-dimensional geometric morphometric study of the effects of erosion on the morphologies of modern and prehistoric footprints. *Journal of Archaeological Science: Reports* 17: 93-102.

One manuscript is currently in preparation:

Wiseman, A. L. A., Bezombes, F. & De Groote, I. The need for non-invasive recording methods: The applicability of UAV technology for recording fossilised footprints *in situ*. *In Preparation*.

This chapter was presented at the following conferences:

Wiseman, A. L. A., Moore, A., Bezombes, F., Checkley, M., De Groote, I. 2017. Methodological approaches to recording *in situ* fossils. *European Society for the Study of Human Evolution 6th Annual Meeting*, Leiden, The Netherlands.

Wiseman, A. L. A. Moore, A., Bezombes, F., De Groote, I. 2017. UAV photogrammetry potential for the recording of fragile fossils: A preliminary assessment. *3D Imaging in Cultural Heritage Conference at The British Museum*, London, UK.

Wiseman, A. L. A. 2017. A multi-disciplinary approach to fossilised trackways: The application of UAV technology and biomechanical assessments. *British Federation of Woman Graduates Annual Meeting*, Liverpool, UK.

Wiseman, A. L. A. & De Groote, I. 2017. A three-dimensional geometric morphometric study of coastal erosion and its implications for biological profiling and biomechanical inferences of fossilised footprints from Formby Point, Merseyside. *UK Archaeological Science Conference 2017*, London, UK.

2.0 Abstract

The discovery of Holocene tracks at Formby Point, UK in 2016 offered a unique opportunity to quantitatively assess rapid fossil degradation. This study, which was published in February 2018, determined that track shape (internal topography and outline metrics) and size are significantly altered by external environmental factors. The results identified numerous issues with currently applied methods of studying fossilised tracks, such as predicting biometrics from morphology: once tracks were exposed to the elements they began to erode, thus introducing previously unknown error in track inferences. Importantly, the results from this study identified the need to rapidly record fossilised tracks after exposure.

Two sets of experimental flights using Unmanned Aerial Vehicles (UAV) were designed whereby the optimal flight path, flight height, camera choice and capture type (video versus camera stills) were identified. Shape and size, the consequence of poorly reconstructed depth dimensionality on surfaces, were found to be affected by flight path and by the height of the UAV, indicating that the optimal method of recording tracks is to use a handheld DSLR camera following a circular or rastered flight path. Results of this study have demonstrated that, currently, UAV technology does not meet the standards required by palaeoanthropologists for the production of high quality, precise data.

Although UAV technology produced unreliable reconstructions, UAVs remain a technological solution when sites may be at immediate risk of destruction. Although the produced models may not have precise depth dimensionality, it is better to have a record of these footprints without risking further damage to the fossil interface via the excavator or jeopardising their complete destruction. The deployment of UAV technology will permit the digital preservation of fossil material which would otherwise be lost. If circumstances permit longer data capture periods, then it is recognised that the best method for recording fossil footprints would be to use handheld recording methods.

2.1.0 Introduction

Tracks are formed in soft substrates that have an adequate water content (Ashton et al. 2014). As a foot impacts the ground, the substrate will deform under the applied load as strain transfers to the surrounding materials, deforming the region around the applied load, leaving an impression of the foot (Morse et al. 2013), which can inform on the biometrics and the kinematics of the track-maker (Bennett and Morse 2014). Tracks will become fossilised if the substrate rapidly dries and is then covered (Morse et al. 2013).

As with any archaeological material, once the fossils are uncovered and exposed to the elements they will begin to erode (Bennett et al. 2013), compromising the shape and size of a track. Tracks may span a large region and are difficult to extract and preserve (Bennett and Morse 2014), creating the need for rapid and accurate recording. Many digital methods have been applied in recent years to accurately capture and record tracks, such as the use of laser scanners (e.g., Domjanic et al. 2013), or photogrammetry (e.g., Bennett et al. 2013). Digital capture facilitates laboratory-based analysis of the tracks (Falkingham et al. 2018), allowing for novel techniques to be applied to investigate the relationship between form and function (Vereecke et al. 2003; Domjanic et al. 2013). Ultimately, digital capture permits the digital preservation of fragile fossils, such as the Laetoli tracks. Upon discovery, casts were made of each of the Laetoli tracks (Feibel et al. 1995). 3D models were created from these casts (Bennett et al. 2016b), which have now become widely available to academics for extensive assessments and to the public in museums worldwide.

However, data from casts is limited and often plagued by noise error (Bennett et al. 2013). New technological advancements have facilitated the digital capture of tracks *in situ*, allowing for more accurate post-excavation assessment (e.g., Falkingham et al. 2018). The use of laser scanners and/or photogrammetry has enhanced the recording of tracks, creating high resolution 3D models. Yet, many of these techniques can be damaging to archaeological sites (Bennett et al. 2013). For example, the use of tripods and trampling from technicians can compromise the rigidity of a track, particularly those found in easily deformable and unlithified materials, such as the Happisburgh tracks (Ashton et al. 2014).

A less invasive method is the use of Unmanned Aerial Vehicles (UAVs). These can be controlled from a far distance, allowing for the fossils to be digitally and remotely recorded without interacting with the fossil material(s). In recent years, UAVs have been increasingly used to record cultural heritage sites (Rinaudo et al. 2012; Nex and Remondino 2014; Achille et al. 2015; Guerrieri and Marsella 2017; Campana 2017;

Nikolakopoulos et al. 2017) and to deploy a variety of payloads e.g., LiDAR and various cameras for remote sensing and photogrammetry purposes. The use of UAVs are increasing in popularity owing to how rapidly an area can be recorded (Smith et al. 2014; Campana 2017), whilst also offering a non-destructive and non-invasive method to capture an area of interest.

To date, only Nikolakopoulos et al. (2017) have examined the reliability of UAV technology to record archaeological remains. High levels of accuracy were determined when comparing traditional methods of aerial data capture (topographic surveys) with that of UAV deployment (Nikolakopoulos et al. 2017), indicating that UAV photogrammetry is a reliable and valid method for recording archaeological sites. However, no study has yet tested the accuracy of 3D model creation of small objects (e.g., a footprint) as captured from different flight paths, camera types, recording heights and UAVs in comparison to traditional handheld methods of photogrammetry. A study that addresses these research questions will determine if UAVs can be used to capture small, detailed items that can be precisely reconstructed and are of a high resolution.

2.1.1 Aims and objectives

The overall aim of this chapter was to identify how the shape and size of a track may be affected by external environmental factors prior to fossilisation and post-exposure. Assuming that track degradation produces varying outline metrics with increasing diagenesis, then the need for the rapid recording of tracks is paramount. The optimal data capture methods for recording fossil tracks were tested.

There were two overarching objectives of this chapter:

- i. To quantify the extent that degradation prior to fossilisation and erosional factors post-exposure will affect the shape and size of a footprint.
- ii. To determine the optimal method of recording *in situ* fossil material rapidly and accurately post-exposure.

2.2.0 The effects of erosion on track morphology and preservation

Fossilised hominin track localities have been discovered across Africa, Eurasia, Australia and the Americas (Leakey and Hay 1979; Behrensmeyer and Laporte 1981; Roberts and Berger 1997; Mietto et al. 2003; Watson et al. 2005; Webb 2007; Bennett et al. 2009; Roberts 2009; Morse et al. 2013; Felstead et al. 2014; Aston et al. 2014; Masao et al.

2016; Bustos et al. 2018). In lieu of skeletal material, fossil tracks can be used to infer body dimensions of the track-makers (Bennett and Morse 2014). Numerous fossil and forensic-based studies were conducted that attempted to find a correlation between track measurements (e.g.; forefoot breadth, heel breadth, length, toe extremity length, etc.) and body dimensions, such as stature, body mass, hip height, sex and age (Krishan 2006; Kanchan et al. 2008; Avanzini et al. 2008; Bennett et al. 2009; Dingwall et al. 2013; Domjanic et al. 2015; Hatala et al. 2016c).

For example, stature is often predicted from fossil tracks by assuming that total track length is 15% of stature (Martin 1914). Depending on substrate material properties, track length within a trackway belonging to a single individual can vary substantially. For example, stature and mass predictions from just one trackway from Walvis Bay have estimated that the individual ranged from 1.35 m to 1.73 m tall, with the individual being either malnourished or clinically obese (Bennett and Morse 2014). Evidently, slight variations within a trackway results in grossly variable biometric predictions.

In other locations, such as at Laetoli, Tanzania and Ileret, Kenya, the substrate material properties are much more uniform across a trackway, and biometric data that is extracted is less variable (Bennett et al. 2009). Less variable measurements have resulted in numerous studies utilising these measurements to predict not only biometric data, but also kinematic data (Schmid 2004; Berge et al. 2006; Vaughan et al. 2008; Raichlen et al. 2008; Raichlen et al. 2010; Crompton et al. 2012; Bates et al. 2013b; Dingwall et al. 2013; Bennett et al. 2016a; Hatala et al. 2016b; Masao et al. 2016; Raichlen and Gordon 2017). These studies have allowed palaeoanthropologists to assess evolutionary trends in bipedal locomotion and body proportions.

It has been previously demonstrated that tracks are susceptible to taphonomic changes prior to diagenesis as the result of a number of variables; weather conditions, changes in surface hydrology and/or bioturbation (Marty et al. 2009; Bennett and Morse 2014; Zimmer et al. 2018). After the tracks have undergone diagenesis and have either become exposed or excavated a number of variables can lead to the tracks becoming eroded, thus affecting track shape (Bennett et al. 2013; Zimmer et al. 2018). It must be acknowledged that weather action, such as wind and/or rain, may affect the size and shape of a track in a similar manner that slight variations in substrate typology may affect track production (Marty et al. 2009; Bennett et al. 2013). No studies have yet quantified the effects of degradation on morphology and how this can affect track outline metrics.

2.2.1 Aims

This study aims to quantitatively assess the effects of taphonomy and erosion on track morphology through the assessment of experimental and Holocene tracks. New discoveries of human trackways at Formby Point, UK has offered a unique opportunity to record a set of Holocene tracks as they rapidly eroded.

This study proposes that tracks are at risk of significant morphological change which will alter body size predictions at two stages. The first stage is immediately after track production. The second stage is post-excavation. It is predicted that a delay in events leading to excavation and recording could result in changes in the shape and size of a track, particularly in easily deformable softer sediments which are more susceptible to morphological changes (Bennett et al. 2013).

A selection of experimentally generated tracks were created to assess changes in track morphology prior to fossilisation. Holocene human and animal tracks discovered along the Sefton Coast were also examined to determine if there were any changes in shape or size per day after exposure. It is predicted that the longer a track is exposed, more significant changes in shape and size of the impression will occur. Shape changes are predicted to affect measurements of the foot used to inform upon body size estimates. An improvement on understanding the effects of erosion on morphology will improve the ability to accurately assess body size estimates from future track sites.

2.2.2 Geological and archaeological context

Formby Point is located along the Sefton Coast in Merseyside, England and is characterised by silty, fine-grained sands and peat sediments and sand dunes (Roberts et al. 1996), preserved in unlithified soft-sediments (Roberts 2009; Bennett and Morse 2014). Encroaching coastlines have led to the exposure of numerous ancient sediments since the 1970s, many of which contain over 145 Holocene human trackways and animal tracks along a 4 km stretch of this coastline (Huddart et al. 1999; Roberts 2009). The Formby Point sediments are similar to other fossilised sediment beds at Terra Amata, a site containing a Neanderthal track (De Lumley 1966), and recent sand dune deposits containing potential Neanderthal tracks in Gibraltar (Muniz et al. 2019). The sediments have yielded dates from 6650 ± 700 OSL BP $\sim 3575 \pm 45$ 14C BP (Roberts 2009).

In June 2016 three human trackways were exposed due to wave erosion at Formby Point immersed in over 700 animal tracks. Auroch, roe and red deer, crane bird, wolf/dog, and

beaver tracks were identified (Roberts et al. 1996; Burns, 2016 pers. comm.). The interaction between many animal and human tracks offer a glimpse into Mesolithic human activity.

The Holocene sediment layer was excavated by staff and students of The University of Manchester. Unfortunately, the bed was destroyed in just under two weeks after exposure due to the destructive nature of the high tide. Twice a day the sediment layer was completely immersed by high tide, with the tracks only reappearing with low tide. Visually, it was possible to see the daily erosion of the tracks as the direct result of wave action (Figure 2.1). The sediment bed was unlithified and despite efforts to prevent human and animal interference with the tracks, tidal action still led to the destruction of the bed. Degradation is hypothesised to have resulted in significant morphological change to the shape and size of the tracks.

Holocene tracks have previously been exposed along the Sefton Coast (Roberts 2009), with fossilised tracks appearing at other coastal sites in the UK, such as at Happisburgh, Suffolk (Ashton et al. 2014). These beds containing unlithified tracks were also destroyed rapidly due to tidal action in just two weeks. If this study is successful in determining that morphological changes are paramount in coastal locations, particularly with tracks that are unlithified, then the biometric data that has been previously published from these sites, such as at Happisburgh (Ashton et al. 2014), are questionable. The sediments are variable between Formby Point and Happisburgh, but it is a fair assumption that two soft, unlithified sediments would have reacted similarly when exposed to the same variables: vigorous tidal action and poor weather conditions that resulted in the rapid deformation and subsequent destruction of both beds. It is expected that both sites also experienced changes in footprint morphology coinciding with the rapid destruction of the beds.

The rapid erosion of the tracks at Formby Point have offered a unique opportunity to quantitatively assess the effects of daily degradation on track morphology. If the current study is successful in determining that tracks undergo daily morphological changes, the results will have considerable implications for future studies that assess track discoveries from coastal locations.

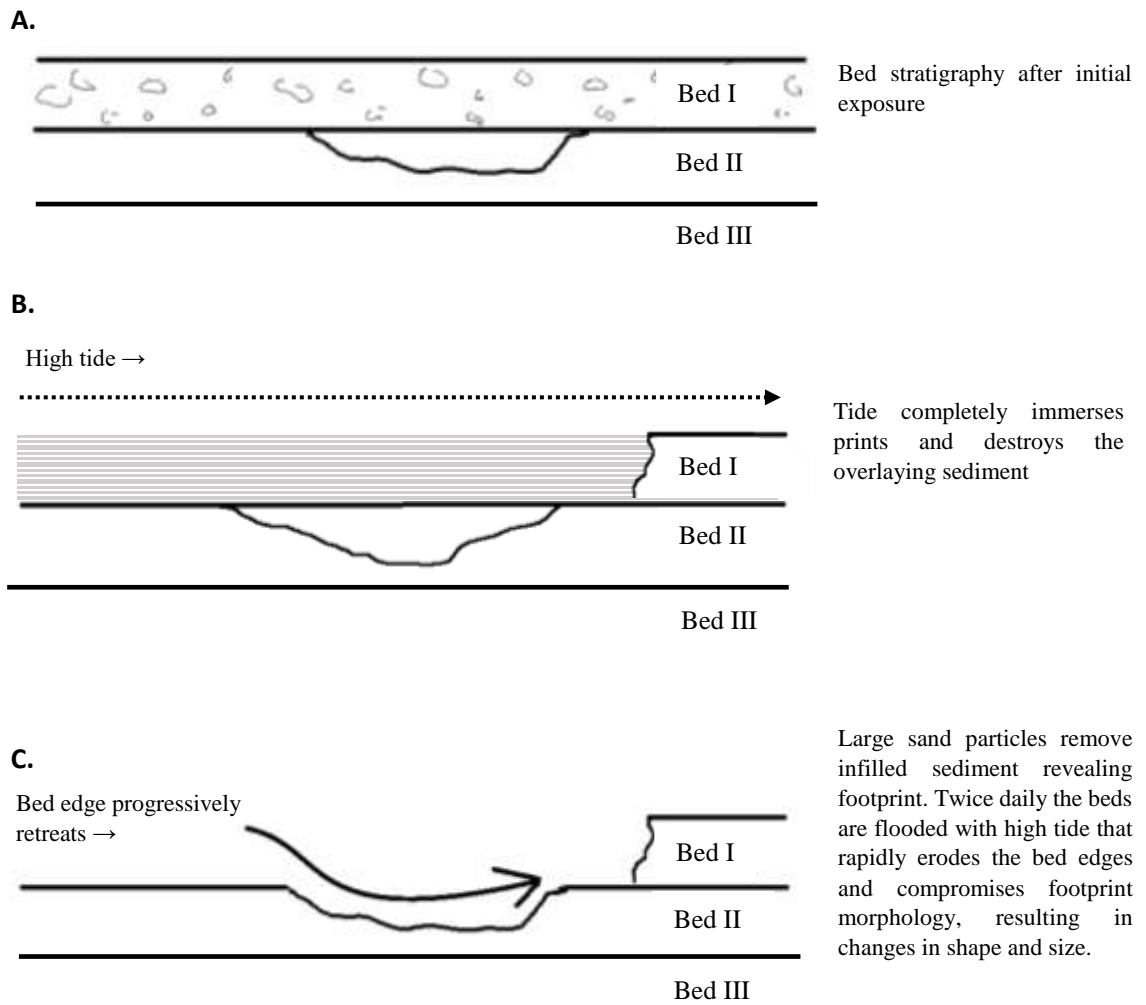


Figure 2.1. Diagram explaining the destructive nature of the high tide. Twice a day the beds were flooded by high tide which resulted in damage to the bed edges and the loss of ~60 cm of the west-facing bed daily. Large sand particles and water eroded the footprint edges resulting in changes in shape and size.

2.2.3 Experimental design

Two experimental tracks contained in one tray were created in homogenous fine-grained sand composed of rounded to sub-angular particles measuring ~0.06-0.7 mm in diameter with ~20% saturation at a 40 mm depth (Figure 2.2). Previous experiments have determined that this is the optimal saturation for track definition, whereby sand composition has no significant effect on morphology after saturation (D'Août et al. 2010; Crompton et al. 2011). The tracks were created inside a container with a drainage system in place. The base of the tray allowed any rainwater that saturated through the overlaying

sediment to drain through to the ground to prevent the tray from flooding. Netting was placed over the tracks to prevent animal interference, but still allowed wind and rain to penetrate through.



Figure 2.2. Set-up of the experimentally generated tracks on the first day of the experiment. Netting was placed over the prints each day to prevent animal interference. Photographs were taken with a DSLR D3300 Nikon camera mounted to a tripod.

The experimental prints were placed outdoors in an open area in Liverpool, Merseyside during winter. During the first 14 days, the weather was dry with low wind speeds and near-freezing temperatures. There was rain and medium-to-high wind speeds during the remaining six days of the experiment. Rain resulted in small dents across the sediment to form. Track features progressively eroded in the final days of the experiment.

These experimental tracks were not created in a material that reflect any sediments belonging to fossilised beds containing tracks. A homogenous material of uniform particle distribution and water content was deliberately selected. The rationale for using this material is to demonstrate that tracks are susceptible to morphological change prior to becoming covered with overlaying material, a process that often leads to fossilisation (Morse et al. 2013). By using this homogenous material, the problem of attempting to replicate sediments from Formby Point, Ileret or Laetoli, etc. was avoided. Any unlithified material (e.g., volcanic ash, fluvial or lacustrine deposits composed of silt, sand or clay of varying material properties) is expected to behave in a similar manner because any material that can be deformed to produce a track with anatomical features will deform as the result of weather action. This must remain an important consideration

when analysing fossilised tracks: any information extracted from the tracks can only be classed as relative information about the track-maker.

2.1.2 Holocene track data collection

Three human trackways were discovered at Formby Point containing a total of 17 complete human tracks of definite ichnology. Due to daily time constraints of the incoming high tide, only one human track was recorded daily and used for this study. It was the longest surviving track before the complete destruction of the bed after seven days. Others were initially selected in addition but were rapidly destroyed after just three to four days, warranting their removal from the dataset. One auroch and two roe deer tracks were also selected (Figure 2.3).

Due to a combination of excavation limitations and bad weather the human footprint was only recorded on four days out of a possible seven days, and the animal prints were recorded on a total of five days. On the seventh day the section of bed containing the human print had completely degraded (Figure 2.3Aiii). The animal prints were destroyed the following day. Because the footprints could not be recorded every day, the greatest morphological changes (i.e., those leading to the destruction of the prints) were potentially not captured.

A DSLR (digital single-lens reflex) D3300 Nikon camera with a macro 60 mm lens of zoom was used to photograph the tracks each day. Due to sporadic weather conditions (a mix of cloud cover and bright sunlight) during each recording period, camera settings were consistently altered to accommodate weather changes using JPG to promote faster data capture time, concurrent with time constraints. The first model of the animal prints was made using a GoPro Hero 4 Silver Edition due to time constraints of the incoming high tide.

2.2.4 Methodology

Photogrammetry is a technique for acquiring geometric information from a selection of photographs captured of an item at various angles to create a 3D object (Falkingham 2012). Photogrammetry was applied to create 3D models of each track daily on the software Pix4Dmapper (v.4.327 Pix4D, Lausanne, Switzerland). Weather conditions during the experiments were consistent with heavy cloud cover. Conditions at Formby Point were mostly very bright, with the ground quite wet, which has visually reduced the resolution for two models by introducing blur as the consequence of capturing reflective

materials. All photographs were taken during dry periods of the day. Model editing was completed using Avizo (v.9.0.1 FEI, Oregon, USA).

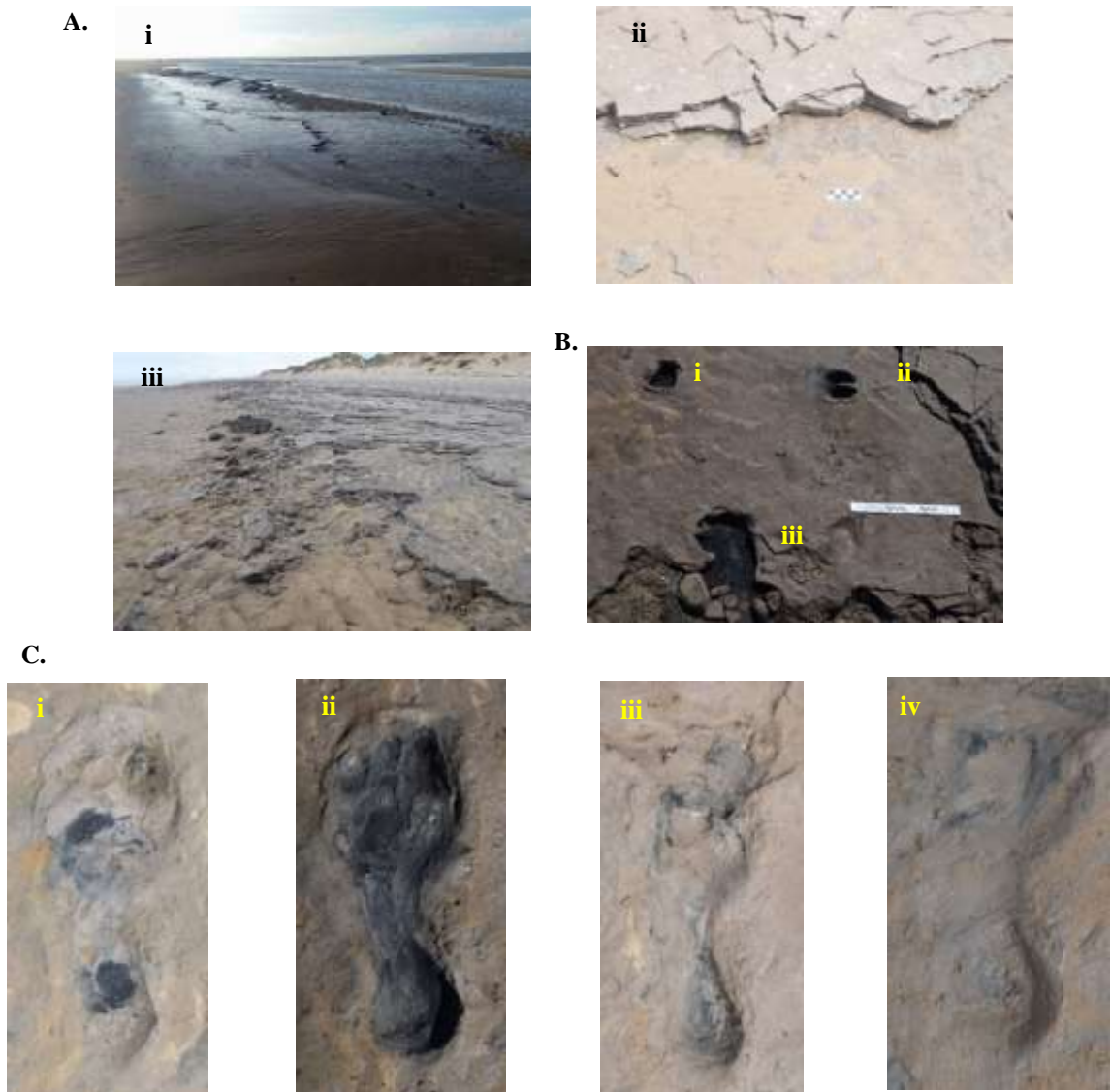


Figure 2.3. (A) High tide completely immersed the bed each day. A.i shows the incoming high tide that later reached on average 8 m high. Overlaying beds were rapidly removed by the tide, revealing lower beds below (A.ii). After repeated tidal immersion, the fossilised beds were destroyed. A.iii shows the bed after just one week. Around 5 m of the west-facing bed was lost in just one week. (B) Photograph of the selected animal prints on the second day. B.i and B.ii belong to roe deer. B.iii belongs to auroch. Note the fragmented posterior region of the auroch print. (C) Photographs of the human print during the four days of recording, with C.i belonging to day one and C.iv belonging to day four.

Track length was calculated by measuring the distance between the most distal point of the hallux and the pternion. The measured length was used to predict stature of the Holocene human print by applying Martin's ratio (0.15), which has repeatedly been found to positively predict stature in modern habitually unshod populations (Martin 1914; Hrdlicka 1935; Dingwall et al. 2013) and has been previously applied at fossilised sediment localities, such as Laetoli (Tuttle 1987) and Happisburgh (Ashton et al. 2014). Robbin's ratio (0.14) (1984) was used for the experimental tracks owing to the track-maker being habitually shod (Bennett and Morse 2014). The validity of stature prediction methods will be extensively explored in Chapter Four. Here, prediction methods were employed to demonstrate that degradation can affect the size of a print. The precision of predicting true track-maker stature was not the aim of this study.

Geometric morphometrics (GM) is a suite of statistical methods employed to measure and compare patterns of similarity and differences in many objects through the process of datum acquisition, processing, analysis and visualisation of geometric information (Bookstein 1991; Slice 2005). These methods allow for morphological changes to be quantified from the statistical application of landmarks (Oxnard and O'Higgins 2009). These techniques were applied in the current study to determine if shape/size change occurs between daily models, and if this is the direct result of coastal erosion. All analyses were computed in R (R Core Team 2017), and two R packages: morpho (Schlager 2017) and geomorph (Adams and Otárola-Castillo 2013).

A total of 44 models were landmarked, representing the experimental prints and the Holocene human print. A further 15 models were landmarked, representing the animal prints. A total of 20 type II landmarks (Bookstein 1990) were used for the human dataset and a total of 10 landmarks were used for the animal dataset (five for the first roe deer print, three for second, and three for the auroch print). Landmarks were digitised as 3D .ply surfaces in Avizo 9.0.1 by the same researcher (Figure 2.4).

To test for consistency in landmark digitisation landmarks were placed daily by the same researcher on one model each for all prints included in these assessments over a period of ten days. A Generalised Procrustes Analysis (GPA) was computed, which translates and rotates each homologous landmark to the origin, whilst scaling to unit-centroid size (CS) (Zelditch et al. 2012). The resulting Procrustes distances between each landmark consensus with the mean landmark configuration were calculated and then divided by the number of repeats (Slice 2005; Zelditch et al. 2012). This process provided the error estimate (Type I error rate of 5%) for landmark placement within a 95% confidence

interval. Mean values (Procrustes distances) over 0.05 specified that the distance between a landmark and the overall consensus was high and that the landmark is non-replicable (Profico et al. 2017). All mean values lower than 0.05 indicated good repeatability in landmark placement. All landmarks were found to be homologous between each daily model, permitting the following assessments to be conducted.

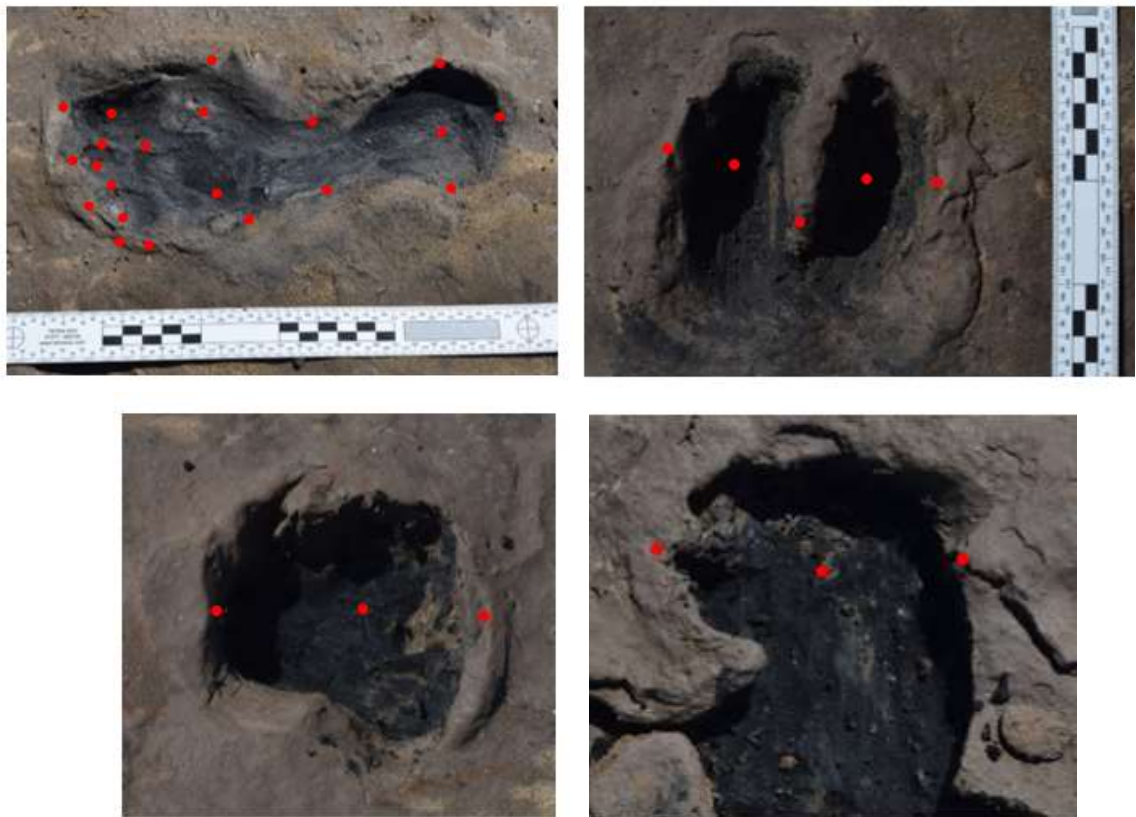


Figure 2.4. Landmark datasets for the human prints and animal prints. A lack of homologous landmarks in the animal dataset has resulted in a reduced landmark dataset. It is expected that landmark homology will be reduced with daily erosion, and that it will be difficult to place landmarks after features have been progressively eroded.

Prior to any GM applications, the depth of four landmarks were calculated for all experimental and Holocene human prints: the medial and lateral forefoot region at the deepest points, and the medial and lateral heel at the deepest points. Two landmarks were used for heel depth because the heel base was uneven and did not form a typical u-shape (Hatala et al. 2018), but rather a w-shaped base. The depth of these landmarks are expected to change, corresponding to increased degradation of the footprint. The landmarks that synthesised the most concave points on the medial and lateral heel and

forefoot were used to calculate the linear distance across these region. Depths were thus measured using simple trigonometry (the cosine rule) for all prints.

A GPA of all landmark configurations was performed (Zelditch et al. 2012). These configurations were all aligned to a single reference specimen, representing the mean shape (Gower 1975) within Kendall's shape space (Kendall 1984). Shape variation was assessed by a Principle Components Analysis (PCA), which is a non-parametric statistical technique used to examine the relationship between a set of variables by calculating the maximum distance between each individual landmark (Bookstein 1991). Each Principle Component (PC) was examined to determine shape variability (Bookstein 1990). Shape changes were visualised by non-affine partial warp grids called thin plate spline (TPS) (Rohlf and Splice 1990). A TPS permits for the visual representation of relative shape deformation and displays landmark transformations which maps a set of GPA-aligned configuration of landmarks between a set of structures, with the grid lines representing the relative amount of bending energy between each landmark (Rohlf and Splice 1990). TPS grids were not created for the animal prints due to a reduced landmark dataset. An ANOVA was computed to assess the relative amount of shape variation per day (Dryden and Mardia 1998). Results were supported by a pairwise test that determined which variable(s) influenced shape variation (Zelditch et al. 2012).

Categorical variables were created for each landmark configuration to assist in assessing the causes of shape change. By adopting the use of categorical variables in the dataset, information about the tracks – such as the sudden appearance of holes in the surface as the direct result of rain – were included in the analyses. Their inclusion in the dataset assigns each configuration of landmarks to a group, allowing for groups to be statistically compared. For example, group one contains two variables: the presence or absence of raindrops. This group were then statistically compared with the second group whereby the configurations were assigned a variable stating if the track has experienced a reduction in height of the landmarks relative to landmark height on day one. Subsequently, it was possible to determine if rain action has resulted in the reduction of landmark height and if these variables have cumulatively resulted in changes to the shape and size of a track.

Two categorical variables were developed for the experimental prints. The first described the presence of rain drops in the bed that left small dents in the sediment towards the end of the experiment. The second described the reduction in height of several landmarks in the forefoot region, corresponding to degradation. Two categorical variables were created

for the animal prints: the presence/absence of toe ridges in the roe deer and the severe erosion of the posterior border of the auroch footprint.

Two categorical variables were established for the Holocene human dataset: the grade of footprint degradation and depth. Two grades were established for degradation: the presence and absence of the forefoot region. Track depth was measured at five separate points across the foot. Two grades were established for depth based upon the significant reduction in hallux depth relative to an increasing heel depth. This is split between the first two days and the final two days for the Holocene print.

The relationship between footprint degradation and size was assessed by regressing log-CS to the first PC (Cooke and Terhune 2014). Because this study wanted to identify the association between erosion with that of shape and size changes in a track, only the PC that explained the majority of shape change was examined. Levels of significance were computed by permutation tests to a 95% confidence level, using 1000 permutations which tests the sampling distributions (Bookstein 1991). Finally, morphological disparity tests were computed to perform a pairwise comparison between-groups (Zelditch et al. 2012).

2.2.5 Results

Morphological change prior to fossilisation (experimental prints)

Foot length was calculated for each model (Table 2.1), with stature being predicted using Robbin's ratio (Robbin 1984) as the track-maker was habitually shod. Here, prediction methods were employed to demonstrate that degradation can affect the size of a print. The precision of predicting true track-maker stature was not the aim of this study, but will instead be refined in Chapter Three. Different statures were produced using Robbin's ratio for the models representing the final two days of the experiment. Foot length increased as much as 6.02%.

PCA of the experimental prints over a period of 20 days revealed that shape variance can be explained by the first two PCs that account for >84.6% of total variance (Figure 2.5; Appendix B). The first two axes (PC1 and PC2) can be cumulatively summarised as accounting for the observations previously identified in the creation of the categorical variables: the reduction in height of the toe ridges (identified in PC2) and the appearance of numerous holes as the direct result of rain/weather (identified in PC1). The maximum (PC1+) and minimum (PC1-) shape difference indicates that changes in foot length are associated with poor weather conditions, with an increased distance between anterior and

posterior landmarks as ridges become shallower and less convex, as supported by the loss of topographical height highlighted in the TPS grids (Figure 2.5).

As expected, weather action has cumulatively resulted in changes in shape/size of the footprint (according to PC1) and changes in footprint depth (according to PC2). This is characterised by the strong separation of negative PC scores for the final two days of the experiment and positive PC scores for the first 18 days of the experiment. The least displacement for both the experimental prints occurs in the heel region, with shape remaining almost static with increasing degradation (Figure 2.5).

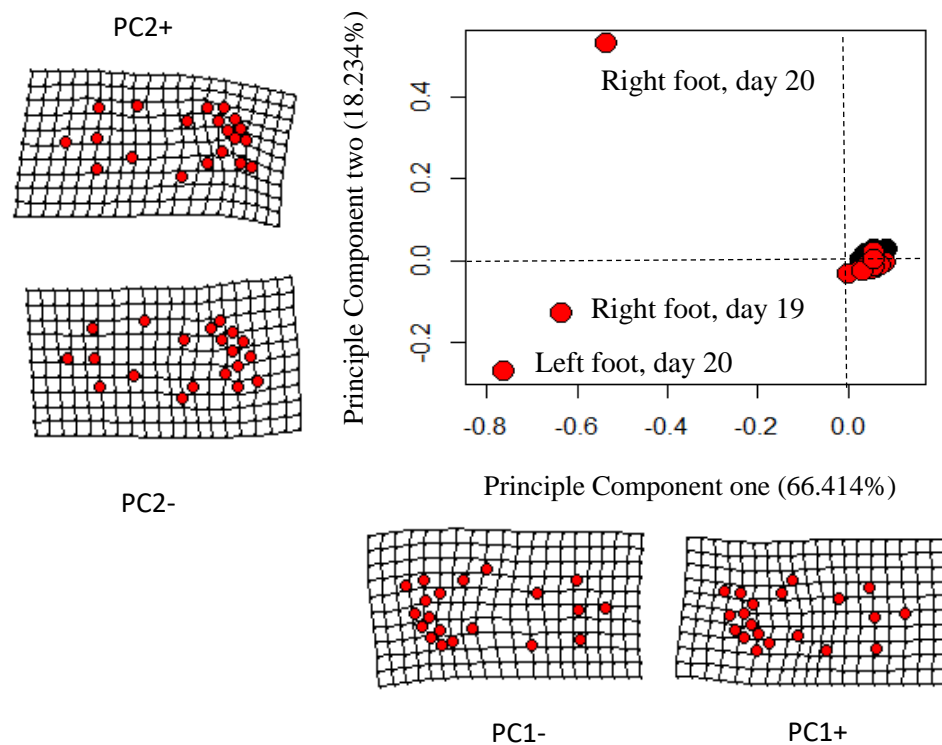


Figure 2.5. PCA graph illustrates the shape change in the experimental tracks along PC1 and PC2. Black dots represent the experimental prints before weather damage. Red dots represent the presence of rain damage. TPS grids display the maximum and minimum relative shape changes along each PC axis.

Table 2.1. Foot length measurements (cm) of the experimental tracks and predicted stature (Robbin 1984). Percentage change difference in foot length values from the first day were calculated. Model numbers correspond to the day that the model was made.

	Model	Foot length	% change in foot length	Predicted stature
Left foot	1	21.59	/	154.24
	2	21.46	0.62%	153.29
	3	21.37	1.06%	152.61
	4	20.64	4.40%	147.45
	5	20.56	4.78%	146.86
	6	20.99	2.80%	149.92
	7	20.54	4.87%	146.74
	8	20.30	6.02%	144.96
	9	20.79	3.74%	148.47
	10	20.98	2.86%	149.84
	11	21.21	1.76%	151.52
	12	21.32	1.26%	152.29
	13	21.62	-0.13%	154.44
	14	21.65	-0.25%	154.63
	15	21.59	0.01%	154.22
	16	22.96	-6.32%	163.99
	17	22.20	-2.79%	158.55
	18	22.07	-2.20%	157.63
	19	22.19	-2.76%	158.49
Right foot	1	22.12	/	157.98
	2	21.84	1.26%	155.99
	3	21.35	3.46%	152.51
	4	21.32	3.58%	145.17
	5	20.84	5.77%	148.86
	6	20.97	5.20%	149.76
	7	21.06	4.77%	150.44
	8	21.70	1.89%	155.00
	9	22.60	-2.20%	161.45
	10	20.89	5.54%	149.22
	11	21.16	4.34%	151.13
	12	21.28	3.80%	151.97
	13	21.41	3.19%	152.94
	14	21.91	0.93%	156.51
	15	22.38	-1.19%	159.86
	16	22.94	-3.74%	163.89
	17	23.42	-5.89%	167.28
	18	22.15	-0.16%	158.23
	19	22.36	-1.08%	159.69

To analyse if the degradation affected print size, shape variability (assessed by using PC1) was regressed against log-CS for all tracks (Figure 2.6). Results indicated that size was significantly affected by degradation in the final two days of the experiment and that the null hypothesis can be rejected, and that there is a statistically significant difference in shape and size between the models, as shown by a one-way ANOVA. This is corroborated by the change in length and in foot width as the direct result of rain. Shape change has a significantly strong association with log-CS ($R^2=0.575$; $P=0.002$) and a weakly positive correlation with weather action ($R^2=0.223$; $P=0.002$).

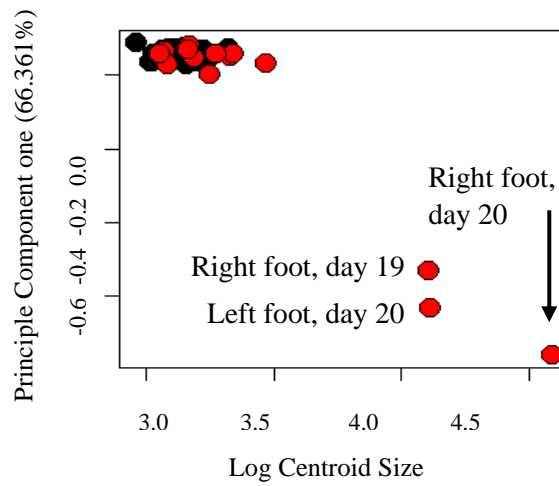


Figure 2.6. Linear regression establishing the positive relationship between log-CS and shape of the experimental prints, as explained by PC1. Red dots represent the presence of rain damage, which increased in the final two days of the experiment. Black dots represent the experiments before weather damage, which are clustered in the graph.

A morphological disparity test found that shape changes were only significantly affected by weather in the final six days of the experiment with the severe degradation of the toe ridges ($P=0.004$) and the increased presence of raindrops ($P=0.002$). No statistically significant shape/size change occurred in the first 14 days of the experiment when weather remained dry. The null hypothesis can be rejected as there is a significant association between weather and shape changes.

Morphological change after exposure/excavation (Holocene human tracks)

Upon visual inspection, it was clear that all of the Holocene tracks selected displayed the collapse of key features of the tracks. The human track suffered severe degradation in the

forefoot, the roe deer prints lost toe ridges, and the auroch print, which was located on the edge of the sediment bed, progressively lost the posterior region of the print each day alongside the erosion of the bed edge. If the bed had been discovered during the final two days of exposure it is questionable whether the tracks would be identified as human or animal, because the hollows that remained resembled bed damage, rather than tracks.

Foot length was calculated for each model (Table 2.2). As expected, four different foot length measurements were generated, although the variance between day one and day two is only 3.8 mm and is not deemed significant. Measurements from the final two days are quite different. The tip of the hallux is still easily distinguishable in the day three model, although the ridge is much less prominent. In day four a more inferior point has been identified as the tip of the hallux, although it was roughly 1 cm shorter than the first two days, and 2 cm shorter than the third day. Evidently, a large margin of error exists in determining track extremities after prolonged exposure. Distinguishing track borders has been previously documented to be difficult (Falkingham 2016), but this is the first study to quantify the inability to identify these borders with increasing erosion.

Stature was predicted using Martin's ratio (Martin 1914) (Table 2.2). Different statures were produced in accordance with varying foot length, with the percentage increase in foot length increasing as much as 6.47% with erosion.

Table 2.2. Foot length measurements (cm) and the predicted stature. Percentage change difference in foot length values from the first day were calculated.

Day	Foot length	% change in foot length	Predicted stature
1	24.64	/	164.26
2	24.64	± 0.01%	164.28
3	25.75	+ 4.42%	171.68
4	23.11	- 6.47%	154.05

PCA of the Holocene human track revealed that shape variance can be explained by the first two axes that account for more than 81% of total variance (Figure 2.7; Appendix B). The first axis can be surmised as describing the significant degradation of the forefoot region and the collapse of ridges between the second to fifth metatarsals that are prominent in the first two days only – these observations were previously identified

during the creation of the categorical variables and have thus informed on the major shape change of the Holocene track. The forefoot region becomes flat (supported by a loss of depth; Table 2.3), with no clear identifiable structures. There are two exceptions: the hallux and the ridge surrounding the extremity of the fifth digit. This is characterised by the strong separation of individual PC scores, represented by negative PC scores for the first two days and positive PC scores for the final two days that the track was recorded. This division was emphasised by the dotted line along the PC1 axis (Figure 2.7).

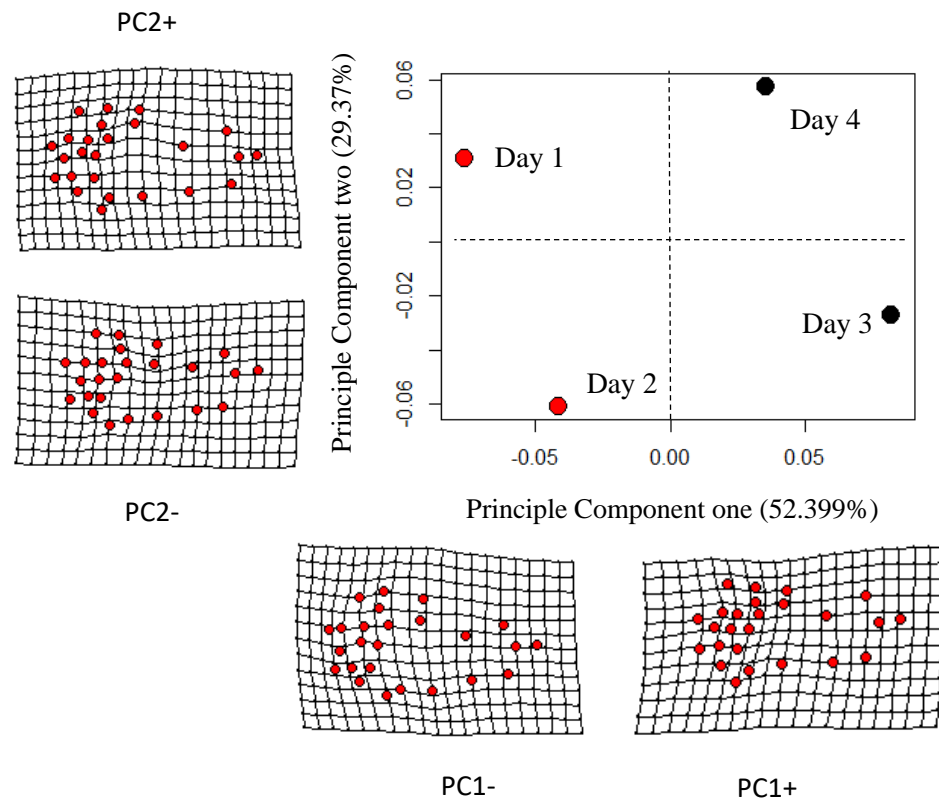


Figure 2.7. This PCA graph illustrates the shape change in Holocene human track. Red dots represent the presence of the forefoot. Black dots represent the severe degradation of the forefoot. TPS grids display the maximum and minimum relative shape changes along each PC axis.

Variation along PC2 described changes in depth of the footprint as a whole. The depth (i.e., landmark heights) of the hallux decreases by 87.7% relative to the heel, which decreases in depth by 52.5% (that is, the heel becomes shallower as the track borders progressively erode). The depth of the lateral foot (second to fifth metatarsals) is found to decrease by 41.1%. The region under the first metatarsal decreases in depth by 27.1%

during the first two days then increases in depth by 65.8% relative to the loss to the lateral border of the foot by the final day. The midfoot region (area lateral to the medial arch) only decreases by 10.3%, displaying the least amount of depth and shape variance across the track.

Table 2.3. The depth of the Holocene human track at five separate locations taken from each model. Long axis of the foot is defined as a line from the second digit passing through the midline of the foot to the pternion. Measurements are in mm.

	TIME			
	Model 1	Model 2	Model 3	Model 4
Depth of hallux	15.345	14.286	2.657	1.894
Depth of long axis	19.207	12.092	11.399	11.324
Depth of first metatarsal	11.549	8.410	10.032	13.939
Depth of midfoot	6.423	6.483	8.004	5.766
Depth of heel	12.114	16.103	17.666	18.481

The shape differences depicted reveal that track shape can be warped into two different shapes, per the forefoot region (the categorical variables). The maximum (PC1+) and minimum (PC1-) shape difference along PC1 indicates that the forefoot region became much more constricted as erosion increased, with a reduced height and a reduced amount of bending energy (PC1-) between each landmark. A likely cause in this displacement may be the degradation of numerous distinguishable features in this region and a reduction in the height of numerous landmarks. Similarly, the most obvious shape changes along PC2 in the experimental tracks occurred in the forefoot region, explaining a reduction in the height of the toe ridge landmarks as the ridges were slowly eroded.

The most obvious shape change along PC2 would appear to be around the head of the metatarsals. This area seems to be wider between PC2+ and PC2-, with the landmarks characterising the medial border of the foot being stretched relative to the lateral border of the foot. This area became much less distinguishable during the last two days making this the likely cause in this displacement. The loss of the medial ridge may further explain this shape variance. This is further corroborated by the depth test which found this area lost considerable depth relative to the medial border of the foot.

A morphological disparity test found that shape change is significantly correlated with changes in size ($P=0.004$) and with depth also significantly affected ($P=0.005$). CS is very weakly correlated to changes in depth ($R^2=0.007$). A poor R^2 value may be explained by a reduced dataset ($n=4$). Therefore, the null hypothesis regarding depth cannot be rejected as a positive association could not be established. Similarly, a pairwise test was computed to establish the amount of shape change relative to footprint depth. The null hypothesis cannot be rejected as the interaction between depth and shape/size was not found to be significant ($P \geq 0.05$).

Morphological change in the Holocene animal tracks

Shape change of the animal prints can be explained by the first three PCs that account for more than 97% of total variance (Figure 2.8; Appendix B). The first axis can be summarised as describing the degradation of the auroch print, which was discovered at the edge of Bed III. By the second day, half of the print had completely disappeared, with the lateral and medial edges of the track progressively eroding until its complete disappearance on the fifth day. By the third day it was no longer identifiable as a print. The loss of identifiable features of this print has resulted in the strong separation of individual PC scores along the first axis, represented by negative PC scores for the first two days and positive PC scores for the last three days.

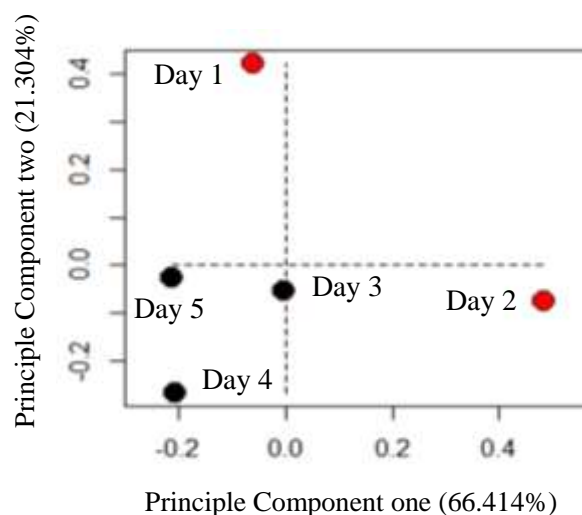


Figure 2.8. This PCA graph illustrates the shape change in Holocene animal tracks. Red dots represent the first two days of recording. Black dots represent the last days of recording when the auroch print became severely degraded.

Shape change along the second axis can be summarised as describing relative changes in depth. With the loss of the toes the base of the prints became less convex. This loss is more evident on the fifth day, represented by negative PC scores for the first two days and a positive PC score for the final day. Variation along the third and fourth axes cumulatively describe changes in the loss of toe ridges in the roe deer tracks. The ridge between the medial and lateral toes had completely vanished by the fourth day. The borders of one of the roe deer prints are no longer undercut but are shallow and slanted. This results in a considerable lack of distinction of internal morphology.

2.2.6 Discussion

Taphonomic changes to track morphology prior to diagenesis

GM methods were applied to quantitatively assess the effects of erosion on track morphology and to assess if degradation affects body proportion estimates. One Holocene human track, two experimental human tracks and three Holocene animal tracks were selected to be recorded daily (n=59). This study was testing the hypothesis that track morphology will change in shape and size prior to fossilisation and post-fossilisation and subsequent exposure. It was predicted that prolonged exposure will significantly affect measurements taken of the foot, thereby decreasing the accuracy of biological inferences.

It has been previously demonstrated that tracks undergo significant taphonomic processes prior to burial and diagenesis (Marty et al. 2009), that may alter the shape of a track thus affecting any inferences extracted, such as body proportion predictions (Bennett and Morse 2014). However, to date, no study has quantified morphological changes due to taphonomic processes and how these changes may affect body proportion predictions.

The results from the current study demonstrate that significant morphological changes may occur in softer sediments prior to diagenesis, concurrent with weather conditions. Shape and size will change significantly after rainy periods or high wind speeds. These shape/size changes affect measurements taken of the foot (length has been used in this study as an example), thereby producing inaccurate predictions of stature. Although not the focus of this study, it can be assumed that other biological predictions will vary greatly if a track is exposed to adverse weather conditions prior to fossilisation. While the current study has only focused on weather action as a taphonomic variable, it is a fair assumption to say that other taphonomic processes such as bioturbation, will also affect morphology. External factors that may affect footprint degradation were not standardised (i.e., rain and

wind were not controlled variables) because this study wanted to provide a realistic representation of erosional processes. Future studies could offer a more mechanistic approach to provide a comprehensive insight into track degradation and how erosional processes can affect the information that is extracted from a track.

The results of the current study have considerable implications for the human evolution fossil record: how accurate are previously published body proportion estimates of fossil tracks? As previously stated, by analysing the morphology of a track, numerous inferences can be made. For example, foot parameters (such as using foot length to predict stature and foot index to predict body mass) were used in conjunction with contemporaneous skeletal data from north-western Europe dated to 950-850 Ka to assign *Homo antecessor* as the maker of the Happisburgh tracks (Ashton et al. 2014). Taphonomic processes, such as changes in surface hydrology or even bioturbation, after track creation may have affected the shape and size of the Happisburgh tracks, thus altering taxon assignment and body proportion predictions. Similarly, taphonomic processes of the tracks from either Laetoli or Ileret may have resulted in the hominin body proportion estimates being under- or over-estimated.

It is suggested that sediment beds should be inspected for evidence of weather damage, particularly in softer lithified sediments in future fossilised bed discoveries as the surface area may have been exposed for several days prior to fossilisation, with a potential loss of information. In particular, a palaeoanthropologist should inspect the sediment bed for rain drops.

Morphological changes to a human track after exposure/excavation

After a track has become covered by overlaying sediment and has begun the process of diagenesis and subsequently exposed, the impression is susceptible to significant changes in shape and size, thereby affecting body size estimates. An example of how degradation can affect track inferences can be found in the high variance of predicted stature values presented in the current study. The first 3D model was created just under a week after the track was first exposed. The rapid degradation of the track after this point has significantly affected stature predictions. Shape change during the first two days is miniscule, and any analyses and subsequent results would not have produced drastically different results. As such, foot size and subsequent body size estimates can be reliably predicted in the initial few days of exposure, assuming that minimal change occurred as a result of taphonomic processes prior to diagenesis. Prolonged exposure after excavation has significant

implications for extracting reliable data. This problem is not unique to Formby Point, it was paramount during the excavations at Happisburgh. The Happisburgh tracks were also found on the coastline and were destroyed rapidly due to tidal action (Ashton et al. 2014). Any delay in recording the tracks may have resulted in stature and mass values that are not true representations of the Happisburgh hominins.

This has considerable implications for other track sites. The Ileret, Kenya tracks are the oldest tracks attributable to the genus *Homo* (Bennett et al. 2009), and are thus of great scientific importance. The sediment bed containing the trackways are composed of fine-grained silt and sands that are unlithified and highly erodible (Bennett et al. 2013). These sediments are quite comparable to the fine-grained sand and peaty sediments from Formby Point. Similarly, the Ileret trackways are at threat of flooding and storm action (Bennett et al. 2013) – two variables that are somewhat comparable to the Formby Point sediment beds. With the exception of changes in water salinity (Formby Point is characterised by salt-water immersion and the threat of flooding at Kenya relates to non-saline lake inundation), the variables highlighted in the current study are applicable to the highly-erodible Ileret tracks. Fortunately, the Ileret trackways were covered post-excavation to geo-protect the trackways (Hatala et al. 2017). However, if the trackways are exposed for excavation or geo-tourism during periods of stormy weather or flooding, it is expected that the tracks will undergo significant morphological change that may affect the interpretation of the track-makers.

The Laetoli, Tanzania trackways were formed in natrocarbonatite ash (Leakey and Hay 1979) and are partially lithified, meaning that these tracks are more robust and firmer than the unlithified trackways from Ileret (Bennett et al. 2013). It is expected that the Laetoli sediments will be less-susceptible to morphological changes as the direct result of wind or rain action, due to much firmer substrates. However, the threat of degradation as the direct result of exposure is not redundant. It is expected that any material that is not fully lithified and preserved will undergo significant changes in shape and size due to a number of external factors. Care should be taken for the immediate preservation of tracks of high interest, such as the Laetoli trackways. Without preservation, a print will continue to be subjected to considerable morphological change, and eventually may be unrecognisable. This occurred with the human print at Formby Point. Due to the severe degradation in the forefoot region in the Holocene human track, it is questionable as to whether the track would be declared human, if discovery was delayed. If it had been declared human, remarkable differences in track measurements would have been made. These

measurements are used to determine body size estimates (age, sex, mass and stature). Any inferences or estimations that could be calculated from these measurements taken in the final few days would have changed drastically from those made in the first day.

Happisburgh is a prime example of severe degradation hampering ichnotaxonomy. Numerous hollows were excluded in the analyses of the Happisburgh tracks due to questionable ichnology; only 14 tracks out of a total of 152 could be definitively declared hominin (Ashton et al. 2014). These hollows could be remnants of hominin tracks whereby only the heel and border of the impressions – the deepest regions that are preserved the longest – have survived, as observed at Formby Point (Figure 2.7). Alternatively, the hollows could be eroded animal tracks. Tidal erosion and a delay in recording these prints that potentially belong to an extinct *Homo* species may have resulted in a considerable loss of data.



Figure 2.9. Comparison of hollows from Happisburgh (left) and Formby Point (right). Many of the hollows from Happisburgh that were disregarded by Ashton et al. (2014) that have questionable ichnology could have been identified as hominin if a delay in recording had not occurred. The photograph from Formby Point was taken on the penultimate day of excavation. The red highlighted tracks were previously identified as human, but on this day appeared as oval hollows with no distinctive features. Photo credit: Photograph of Happisburgh sediment bed by Simon Parfitt, May 2013.

The results from the current study are a prime example of how rapidly a track can degrade. Within two weeks the Formby Point Holocene sediment bed had completely vanished. During this time, one of the human trackways had completely eroded, with only one very deep trackway remaining *in situ*. The track that formed the basis of this study lay towards the west of Bed II and was the first track to be immersed by high tide. By the end of the

first week Bed II had completely eroded, revealing another bed below. Bed III (towards the north) was the final bed to disappear. Severe erosion in Bed III by end of the week made 3D modelling impossible due to the numerous pockets of water that remained during low tide. The rapid degradation of these tracks has demonstrated the pivotal need for digital recording for the preservation and future scientific investigation of these fragile fossils.

Morphological changes to animal tracks after exposure/excavation

In the current study, it was demonstrated that the Holocene animal tracks also experienced a significant change in shape and size as the direct consequence of weather action. The roe deer tracks, which were deeply pressed, exhibited no significant change in shape nor size (except for the toe ridge region). This implies that lightly pressed tracks are more susceptible to degradation. Prolonged exposure will affect track definition and depth.

The complete loss of the posterior region of the auroch track from Formby Point further raises questions regarding ichnology. By the second day, the track would have been identified as sediment damage, rather than an extinct species of cattle. Although not the focus of the current study, the auroch trackways provide a unique opportunity to study the gait dynamics of an extinct animal that would have been lost if the Formby Point tracks were not rapidly recorded. Similarly, the delayed excavation at Happisburgh resulted in numerous damaged tracks – poor anatomical definition has resulted in many of the Happisburgh tracks not being assigned to any taxa (Ashton et al. 2014) – being unidentifiable and rightly excluded from analyses. However, the loss of this data may have resulted in a lost opportunity to identify an extinct species of animal present in Britain during MIS 21/25.

Fortunately, better preservation resulted in the identification of numerous animal hollows within the Laetoli trackways, representing a range of extinct Pliocene species within the carnivora, equidae, suidae, and bovidae mammalian orders (Leakey and Hay 1979). However, taphonomic and/or post-excavation erosion of these tracks may have resulted in a warping of anatomical features. A loss of this data may have resulted in the incorrect ichnotaxonomy of the tracks, or unreliable biological data of the species.

While rapid recording is recommended in order to extract the most reliable data, it must be acknowledged that taphonomic changes may have occurred prior to diagenesis, resulting in a loss of reliable data. Tracks that display poor anatomical features are

concluded to be unreliable. Tracks that are deeply pressed, with clear anatomical details will undergo insignificant morphological changes in the period immediately after exposure. It is expected that clearly defined tracks will be the most reliable to inform on the track-makers.

2.2.7 Remarks on the effects of diagenesis in track morphology

By applying GM techniques, it was possible to identify the effects of erosion on track interpretation, particularly in softer sediments. The use of statistical techniques created a fundamental tool for the evaluation of track erosion. Results show that weather action can result in significant morphological change to a track prior to and after fossilisation. If a surface is free from weather damage, which can be assessed visually, it may be assumed that there has been no significant loss of reliable data prior to fossilisation. After fossilisation and exposure, a track will undergo considerable morphological change directly associated with weather and coastal activity. Morphology was not found to be significantly affected in the first few days after initial exposure, necessitating the need for rapid recording to provide the most accurate results, particularly in highly erodible substrates. It is recommended that inferences made on tracks that have a questionable time frame of exposure should be treated with caution. By creating high resolution 3D models rapidly these fragile fossils were digitally preserved for further analyses.

2.3.0 The need for non-invasive recording methods: The applicability of UAV technology for recording fragile fossils *in situ*

As demonstrated in section 2.2, there is the need to rapidly record archaeological remains that are at risk of destruction, with a delay in recording resulting in modelled tracks that may have unaccounted-for error in both outline metrics and tracks depths (Wiseman and De Groote 2018; Zimmer et al. 2018). If the excavator records these remains by hand there is often the risk of inadvertently destroying the fossils by accidental trampling, as documented during fieldwork at Formby Point, UK in 2017, and by other studies that have recognised track degradation at Engare Sero, Tanzania (Zimmer et al. 2018).

At Formby Point in winter 2016-2017, a new sediment bed containing additional Holocene tracks was extremely saturated as the direct result of repeated salt water immersion by the high tide. Poor winter weather conditions prevented the sediment bed drying through periods of exposure. The sediment bed, which was composed of

unlithified soft silts and a high salt water composition, was very soft and deformable. Consequently, the excavation team were inadvertently leaving their own impressions behind on the sediment bed which destroyed underlying tracks in the bed directly below. Furthermore, the sediment bed was located on public land with ease of access by members of the public. Consequently, the Holocene tracks were destroyed by modern human and animal (primarily horse and dog) trampling. This identified the need to use a recording method that can remove the excavator from the locality, whilst also rapidly recording the tracks before damage can occur.

Advances in cost-effective 3D model creation have pioneered methodological approaches to analysing fossilised remains. However, exposed and erodible sites where fossil extraction can be difficult often warrants the need to record fossils *in situ*. Often, these fossil sites can be large. For example, the sediment beds at Formby Point can often be $>100\text{ m}^2$, necessitating the need to identify a recording method that can quickly and efficiently capture data.

UAVs offer a non-destructive and non-invasive method to record an area of interest quickly (Achille et al. 2015; Fernandez-Hernandez et al. 2015; Guerrieri and Marsella 2017; Campana 2017). A UAV is a remotely controlled unmanned aircraft with a platform allowing the attachment of a recording device (Pajares 2015), such as a camera for photogrammetric purposes. Multi-rotor UAVs offer a considerable advantage over more traditionally used methods of aerial photography in cultural heritage (Smith et al. 2014), such as recording equipment attached to kites or balloons (Mozas-Calvache et al. 2012; Nikolakopoulos et al. 2017). UAVs typically have a larger range, can be used in a greater variety of weather conditions and can be manually controlled to target specific areas of interest (Dell'Unto 2017), thereby removing the excavator from site to minimise damage to the fossil interface whilst rapidly recording the research area.

However, capturing sufficient data via aerial photogrammetry is problematic. Occlusion is a well-documented issue in UAV applications whereby (1) overlaying objects will prevent the data capture of underlying objects or those in close proximity and/or (2) the shape of an object may hinder the capture of the full object through a process called self-occlusion (GIM International: Oblique Airborne Photogrammetry, 2014). Self-occlusion causes parts of the object boundaries to become 'lost' in the 3D model as the deployed flight path and chosen method of recording inadequately captures the required ~80% overlap of photographs necessary to reconstruct a 3D model via photogrammetry.

This is a common occurrence in archaeological research whereby complex sites inhibit a comprehensive 3D model to be captured. To circumvent this issue, one study used a combination of LiDAR technology and Structure from Motion photogrammetry to capture the complex archaeological remains of the city of Dedan, Saudi Arabia (Smith et al. 2014), producing a somewhat ‘complete’ model with little sparsity in the dense cloud reconstruction. The accuracy of the 3D model and the full extent of occlusion which may have prevented the reconstruction of minute features (e.g., the stone wall interface of each building/structure) was not reported.

Another study tested photograph overlap via various methods of aerial photogrammetry as deployed by single-rotor UAV and Remote Piloted Vehicles in Piedmont, Italy (Chiabrando et al. 2011). The study aimed to map a large historical landscape via various methods to identify the best practise for aerial photogrammetry and to investigate the extent of occlusion in data capture. Severe rates of occlusion were identified during the flights (only 28.3% of data points were matched), even at low altitude data capture. Edge reconstruction in the areas around the walls (e.g., the detailed brick overlay) were mostly lost (Chiabrando et al. 2011).

The Piedmont study utilised a single-rotor UAV (Chiabrando et al. 2011). A multi-rotor UAV has a compelling advantage over single-rotor UAVs as the user has significant command over the positioning and movement in comparison to the single-rotor, thus permitting greater control over the framing of data capture. The inclusion of a multi-rotor UAV in the Piedmont mapping study could have resulted in improved photograph overlap, thereby reducing the issue of occlusion.

However, the needs of the collected 3D model in any site will depend on data capture ‘efficiency’. The researchers at Piedmont, Italy (Chiabrando et al. 2011) sought to map the archaeological terrain, like the research in Dedan, Saudi Arabia (Smith et al. 2014). The produced models were sufficient for the requirements of the respective studies, whereas the comprehensive reconstruction of intricate details, such as the brick overlay patterns, were not the target.

With recent technological advancements and applications in UAV technology (Sauerbier and Eisenbeiss 2011; Rinaudo et al. 2012; Nes and Remondino 2014; Achille et al. 2015; Guerrieri and Marsella 2017; Campana 2017; Bergstrom et al. 2019) it is questionable as to whether a UAV can be used to record smaller, intricate details with high resolution, such as a fossil track, if considerable care is given to a number of parameters; camera

selection, designed flight path and camera positioning (Bemis et al. 2014). Fossil tracks are negative impressions in the ground susceptible to erosion and/or destruction by the excavation team (Wiseman and De Groote 2018; Zimmer et al. 2018). The use of a multi-rotor UAV will remove the researcher from the locality thereby minimising damage to the fossil interface. A multi-rotor UAV will also offer a considerable advantage over traditional aerial methods of photogrammetry to digitally record footprints by theoretically manoeuvring the deployed camera into an optimal position(s) to capture adequate photograph overlap of the complex internal structure of a track (Figure 2.10).

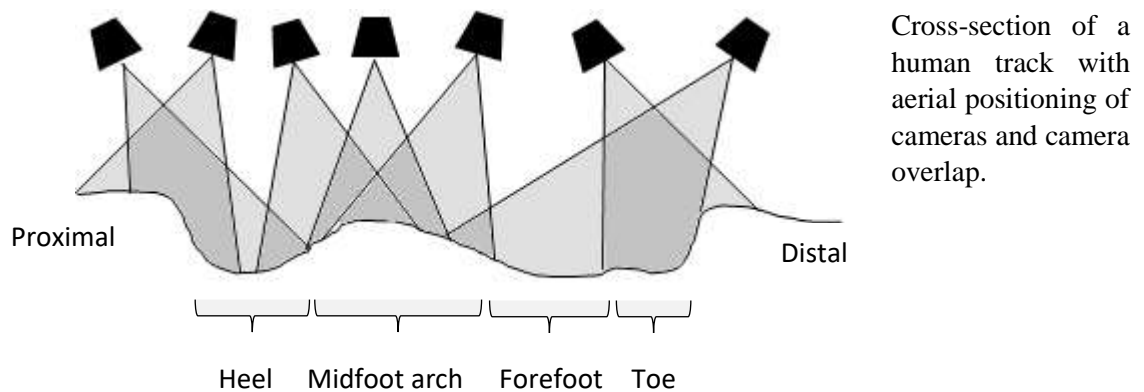


Figure 2.10. By careful design and selection of flight path and camera positioning it may be possible to capture a high-resolution model of the negative impression of a track without losing the complex internal structure. Diagram adapted from Bemis et al. (2014).

No study has yet tested the accuracy of flight data as captured from a multi-rotor UAV compared with traditional handheld methods of recording to determine if UAVs can be used to capture intricate details requiring high resolution and which can be used to create a precise 3D reconstruction of an object.

2.3.1 Aims

A series of experimental UAV flights were designed to identify the best practice for recording small fossils using photogrammetry. The data from these flights were compared to traditional handheld methods of recording. Two UAVs were tested: a DJI f550 and a DJI s900. The applicability of two types of the most commonly used cameras in aerial photogrammetry, a DSLR (digital single-lens reflex) and an action camera, were tested (GIM International: Mapping the World, 2016). The experimental area was also recorded via handheld methods. To combat the issue of occlusion hindering minute depth reconstruction, flight path was carefully considered to capture sufficient data (e.g., the

negative impressions of a footprint which will not have a uniform shape nor depth). By incorporating multiple camera positions and angles, occlusion should be drastically reduced (Bemis et al. 2014).

2.3.2 Experimental Design

A selection of experimental tracks were created in homogenous fine-grained sand composed of rounded to sub-angular particles measuring $\sim 0.06\text{-}0.7$ mm in diameter with $\sim 20\%$ saturation at a 40 mm depth (Figure 2.11). The recording area was constructed indoors to control for lighting and external factors, such as wind speed. Additional lighting was used to highlight the recording area clearly, thus increasing the visibility contrast of the negative impressions of the tracks.

A second set of flight tests were designed following this first round of experiments (Figure 2.11). The second set of experiments refined issues identified during the first testing phase and incorporated the recording of various objects that were not included initially. The inclusion of additional items in the second set of experiments permitted the assessment of whether other objects are affected by changes in shape and size, or if it is just negative impressions on a surface (e.g., a track) that is altered by various recording methods, thus permitting a more comprehensive assessment. The second set of UAV flights followed a similar experimental set-up as the first round of flights: experimental tracks were created in identical sand composition. Plastic replicas of the Laetoli tracks were placed within the recording area.

First set of experiments



Second set of experiments



Figure 2.11. The recording areas of the first set of experiments (left) and the second set of experiments (right).

2.3.3 Methodology

All models/data capture pertaining to the handheld method of recording will subsequently be referred to as ‘close range photogrammetry’ and data captured from the UAV will be referred to as ‘aerial photogrammetry’.

Prior to aerial photogrammetry, the experimental area was initially recorded via close-range photogrammetry. After recording the area by hand, the cameras were attached to two different UAVs: f550 and s900. A Nikon DSLR D3200 camera with a fixed focal length of 35 mm was used during the first set of flight testing. A Panasonic Lumix DMC-GH4 DSLR camera with a fixed focal length of 35 mm was used during the second set of flight testing. Camera type changed to incorporate the use of a camera with greater specifications and a greater buffer speed, and to allow the use of a lighter camera (210 g less weight) to promote longer battery life of the UAV. Both experiments incorporated the use of an action camera (a GoPro Hero 4 Black Edition) (Table 2.4).

Table 2.4. Camera specifications for the cameras used during the study.

First set of experiments: f550 UAV		Second set of experiments: s900 UAV
Nikon Digital SLR Camera D3200	GoPro Hero 4 Black Edition	Panasonic Lumix DMC- GH4 4K Digital SLR Camera
File Format: RAW/MOV	File Format: JPEG	File Format: RAW/MOV
ISO: 200	ISO: Automatic	ISO: Automatic
Aperture: F6.3	Aperture: Automatic	Aperture: Automatic
Exposure: 1/20	Exposure: Automatic	Exposure: Automatic
Focal length: 35 mm	Focal length: wide angle (160°)	Focal length: 35 mm
Weight: 505 g (camera) + 265 g (lens)	Weight: 88 grams	Weight: 560 g in total

Camera settings of the Panasonic Lumix DMC-GH4 DSLR camera were changed during the second set of experiments to ‘automatic’ to circumvent the issue of external factors (height or shadow changes) affecting photograph quality and, potentially, affecting model

quality. During the first set of experiments, the Nikon DSLR D3200 camera was attached to the DJI f550 UAV. This camera only recorded via camera stills and the action camera only recorded via video. During the second phase of experiments the recording methods were expanded: the Panasonic Lumix DMC-GH4 DSLR camera (attached to the DJI s900 UAV) and action camera (attached to the DJI f550 UAV) recorded via both video and camera stills.

Following close range photogrammetry, an f550 UAV was used to record the area during the first set of experiments. An s900 UAV was used during the second set of experiments to assist in stabilisation of the DSLR camera. As the flights were conducted within an indoor space, GPS (Global Positioning System) signal was unreliable. The UAV was flown in ATTI (attitude) mode at two different heights: 1-3 m and 3-5 m with a DSLR camera (the Nikon DSLR D3200 during the first set of flights and the Panasonic Lumix DMC-GH4 DSLR during the second set of experiments) mounted and then with the action camera attached.

The UAV was flown at a steady height across the recording area, but slight error in the absolute vertical position can be introduced with the lack of GPS stabilisation. As such, it is more accurate to report that the UAV was flown between 1-3 m and 3-5 m. It was expected that if the UAV was flown below the 1 m benchmark that the airflow from the UAV would disturb the sand, thus introducing noise error and ultimately destroying the true shape of the experimental tracks. This would also be true for fossilised tracks: if the UAV is flown too closely to the fossil there is risk of destroying the sediment.

The action camera and the Nikon DSLR D3200 were mounted to the UAV via a custom designed, 3D printed gimbal. Camera lens angle was of least concern when recording via the action camera, which had a fixed angled lens of 160° and thus a greater range of captured area. An angled lens of 160° captures an area of 18.47 m² in a single frame if flown at 3 m which is more than adequate considering that the area containing the experimental tracks measured 5 m by 3 m. The fixed camera lens angle of both DSLRs with a zoom of 35 mm was 54.4°, whereby the Angular Field of View (AFOV) was calculated using the following equation:

$$AFOV(^{\circ}) = 2 \times \tan^{-1} \left(\frac{\text{Camera Focal Length}}{2 \times \text{camera height}} \right)$$

As the AFOV was smaller in both DSLR cameras compared to the wide angled action camera (Table 2.5), the angle of the DSLR whilst attached to the f550 UAV had to be

carefully considered to sufficiently capture the experimental area. During the first set of experiments the action camera and the Nikon DSLR D3200 were attached to the f550 at a fixed 30° angle. This was later refined to a fixed 45° angle during the second set of experiments to allow for a greater area to be recorded (Figure 2.12). The s900 gimbal permitted the user-controlled yaw rotation of the DSLR whilst maintaining a fixed angle of 45°.

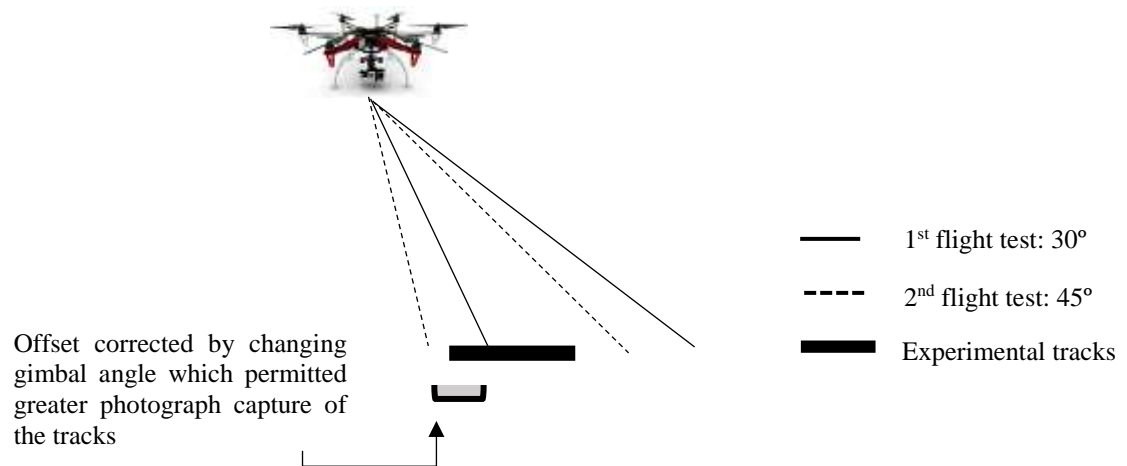


Figure 2.12. Diagram demonstrating the effect of camera offset angle. By reducing the offset when using a fixed 45° angle gimbal, the UAV can be flown more closely to the item of interest during each of the designed flight paths.

The area (m²) captured via aerial photogrammetry was increased with the increasing height of the UAV as a direct correlation with the fixed camera angle (Table 2.5). However, preliminary results from the first set of experiments demonstrated that an increase in recording equipment height came at the expense of a lower resolution model (Table 2.6), which was presumably due to poor photograph overlap during each flight path (see Section 2.3.5). To test this, greater consideration was thus given to camera angle during the second set of flight tests. By changing the fixed angle of the custom designed gimbal from 30° to 45°, the camera is optimally positioned relative to the ground points for recording (Table 2.5).

By changing the gimbal angle the camera offset is corrected, allowing for the deployed camera to be optimally positioned (Figure 2.12). If the offset remained at a 30° angle during the second set of flight tests then this would have resulted in either (1) longer flight times or refined flight paths to capture data missed by the offset (although deciding

if/when sufficient photograph overlap had been captured would have been subjective), or (2) the full extent of camera offset would not be recognised until model creation whereby poor photograph overlap of the objects may have resulted in increased self-occlusion, resulting in poor edge and structure reconstruction. By changing the camera offset distance from 30° to 45°, greater photograph overlap was captured as the UAV recorded data at an improved distance to the experimental tracks (Table 2.5; Figure 2.12).

Table 2.5. The effect of camera angle on the captured area, and the offset of the camera created by attaching the camera to the f550 via a custom designed, 3D printed gimbal.

		Captured Area		Camera offset using the 3D printed gimbal	
		160° fixed angle action camera	54.4° fixed angle DSLR camera	Fixed 30°	Fixed 45°
Height:	1 m	6.16 m ²	0.91 m ²	1.38 m ²	0.85 m ²
	3 m	18.47 m ²	2.73 m ²	4.13 m ²	2.56 m ²
	5 m	30.77 m ²	4.55 m ²	6.88 m ²	4.27 m ²

To capture the optimal amount of data at the greatest possible quality, flight path was also a consideration. During the first set of experiments, three flight paths were developed for both the handheld methods and the UAV flights to follow. All recording methods (handheld and flight data with both camera types using the f550 and, later, the s900) followed a circular path, a linear path and a rastered path. This was expanded to incorporate an additional flight path during the second set of experiments: the arched path (Figure 2.13).

Unfortunately, the Nikon DSLR D3200 using the f500 from the first set of experimental flights produced poor photograph overlap, resulting in many of the models failing to calibrate. This issue was rectified during the second set of experiments by using the Panasonic Lumix DMC-GH4 DSLR mounted to the s900 which has a greater buffer speed for rapid photograph capture.

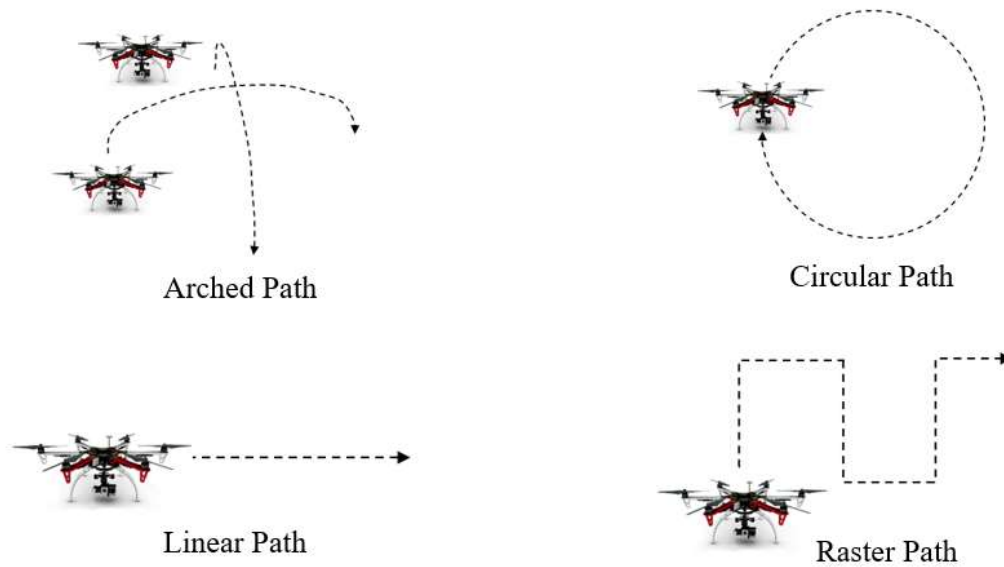


Figure 2.13. Flight paths designed for the experiments.

2.3.4 Model creation

Point cloud production

All photographs and videos were imported into Pix4Dmapper (v.4.327 Pix4D, Lausanne, Switzerland). Photogrammetric 3D models of all close-range and aerial data were created. To increase reconstruction accuracy manual tie points (MTPs) were utilised in every model. MTPs are 3D matching points in a selection of photographs that are defined by the user (Pix4D, Lausanne, Switzerland, 2018). MTPs are also efficiently used to calibrate images that the software is unable to calibrate, thus increasing the amount of tie points in each model.

To avoid the issue of working with large file sizes (e.g., a scaled point cloud of 60 million points produces a LAS file size of 1.9 GB), all point clouds were exported into CloudCompare (v.2.10 OpenGL 2018) where each of the models were scaled. Scaled point clouds were checked using various measurements of numerous scale bars present in the model. All point clouds were comparatively assessed to identify the best flight path and recording method for producing high quality models with precision.

Mesh creation

As this study incorporated the use of GM analyses, mesh production was necessary. The meshes created in Pix4Dmapper were determined to be of low quality as the maximum

number of triangles during creation is 20,000,000. Upon visual inspection of the meshes it was determined that this threshold simplified smaller details in the tracks to utilise the full range of triangles uniformly across the mesh, necessitating the need to create the meshes in another manner (Figure 2.14). Although the models in Pix4D could have been cropped to the size of the prints, this study wanted to test the precise reconstruction of a specified area. To remove the issue of limited mesh reconstruction, another software was utilised for mesh reconstruction: CloudCompare because the triangles created for the meshes are infinite. After point cloud production, all data processing and analyses were computed in CloudCompare. Computing all processing (e.g., cropping point clouds) in the same software allowed for a user-efficient workflow process to be established.

All point clouds were cropped to the desired region of interest and 3D meshes were created in CloudCompare using an Octree depth of 9. Octree value was determined via visual inspection of mesh output.

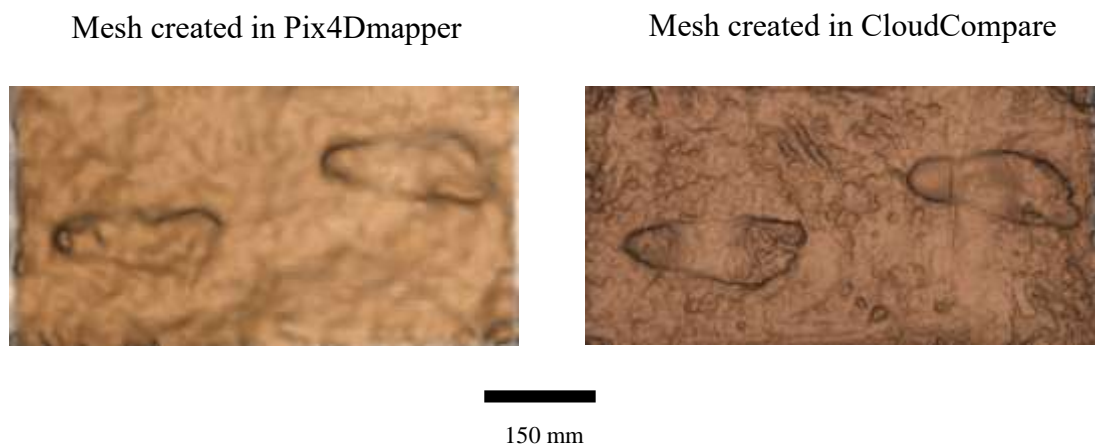


Figure 2.14. Mesh production in different software of the same model created from close-range photogrammetry using the Nikon DSLR D3200 following a rastered path.

2.3.5 Analyses

Point cloud density

To address the question of which flight path and recording mode would provide the greatest quality model, point cloud density was quantified for each model. A comparison of point density will only provide a relative measure of quality because the method does not consider point cloud noise. Noisy point clouds were excluded from this comparison (see: Table 2.6) and Cloud to Cloud Distance methods (the following analyses) were used in conjunction with this comparison to provide a rounded overview of model quality and precision.

For both sets of experiments, a selection of the recording area was cropped. For the first set of experiments, a cropped section in the centre of the model was selected. For the second set of experiments, the centre tray was selected. Both selected areas measured 1 m by 0.5 m. The central items were selected on the assumption that point cloud density would likely be greater in this region. Using CloudCompare point cloud density was calculated for each of the selected areas. A two-tailed Student's *t*-test was computed in R (R Core Team 2017) to statistically compare point cloud densities between models.

Point cloud comparisons

As the second set of experiments were more comprehensive than the first, only models belonging to the second set of experiments were used for the point cloud comparison assessment in CloudCompare. The Cloud to Cloud Distance method (Olsen et al. 2010; Lague et al. 2013) compares two point clouds of equal scale whilst calculating the distance between two clouds, using one of the point clouds as a ground truth (reference) and the other as the comparative entity. All distances between clouds were calculated from the reference cloud to the compared cloud, producing a scalar field of distances. The reference cloud was always selected by the user based on which cloud produced the greatest point cloud density with the lowest noise and misalignment (see: Figure 2.17). For example, a handheld method would always be selected by the user as a reference, with a model from one of the UAV methods used as the comparative entity. Recording heights of 1-3 m were always selected by the user as the reference, with the recording heights of 3-5 m as the comparison. Similarly, a model created from DSLR camera stills would always be selected by the user as the reference cloud, with a model created from an action camera recorded via video as the comparative entity.

Assessing shape/size distortion in the 3D mesh analyses

While it was expected that no shape/size disparity would be identified between models of the exact same object, the small possibility that flight path or camera angle may have distorted object shape/size by introducing camera parallax issues could not be ignored (Westoby et al. 2012; Mallison and Wings 2014). Parallax is the displacement/distortion of an object when photographs are captured from differing angles (Seiz et al. 2002). Although the initial processing stages in Pix4Dmapper account for this distortion by applying correction parameters (Pix4D, "Camera Distortion", 2018), the possibility that slight distortion may be present in model reconstruction was considered. GM methods

were utilised to determine if any of the flight paths or recording modes produced disparate models. Analyses were computed in morpho (Schlager 2017) and geomorph (Adams and Otárola-Castillo 2013), R packages (R Core Team 2017).

For the first set of experiments three tracks were selected for the analysis with a comprehensive landmark configuration. For the second set of experiments all objects within the recorded area were selected: the three trays were analysed individually, alongside two plastic casts of the Laetoli track copies. Homology of landmarks for these objects was reduced with increased height of the UAV and, occasionally, flight path due to increased photograph blur – this was not an issue with the tracks from the first set of experiments as numerous UAV models were discarded due to poor reconstructions (see: Section 2.3.3.). The increase of blur in these specific models produced reconstructions with little topographical features (e.g., the loss of toe ridges). Visually, it was not possible to place any more than 14 landmarks on the trays containing the experimental tracks due to a lack of homology between models. Consequently, the landmark configuration for all objects remained simple, addressing outline metrics and depth (Figure 2.15). All items from the second set of experiments were computed separately, offering the greatest amount of assessment between models.

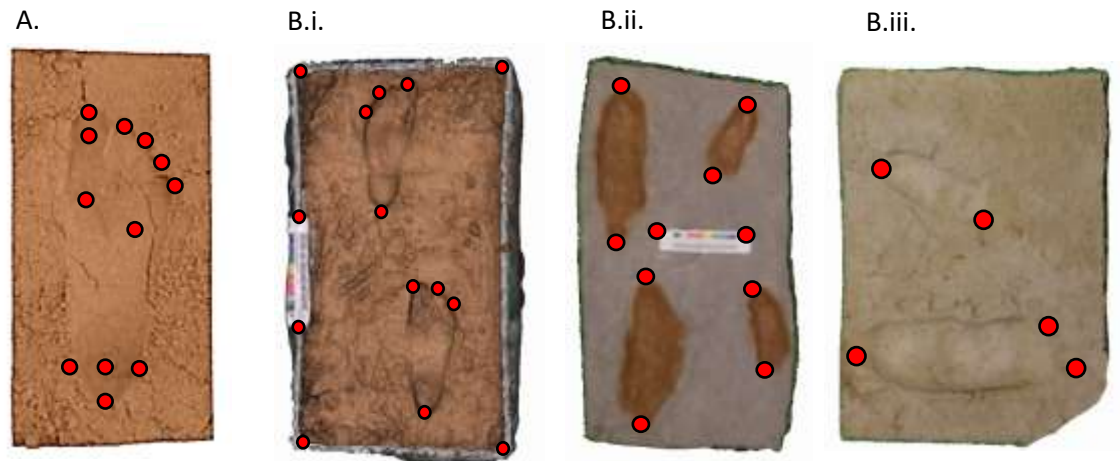


Figure 2.15. Landmark datasets for the first (A) and the second (B) set of experiments placed on meshes. Objects were sub-divided from the second set of experiments to incorporate the inclusion of experimental tracks (x3 trays) (B.i), replica casts of the Laetoli tracks with colour (B.ii), and replica casts of the Laetoli tracks without colour (B.iii). Objects not to scale.

Reliability tests of landmark placement were conducted in Morpho (Schlager 2017) to ensure that landmarks could be consistently identified within and across samples.

Through this process, landmarks found to be non-replicable between objects were removed (e.g., the deviation from the landmark consensus was found to be >1.5 mm which was deemed to be too great an error margin for replicable landmark placement). This process resulted in the selection of 14 type II geometrically-defined landmarks (Bookstein 1991) that were all within 0.6 mm deviation from the consensus; whereby deviations within this threshold are deemed by the user to be observer-error. Landmarks were digitised on each object using Avizo (v.9.0.1 FEI, Oregon, USA).

A GPA was performed on each landmark configuration. Shape variation was assessed using a PCA on the resulting GPA coordinates. Each PC was examined to determine shape variability. An ANOVA was computed on each landmark consensus to assess the relative amount of shape variation between each model. Categorical variables were created to assess the cause of any shape change. Both sets of experiments used the same categorical variables: flight height (close-range and aerial photogrammetry at 1-3 m and at 3-5 m), flight path (a circular path, a linear path, a rastered path and the arched path) and camera mode (video or camera stills). The use of categorical variables will determine the best flight path for recording intricate details or will identify if any of the listed variables have cumulatively resulted in changes in shape and/or size to an object. For example, it will be possible to determine if a handheld Nikon DSLR D3200 camera recording via camera stills following a circular path is a more suited method than a UAV at 3-5 m high with an action camera recording via video following an arched path.

2.3.6 Results

Model reconstruction

Numerous models had to be discarded due to poor model reconstruction. This was an issue for several models, with the underlying cause being identified as severe motion blur (Figure 2.16). Problematic images were removed, and the models were recalibrated without these images in conjunction with an increased number of MTPs. Often, this rectified the issue of poor model calibration. Eight of the models from the second set of experiments were unsalvageable: this issue was detrimental for all models related to the arched paths and most models related to the linear paths.

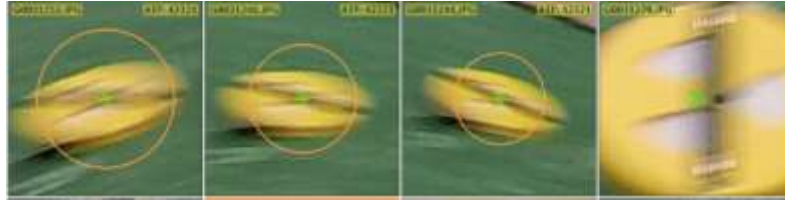


Figure 2.16. An example of camera motion blur during the UAV flight tests. These images belong to the UAV flown at 1-3 m high with an action camera attached, recording via video, following a circular path.

Two flight paths (the linear path and arched path) were identified as consistently producing poor model reconstruction, despite the use of numerous MTPs (~20) and the removal of photographs that exhibit motion blur. Issues were present in both close-range and aerial photogrammetry. The arched path produced severely distorted reconstructions that were unsalvageable despite the use of multiple MTPs (Figure 2.17a.i). It is expected that the issue is related to camera parallax (Figure 2.17b). The path followed an arched trajectory, that came within 10 cm of the ground when the Panasonic Lumix DMC-GH4 DSLR was handheld (no tripods were utilised), and within 50 cm to 100 cm (estimation) when the UAV was used to record the area. Accordingly, the worst reconstructed models were those recorded via close-range photogrammetry as the camera was positioned at more severe conflicting angles throughout the flight path trajectory. Photographs that were deemed to be close to the ground were removed and the tie points were re-calibrated without these photographs. Model accuracy did not improve despite the majority of ‘problematic’ images being removed, resulting in an extremely sparse and unusable point cloud (Figure 2.17a.ii). As the height of the UAV is increased and the camera angles became less conflicted, then model reconstruction improved slightly, but did not reach the standards nor expectations of a usable model due to severe distortion. Consequently, it was determined that the arched path was not a reliable method for capturing data.

All models recorded from linear paths produced noisy point clouds, and poor quality meshes. The most likely explanation for this issue would be camera parallax. As the camera was only travelling in one direction at a fixed angle (30°/45°), there were no reference points for recreating accurate depth (e.g., Westoby et al. 2014; Mallison and Wings 2014), resulting in increased noise error for this flight path. Consequently, it was determined that the linear path at 30°/45° was not a reliable method for capturing data.

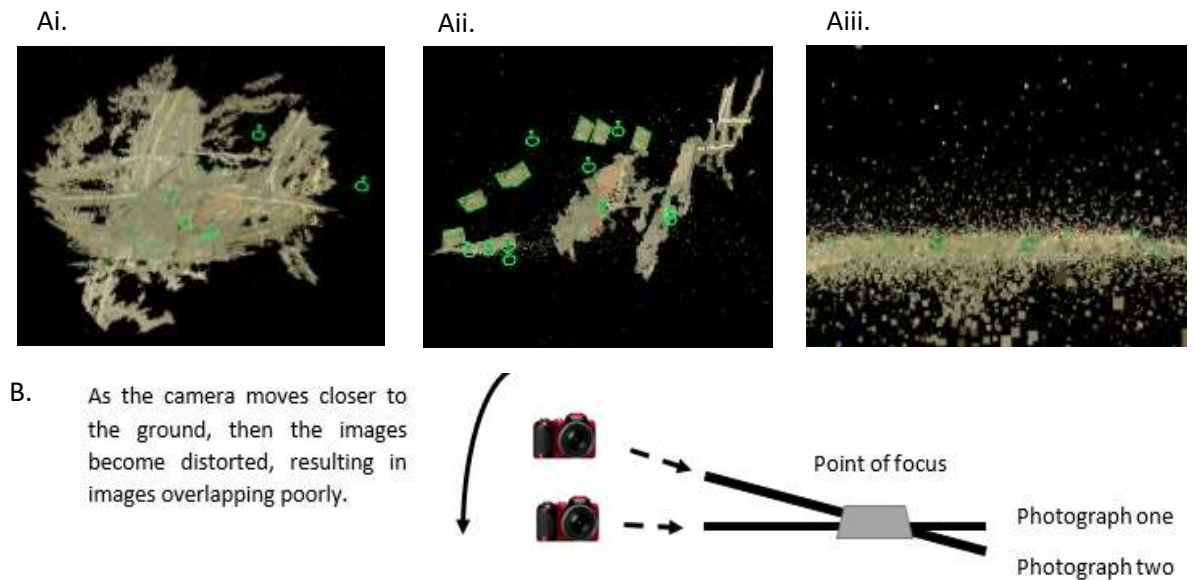


Figure 2.17. Examples of poor model reconstruction in the arched path (Ai; Aii) and linear path (Aiii). Ai was created from the UAV at 3-5 m, with an action camera following the arched path, and recording via video. To attempt to improve model reconstruction, numerous photographs were removed (Aii). However, model accuracy remained low, suggesting the issue could be camera parallax (B).

2.3.7 Model quality

The point cloud density of each model from both sets of experiments were calculated within a 1 m by 0.5 m selected area (Table 2.6). The numbers of points within a given selection were greater for the second set of experiments, but the overall results were broadly uniform between each set of experiments: close range photogrammetry produced the greatest point cloud densities, although model density was greater during the second set (e.g., during the first set of experiments the linear path recording via Nikon DSLR D3200 stills produced a point cloud density of 1,567,744 points in an area measuring 1 m by 0.5 m; and during the second set of experiments the rastered path recording via the Panasonic Lumix DMC-GH4 DSLR stills produced a point cloud density of 11,056,290 points in an area measuring 1 m by 0.5 m). Similarly, aerial photogrammetry produced models with low point cloud densities, regardless of whether a DSLR camera or action camera was attached (e.g., during the first set of experiments the rastered path recording via video using the action camera produced a point cloud density of 3258 points in an area measuring 1 m by 0.5 m; and during the second set of experiments the rastered path recording via stills using the action camera produced a point cloud density of 8664 points in an area measuring 1 m by 0.5 m).

Except for one model from the first set of experiments (the handheld Nikon DSLR D3200 camera using camera stills following a linear path), all flight paths generally produced comparable point cloud densities (Figure 2.18). For example, as the height of the recording device increased, a trend for decreasing point cloud density was apparent (Figure 2.18a), although this was often non-significantly disparate (Table 2.7). Often model resolution was very poor to the extent that it was difficult to distinguish track morphology clearly. In the two examples provided in Figure 2.18b, it is possible to see the loss of detail once the height of the recording device is increased from 1-3 m to 3-5 m, further amplified by using video to record the experimental trackway, rather than camera stills. There is complete loss of the toe region of the track, coupled with a loss of depth dimensionality, noticeable when the texture is removed from the 3D mesh, resulting in a flat model with no morphological features. Texture mapping is a method of distinguishing coloured details on a 3D-generated model (Catmull 1974). The texture maps preserved general track outline, but if they are removed then the underlying 3D reconstruction is void of definition in this particular model.

Models with an improved point cloud density (Table 2.6) have greater morphological detail, highlighting that these models (e.g., any of those created from a handheld DSLR camera) have adequately captured the complex structure of a track. Whereas, using an action camera deployed through aerial photogrammetry to record tracks results in failure to reconstruct track edges, represented by (1) a flat model once texture is removed and (2) a reduced point cloud density (e.g., a total of 3258 points in an area measuring 1 m by 0.5 m when the UAV is at 3-5 m). A reduced point cloud density subsequently produced a ‘simplified’ 3D mesh due to the interpolation of sparse vertices that distorted and ‘simplified’ the topographical features of each track despite point clouds being non-significantly variable with those of a denser point cloud ($P \geq 0.05$), as supported by a two-tailed Student’s *t*-test (Table 2.7).

The second set of flight tests corrected the camera offset by changing the fixed angle of the custom designed gimbal from 30° to 45° to determine if greater photograph overlap can be captured during each of the flight paths as the camera lens is more optimally suited to record the experimental trackway (see: Section 2.3.3; Table 2.5). As the height of the recording device increased then model quality decreased (e.g., the maximum number of points was 11,056,290 in an area measuring 1 m by 0.5 m following a rastered path with a handheld Nikon DSLR D3200; whereas, the minimum number of points within the exact same area was 3258 in an area measuring 1 m by 0.5 m following a rastered path

with an action camera using stills to record) (Figure 2.18b), although this was determined to be non-significantly variable between-groups ($P \geq 0.05$) (Table 2.7). Levels of non-significance detected between-groups is likely explained by either a spread of data points (from 3258 to 116,462 in the action camera data, and 8664 to 11,064,954 in the DSLR camera data), or due to somewhat unequal group sizes (Cohen 1988).

Video from the action camera produced greater quality models than action camera stills across all variables ($t = -3.386$; $P = 0.007$), as determined by comparing point cloud densities between models (e.g., point cloud density of the exact same area measuring 1 m by 0.5 m when recorded via close range photogrammetry following a circular path was 112,121 points when recorded via video compared to 32,506 points when recorded via stills). Increased photograph overlap in the video likely compensated for reduced image quality, suggesting that action camera stills is a non-preferable method of data capture. Despite increased photograph overlap in the action camera video, recording via video with the Panasonic Lumix DMC-GH4 DSLR consistently produced greater quality models than that of the action camera ($t = 2.34$; $P = 0.030$) (Table 2.7), indicating that if possible a DSLR camera would be the optimal choice for capturing an area of interest regardless of whether recording via video or stills. In sum, by correcting the camera offset angle from 30° to 45° point cloud density is improved concurrent with improved photograph overlap (Table 2.6), as reflected in the subsequent 3D mesh creation (see Section 2.3.7). If comparing within-sets, no significant disparity was identified in the point cloud density between models created from various flight paths ($P \geq 0.05$), or between models created from any DSLR camera stills in comparison to DSLR video capture ($P \geq 0.05$).

Close-range photogrammetry or aerial photogrammetry?

Results demonstrate that the point cloud density of models between close-range photogrammetry and aerial photogrammetry are non-significantly variable ($P \geq 0.05$) (Table 2.7). Despite the established non-statistically significant disparity, an inspection of the data ranges between close-range and aerial-capture point clouds indicates that density is always greater when close-range photogrammetry is employed (Table 2.8). Non-significance may have been detected due to unequal sample sizes and/or the testing of small group sizes (Cohen 1988). Additionally, the models created from aerial data may have increased noise, thus warping a true reflection of point cloud density. Regardless, close-range photogrammetry produces greater resolution models.

Table 2.6. The number of points per point cloud within a 1m by 0.5 m selection of each model. A shaded black box indicates that a particular variable was not included in the first set of experiments (the arched path, the use of stills as deployed by an action camera nor the use of video as deployed by the Nikon D3200 DSLR camera. Due to hardware failure, no video was captured via the Panasonic Lumix DMC-GH4 DSLR during UAV deployment). A shaded grey box indicates that the model was too poorly reconstructed to obtain a point cloud density result despite the inclusion of multiple MTPs (see: Section 2.3.6). ‘AC’ represents action camera data. Set 1 (the first set of flight tests) DSLR data used the Nikon DSLR 3200 to capture data. Set 2 (the second set of flight tests) DSLR data used the Panasonic Lumix DMC-GH4 DSLR to capture data.

			Circular Path		Linear Path		Rastered Path		Arched Path	
			Set 1	Set 2	Set 1	Set 2	Set 1	Set 2	Set 1	Set 2
Close range photogrammetry:		DSLR stills	117904	421328	1567744	4250706	71537	11064954		3498484
		DSLR video		105879		3398617		533353		768076
		AC stills	32506	76492	156744	106935	93159	106202		32056
		AC video	112121	247368	45010	224432	116462	203618		234355
Aerial photogrammetry:	3 m	DSLR stills	51992	593658		915747	56903	1308202		215813
	3 m	AC stills		15137		35423		126172		29525
	3 m	AC video	6711	120961	12132	86985	6344	241527		70132
	5 m	DSLR stills		130752		274450		288842		134125
	5 m	AC stills		8925		18133		8664		30600
	5 m	AC video	3490	48053		78331	3258	32312		

Table 2.7. Results of the two-tailed Student's *t*-test for unequal variances of point cloud densities of an area measuring 1 m by 0.5 m. 'Between-sets' represents that the data from the first set of experiments has been statistically compared to the data from the second set of experiments. 'Within-sets' data represents the second set of flight test data. Because the second set of flight tests produced greater point cloud densities, comparisons were made between flight paths using the second set of flight test data only. As the arched path was not implemented until the second set of flight tests then this data is missing from all statistical analyses. AC represents 'action camera' data. Significant P values can be found in bold.

						95% Confidence Interval of Difference		t	P
		DF	Mean Variance	Std. Deviation	Std. Error Mean	Lower	Upper		
Between-sets	Close range ~ aerial: Set1	3	448783.75	743923.40	371961.70	-734964.39	1632531.89	1.207	0.314
	Close range ~ aerial: Set2	10	1303902.64	3403239.00	1026115.00	-982424.54	3590229.82	1.271	0.233
	Aerial: Set1 ~ aerial: Set2	2	-1221.57	123005.77	71017.45	-427719.21	184305.88	-1.720	0.228
	Circular Path	5	-197189.33	193614.00	79042.57	-400374.72	5996.05	-2.495	0.055
	Rastered Path	5	-2101525.33	4381471.00	1788728.00	-6699597.00	2496546.37	-1.175	0.293
	Linear Path	3	-721857.00	1310757.00	655378.50	-2807563.80	1363849.77	-1.101	0.351
Within-sets	Circular ~ Linear	9	-762120.60	1484228.00	469354.10	-1823873.30	299632.08	-1.624	0.139
	Circular ~ Raster	9	-1214529.30	3321381.00	1050313.00	-3590502.40	1161443.82	-1.156	0.277
	Raster ~ Linear	9	452408.70	2421798.00	765839.90	-1280041.50	2184858.87	0.591	0.569
	DSLR stills: DSLR video	3	3607386.75	4730833.42	2365416.71	-3920424.92	11135198.42	1.525	0.225
	AC stills: DSLR stills	11	1875233.08	3161033.22	912511.69	-133191.61	3883657.77	2.055	0.064
	DSLR video: AC video	3	974038.00	1493770.70	746885.35	-1402884.52	3350960.53	1.304	0.283
	DSLR stills: AC video	10	1935743.09	3260592.07	983105.50	-254752.47	4126238.65	1.969	0.077
	DSLR video: AC stills	3	1121060.00	1475704.95	737852.48	-1227115.88	3469235.89	1.519	0.226
	AC stills: AC video	10	-93030.45	91122.16	27474.36	-154247.15	-31813.76	-3.386	0.007
	DSLR: Action Camera	15	1649934.31	2817137.46	704284.36	148787.72	3151080.90	2.340	0.030
	Video: Stills	14	1132846.07	3161725.65	816354.05	-618059.24	2883751.37	1.390	0.190

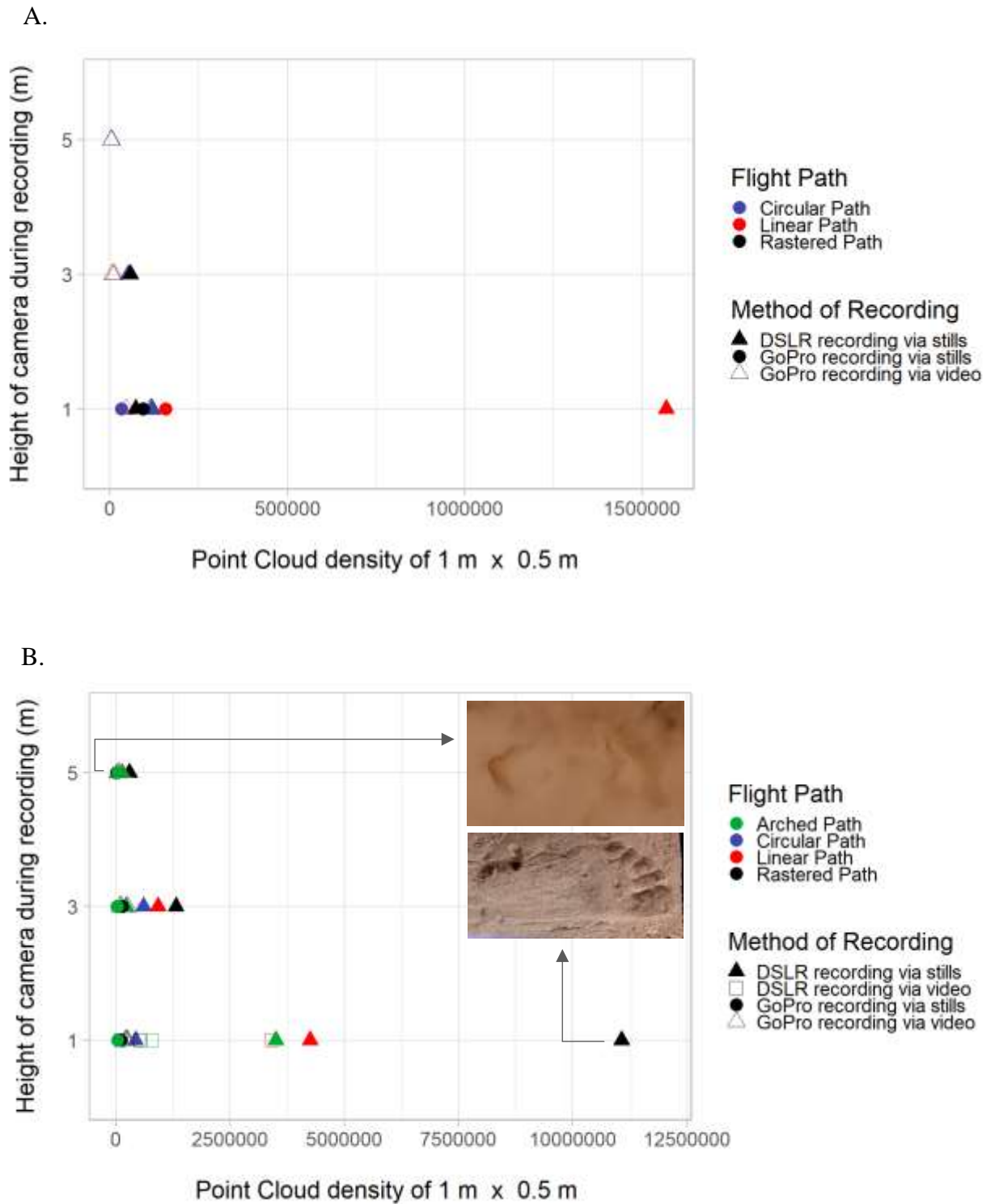


Figure 2.18. Point cloud density results from the first (A) and second (B) set of experiments, with two examples of point clouds displaying stark contrast in model quality (A). Higher points per cloud in each model produced more defined object outlines, as demonstrated in the two track examples (B). A height of 1 m represents the handheld recording devices, and heights of 3 m and 5 m represent aerial photogrammetry.

Table 2.8. The descriptive statistics for point cloud density between the close-range photogrammetry and aerial photogrammetry during the first set of flights tests (Set 1) and the second set of flight tests (Set 2).

		Range				
		Mean	Std. Dev	Std. Error	Minimum	Maximum
Set1	Close-Range	355,767	60,049	181,056	32,506	1,567,744
	Aerial	22,332	24,891	8297	3258	56,903
Set2	Close-range	1,579,553	2,894,507	723,627	32,056	11,064,954
	Aerial	209,237	319,838	66,691	8664	1,308,202

2.3.8 Comparing point cloud entities

During the point cloud comparisons, it was established that models created from close-range photogrammetry and from aerial photogrammetry were non-significantly variable, suggesting that both methods produce comparable resolution (however, see: Table 2.8). An inspection of some of the aerial models suggest that increased noise may exist in the aerial photogrammetry (e.g., Figure 2.17iii), thus warping a ‘true’ reflection of point cloud density. Increased noise and floating “artefacts” will suggest that point cloud density may in fact be greater than the points actually representing the footprint. Consequently, there may then be an issue in model reconstruction precision.

Cloud to Cloud comparisons were conducted for the two flight paths that displayed no visually evident distortion: the circular path and the rastered path. These paths produced the best model reconstructions with the least amount of sparsity (e.g., see Figure 2.16). Both the circular path and the rastered path produced similar cloud to cloud results. Graphical results presented in the following sections belong to the circular path as example.

Comparing point cloud entities: camera stills versus video recording

Point cloud comparisons were computed between models. Results show little disparity in absolute distances between camera stills and video when these recording devices are handheld as the average distance between points was 0.91 mm (Figure 2.19a; Table 2.9). This small discrepancy increases stature prediction (Martin 1914) by just 0.61 mm (e.g., predicted stature was calculated as 164.60 cm using Martin’s ratio from the tracks as

measured during the experiments using a handheld tape measure; whereas, predicted stature from the point clouds with a discrepancy of 0.91 mm produces a predicted stature value of 164.61 cm, although this has been calculated to be within the ranges of observer error when extracting track measurements in Section 4.3.3). Consequently, this disparity is considered minute and acceptable.

A few problematic areas were identified: around the edges of each of the objects where the distance was ~10 mm between points. This increased distance between points representing the edges of each object may be caused poor reconstruction in the camera stills model whereby camera overlap is reduced relative to the video capture which can capture more frames per second (Table 2.4), resulting in less points per region around object edges. This suggests that video camera as deployed by the action camera is preferable relative to the action camera stills, concurrent with the point cloud density results which stipulated that the action camera video produces a greater overall number of points per region (0.5 m by 1 m).

When the action camera is attached to a UAV at 1-3 m the distance between the two point clouds (camera stills and video) is greater than that of the handheld comparative models, with an average distance between points of 19.34 mm (Figure 2.19b; Table 2.9). However, this averaged disparity is of little concern: this area is mostly tarpaulin, and despite efforts to weigh down the tarpaulin there was still airflow from the UAV that caused the tarpaulin to make slight movements. The models of the trays of sand containing the experimental tracks and the Laetoli tracks remain mostly similar, with little disparity between the point clouds in these regions with some discrepancy around object edges (~0-10 mm). A ~10 mm distance between points around object edges regardless of camera mode or height of the recording device suggests a loss of precise depth reconstruction when employing action camera stills to record the area.

Aerial photogrammetry at 3-5 m using an action camera produced poorly reconstructed models. When recording via camera stills large areas failed to reconstruct, resulting in a sparse point cloud with an average distance between points of 74.21 mm and a maximum distance of 340.26 mm (Figure 2.19c). The model created from the video produced better model reconstruction, free from sparse regions. However, this model was noisy with severe distortion around object edges, resulting in the distances between the two point clouds often being as high as ~340 mm. Although multiple MTPs were employed during model creation to rectify this issue, attempts were unfounded.

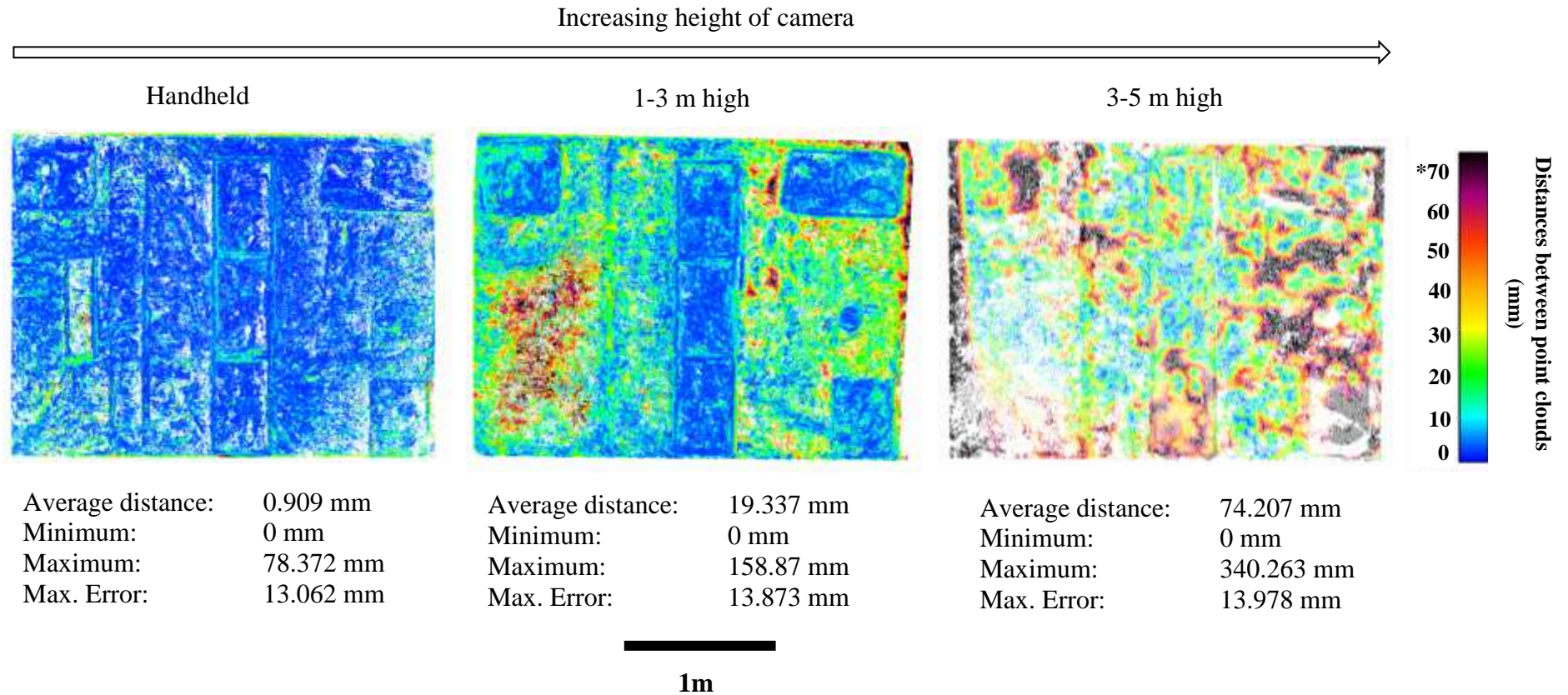



Figure 2.19. Point cloud comparisons from the comparative assessment of two recording methods: camera stills versus video recording. Images show disparity in point cloud distances between two equally scaled point clouds. Examples are created from the action camera of the circular path with the camera stills used as the reference entity. A value of *70 refers to (1) areas of the point cloud that are missing due to poor camera overlap and (2) an extremely noisy point cloud whereby the maximum disparity is 0.34 m (as represented by the black regions).

Table 2.9. The number of points per cloud to cloud comparison grouped to the nearest 10 mm. Points exceeding 70 mm between models were less common than those displaying 0 mm between models (e.g., there was 70 mm distance between 193 points in comparison to the 5,207,656 points where the distance was 0 mm when comparing handheld camera types). Generally, points that were >30 mm between clouds belonged to regions of the models that were poorly reconstructed and sparser than regions demonstrating <30 mm distances between points. ‘AC’ represents action camera data. ‘DSLR’ represents all data captured via the Panasonic Lumix DMC-GH4 DSLR. Points exceeding 75 mm+ were not quantified.

		0 mm	10 mm	20 mm	30 mm	40 mm	50 mm	60 mm	70 mm	75 mm+
										
Camera Height										
DSLR ~ AC:	Close-range	5,207,656	0	929,878	1961	26,991	1866	5113	193	NA
	1-3 m	252,457	11,447	6414	5377	2461	1251	575	188	NA
	3-5 m	86,235	47,518	11,199	2980	1210	676	265	118	NA
Camera stills ~ Video:	Close-range	1,518,678	142,275	13,147	5842	1241	284	51	13	NA
	1-3 m	1,400,899	493,509	77,948	37,381	14,406	5578	461	123	NA
	3-5 m	161,450	138,034	76,672	47,919	16,799	8758	3409	154	NA
Action camera:	Close-range ~ 1-3 m	161,743	67,421	3872	1859	1039	645	33	40	NA
	Close-range ~ 3-5 m	126,762	86,794	15,067	5017	1419	1112	411	70	NA
	1-3 m ~ 3-5 m	61,302	37,533	15,126	2940	1371	247	124	7	NA
DSLR camera:	Close-range ~ 1-3 m	3,258,505	213,714	25,505	10,865	4466	805	8	8	NA
	Close-range ~ 3-5 m	2,766,895	706,018	23,937	8624	7235	1138	21	8	NA
	1-3 m ~ 3-5 m	816,738	317,595	42,350	15,090	5831	2547	1460	155	NA

Alternatively, the successful reconstruction of close-range and aerial photogrammetry at 1-3 m demonstrates that flight paths were successfully implemented at lower altitudes. Other factors are likely responsible for the poor reconstruction of objects during aerial photogrammetry at 3-5 m, such as the lack of GPS signal when flying indoors which reduced UAV stabilisation and/or insufficient photograph overlap production of smaller objects when the height of the recording device was increased.

Importantly, the experimental tracks measured 246 mm in length (as determined using a handheld tape measure during the experiments). A disparity of ~340 mm between point clouds is clearly unacceptable for use in ichnological studies.

Comparing point cloud entities: camera type

Point cloud comparisons were computed between models created from a Panasonic Lumix DMC-GH4 DSLR camera and an action camera to determine the optimal camera type for recording small items (Figure 2.20; Table 2.9).

Results show that little disparity in absolute distances are identified between the Panasonic Lumix DMC-GH4 DSLR camera and the action camera when the cameras are handheld with an average distance between points of 15.79 mm (Figure 2.20a). However, the area containing the experimental tracks and the Laetoli tracks were identified to have a smaller than average distance of ~0-10 mm between clouds, similar to the comparison of camera stills and video.

The distances between the point clouds increase when aerial photogrammetry at 1-3 m using an action camera is utilised, although the average distance between points was 8.90 mm (Figure 2.20b). However, the internal structure of each tray of sand displayed ~20-30 mm between clouds, particularly in each individual track – this is an increase of 77% disparity in the reconstructed track structure from the close-range photogrammetry. This increase of 30 mm in track length would produce a stature prediction of 184 cm, a discrepancy of 20 cm (+12.2% increase) from the ‘true’ stature of 164 cm.

A maximum of ~50 mm in distance between points in one of the track-bearing trays produced a stature prediction of 197.33 cm (an increase of +20.33%). Distances >50 mm between points were once again found in the area with the reflective tarpaulin.

When the cameras are attached to a UAV at 3-5 m high the models exhibit improved model reconstruction than those created at a lower height with an average distance between points of 9.56 mm which is more uniformly distributed across the experimental

trackway than that of the 1-3 m models. Quite possibly this is due to greater photograph overlap and capture area with the increased height of the recording device, despite this coming at the expense of reduced point cloud density (Figure 2.17; Table 2.9). However, the base of each track is ~20 mm distance between point clouds, with the edges of the objects (e.g., the trays containing the tracks) exhibiting a ~50 mm disparity between clouds (Figure 2.20c). Evidently, an increase of the recording device height to 3-5 m insufficiently captures the object boundaries when recording via Panasonic Lumix DMC-GH4 DSLR camera stills, with the models displaying inadequate levels of self-occlusion.

UAV airflow caused movement in the tarpaulin. Consequently, four heavy weights were placed on the tarpaulin between flights (Figure 2.20), resulting in these regions being misconstrued as large distances (+75 mm) between clouds with the sudden appearance of 'new' items. To test if this had any effect on 'cloud to cloud' disparity, two point clouds were cropped to exclude these items prior to the cloud to cloud analysis. The scalar maps produced were identical to those already generated with these items included with the same distribution of point to point distances (e.g., Figure 2.20). The only difference was the absolute distance between the two clouds. However, this absolute value was not considered in the current analyses as the hypotheses regard shape and/or size differences within small objects; e.g., a singular track. These nuanced variabilities of the internal morphology of the tracks would be lost if only the absolute differences were reported.

Close range photogrammetry versus aerial photogrammetry

Point cloud comparisons were computed between handheld and UAV data to determine the optimal height for recording intricate detail, and to determine if a UAV can be used to reliably record tracks. Results show that little difference in absolute distances were identified between close-range photogrammetry and aerial photogrammetry at 1-3 m using the action camera with an average distance between points of 6.71 mm (Figure 2.21a; Table 2.9). Like the comparison of camera stills and video, the edges of each object have discrepancies in depth (~20 mm). Items that are located further from the centre of the recording area have increased loss of accurate depth reconstruction.

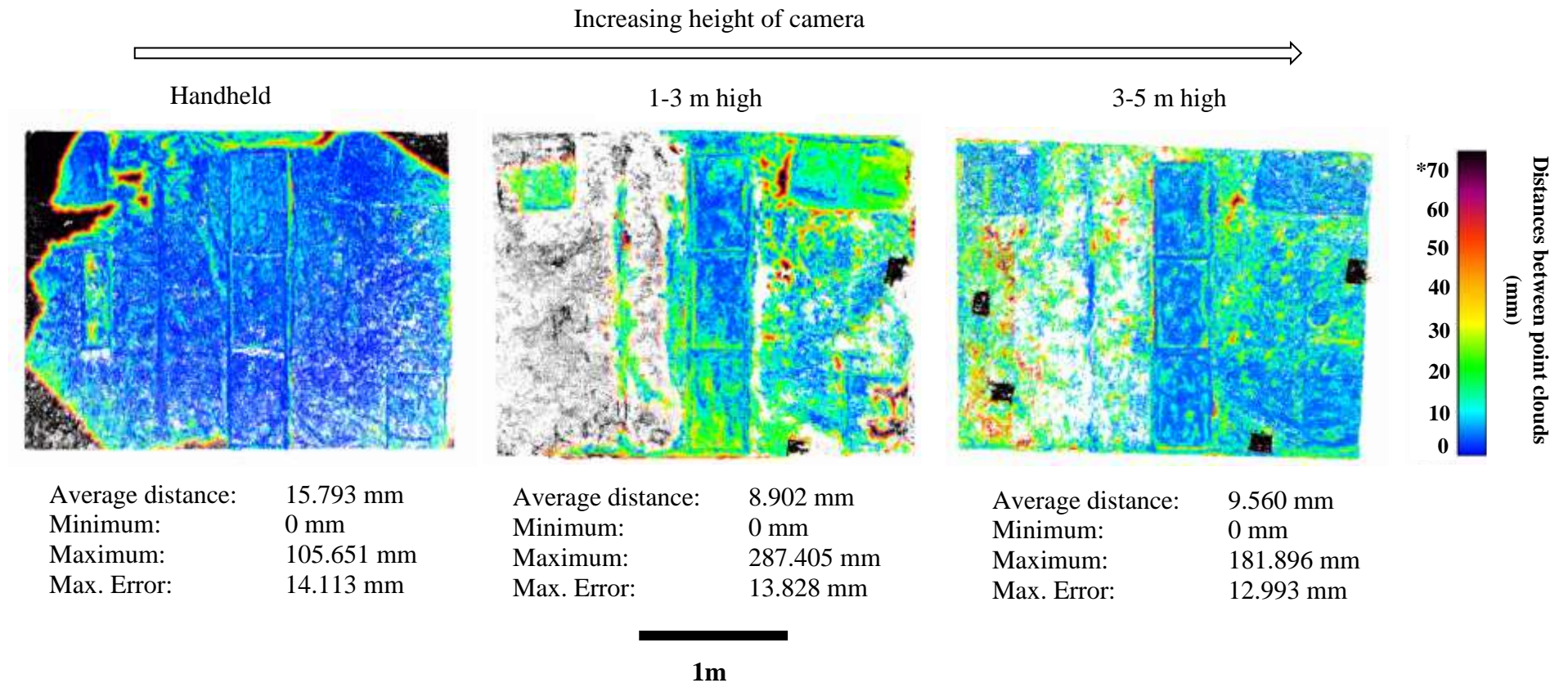


Figure 2.20. Point cloud comparisons from the comparative assessment of camera type: Panasonic Lumix DMC-GH4 DSLR camera compared to an action camera. Images show disparity in point cloud distances between two equally scaled point clouds. These examples are created from the circular path with the camera stills used as the reference entity. A value of *70 refers to areas of the point cloud where heavy weighted items were added between flights.

Results show large disparity in absolute distances between close range photogrammetry and aerial photogrammetry at 3-5 m with an average distance between points of 13.69 mm (Figure 2.21b). The distance between the two point clouds is ~50 mm in one of the trays containing experimental tracks, highlighting that the higher that a UAV is flown, then model accuracy is reduced by 20.33% relative to recording via close-range photogrammetry. This has considerable implications for recording smaller objects to a high standard: the dimensions of the model are unreliable.

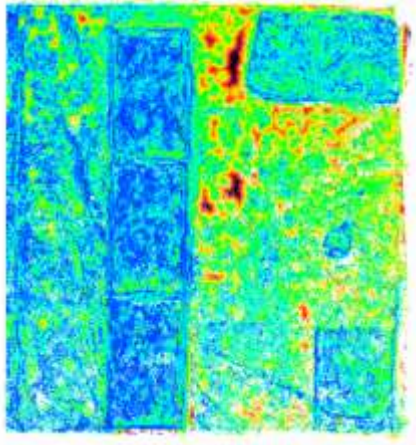
Interestingly, one of the Laetoli replica tracks (G2/3-25) demonstrates ~0 mm distance between points belonging to the close-range models and aerial models at 3-5 m (object in the top right corner of Figure 2.21b). G2/3-25 has a standardised depth of 30 mm, which is comparable to the other Laetoli tracks (Masao et al. 2016) included in the flight tests. However, G2/3-25 exhibits steep track borders with a uniformly distributed base relative to the other tracks whereby the basal depth of the other tracks are uneven. A combination of steep track borders, a uniform track base and the cast colours (the casts were manufactured with a grey background with the tracks in brown) likely emphasised the track outline in each photograph, aiding precise reconstruction of deep tracks. This indicates that complex shallower track morphologies with uneven bases may be reconstructed less accurately using aerial photogrammetry.

The model created from aerial photogrammetry at 3-5 m was sparse, with less density of points per region than the other models (Figure 2.21c; Table 2.9). The average distance between points belonging to the UAV flight at 1-3 m and 3-5 m was 12.12 mm. The greatest disparity between these two models exist around the object edges of up to ~40 mm discrepancy. This confirms the conclusion that using a UAV at a greater height with an action camera produces unreliable depth dimensionality.

The Panasonic Lumix DMC-GH4 DSLR at various heights

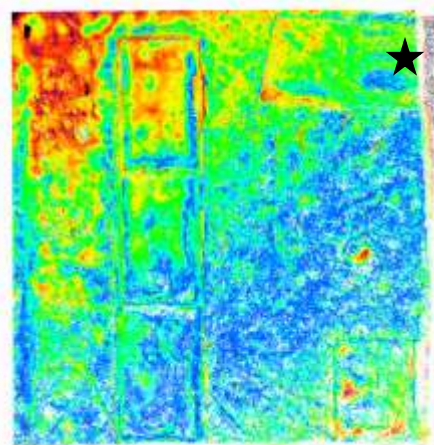
Cloud to cloud comparisons of the above results have all incorporated the action camera data. The specifications of the action camera are not as advanced as the Panasonic Lumix DMC-GH4 DSLR (Table 2.4). The issue discussed in point cloud disparity at various heights and recording methods (stills versus video) may be influenced by use of the action camera. The point cloud comparisons were recomputed using the Panasonic Lumix DMC-GH4 DSLR camera which captures data with an effective 16.1 megapixels in comparison to the action camera which captures data with an effective 12 megapixels (Table 2.4; Figure 2.22).

(A) Handheld action camera compared to an action camera attached to a UAV at 1-3 m high



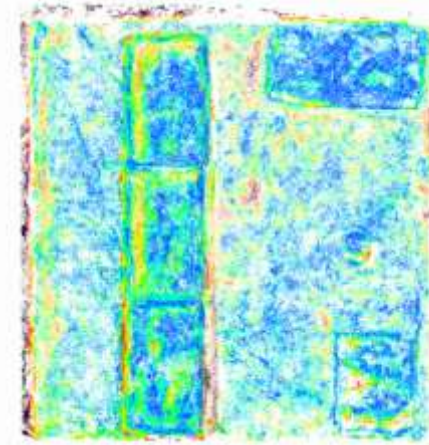
Average distance: 6.705 mm
 Minimum: 0 mm
 Maximum: 87.573 mm
 Max. Error: 9.786 mm

(B) Handheld action camera compared to an action camera attached to a UAV at 3-5 m high

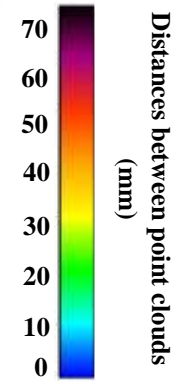


Average distance: 13.688 mm
 Minimum: 0 mm
 Maximum: 136.64 mm
 Max. Error: 9.992 mm

(C) An action camera attached to a UAV flown at 1-3 m compared to an action camera attached to a UAV at 3-5 m high



Average distance: 12.119mm
 Minimum: 0 mm
 Maximum: 105.397 mm
 Max. Error: 9.786 mm



1m

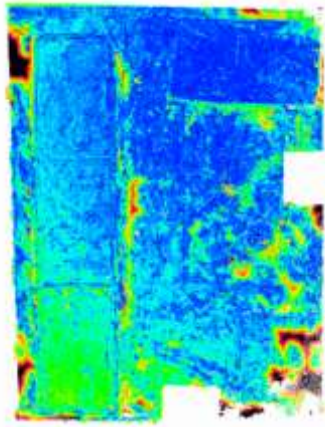
Figure 2.21. Point cloud comparisons from testing the effect of the action camera height on point cloud resolution. Images show disparity in point cloud distances between two equally scaled point clouds. These examples are created from the action camera of the circular path with the camera stills used as the reference entity. The recording area relative to those shown in Figures 2.19 and 2.20 was shortened due to the loss of a light-weighted item that was blown out of the area by the airflow of the UAV. ★ refers to print G2/3-25 (B).

Results show that little disparity in absolute distances were identified between close-range photogrammetry and aerial photogrammetry at 1-3 m, with an average distance between points of 6.71 mm. One of the trays exhibits a cloud to cloud distance of ~20 mm, which would increase any predicted stature value by 8.13% (e.g., an increase of 20 mm in track length would produce a stature prediction of 173.33 cm rather than an accurate stature prediction of 164 cm). There is poor reconstruction of the edges of the other objects (Table 2.9). This indicates that DSLR flight data cannot be used to reconstruct object edges precisely.

Results show disparity in absolute distances between close-range photogrammetry and aerial photogrammetry at 3-5 m, with an average distance between points of 13.69 mm. The distance between the two clouds was ~20 mm in the experimental tracks, but ~50-60 mm in the Laetoli casts. This indicates that if the height of the recording device is increased, model quality declines. This has considerable implications for recording smaller objects to a high standard: with the loss of reliable depth dimensionality (imperative for quantifying the internal morphology of a track) it will be impossible to accurately reconstruct the biometrics and/or biomechanics of the track-maker.

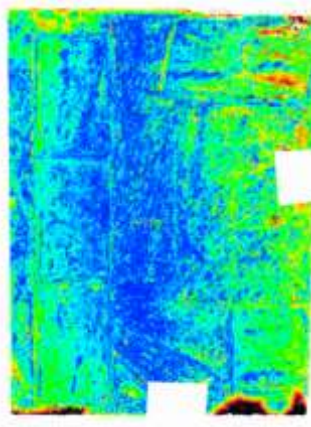
Results show large disparity in absolute distances between each of the aerial photogrammetry models at 1-3 m and at 3-5 m, with an average distance between points of 12.12 mm. The greatest disparity between these two models exist around the edges of the objects of up to ~50 mm discrepancy, with one tray exhibiting ~30 mm in the structures of two tracks. Consequently, the null hypothesis can be rejected as it can be identified that an increase in the height of the UAV consequently decreases model accuracy, similar to the results using the action camera. An UAV at a greater height produces unreliable model reconstructions, regardless of the type of camera attached (Figure 2.22).

(A) Handheld camera compared to a camera attached to a UAV flown at 1-3 m high



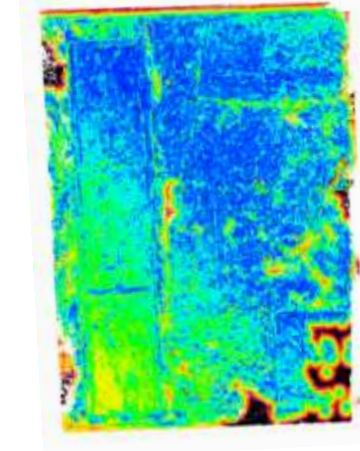
Average distance: 6.705 mm
 Minimum: 0 mm
 Maximum: 87.573 mm
 Max. Error: 9.786 mm

(B) Handheld camera compared to a camera attached to a UAV flown at 3-5 m high

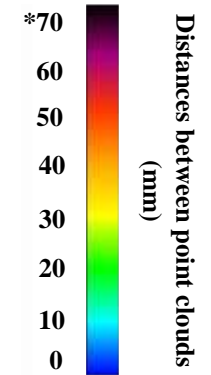


Average distance: 13.688 mm
 Minimum: 0 mm
 Maximum: 136.64 mm
 Max. Error: 9.992 mm

(C) A camera attached to a UAV flown at 1-3m compared to a camera attached to a UAV flown at 3-5 m high



Average distance: 12.119 mm
 Minimum: 0 mm
 Maximum: 105.397 mm
 Max. Error: 9.786 mm



1m

Figure 2.22. Point cloud comparisons from testing the effect of the camera height on point cloud resolution between two equally scaled point clouds. These examples are created from the Panasonic Lumix DMC-GH4 DSLR camera of the circular path with the camera stills used as the reference entity. Recording area was shortened due to the loss of a light-weighted item that was blown away from the area by the airflow of the UAV. Point clouds were cropped to exclude the additional weighted items as other areas of the models (in black) experienced distances of 75 mm+ between points.

2.3.9 Shape variability in model reconstruction

To determine if shape/size was variable between each 3D mesh belonging to variable flight paths, height of the recording devices and camera type, GM methods were applied. During the first set of experiments only two tracks were selected for this analysis. During the second set of experiments, the entire recording area was used, but the area was sub-divided into five sections (Figure 2.23). This permitted a comprehensive assessment of shape change that incorporated most objects. All analyses from each object were computed separately due to issues with landmark placement. The loss of some regions of meshes during model reconstruction or poor mesh quality inhibited homologous landmarks to be reliably placed on all models (e.g., poor reconstruction of the Laetoli casts from the model created using an action camera at 3-5 m high prevented adequate landmark placement. If all objects were to be inclusive in one set of shape-space assessments, then this model would have been excluded due to the poor reconstruction of just one region of the model). Sub-division of the area incorporated all objects in the recording area to be included in the statistical analyses. In total, this sub-division of both sets of experimental data provided seven sets of shape-space results. All statistical results will be presented here, but only one set of results will be graphically displayed as an example: object two (which contains two experimental tracks) from the second set of experiments.

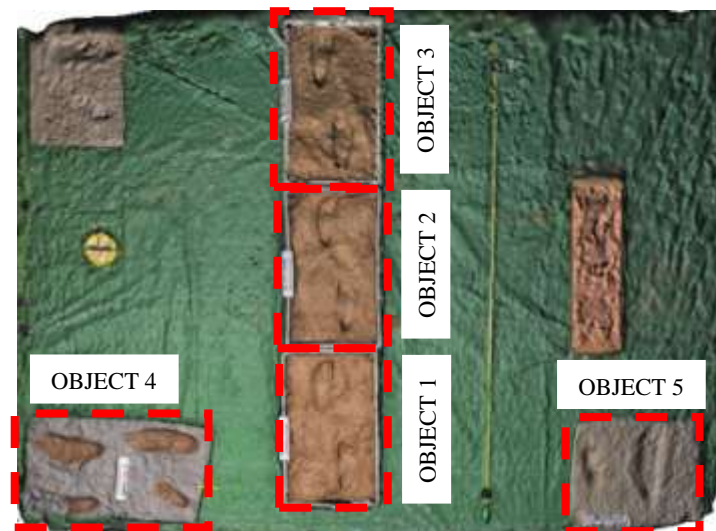


Figure 2.23. Example of a 3D mesh with the sub-division of each object.

Shape variability determined during the first set of flight experiments

The results from the first set of experiments displayed significant variability between flight height ($F=4.987$; $P\leq 0.001$) and flight path ($F=5.288$; $P\leq 0.001$), as shown by a one-way ANOVA (Table 2.10). Levels of significance were computed by permutation tests to a 95% confidence level, using 1000 permutations which tests the sampling distributions. The results of the PCA show a cluster of data points belonging to all close-range and aerial photogrammetry data using the Nikon DSLR D3200 at 1-3 m, with configurations belonging to aerial data of increased height (3-5 m high) for the Nikon DSLR D3200 and all action camera (1-3 m and 3-5 m high) identified as outliers (e.g., shape was significantly variable in these models). Importantly, flight height negatively affected track shape, producing incorrect outline shape and depth dimensionality. This was further affected by flight path. Camera mode (recording via camera stills versus video) did not affect the accurate reconstruction of track morphology ($P=0.229$).

An ANOVA was computed to determine if there were any patterns of shape covariations with size (Table 2.10). No disparity was found between shape (each landmark configuration) and CS ($P\geq 0.05$).

Table 2.10. ANOVA results of intra group variability within the first set of experiments, grouped according to three categorical variables. P values in bold represent statistically significant variability in shape.

Variable	DF	SS	MS	R ²	F	P
Camera Height	2	0.048	0.024	0.227	4.987	0.001
Flight Path	3	0.028	0.004	0.131	5.288	0.001
Camera Mode	2	0.013	0.007	0.063	1.301	0.229
Shape:Size	3	0.014	0.005	0.068	0.796	0.861

Shape variability determined during the second set of flight experiments

The results from the second set of experiments produced comparable results to those from the first set: there was significant variability determined between flight heights, as shown by a one-way ANOVA (Table 2.11). The results of the PCA for all objects generally show

a clustered mix of PC scores of all models, with the same factors producing outliers across all objects along PC1 and PC2: the action camera video consistently produced models with inaccurate depth dimensionality and shape reconstructions, regardless of whether close-range or aerial photogrammetry was employed (Figure 2.24a). Yet, the cloud to cloud comparisons demonstrated that action camera video produced preferable point clouds, particularly around object edges compared to the Panasonic Lumix DMC-GH4 DSLR camera stills during aerial photogrammetry (Table 2.9), although the point cloud density was identified to be low in the action camera models. The interpolation of sparse vertices within the dense clouds (Table 2.6) during mesh creation ‘simplified’ the topographical features of each model captured, regardless of the flight path or height implemented. Consequently, landmark heights may have been increased/decreased relative to other landmark positions, thus warping the landmark configurations used in these analyses. Alternatively, the homology of each landmark positioning could have been affected by the interpolation of vertices during mesh creation, resulting in models with poor outline definition (e.g., see Figure 2.17b). Although the inclusion and exclusion of each model based on homology and clear model definition was carefully considered prior to these assessments (Section 2.3.5; Figure 2.14), the presence of the two outliers on the PCA plot (Figure 2.24a) demonstrate that models created from action camera video data are morphologically disparate from those created via other methods and that landmarks cannot be adequately placed onto these models. Landmarks are used to extract linear measurements of a track, which are subsequently used to predict biometric information and/or biomechanical inferences about the track-maker (Bennett and Morse 2014). Ultimately, these results determine that action camera video cannot be used to reconstruct fossil tracks. Any 3D models created via this method will produce grossly incorrect biometric predictions and biomechanical inferences.

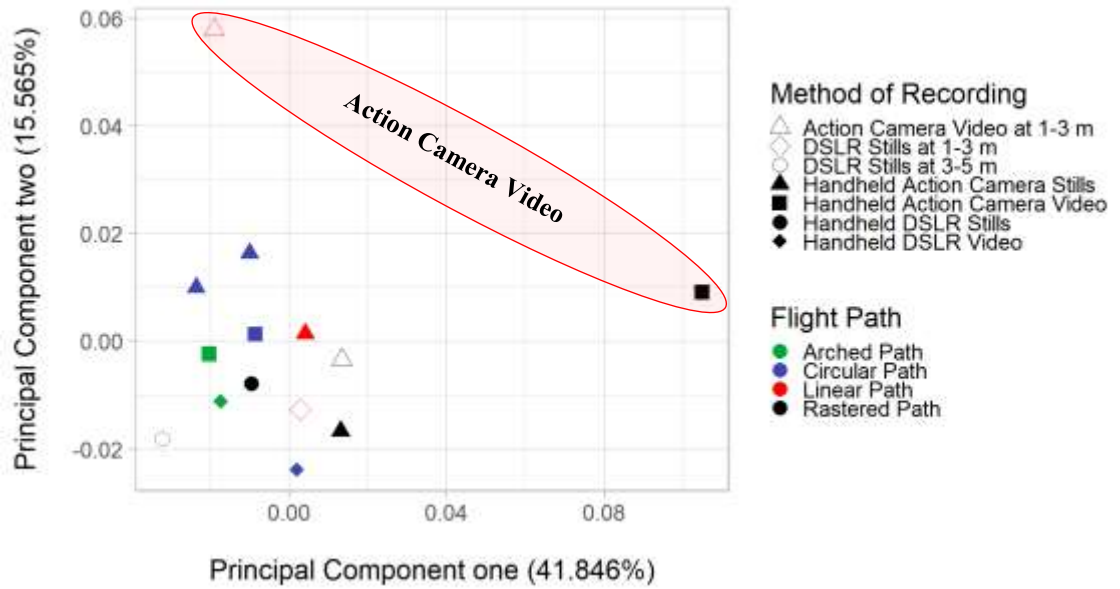
Shape change along PC3 and PC4 was represented by a cluster of data points (similar to shape change along PC1 and PC2), with no clear identification of the causal factor, as shape disparity was not caused by flight path or camera mode. The identified variance between the clustered points is likely observer error, which is an expected factor for any study employing GM methods (Bookstein 1991; Zelditch et al. 2012). Reliability tests of landmark placement determined that all landmarks were consistently and reliably placed. The only evident causal factor for disparity between models was via the deployment of aerial photogrammetry.

One outlier was identified along PC3 and PC4: the model captured via the Panasonic Lumix DMC-GH4 DSLR camera stills at 3-5 m. This model had a reduced point cloud density (Table 2.6) and inaccurately reconstructed model edges relative to the other Panasonic Lumix DMC-GH4 DSLR data (Figure 2.22c). This is most likely the result of reduced photograph overlap as a combination of shutter speed and captured area at an increased height (3-5 m), with a rolling shutter potentially warping true shape.

Table 2.11. Results of the one-way ANOVA computed on the landmark configurations of the second set of experiments. P values in bold represent statistically significant variability in shape.

		DF	SS	MS	R ²	F	P
Object 1	Camera Height	4	0.013	0.003	0.365	2.423	0.011
	Flight Path	3	0.008	0.003	0.214	1.226	0.227
	Camera Mode	1	0.003	0.003	0.079	1.357	0.149
	Shape:Size	1	0.004	0.004	0.106	1.667	0.106
Object 2	Camera Height	2	0.006	0.003	0.183	1.231	0.244
	Flight Path	3	0.008	0.003	0.245	1.083	0.343
	Camera Mode	1	0.002	0.002	0.068	0.872	0.628
	Shape:Size	1	0.005	0.005	0.157	2.236	0.077
Object 3	Camera Height	1	0.290	0.290	0.193	3.601	0.060
	Flight Path	3	0.199	0.066	0.132	0.610	0.706
	Camera Mode	1	0.083	0.083	0.055	0.823	0.575
	Shape:Size	1	0.148	0.148	0.099	1.534	0.137
Object 4	Camera Height	2	0.024	0.012	0.432	2.069	0.013
	Flight Path	2	0.017	0.013	0.293	1.037	0.464
	Camera Mode	1	0.011	0.011	0.196	1.464	0.207
	Shape:Size	1	0.014	0.014	0.244	1.947	0.145
Object 5	Camera Height	6	0.031	0.005	0.589	3.157	0.004
	Flight Path	3	0.031	0.010	0.578	3.152	0.067
	Camera Mode	2	0.012	0.012	0.223	3.652	0.003
	Shape:Size	1	0.018	0.018	0.327	2.910	0.044

A.



B.

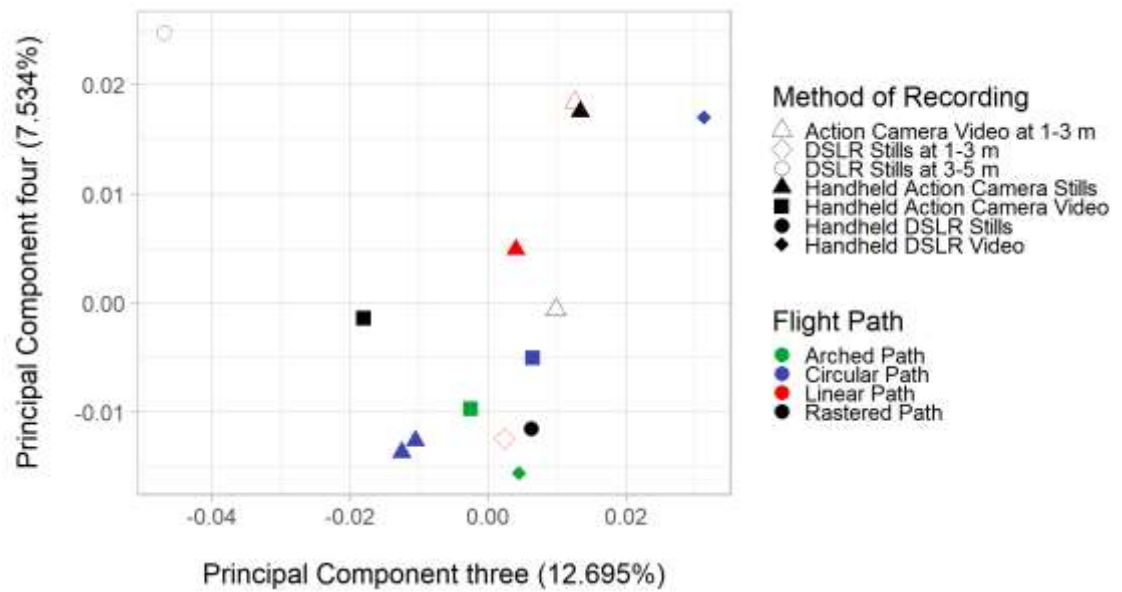


Figure 2.24. Example of PCA plots for object two. These PCA graphs illustrate the shape change between models along PC1 and PC2 (A) and PC3 and PC4 (B) created from different heights; handheld, a UAV flown at 1-3 m high and at 3-5 m high. The outliers identified in (A) belong to the action camera video models and the outlier in (B) belongs to the Panasonic Lumix DMC-GH4 DSLR camera at 3-5 m.

No pattern was determined for flight path or the recording mode of the camera, as both factors produced non-significant shape parameters between models ($P \geq 0.05$ across all objects, with the exception of object five whereby $n=1$ for the outlier which weighted significance values) along PC1 and PC2 and along PC3 and PC4 (Figure 2.22).

An ANOVA was also computed between each landmark configuration and its corresponding CS. No disparity was found between shape (each landmark configuration) and CS ($P \geq 0.05$), except for object five (Table 2.11). This object was located furthest from the centre of the model and was captured by fewer photographs than the other objects due to its position, although this is an unlikely explanation to account for a statistically significant value, which would be best described as marginally non-significant ($P=0.044$). The distortion caused by camera parallax in the linear and arched paths (despite the poorer models being excluded from these analyses) coupled with reduced photograph overlap that impeded accurate model reconstruction is the probable cause for this result.

2.3.10 Size variability in model reconstruction

Finally, linear measurements of each of the tracks and of the objects of known dimensions were collected on the 3D models. Measurements were not collected on the models created from the UAV at 3-5 m high via an action camera due to poor model quality inhibiting the tracks from being distinguishable. A paired samples Student's *t*-test was computed on the linear measurements, which were grouped according to the same categorical variables that were used in the GM analyses. No variability was determined between the action camera and the DSLR camera at any height, or between flight paths ($P \geq 0.05$ between all measurements) (Table 2.12).

Despite no significance being determined between linear measurements in the Student's *t*-test, the results must be considered in terms of applicability for ichnological studies. The greatest discrepancy of one of the modelled experimental tracks (created from the action camera using video, following a linear path and flown at 1-3 m) is +11.12% greater than the true track length measured during the experiments. Foot length is commonly used to predict stature of fossil and forensic tracks (e.g., Domjanic et al. 2010; Bennett and Morse 2014). By using Martin's ratio (Martin 1914), stature prediction of the true foot length measured from the track-maker accurately provides a stature of 164 cm. Whereas, if stature is predicted using the foot length value that is 2.56 cm greater in length, then

stature prediction is found to be 181.07 cm, suggesting that the track-maker is 17.07 cm taller than reality. This indicates that this method of recording and others, whereby depth is poorly reconstructed around the track borders, are not reliable for recording smaller items that need to be accurately recorded for extensive post-excavation assessment, despite statistical assessments suggesting values are non-significantly disparate.

Size discrepancies may be construed as a scaling issue. Models were checked for scale by re-measuring numerous scale bars placed within the recording area. All models were accurately scaled. The issue may then be related to problems with reconstructing depth, which have consequently affected the outline shape of the tracks – these issues were identified during the point cloud comparisons. Determining the ‘true’ border of a track can be complex, with the outline shape changing between various researchers depending on interpretations of outline sediment displacement (Lockley and Hunt 1995; Manning 1999; Marty et al. 2009; Bennett and Morse 2014), although in recent years researchers have established a consistent method for measuring fossil tracks (Bates 2006; Bennett and Morse 2014; Falkingham 2016; Falkingham et al. 2018).

With a loss of depth dimensionality around the borders of a track from UAV data (~10 mm), interpretations on ‘true’ track outline can be lost, leading to discrepancies in track-maker inferences. The results presented here indicate that size variability exists between models. However, this seems unlikely as scale was found to be accurate. Rather than flight data producing models of variable size, the issue presented here is most likely the result of a loss of accurate depth reconstruction that impeded precise landmark distinction on the outline shape of each track, emphasised by the interpolation of sparse vertices during mesh creation that ultimately distorted and ‘simplified’ the topographical features of each track. The variability identified may be the result of either (1) observer-error in misidentifying landmark placement as the direct consequence of poorly reconstructed models; or (2) self-occlusion during data capture that inadequately recorded the complex internal structure of a track.

Table 2.12. Results of the dependent, two-tailed Student’s *t*-test for paired samples of object measurements (mm), using one of the experimental tracks as a statistical example. All objects (n=20 objects, including tracks) produced comparable results, whereby no linear measurements of any of the objects were identified to be significantly different. ‘Var1’ represents the mean of the first variable included in the test (e.g., close-range photogrammetry with all flight paths included). ‘Var2’ represents the mean of the second variable (e.g., aerial photogrammetry at 1-3 m with all flight paths included).

		DF	Mean		Mean Variance	Std. Deviation	Std. Error Mean	95% Confidence Interval of Difference		t	P
			Var1	Var2				Lower	Upper		
Camera stills:	Close range ~ aerial: 1-3 m	1	255.535	254.850	-2.785	6.357	4.495	-5.9899	5.4329	-0.620	0.647
	Close range ~ aerial: 3-5 m	1	255.535	252.750	8.956	6.160	4.356	-4.6386	6.4297	2.056	0.288
	Aerial: 1-3 m ~ aerial: 3-5 m	1	254.850	252.750	11.741	12.516	8.851	-10.0716	12.4197	1.327	0.411
Video capture:	Close range ~ aerial: 1-3 m	1	253.690	256.770	-24.911	19.489	13.781	-20.0015	15.0193	-1.808	0.322
	Close range ~ aerial: 3-5 m	1	253.690	233.843	-28.360	30.151	21.320	-29.9256	24.2536	-1.330	0.410
	Aerial: 1-3 m ~ aerial: 3-5 m	1	256.770	233.843	-3.449	10.662	7.539	-9.9241	9.2343	-0.457	0.727
Handheld:	Camera stills ~ video capture	1	255.535	253.690	29.200	24.126	17.060	-18.7568	24.5968	1.712	0.337
Aerial: 1-3 m:	Camera stills ~ video capture	1	254.850	256.770	7.074	10.994	7.774	-9.1704	10.5852	0.910	0.530
Aerial: 3-5 m:	Camera stills ~ video capture	1	252.750	233.843	-8.116	12.184	8.616	-11.7586	10.1355	-0.942	0.519
Between-groups	Circular ~ raster	1	255.140	256.125	-0.985	31.445	22.235	-28.3507	28.1537	-0.044	0.972
	Circular ~ linear	1	255.140	248.060	7.080	3.635	2.570	-2.5575	3.9735	2.755	0.222
	Circular ~ arched	3	255.140	250.035	0.035	19.000	9.500	-3.0198	3.0268	0.004	0.997
	Raster ~ linear	1	256.125	248.060	8.065	27.811	19.665	-24.1803	25.7933	0.410	0.752
	Raster ~ arch	1	256.125	250.035	6.090	10.055	7.110	-8.4251	9.6431	0.857	0.549
	Linear ~ Arch	1	250.035	248.060	-1.975	17.755	12.555	-16.1501	15.7551	-0.157	0.901

2.3.11 Discussion

This study had one main objective: to determine if high quality models with high precision can be captured via UAV. The results have demonstrated that currently UAV technology coupled with photogrammetry does not meet the standards required by ichnologists, whereby 3D models of tracks are required to be precise to permit linear measurements to be extracted and a comprehensive assessment of morphology to be conducted (Bennett and Morse 2014). Models are required to be accurate and of high quality to facilitate extensive post-excavation analysis (Belvedere et al. 2018; Falkingham et al. 2018). A comprehensive set of experiments including various flight paths, camera types and camera modes were tested, following in-field practises of using the most commonly deployed camera types (DSLR and action cameras) and recording methods. Results show that close-range photogrammetry (any camera model) produced the greatest quality models, whereas an action camera attached to a UAV at 3-5 m high produced the lowest quality models, corresponding to the trade-off in camera specifications.

These results have considerable implications for palaeoanthropology. As demonstrated in Section 2.2, there is a requirement to rapidly record fossils before extensive erosion occurs (Wiseman and De Groote 2018). There is also the need to remove the excavator from a locality to minimise potential damage to fragile fossils and to allow greater digital preservation of a site. However, currently if a UAV is used to record an area of interest then poor quality models are produced. Numerous explanations can be presented to account for a reduction in quality: (1) there is the loss of control over camera settings once the UAV is airborne, coupled with a potential lack of capturing sufficient data for digital reconstruction; (2) motion blur is often unavoidable and will be problematic on all sites, particularly in natural areas whereby simple occurrences of grass movement etc. in the wind will cause significant motion blur to occur; and (3) minute changes in depth of a surface, such as those present in the negative impression of a shallow track, cannot be captured by a UAV flown at any height when the UAV is deployed indoors, as the flight path is insufficiently designed to capture enough photographs to reconstruct these intricate details. If these experiments were repeated in an outdoor environment, then GPS stabilisation may result in improved model resolution and accuracy. However, the results presented here do suggest that aerial photogrammetry (particularly at 3-5 m) is insufficient to record small objects, such as a track. Further investigation incorporating a greater range of variables is required.

Although it may be argued that discrepancies in depth reconstruction are quite small, the loss of any depth as the direct result of the method of recording is non-conformable with the requirements of palaeoanthropology. Changes in outline metrics and internal morphology, no matter how statistically insignificant, can have significant effects on biometric predictions and kinematic inferences of the track-maker.

The question now exists: at what threshold is data captured from an UAV unreliable? The maximum size discrepancy in the tracks (disregarding noisy and poorly reconstructed point clouds) presented in this study was ~30 mm. This value would significantly change any biometric predictions and/or biomechanical inferences (e.g., Section 2.3.8). Based upon the results of these sets of experiments, it is recommended that, if possible, objects should be recorded via a handheld DSLR camera following either a circular or rastered path. If the area must be recorded via UAV to minimise loss of fossil data due to time constraints (e.g., an incoming tide in coastal localities that would lead to the immersion and probable destruction of fossilised objects) or to utilise a non-destructive recording method (e.g., to remove the excavator from site to minimise destruction to the fossil sediments), it is recommended to use a DSLR camera attached to the UAV flown as close to the object as possible following a circular path, rather than the traditionally used action camera. If a linear or arched path is used, depth dimensionality is expected to be lost, with incorrect object dimensions. If the height of the UAV exceeds 3 m, the shape of the model is expected to be poorly reconstructed.

Campana (2017) stated that the use of UAV technology for the creation of high quality 3D models has improved in recent years, but that there remains room for improvement. The current study has identified considerable methodological issues with UAV height (and, subsequently, camera stabilisation), flight path (that caused significant camera parallax issues) and camera choice that will need to be refined in the future, complimenting previous concerns with UAV use.

2.3.12 Limitations of the study

This is a preliminary assessment of UAV applicability that is not without its limitations. This study only tested the use of two types of UAV: the f550 and the s900. Other UAVs may provide greater camera stabilisation during flight trajectories, thus potentially reducing the amount of motion blur, which would be augmented by conducting these flights outdoors to improve GPS stabilisation of the UAV platform. The UAVs used in this study produced the greatest amount of motion blur when the UAV was turned to

follow the flight path trajectory. Greater stabilisation of the camera when the yaw of the UAV is altered (e.g., during the circular path to maintain a focused 45° fixed angle) would produce higher quality photographs, improving model quality, and quite possibly precision also.

The use of a 3D gimbal that controls movement and improves stabilisation would likely improve photograph quality. Quality would also likely be improved by replicating these experiments in an outdoor space. The current experiments were conducted within an indoor space, thus omitting the use of GPS stabilisation. An outdoor use of UAV technology would likely increase aircraft stability due to GPS stabilisation, thus reducing the amount of blur in photographs by utilising GPS stabilisation of the camera platform but environmental factors, such as wind, may cause further issues.

Outdoor flights were not conducted as a part of this chapter due to issues with gaining licensed flying permission/insurance in areas suitable to implement the experimental trackways (e.g., the surrounding areas in Liverpool, Merseyside are prohibited due to nearby airports and Site(s) of Special Scientific Interest for wildlife protection). Consequently, it was decided to conduct all flight trials indoors.

Data capture length could be another factor causing poor model reconstruction. Although recording time was not too variable (Table 2.13), a reduced recording period (albeit, a matter of seconds) is expected to have resulted in less photographs captured. Future experiments would be enhanced by controlling for the time spent recording an area of interest. Additionally, if these experiments are repeated outdoors then the number of photographs discarded due to blur should be reduced, thus augmenting the available photograph selection for 3D reconstructions.

The choice of UAV in this study also limited the type of camera and lens that could be attached to the payload. UAVs are limited by the weight of the payload, with heavier items diminishing battery life (GIM International: Mapping the World, 2016; Mansouri et al. 2017). Future experiments could incorporate a larger and more powerful UAV, such as a high-end multicopter UAV (although this would likely come at the expense of increased airflow that may destroy the sediment if flown too lowly), permitting an improved choice of camera and lens; or could use a powerful, light and compact DSLR camera.

Table 2.13. Data capture time in seconds from the second set of UAV flight tests to record an area measuring 5 m by 3 m. No video data was captured of the Panasonic Lumix DMC-GH4 DSLR due to UAV/propeller damage during the flights. Flight duration was not recorded during the first set of experiments. Duration of each flight path during close-range photogrammetry is also reported.

	Action Camera: GoPro Hero 4 Black				Panasonic Lumix DMC- GH4 DSLR	
	1-3 m high		3-5 m high		1-3 m high	3-5 m high
	<i>Stills</i>	<i>Video</i>	<i>Stills</i>	<i>Video</i>	<i>Stills</i>	<i>Stills</i>
Arched Path	21.12	22.98	26.67	33.44	35.30	28.74
Circular Path	63.10	42.38	67.71	55.75	47.24	39.56
Linear Path	16.52	14.17	17.30	14.86	15.12	16.22
Rastered Path	38.93	39.50	35.65	34.23	31.76	31.62
	Handheld				Handheld	
	<i>Stills</i>		<i>Video</i>		<i>Stills</i>	<i>Video</i>
Arched Path	120.00		35.00		120.00	41.00
Circular Path	60.00		42.00		120.00	31.00
Linear Path	60.00		12.00		60.00	15.00
Rastered Path	120.00		28.00		180.00	29.00

However, neither of these suggestions could be implemented without consideration of an improved flight path. Within the current study there is the possibility that insufficient data was captured as the direct result of the designed flight paths, resulting in poor quality models being reconstructed. Flight paths that are refined and specifically designed to capture minute changes in depth across a surface would be essential. Furthermore, it is recommended that future tests use a combination of longer flights and repeated flight paths in an outdoor setting to utilise GPS stabilisation thereby increasing photograph overlap. Flight data designed in this manner may find that high quality models can be produced than those created during the experiments presented in this chapter.

Finally, if issues with flight path and payload can be refined and rectified, issues with software may still be paramount. This study reconstructed all models in just one software: Pix4Dmapper. A few of the models discussed in this chapter were also reconstructed in

Agisoft PhotoScan Professional (v.1.3.4. Agisoft, St. Petersburg, Russia). Whilst no analyses were conducted on these reconstructions, visual inspection of the reconstructions have identified models that are plagued by distortion (the linear and arched paths), similar to the Pix4Dmapper reconstructions. Although the distortion in the Agisoft PhotoScan reconstructions are not as severe as those reconstructed from the arched and linear paths in Pix4Dmapper, any identified distortion results in unusable models. In field practises, data would likely need to be recollected.

The rastered and circular flight paths were reconstructed in Agisoft PhotoScan with no distortion and with little noise error. However, the produced meshes were automatically simplified and smoothed in comparison to the replica reconstructions from Pix4Dmapper. This suggests that Agisoft PhotoScan cannot be used to reconstruct minute changes in depth (e.g., the negative impression of a track) if the height of the recording device is increased (e.g., via UAV). Other photogrammetry software may reconstruct models with minimal distortion/parallax and noise error. Future flight tests should incorporate a range of photogrammetry software, including a re-test of Pix4Dmapper and Agisoft PhotoScan with new datasets, to validate these results.

This study does not entirely dismiss the use of UAV technology for the recording of heritage sites, but instead highlights that there are considerable methodological issues with depth reconstruction that ultimately affects the shape and size of objects. Rather, it is recommended that flight paths are refined and that there is careful consideration of the recording method. If precise models are desired, such as those of tracks, then the results of this study do not currently endorse the use of a UAV.

Chapter Three

Investigating the relationship between lower limb kinematics, biometrics and track morphology across various types of substrates and speeds

In this chapter track morphology was analysed to investigate shape patterns that can be used to identify the track-maker's biometrics and locomotory behaviour. Experimental tracks were created in substrates of differing compliance at varying speeds and limb postures. Changes in substrate caused variations in track outline metrics which negatively affected biometric predictions, indicating that biometric information (mass, age and sex) cannot currently be reliably extracted from track dimensions, particularly when the underlying substrate moisture content is increased and/or traversing at different speeds, such as a walk to a jog. Patterns of shape disparity were visually identified between experimental tracks. To investigate the interaction between limb kinematics and substrate deformation with the resulting track morphology, 3D Motion Capture Systems were employed to capture modern human movement across a range of substrates. Changes in joint angles were associated with variations in track shape production. Shape variations were also identified in fossil tracks, permitting a potential insight into hominin locomotion.

This chapter forms the basis of three manuscripts which are currently in preparation:

Wiseman, A. L. A. O'Brien, T. & De Groote, I. Revisiting the bent-hip bent-knee hypothesis: a biomechanical investigation of hominin track morphology. *In Preparation*.

Wiseman, A. L. A. O'Brien, T. & De Groote, I. A 3D motion capture approach for investigating the relationship between substrate deformation, limb movement and track formation. *In Preparation*.

Wiseman, A. L. A. O'Brien, T. & De Groote, I. An experimental approach to refining stature prediction of footprints produced in different substrates and several speeds. *In Preparation*.

This chapter was presented at the following conferences:

Wiseman, A. L. A. O'Brien, T. & De Groote, I. 2018. Assessing 3D kinematics across various substrates and speeds in modern humans and the implications for human evolution. *European Society for the Study of Human Evolution 7th Annual Meeting*, Faro, Portugal.

Wiseman, A. L. A. 2017. A multi-disciplinary approach to fossilised trackways: The application of UAV technology and biomechanical assessments. *British Federation of Woman Graduates Annual Meeting*, Liverpool, UK.

This chapter will be presented at the following upcoming conference:

Wiseman, A. L. A. O'Brien, T. & De Groote, I. 2019. Capturing 3D locomotor kinematics of modern humans to determine behavioural substrate navigation. *American Association for Physical Anthropology*, Cleveland, Ohio, USA.

3.0 Abstract

Hominin fossil track discoveries have been used to predict both biometrics and locomotion of the track-makers, yet the relationship between movement and the foot's interaction with the substrate remains poorly understood, inhibiting a comprehensive reconstruction of evolutionary locomotion. To determine the relationship between track morphology, biometrics, limb kinematics and substrate deformation this study employed 3D motion capture systems to characterize movement (hip, knee and ankle) in modern humans across a range of substrates and speeds.

Variations in track outline metrics produced inaccurate biometric predictions. Changes in foot lengths between different substrates and variable speeds were successfully corrected, resulting in the accurate stature and hip height prediction from tracks. Foot width variations could not be corrected-for, resulting in the unreliable predictions of body mass, age and sex, particularly when substrate moisture content is increased and/or speed is altered.

Track shapes were also variable. To identify if shape patterns could be characterised and used to reconstruct limb movement, 3D kinematics were captured of 20 males and 20 females. Significant increases in hip and knee flexion and plantarflexion were associated with distinct track shapes. Hip and knee movement corresponded to pronounced changes in the midfoot arches, signifying that the prominence of arch impressions was susceptible to increases in height (when walking) and volume (fast walking and jogging) if substrate pliancy is decreased. Plantarflexion on a looser substrate caused a ridge-like appearance that extended mediolaterally across the foot, which is reflective of an efficient toe-off. This ridge-like morphology was identified in numerous *Homo* fossil tracks.

Additionally, the association between track shapes with limb posture was analysed. Variable depth distributions and under-represented midfoot shapes were identified when moving with a flexed limb in comparison to an erect limb. Hallux abduction was also determined to be significantly correlated with increasing knee angle. This morphology is similar to the Laetoli, Tanzania tracks suggesting that australopithecines may have walked with a more flexed limb than modern humans.

This study shows that humans alter limb kinematics to accommodate changes in substrate pliancy producing distinct track shapes. Shape patterns were also identified in fossil tracks, permitting a potential insight into hominin locomotion as reflected in footprints.

3.1.0 Introduction

Fossil tracks have been instrumental in palaeoanthropological debates regarding the origins of bipedal behaviour since the first discovery of hominin trackways in 1978 (Leakey and Hay 1979). These interpretations have subsequently influenced the development of novel techniques into reconstructing foot anatomy and locomotion, alongside biometric inferences from track morphology to allow interpretations into track formation (e.g., Day and Wickens 1980; Stern and Susman 1983; Ward 2002; Falkingham 2014; Hatala et al. 2018). The dynamic movement of the plantar surface of the foot interacts with the underlying substrate which displaces accordingly to support body mass during stance (Morse et al. 2013). Ultimately, a footprint is created that is a direct representation of the track-maker. Yet, the footprint is not a true reflection of movement, but rather that of a sequence of integrated dynamic motions of the foot which are associated with substrate mechanics and of biometrics which are reflected in outline metrics (Hatala et al. 2018).

Outline metrics are commonly used to predict biometric information about the track-maker, such as stature, body mass, sex and age (Day and Wickens 1980; White 1980; Charteris 1981; Bennett et al. 2009; Raichlen et al. 2010; Crompton et al. 2012; Ashton et al. 2014; Bennett and Morse 2014; Masao et al. 2016; Hatala et al. 2016c, 2016b). For example, foot length can be used to predict the track-maker's stature (Martin 1914; Robbin 1984; Dingwall et al. 2013). Variations in substrate mechanics which produce variability in track dimensions (Gatesy et al. 1999; Milán 2006) will not accurately identify the track-makers (Bennet and Morse 2014). The error in extracting accurate dimensions from a track increases for those produced on deeper and less compliant substrates due to sediment instability around track borders (Milán 2006; Gatesy and Falkingham 2017). Consequently, extracting biometric information from deep tracks is problematic owing to a poor relationship between track shape with foot shape (Gatesy and Falkingham 2017; Hatala et al. 2018).

This discrepancy in track dimensions which affected biometric predictions was quite pronounced at Walvis Bay, Namibia (Morse et al. 2013). A long singular trackway belonging to one individual was discovered spanning four different substrate typologies ranging from soft to firm, producing track shapes that vary in length and width, thus over- and/or under-estimating the biometrics of the track-maker (Morse et al. 2013). Body mass ranged from severely obese to critically underweight in this individual, as the direct consequence of changes in substrate mechanics.

Due to a poor understanding of the relationship between substrate mechanics and lower limb movement with that of biometrics (D'Août et al. 2010; Falkingham and Gatesy 2014), it is problematic and difficult to extract biomechanical and biometric information from a track (Morse et al. 2013; Hatala et al. 2018). Consequently, no consensus exists between researchers on the locomotory behaviour of the earliest fossil trackways despite the recent employment of new experimental methods (Berge et al. 2006; Bennett et al. 2009; Raichlen et al. 2010; Crompton et al. 2012; Hatala et al. 2016a; Raichlen and Gordon 2017).

In recent years, studies have begun to explore the relationship between substrate deformation and lower limb kinematics by directly testing the effect that biomechanical variables (e.g., joint angles and limb posture) have on track morphology across a range of different substrate typologies with a consideration of biometric characteristics (e.g., Raichlen et al. 2010; Hatala et al. 2016b; Raichlen and Gordon 2017), building upon the pioneering studies that investigated limb posture of the Laetoli track-maker (Day and Wickens 1980; White 1980; Tuttle 1985; White and Suwa 1987). By addressing this issue, biomechanical and biometric variables from fossil tracks can be more reliably predicted. For example, the Laetoli tracks are often used to examine locomotor biomechanics in australopithecines (e.g., Raichlen et al. 2008), but limb posture – and consequently locomotion – remains uncertain (Stern and Susman 1983; Bennett et al., 2009; Hatala et al. 2016a). Changes in locomotion (e.g., employing an erect limb) may be reflected in the outline shape of a track (Hatala et al. 2016a), which could possibly affect biometric predictions. Consequently, biomechanics and biometrics should be treated cumulatively.

Numerous studies within the last five years have explored the relationship between substrate deformation with that of kinematics and biometrics by examining a variety of morphological track traits. One such study identified correlations between proportional toe depths and limb kinematics to explore inferences on limb posture in the Laetoli track-maker (Site G) using comparative trackways from extant primate analogies (*Pan troglodytes*) and concluded that limb posture in fossil tracks could not be reliably established (Hatala et al. 2016a). Yet, another study employed a similar method which permitted the reconstruction of an erect limb posture in the newly discovered Site S trackways (Raichlen and Gordon 2017).

Other studies have explored the relationship between general track depth and foot pressures (D'Août et al. 2010; Bates et al. 2013b; Hatala et al. 2013). Many of these studies reached a consensus that neither foot pressure nor kinematics influence track

morphology, which is generally accepted (Bennett and Morse 2014). However, numerous independent researchers have concluded studies with conflicting results and have so far been unsuccessful in establishing an accepted association between track depths with that of lower limb movement and biometrics (e.g., conclusions drawn from proportional toe depths versus inferences on foot pressures with track depths). Other avenues of morphology must be explored to determine if biomechanical and/or biometric variables are reflected in track morphology so that both factors can be accurately extracted from fossil material (Hatala et al. 2018).

A new, novel method developed by Falkingham and Gatesy (2014) to explore dinosaur track formation and later employed by Hatala et al. (2018) to investigate hominin track formation used biplanar X-ray to assess the dynamic movement of the foot which leads to track production in a variety of substrates. This method permits the direct observation of foot movement through heel strike to toe-off on a given substrate, which was aided by lead ball marker-sets on the foot's plantar surface in Hatala et al.'s (2018) study. 3D motion of the foot was successfully captured and compared to the deformity of the substrate, thus offering an insight into the relationship between motion and substrate deformation in human (n=3) track production for the first time. For example, the shape of the midfoot impression and the heel were both found to be associated with substrate rigidity, with the medial longitudinal arch being quite deformable and susceptible to changes in height as substrate pliancy was altered. Heel width was found to expand on more rigid substrates, producing a U-shape, whereas a V-shape was produced on a more compliant substrate (Hatala et al. 2018). Evidently, biplanar X-ray is a promising advancement for the field of palaeoanthropology.

However, the adoption of biplanar X-ray methods is currently limited. The costs of the laboratory set-up will usually prohibit the capture of a complete gait cycle. Additionally, natural minerals in the substrate will interfere with the subsurface imaging, thus necessitating the research team to utilise synthetic materials (Falkingham and Gatesy 2014; Hatala et al. 2018).

An alternative quantitative approach using 3D kinematic data capture utilising a rigid landmark-based marker-set on the complete lower limb across various types of non-synthetic materials and different speeds offers an opportunity to explore the association between complete limb motions and posture with that of substrate deformity. In doing so, important questions regarding the functional interpretations of track morphology can be

investigated, including an insight into how this may be associated with biometric variables.

3.1.1 Aims and objectives

The overall aim of this chapter was to identify how track morphology will vary between substrates of differing compliancy, and to determine if morphology can be used to identify the track-maker. Additionally, this chapter will explore the relationship between track morphology with lower limb kinematics to provide a comprehensive insight into the locomotory behaviour of the track-maker.

The following objectives were addressed:

- i. To determine if track shapes and dimensions will be variable when created in different substrates and from several types of movement across a given substrate. It was hypothesised that track dimensions would be variable between tracks produced on different substrates at various speeds.
- ii. To identify how lower limb kinematics may vary when a modern human walks across different types of substrate, and if kinematics are further affected when speed is introduced as a variable. In conjunction with variable track dimensions, it was predicted that track shapes would be disparate across these variables because of the direct consequence of changes in lower limb kinematics. Shape patterns will be explored.
- iii. To explore the relationship between increased lower limb flexion with track morphology, and to determine how this relationship may be affected with changes in substrate pliancy.

3.2.1 Study protocol

All data pertaining to the following study was recorded in the Biomechanics Laboratory in the Tom Reilly Building, Liverpool John Moores University. Ethical approval was granted by the Liverpool John Moores University Research Ethics Committee (REC: 16/NSP/041). An overview of the workflow process for testing the objectives of this study can be found in Figure 3.1.

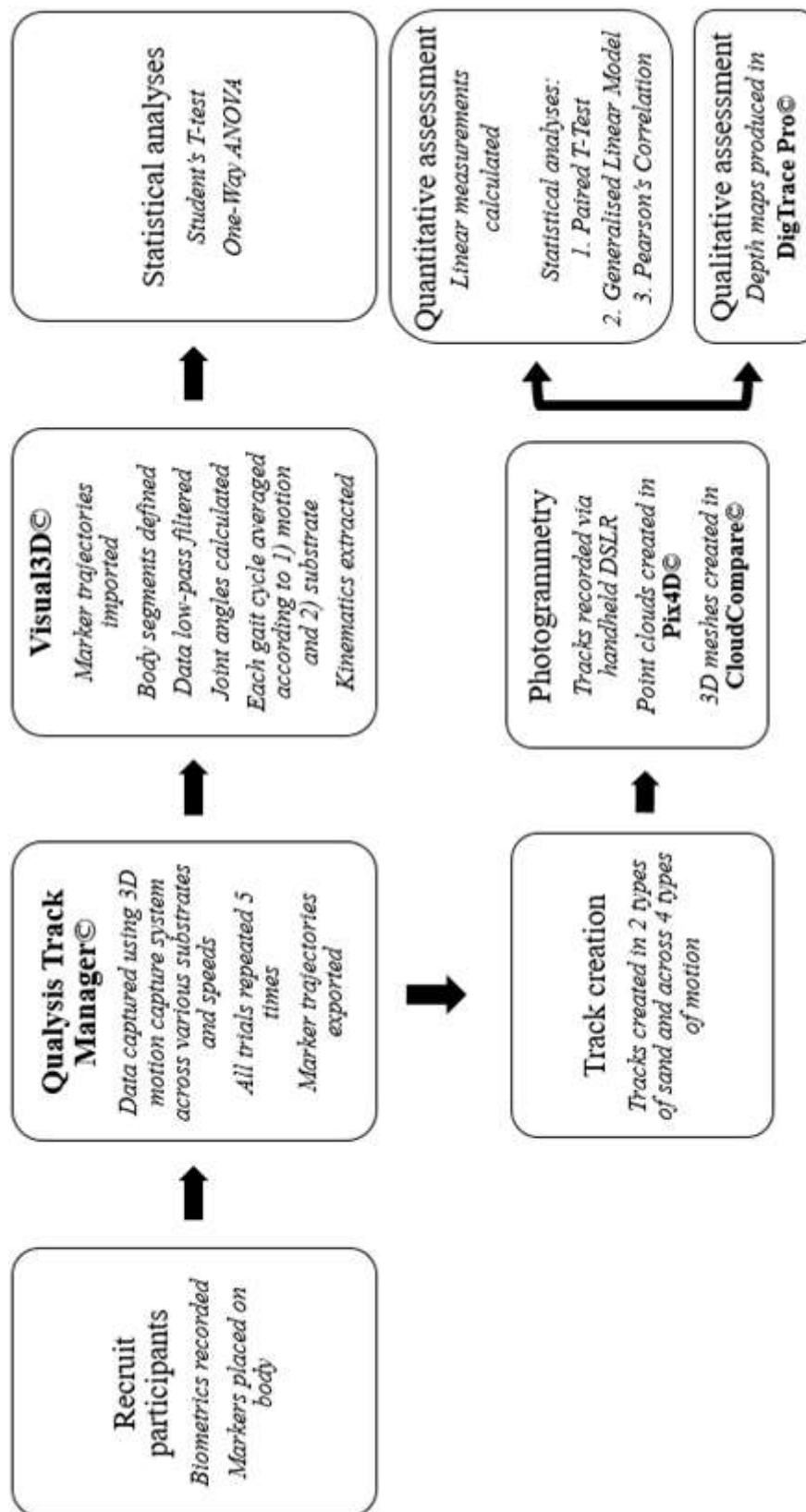


Figure 3.1. Diagram providing an overview of the workflow process for the current study.

Participants were recruited from local university staff and students (see: Appendix D). Adult participants (19 - 40 years old) that were free from current lower limb or spinal

pathologies who were able to move unassisted and whom did not have a history of major limb/spinal trauma were recruited. This resulted in 35 males and 25 females volunteering for the first set of experiments which assessed track morphology, and 21 females and 20 males volunteering to be a participant in the biomechanical trials which repeated the primary experiment protocol, but with the addition of 3D motion capture to record kinematics. Unfortunately, one female participant was later excluded from the latter study due to loss of data (see: Appendix D for information on recruited participants). Participants were selected with the aim to maximise variation in ethnicity, body mass and activity.

Prior to beginning the trials, each participant read a Participant Information Sheet which documented any risks and signed a consent form. Participants were not informed of the hypotheses/predictions of the study. This was a conscious decision by the researcher to prevent any in-depth knowledge of hypotheses/predictions affecting the outcomes of any motion trial.

Additionally, biometric information of each participant was recorded. This included measuring each participant's height, weight, foot length (left and right), hip height, sex, date of birth, and a record of any historical pathology in the lower limb and/or spine; and a record of habitual shoe-wear (i.e., the frequency of wearing high-heeled shoes). Finally, participants completed a short questionnaire regarding their exercise and lifestyle habits (Appendix E). Participants were assigned a unique identification number to anonymise data.

3.2.2 Experimental design

Two trackways were constructed that were filled with fine-grained homogenous sand composed of rounded to sub-angular particles measuring $\sim 0.06\text{-}0.7$ mm in diameter, with an initial standardised depth of 38 mm. Two different water contents were chosen for each trackway: a low-water content and a high-water content. The standards set by Crompton et al. (2012) were employed for track saturation whereby the high-water content trackway was saturated to 20%. This was found to be too saturated, resulting in the immediate water infill of footprints after creation. Water contents were revised to reflect the protocol employed by Raichlen et al. (2010). The high-water content trackway had a saturation of 12% and the low-water content trackway had a saturation of 8%.

Each trackway measured 12 m long by 0.6 m wide, following the recommendation that the minimum length required for adequate gait assessment should be 8 m in length, with a desired length of 12 m for studies that incorporate high-speed running to allow the participant to gain stride prior to data capture (Levine et al. 2012).

Participants were asked to move across each of the substrates at three different speeds: a walk, a fast walk and a run. All participants then employed a flexed limb (that is, they were asked to walk with a bent-hip bent-knee (BHBK) gait. Participants were requested to flex the limb as much as possible during walking to provide a realistic replication of a flexed limb per participant). During the pilot testing of the experimental design it was discovered that when participants ran that their foot penetrated completely through the substrate, coming into contact with the underlying ground. Consequently, two major changes were made to the experimental design of the trackways during the next stage of experiments: the kinematic testing. The trackways were shortened to 9.66 m (although this length may seem arbitrary, this was the length of the uncut planks of wood). Shorter trackways increased the depth of the sand to 44 mm, following the protocol set by D'Août et al. (2010). Additionally, the running pace was removed as a motion, and a jogging pace was introduced instead. By removing the running motion from the trials, it was possible to prevent further loss of data, as any trial with complete substrate penetration would need to be removed from the dataset.

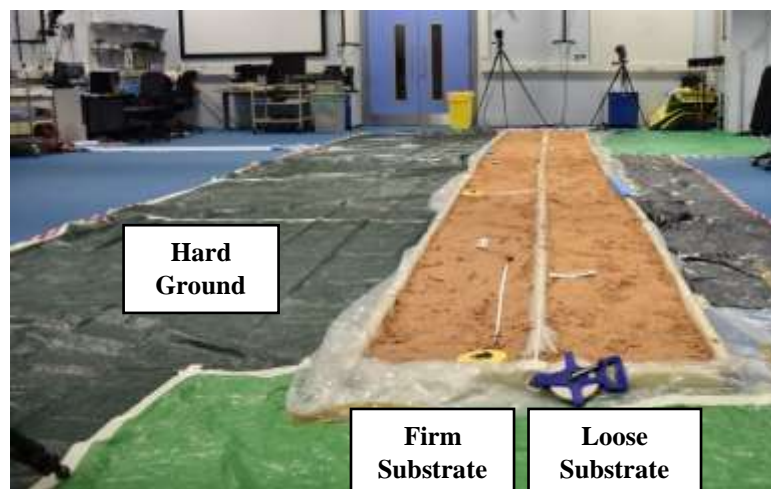


Figure 3.2. Photograph of laboratory set-up.

3.2.3 Photogrammetry

To test for patterns of morphological variability in track shape production, 60 participants were recruited for the first set of experiments. All trials were repeated three times across each substrate at a steady speed to capture the most accurate representation of each participant's movement (Levine et al. 2012) as reflected in a footprint. Speed was controlled for each repeated movement via the use of timing gaiters (Browser TCi Timing System). If speed differed by >1 m/s, then the trial was discarded and redone.

Most importantly, modern shod humans are not accustomed to walking unshod across looser substrates necessitating the need for numerous trials to be repeated for consistency in data. Upon successful completion of the first set of experiments, a further 40 participants were recruited to repeat these experiments, providing a total of 100 participants from a variety of ethnicities, biometrics and ages to permit a comprehensive assessment of track morphology.

Between each individual trial the experimental trackways were flattened using a garden hoe to ensure that all steps were conducted on a flat surface. The trackways were photographed after the final motion from each set of repeated trials. This resulted in eight trackways being recorded per participant in total ($n=100$ participants). All trackways were recorded using a handheld Black Nikon DSLR 5500, with a zoom length of 24 mm following a circular/oval path around the trackways (see: Section 2.3.4). An ISO of 200 was selected, with an aperture of f4 and an exposure of 1/40. A higher aperture was not selected because the saturated sand was quite reflective, necessitating the camera's aperture to remain low for adequate data capture.

Photogrammetry was employed to create point clouds of the tracks in Pix4Dmapper. Point clouds were exported into CloudCompare (v.2.10 OpenGL 2018) for scaling and 3D mesh creation (see: Section 2.3.2).

3.2.4 Statistical analyses of tracks

To determine if track dimensions vary when speed/motion and/or substrate is altered, linear measurements were measured on all tracks. Measurements were conducted on 3D models using CloudCompare (v.2.10 OpenGL 2018) at five points: foot length (from the tip of the hallux to the pternion), the long axis of the foot (from the tip of the 2nd digit to the pternion, passing through the ball of the foot), the forefoot width, and the heel width (Figure 3.3).

Before determining the variability of tracks produced on different substrates at several speeds/motions, sources of error needed to be identified. Error may be introduced in two ways: observer error and via intra-track variability. A two-tailed Student's *t*-test for unequal variances was computed to (1) quantify observer error using repeated measurements of the same tracks (n=5 participants; n=40 tracks); and (2) assess the standard error of step-to-step variance to define intra-track variance (n=100 participants).

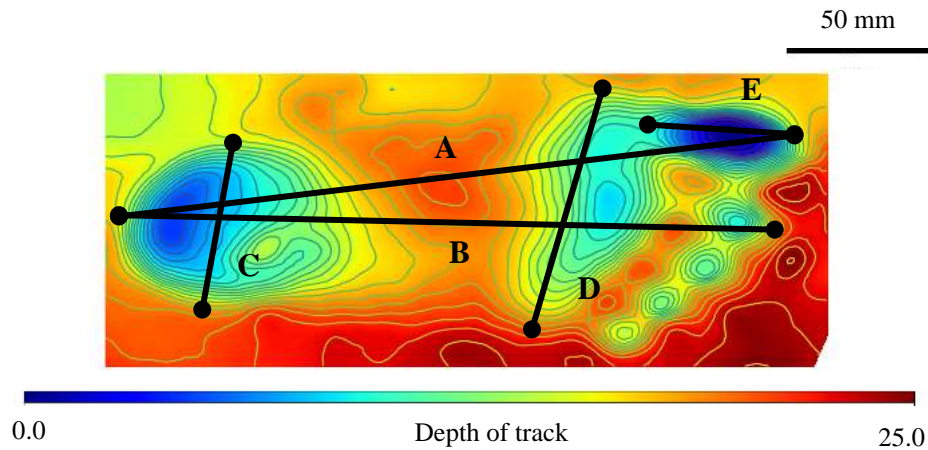


Figure 3.3. Linear dimensions measured in this study. A – Total track length; B – long axis of the foot; C – heel width; D – forefoot width; E – hallux length.

As intra-track variance was identified to exceed that of observer error (see: Table 3.1), then all measurements pertaining to a single individual were averaged. A two-tailed paired Student's *t*-test for sampled means was computed to test for disparity between measurements belonging to the same individual but produced on different substrates at various speeds to determine if track dimensions remain consistent when created in substrates of varying compliancy at several speeds and limb postures. All statistics were computed in R (R Core Team 2017).

Correcting discrepancies in track dimensions

For tracks which were identified to have a significant change in length (an increase or decrease) similar to what was observed in previous studies (e.g., Hatala et al. 2018), a correction factor for that length at a given speed for each of the two substrates was calculated using the unstandardized coefficient of a between-groups regression and the standard error:

$$\text{Corrected Track Length} = m(x) + c$$

The corrected track length was calculated for all track length measurements (n=1776 tracks) using the above equation so that all measurements were consistent between variables to allow for the valid prediction of biometric information from a track. For example, some track lengths were longer on a looser substrate than on a firmer substrate. By using the corrected measurements, these values were less variable per individual across a range of substrates and movements.

3.2.5 Biometric predictions

Stature, age, sex, body mass and hip height are all biometric variables that have been previously predicted from track dimensions (e.g., Bennett et al. 2009; Atamturk 2010; Crompton et al. 2012; Dingwall et al. 2013; Kanchan et al. 2013; Domjanic et al. 2015). To validate the applicability of predicting these variables, each factor (with the exclusion of age and sex) was regressed against true foot length as measured during the experiments using a foot/osteometric board. Where positive associations could be determined, prediction methods were applied to experimental track dimensions to determine if the variable could be accurately predicted despite measurement discrepancies between tracks produced on different substrates and several speeds.

Stature predictions

To test the validity of the correction factors, stature – the most commonly predicted biometric variable – was predicted for all participants using Robbin's Ratio (1984) and Martin's Ratio (1914) (the two most commonly applied stature prediction methods) using track measurements and then using the corrected measurements. Percentage errors were calculated for each predicted stature value using actual stature which was measured during the trials. Results were supported by a Bland-Altman analysis which is a method used to compare two measurements of the same variable (Bland and Altman 1986). The Bland-Altman analysis was primarily used to determine the best method (corrected or non-corrected dimensions) for identifying the track-maker's stature.

Age and sex predictions

To test the accuracy of predicting age and sex from track dimensions, track-maker age was estimated using modern growth curves of the foot derived from the WHO (de Onis 2006) as employed by Ashton et al. (2014) for the prediction of relative age of the Habbisburgh track-makers using 2D measurements, and refined for the Gombore II-2,

Ethiopia trackways (Altamura et al. 2018). Although defining track-maker age is problematic due to ontogeny remaining unknown in hominin species (e.g., the inferred species for the creation of a fossilised trackway), relative age was predicted using an age growth curve for all experimental tracks incorporated into this study using the method defined by Altamura et al. (2018). This method incorporates sex as a covariate. Slight error in age prediction may be present as the boundary between sub-adult and adult is poorly defined (e.g., an adult female could produce a similar track to a sub-adult male). An adult track is classed as 20+ years of age. Because this study only recruited adult participants (19+ years of age), this method produced only a relative age (sub-adult or adult, with the former being incorrect for the assessed population) with an associated sex determinant. Age prediction was included in these analyses to determine if an individual with a small foot could be correctly identified as an adult, or if these methods incorrectly classify these individuals as a sub-adult.

Age and sex were predicted using the averaged track length following the protocol developed by Dingwall et al. (2010) whereby using averaged lengths were identified to reduce the error margin in true foot length by removing nuances in foot slippage and step-to-step variance, particularly for tracks left in deformable materials.

Mass predictions

To test the validity of previous methods of mass prediction, corrected track dimensions (mm) were regressed against body mass (Kg) for the current population. Pearson's Correlation Coefficients were computed to identify associations between variables. This was supported by multivariate regressions of body proportions (stature and body mass) with track dimensions to determine if body mass can be extracted from track impressions.

Hip height

To test the validity of using hip height to predict limb posture, a regression and Pearson's correlation were computed to determine if hip height could be positively calculated from track dimensions using measurements extracted from each participant during the trials. If hip height can be accurately predicted from track dimensions, this will validate previous studies that have used this variable to predict limb posture and to improve speed predictions from fossil tracks. As numerous outliers existed within the dataset, a Generalised Linear Model (GLM) was computed to explore the relationship between total foot length and hip height, with mass introduced as a nested effect.

3.2.6 3D motion capture

To explore the relationship between kinematic variables and substrate deformation, 3D motion capture systems (Qualysis AB, Gothenburg, Sweden) were employed to characterise movement across three different substrates via the application of a reflective marker-set which captured real-time movement across each of the substrates.

A 14-optoelectronic high-speed camera motion system (Oqus Cameras, Qualysis AB, Gothenburg, Sweden) was employed to record movement across each of the trackways (Figure 3.2). During quality testing of the camera set-up ($n=3$ participants from the pilot trials using 10-optoelectronic high-speed cameras) it was determined that markers placed onto the foot were regularly lost on the looser substrate, regardless of the depth of substrate penetration during movement. Consequently, the camera system was redesigned by adding additional cameras at lower heights to address this issue. Ten cameras were wall mounted and four cameras were free-standing on the ground at a height of 1.5 m. By placing these free-standing cameras at a 60° angle (angle determined through trial and error of repeated calibrations and via visual inspection) and at a distance of 1 m/2 m from the track corners at the start and end of the tracks respectively, it was possible to capture all markers during the complete gait cycle, without any loss of marker visibility (Figure 3.4).

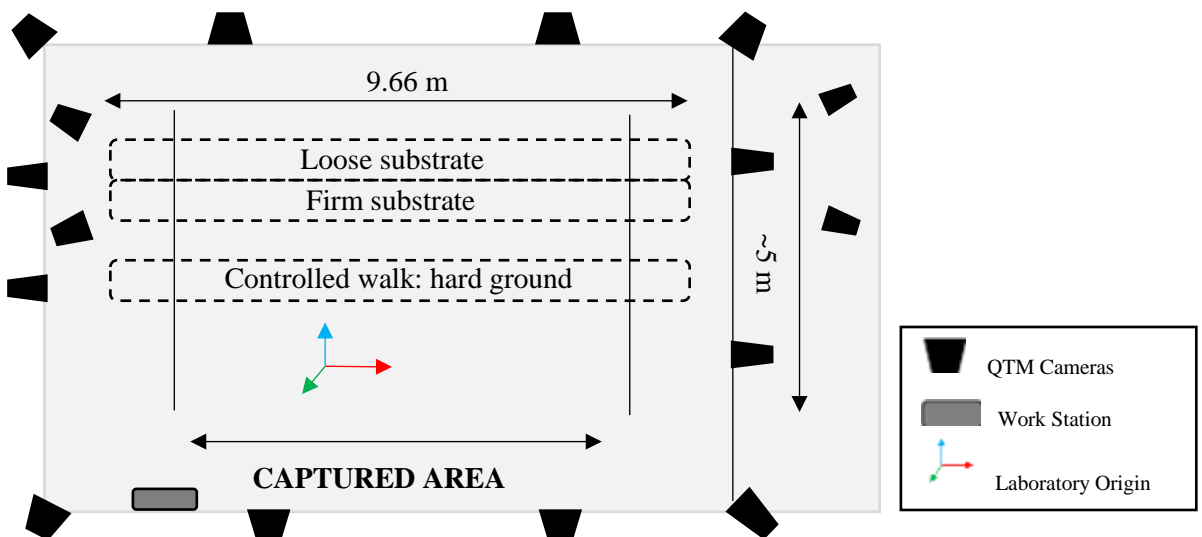


Figure 3.4. Diagram of laboratory set-up and position of each camera.

After camera set-up and trackway design was refined (Section 3.2.2), 40 participants were recruited for the biomechanical trials. All participants agreed to wear minimal clothing for adequate marker placement directly onto the majority of bony anatomical landmarks.

A Liverpool John Moores University Lower Limb and Trunk Model was applied (Figure 3.5), allowing six degrees of freedom for the functional assessment of the hip, knee and ankle joints (Vanrenterghem et al. 2010; Robinson and Vanrenterghem 2012). Representation of the arms was not included in this study because the research questions only addressed movement of the lower limb.

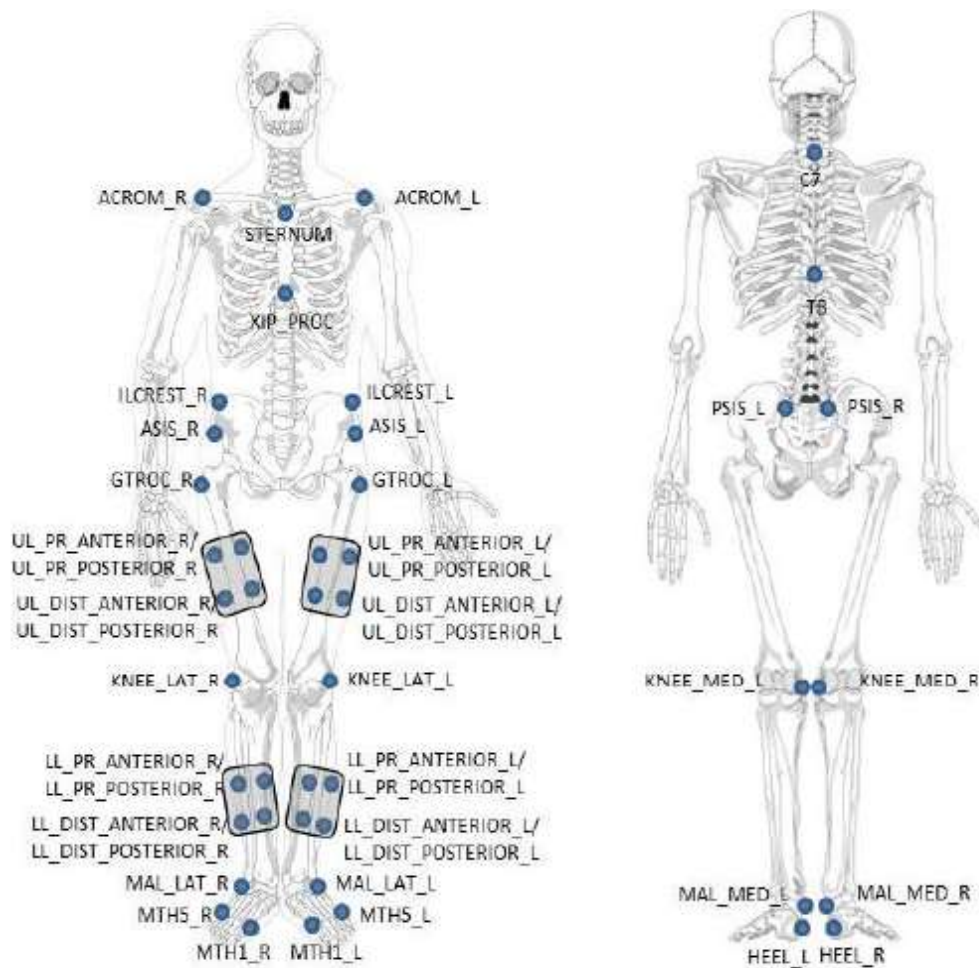


Figure 3.5. The LJM Lower Limb and Trunk Model (Vanrenterghem et al. 2010) used in the current study. Forty-four spherical reflective markers were used in total.

Calibrated volume and QTM camera settings

Prior to data collection, the system was manually calibrated each day via the use of a wand (length of 751.1 mm) with reflective markers attached, relative to a global reference system: the laboratory origin (Di Marco et al. 2016). Calibration was deemed suitable once the standard error of each camera was <0.4 mm. The system was manually calibrated twice a day (or, after every third participant) to prevent a drift in noise error which was otherwise introduced by the presence of reflective materials (e.g., the wet sand and the tarpaulin) ~8 hours after calibration.

As one of the experimental tracks had a water saturation of ~12% and was quite reflective, an aperture of f/5.6 was required to circumvent the issue of the reflective sand being captured. Camera exposure values varied per camera, with the majority being a value of 150 exposure, and others ranging from 180 – 200 exposure. High exposure values belonged to the free-standing cameras on the ground that were much closer to the reflective materials. Marker threshold values were set quite low to reduce the capture of unwanted objects. Threshold values were predominantly set at 15%, with values ranging from 8% – 10% for the free-standing cameras. These settings allowed all markers to be adequately captured with minimal noise.

Static/calibration trials

A static/calibration trial was collected from each participant which permitted an anatomical reference system to be generated, and later used in Visual3D (C-Motion Inc., Germantown, USA) to define body segments. The positions of 44 reflective markers during the static and motion trials were recorded at a frequency of 250 Hz. An Automated Identification of Markers model was generated in Qualysis Track Manager (QTM) for the identification and labelling of all markers.

Motion trials

All motion trials were repeated five times for repeatability (Levine et al. 2012). This resulted in a total of 45 trials per participant (four motions across the loose and firm substrates, and an additional controlled walk across the hard ground). The QTM cameras captured a minimum of five gait cycles per substrate, resulting in a minimum of 225 gait cycles per participant (split between each type of motion). In total, this study captured ~9,000 gait cycles across four different motions.

The hard ground was used as the control experiment. Modern shod humans are accustomed to traversing across hard, even terrains (Bennett and Morse 2014). By recording movement across the hard ground, it is possible to have a record of each participant's lower limb movement across a hard ground in a controlled environment. The controlled experiment was then compared to each motion across the experimentally designed trackways to determine how variable kinematics are when substrate pliancy is increased and limb posture is altered to accommodate changes in substrate deformity.

Each participant was told to walk at a self-selected, comfortable walking pace, then to walk swiftly at their chosen increased walking pace, and then to jog at a pace that they believed would be sustainable for at least a few minutes (Figure 3.6a). By allowing the participants to choose comfortable speeds rather than controlling step and stride lengths per motion, intra-group variability in gait dynamics will be increased. The purpose of the current study is to determine kinematic changes corresponding to modifications in substrate navigation in respect to fossil hominins. By introducing intra-group variability from unconstrained gait data, the ranges of lower limb kinematics will be much greater (Levine et al. 2012), allowing for the results of this study to reflect real-time substrate navigation of modern humans, whereby it will be much more applicable to make inferences regarding hominin locomotion.

Trials were discarded and re-captured if a participant was deemed to have altered their gait in any manner during movement (Figure 3.6b). For example, one participant over-emphasised toe-clearance during the swing phase resulting in numerous re-trials.

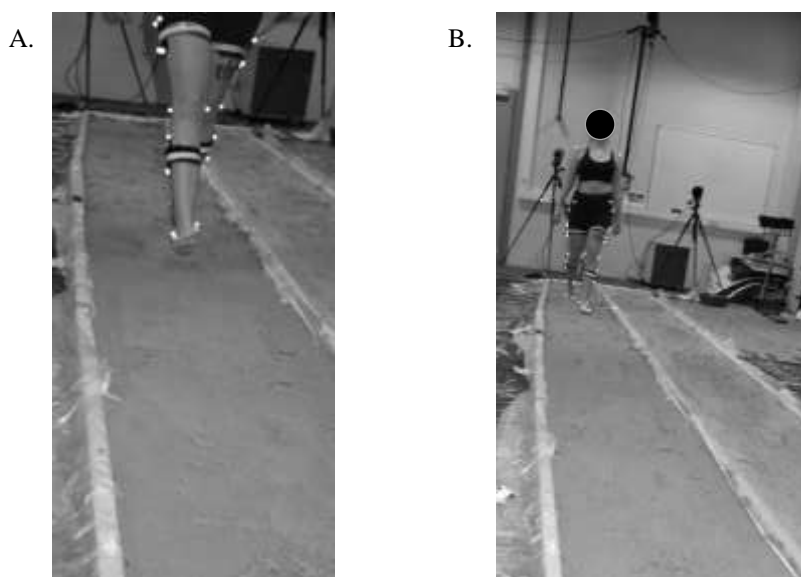


Figure 3.6. Examples of movement across the firm substrate.

During the jogging trials <5% of individuals (those with a body mass >82 Kg, or those who trained regularly in jogging/long distance running) displayed complete substrate penetration of the less compliant substrate. This resulted in the jogging trials for these individuals being disqualified from the study. All other trial data pertaining to those heavier individuals were incorporated into the study to allow a comprehensive assessment of how kinematics may change within the same motion across different types of substrates.

Prior to the BHBK motion trials, all participants were instructed to practise the movement on the hard ground several times at a self-selected walking pace. This practise ensured that each individual was acclimatised to the BHBK postural positioning during the motion, and that the body had become temporarily accustomed to moving in that manner.

Identified issues with the BHBK trials

Unfortunately, 50% of the trials were discarded for the BHBK movement. Upon assessment of the ankle kinematics it was determined– despite visual controls of movement during the trials – that half of the participants kept their foot in a dorsiflexed position throughout the gait cycle, and the other half used a plantarflexed posture of the ankle during the swing phase. Using extant non-human primate analogs of bipedal movement, high ranges of dorsiflexion – which would be necessitated (and utilized by half of the participants within the current study) for toe clearance of the substrate if the foot was kept in a dorsiflexed position during toe-clearance – are not present in the primate model of bipedal locomotion (Fernandez et al. 2016). Consequently, all trials belonging to a participant whom kept their foot in a dorsiflexed posture during the BHBK motion have been discarded. If these participants were included then all statistical results of all lower limb joint angles between motions yielded significant variability in movement across different substrates, which was not a true representation of this motion.

3.2.7 Data processing and extraction

Missing marker trajectories were linear filled in QTM (gaps <10 frames). Marker trajectories were imported into Visual3D (v.5.02.30 C-Motion Inc., Germantown, USA) for the creation of a biomechanical model to estimate kinematics. Rigid segments were defined using the Visual3D protocol based upon each of the static trials. Data was interpolated to fill any remaining gaps and a low-pass filter of 6.0 was used to smooth marker trajectories. Events were defined for all gait cycles via the visual identification of

events: both heel strike and toe-off for the left and right limbs were established. All gait cycles belonging to each participant from each motion on a particular substrate were averaged to provide one mean gait cycle (e.g., one gait cycle with a standard deviation was produced for participant BK001 when walking on a less compliant substrate). All joint angles (defined as the angle between body segments) from heel strike to heel strike in the sagittal plane were calculated using the automated functions in Visual3D.

3.2.8 Statistical analyses

Despite sex from experimental tracks being largely non-determined (Section 3.3.4), all statistical analyses were grouped and computed separately according to sex to avoid the small possibility of introducing sex as an additional, non-crucial variable (Bruening et al. 2015), although some studies have argued that sexual dimorphism does not exist in limb posture or kinematics in modern human gait cycles (Kerrigan et al. 1998; Cho et al. 2004; Hurd et al. 2004). This study took a conservative approach and grouped data was not compared statistically, nor included as grouping variables in linear models.

To identify how lower limb kinematics may vary when walking across different types of substrate at variable speeds and limb postures, the peak flexion and extension of the hip and knee and the peak dorsiflexion and plantarflexion of the ankle from each averaged gait cycle were extracted. Extracted data was grouped according to each motion: a walk, fast walk, a jog, and BHBK movement. Data was sub-divided according to substrate (the firm and loose substrates) to permit an assessment of how kinematics may differ when variables are changed.

A two-tailed paired Student's *t*-test for equal variances was used to determine if there was any asymmetry in motion between the left and right leg. A one-way ANOVA was computed to determine if kinematics belonging to a particular motion were affected by movement across different types of substrates, and to determine if kinematics were changeable between speeds across the same type of substrate. All statistics were computed in R (R Core Team 2017).

3.2.9 'Averaged' track creation

To explore the relationship between track morphology with lower limb kinematics, the averaged gait cycle from each participant was compared to the corresponding internal track morphology. As no intra-trackway variability was identified within steps when

assessing track dimensions (Section 3.2.4), then the creation of an ‘averaged’ 3D mesh of each track (Belvedere et al. 2018) corresponding to each variable was possible.

To create ‘averaged’ tracks, 3D meshes were exported into DigTrace Pro (v.1.0, Budka et al. 2016). Each left and right track from an individual across a specific trackway were registered using a global landmark-defined approach for a rigid transformation to provide an averaged track shape following a standardised track registration protocol (Pataky and Goulermas 2008; Bennett et al. 2016b). Although track registration can remove nuanced features (Belvedere et al. 2018) and can be undesirable for fossilised tracks for this reason, registration is suited for experimental tracks whereby the desired outcome is to determine general track morphology from movement across a specific substrate.

Individual tracks were discarded if the standard error was >3 mm during registration (a user-defined threshold value). Discarded tracks were always the first two steps and last two steps of a given motion as the participant stepped onto and off the substrate – these steps were also removed for the kinematic testing (Section 3.2.6). Because the greatest discrepancy during track registration was found in track depths rather than outline shape (Figure 3.4a), averaged tracks were thus confidently created with minimal standard error (Figure 3.4b) to permit the following assessments. Track registration provided 312 mean tracks (left and right) for assessment. Depths were qualitatively assessed to determine the general depth patterns and morphologies across a given track.

The registered track shapes were visually assessed for morphological patterns corresponding to particular changes in kinematics (e.g., increased knee flexion when walking swiftly across the less compliant substrate).

Discrepancies in arch height were observed. To test the prediction that arch height was variable across different substrates, arch height was quantified by measuring the absolute height from the deepest point in each averaged track in CloudCompare. Absolute height was recorded so as to treat the entire track as a representation of integrated, dynamic movements. A two-tailed paired Student’s *t*-test for equal variances was computed in R to test for discrepancy between arch height, grouped according to factors (motions and substrate typology).

Similar to previous studies (e.g., Hatala et al. 2018) this study identified that arch height was variable between different substrates. To identify if the increase in arch height was associated with lower limb movement (e.g., hip and/or knee flexion, and/or ankle plantarflexion/dorsiflexion), a between-groups ANOVA was computed.

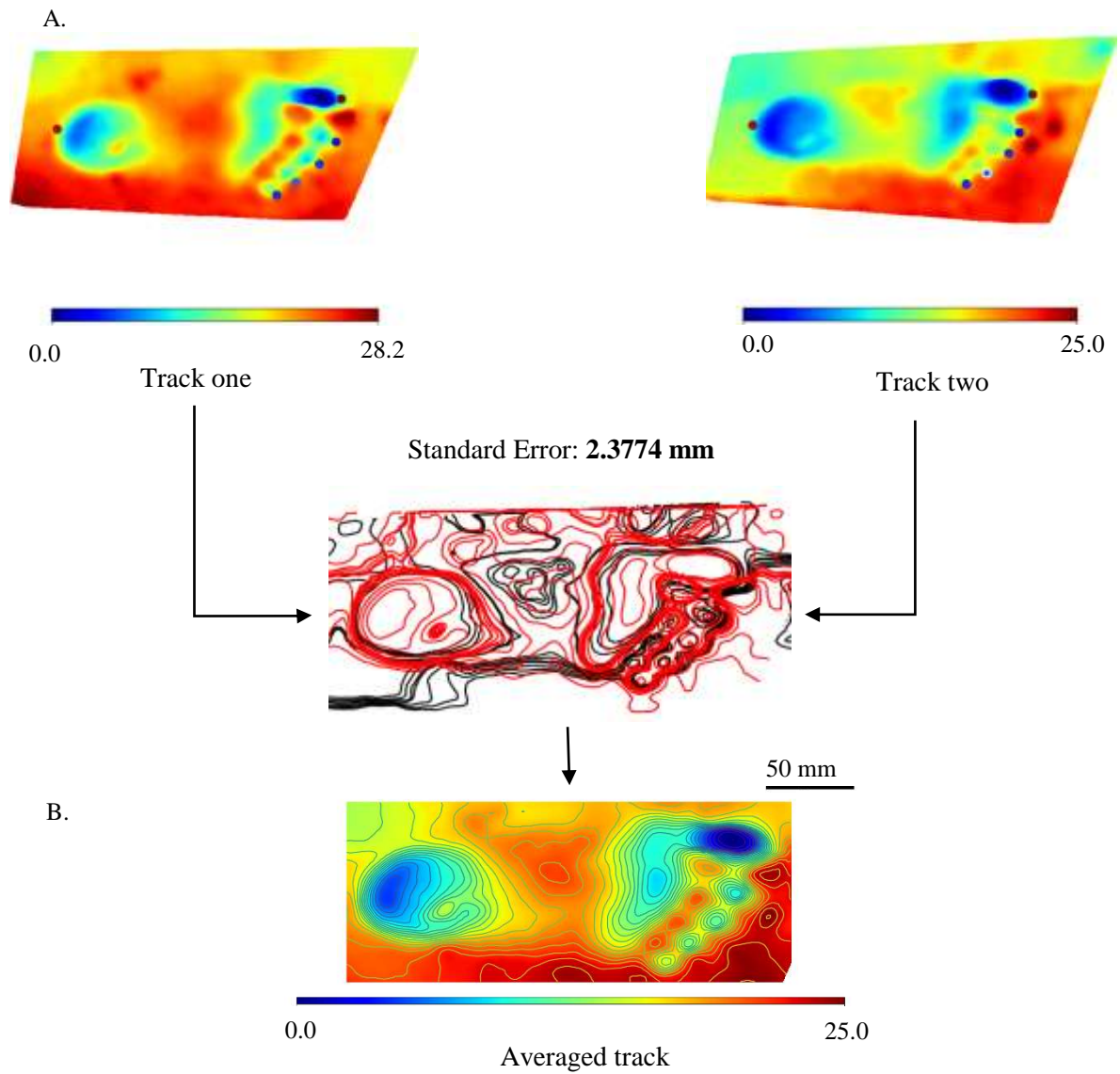


Figure 3.7. Example of the rigid-track registration method employed in this study (A), with the landmarks used for registration (the red and blue dots). The black outline track is the initial track. The red outline track is the computed mean between each track. The red contoured lines within the track show that the greatest intra-trackway discrepancy can be found in track depths, rather than the outline. Averaged tracks were created (B).

Identifying the influence of kinematics on track production

Previous studies that have assessed the midfoot impression in fossil tracks have not only used arch height but also the shape/prominence of the midfoot impression to ascertain functional morphology (e.g., Crompton et al. 2012; Bennett et al. 2016a; Holowka et al. 2017). To examine how the shape and size of the midfoot changes when tracks are produced on differing substrates when employing a range of motions, mesh to mesh comparisons were created in CloudCompare using a rigid transformation. To avoid scale (e.g., variable track dimensions) introducing error into the mesh comparisons, tracks were scaled to the length of a walking track on the firm substrate for consistency in measurements.

Hallucal abduction angles

Upon visual inspection of each registered track, it was observed that those tracks made with a flexed limb (BHBK) potentially displayed increased hallucal abduction. To test this prediction, hallucal angle for each registered track was calculated. First, a one-tailed paired Student's *t*-test for equal variances was computed to determine if hallucal abduction was differential between tracks made on each substrate. A GLM was then computed to determine if the predicted variation in hallucal abduction was associated with increased hip and/or knee flexion (peak flexion values were extracted from the kinematic tests; Section 3.2.5) across the two substrates. Results were supported by a Pearson's Correlation Coefficient.

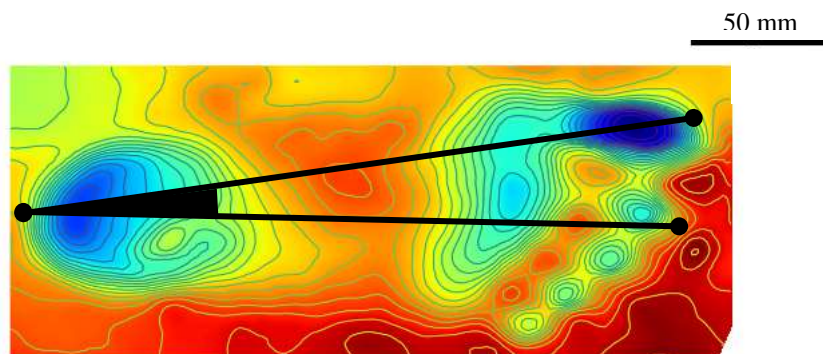


Figure 3.8. Calculation of hallux angle for each registered track. Angle is measured as an intersecting line through the midpoint point of the hallucal impression and through the deepest point of the medial pad of the foot relative to the foot's long axis.

3.3.0 Results

3.3.1 Measurement repeatability in linear measurements of tracks

Error may be introduced in two ways when taking measurements of tracks: observer error and via intra-track variability. Replicability tests were computed to test observer error via assessing the reliability of measuring linear measurements from tracks. The mean standard error of all measurements was determined to be <1.92% (Table 3.1). The threshold for observer error was thus established to be within 0-1.92%.

Step to step variance likely exists in a single trackway (Bennett and Morse 2014). To examine intra-print variability, the standard error of all measurements taken from an individual trackway were calculated (Table 3.2). As demonstrated by the mean standard error of each measurement, intra-track variability exceeds that of the observer error, ranging from 3.637% to 9.254%. To circumvent the issue of intra-track variability in linear measurements introducing noise error to between-group assessments, all subsequent analyses used averaged linear measurements (≥ 9 prints per variable).

Table 3.1. Observer-error for extracting linear measurements from tracks (n=5 participants). Dimensions were consistently measured. M.S.E values sorted from minimum (white) to maximum (dark green).

	Foot length		Long Axis		Hallux Length	
	M.S.E	Variance	M.S.E	Variance	M.S.E	Variance
Walk_loose	0.678%	0.454% \pm 1.050	0.653%	0.807% \pm 1.012	0.234%	0.449 \pm 0.362
Walk_firm	1.107%	0.069% \pm 1.715	0.877%	0.126% \pm 1.359	0.627%	1.716% \pm 0.971
Fast Walk_loose	0.442%	-0.416% \pm 1.051	0.678%	-0.416% \pm 1.051	0.899%	-0.422% \pm 1.392
Fast Walk_firm	0.802%	-0.045% \pm 1.242	0.424%	-0.434% \pm 0.785	0.318%	-1.829% \pm 0.493
Jog_loose	0.288%	-0.116% \pm 0.446	0.377%	-0.181% \pm 0.584	0.408%	-1.076% \pm 0.632
Jog_firm	0.857%	-0.798% \pm 1.355	0.421%	-0.117% \pm 0.653	0.926%	0.237% \pm 1.434
BHBK_loose	0.455%	-0.179% \pm 0.705	0.230%	-0.185% \pm 0.356	0.067%	-0.186% \pm 0.104
BHBK_firm	0.489%	-0.494% \pm 0.757	0.587%	0.281% \pm 0.909	0.411%	0.691% \pm 0.637

	Forefoot Width		Heel Width	
	M.S.E	Variance	M.S.E	Variance
Walk_loose	0.47%	0.963% \pm 0.723	0.37%	1.409% \pm 0.567
Walk_firm	1.03%	-1.598% \pm 1.600	0.59%	-1.922% \pm 0.910
Fast Walk_loose	0.135%	0.363% \pm 0.209	0.33%	0.193% \pm 0.509
Fast Walk_firm	0.31%	0.694% \pm 1.076	0.14%	0.325% \pm 0.211
Jog_loose	0.72%	-1.837% \pm 1.113	0.48%	-0.830% \pm 0.749
Jog_firm	0.25%	-0.046% \pm 0.389	0.94%	-0.420% \pm 1.458
BHBK_loose	0.61%	-0.471% \pm 0.942	0.24%	-0.911% \pm 0.367
BHBK_firm	0.84%	-1.596% \pm 1.307	0.52%	-1.612% \pm 0.789

Table 3.2. Intra-trackway variability of each participant's movement across the loose and firm substrates (n=100 participants). Intra-trackway dimensions exceeded that of observer-error (Table 3.1) but were still established to be consistently measured. M.S.E values sorted from minimum (dark green) to maximum (yellow).

	Foot length		Long Axis		Hallux Length	
	M.S.E	Variance	M.S.E	Variance	M.S.E	Variance
Walk_loose	4.06%	5.513% ± 4.294	3.82%	4.653% ± 3.601	1.95%	5.120% ± 4.057
Walk_firm	4.03%	4.467% ± 3.585	3.91%	5.044% ± 3.810	1.76%	3.637% ± 2.774
Fast Walk_loose	4.05%	5.707% ± 4.430	5.06%	5.507% ± 4.268	1.75%	6.676% ± 4.367
Fast Walk_firm	3.96%	4.954% ± 3.720	4.14%	6.134% ± 4.574	1.37%	3.696% ± 2.829
Jog_loose	3.30%	7.766% ± 5.211	3.17%	5.299% ± 3.900	4.63%	7.063% ± 4.657
Jog_firm	2.90%	4.603% ± 3.514	2.82%	6.617% ± 4.899	3.34%	4.605% ± 3.414
BHBK_loose	2.95%	6.300% ± 4.999	3.19%	7.848% ± 5.989	1.94%	6.064% ± 4.547
BHBK_firm	3.37%	5.534% ± 4.261	3.75%	6.327% ± 5.037	1.85%	4.317% ± 3.410

	Forefoot Width		Heel Width	
	M.S.E	Variance	M.S.E	Variance
Walk_loose	2.82%	6.830% ± 5.647	2.27%	4.893% ± 3.996
Walk_firm	2.10%	4.937% ± 3.789	1.42%	3.986% ± 3.006
Fast Walk_loose	5.44%	6.517% ± 4.771	1.42%	3.927% ± 2.956
Fast Walk_firm	2.02%	4.304% ± 6.517	1.36%	4.457% ± 3.351
Jog_loose	2.36%	9.254% ± 5.872	3.22%	4.927% ± 3.232
Jog_firm	2.50%	4.252% ± 3.357	1.48%	4.984% ± 3.588
BHBK_loose	1.87%	6.181% ± 4.472	1.77%	5.533% ± 4.043
BHBK_firm	2.15%	7.814% ± 5.620	1.71%	4.908% ± 3.677

3.3.2 Variability in track dimensions across difference substrates and speeds

No discrepancies were established in the majority of track dimensions between the firm and loose substrate for any given speed: foot length ($P \geq 0.05$, $SE=1.359$), the long axis ($P \geq 0.05$, $SE=1.357$), heel width ($P \geq 0.05$, $SE=1.016$) or the hallux length ($P \geq 0.05$, $SE=1.041$), as shown by a paired Student's *t*-test (Table 3.3). Only forefoot width was identified to become wider on a looser substrate ($P \geq 0.05$, $SE=1.041$). When the walking speed was increased then tracks on the looser substrate were significantly wider in both the forefoot ($P=0.001$, $SE=2.092$) and the heel ($P=0.004$, $SE=1.093$). All other linear measurements were found to be comparable between tracks made on the different substrates (Table 3.3).

If comparing walking tracks with those created from a fast walk, only the length of the hallux was found to be marginally greater on the looser substrate ($P=0.032$, $SE=1.595$) and the firmer substrate ($P=0.043$, $SE=0.924$). All other measurements remained consistent across the same substrate with an increase in speed (Table 3.3).

When a participant was jogging, foot length ($P \leq 0.001$, $SE=1.363$), the long axis of the foot ($P=0.0026$, $SE=1.562$), the length of the hallux ($P \leq 0.001$, $SE=2.752$), forefoot width ($P=0.003$, $SE=1.645$), and heel width ($P=0.003$, $SE=1.459$) were significantly disparate between the substrates (Table 3.3).

If comparing tracks created from a fast walk with those created from a jogging pace, variability was always found on the firmer substrate rather than the softer substrate. Foot length ($P=0.001$, $SE=2.536$), the long axis of the foot ($P=0.037$, $SE=2.800$) and forefoot width ($P=0.011$, $SE=1.531$) were all found to be greater when speed is increased (Table 3.3).

During the BHBK motion, foot length, heel width and length of the hallux were all found to be significantly variable when created in different substrates ($P=0.006$, $SE=1.735$; $P=0.003$, $SE=1.535$; $P=0.003$, $SE=1.425$, respectively). Forefoot width and the long axis of the foot were found to be similar when the tracks are created in different substrates (Table 3.3).

To determine if track measurements change linearly between individuals, the percentage change and standard error in measurements between different motions across the two substrates were calculated (Table 3.4). Track dimensions from the two different substrates grouped according to motion were regressed (Figure 3.9). Results are summarised below.

Table 3.3. Results of the two-tailed paired Student's *t*-test for sampled means of the five linear measurements of each track for grouped motions across the two substrates within this study: loose and firm. Measurements in mm.

		Mean Variance	Std. Deviation	Std. Error Mean	95% Confidence Interval of the Difference		<i>t</i>	R ²	DF	P
					<i>Lower</i>	<i>Upper</i>				
Foot length	Walk_loose ~ Walk_firm	-1.807	13.454	1.359	-4.504	0.890	-1.330	0.849	97	0.187
	Fast Walk_loose ~ Fast Walk_firm	-3.063	16.904	1.802	-6.645	0.519	-1.700	0.898	87	0.093
	Jog_loose ~ Jog_firm	-5.284	10.473	1.363	-8.013	-2.555	-3.875	0.842	58	<0.001
	Walk_loose ~ Fast Walk_loose	-0.623	19.378	2.300	-5.210	3.964	-0.271	0.693	70	0.787
	Walk_firm ~ Fast Walk_firm	-2.125	16.720	1.957	-6.026	1.776	-1.086	0.744	72	0.281
	Fast Walk_loose ~ Jog_loose	9.084	18.978	2.536	4.001	14.166	3.582	0.489	55	0.001
	Fast Walk_firm ~ Jog_firm	4.106	18.907	2.729	-1.384	9.596	1.505	0.672	47	0.139
	BHBK_loose ~ BHBK_firm	-5.023	12.634	1.735	-8.505	-1.541	-2.894	0.688	52	0.006
	Walk_loose ~ BHBK_loose	-2.767	12.135	1.829	-6.456	0.922	-1.512	0.738	43	0.138
	Walk_firm ~ BHBK_firm	-8.112	17.442	2.517	-13.177	-3.048	-3.222	0.457	47	0.002
Long Axis	Walk_loose ~ Walk_firm	-1.156	13.363	1.357	-3.849	1.537	-0.852	0.884	96	0.396
	Fast Walk_loose ~ Fast Walk_firm	-3.653	28.764	3.084	-9.783	2.478	-1.185	0.868	86	0.239
	Jog_loose ~ Jog_firm	-3.563	11.796	1.562	-6.693	-0.433	-2.28	0.833	56	0.026

Table 3.3 cont. Results of the two-tailed paired Student's *t*-test for sampled means of the five linear measurements of each track for grouped motions across the two substrates within this study: loose and firm. Measurements in mm.

		Mean Variance	Std. Deviation	Std. Error Mean	95% Confidence Interval of the Difference		<i>t</i>	R ²	DF	P
					<i>Lower</i>	<i>Upper</i>				
<i>Long Axis cont.</i>	Walk_loose ~ Fast Walk_loose	-1.776	16.909	2.021	-5.807	2.256	-0.879	0.764	69	0.383
	Walk_firm ~ Fast Walk_firm	-1.949	15.874	1.871	-5.679	1.781	-1.042	0.762	71	0.301
	Fast Walk_loose ~ Jog_loose	5.978	20.772	2.801	0.362	11.593	2.134	0.592	54	0.037
	Fast Walk_firm ~ Jog_firm	1.016	19.511	2.816	-4.649	6.681	0.361	0.653	47	0.72
	BHBK_loose ~ BHBK_firm	-3.900	14.621	1.990	-7.891	0.091	-1.96	0.647	53	0.055
	Walk_loose ~ BHBK_loose	-2.993	14.921	2.249	-7.530	1.543	-1.331	0.599	43	0.19
	Walk_firm ~ BHBK_firm	-6.864	17.720	2.558	-12.009	-1.718	-2.684	0.441	47	0.01
Forefoot width	Walk_loose ~ Walk_firm	-5.057	13.829	1.397	-7.830	-2.284	-3.62	0.423	97	<0.001
	Fast Walk_loose ~ Fast Walk_firm	-7.362	19.620	2.091	-11.519	-3.205	-3.52	0.200	87	0.001
	Jog_loose ~ Jog_firm	-5.753	12.635	1.645	-9.046	-2.461	-3.498	0.418	58	0.001
	Walk_loose ~ Fast Walk_loose	1.940	11.953	1.419	-0.889	4.770	1.368	-0.206	70	0.176
	Walk_firm ~ Fast Walk_firm	-1.043	22.898	2.680	-6.386	4.299	-0.389	0.496	72	0.698

Table 3.3 cont. Results of the two-tailed paired Student's *t*-test for sampled means of the five linear measurements of each track for grouped motions across the two substrates within this study: loose and firm. Measurements in mm.

		Mean Variance	Std. Deviation	Std. Error Mean	95% Confidence Interval of the Difference		<i>t</i>	R ²	DF	P
					<i>Lower</i>	<i>Upper</i>				
<i>Forefoot width cont.</i>	Fast Walk_loose ~ Jog_loose	-4.044	11.456	1.531	-7.112	-0.976	-2.641	-0.165	55	0.011
	Fast Walk_firm ~ Jog_firm	-1.048	25.143	3.629	-8.349	6.252	-0.289	0.304	47	0.774
	BHBK_loose ~ BHBK_firm	-2.827	24.687	3.360	-9.565	3.912	-0.841	0.146	53	0.404
	Walk_loose ~ BHBK_loose	3.940	3.445	1.989	-4.617	12.497	1.981	0.181	2	0.186
	Walk_firm ~ BHBK_firm	-2.395	14.480	2.090	-6.600	1.809	-1.146	0.115	47	0.258
Heel width	Walk_loose ~ Walk_firm	-6.995	10.062	1.016	-9.013	-4.978	-6.882	0.369	97	<0.001
	Fast Walk_loose ~ Fast Walk_firm	-4.444	10.250	1.093	-6.616	-2.273	-4.067	-0.024	87	<0.001
	Jog_loose ~ Jog_firm	-4.023	11.204	1.459	-6.943	-1.104	-2.758	0.381	58	0.008
	Walk_loose ~ Fast Walk_loose	-2.766	8.543	1.014	-4.788	-0.743	-2.728	0.290	70	0.008
	Walk_firm ~ Fast Walk_firm	-0.030	11.149	1.305	-2.632	2.571	-0.023	0.217	72	0.981
	Fast Walk_loose ~ Jog_loose	1.518	11.424	1.527	-1.541	4.578	0.995	0.157	55	0.324
	Fast Walk_firm ~ Jog_firm	0.441	10.842	1.565	-2.707	3.589	0.282	0.179	47	0.779
	BHBK_loose ~ BHBK_firm	-4.515	10.478	1.426	-7.375	-1.655	-3.166	0.130	53	0.003

Table 3.3 cont. Results of the two-tailed paired Student's *t*-test for sampled means of the five linear measurements of each track for grouped motions across the two substrates within this study: loose and firm. Measurements in mm.

		Mean Variance	Std. Deviation	Std. Error Mean	95% Confidence Interval of the Difference		<i>t</i>	R ²	DF	P
					<i>Lower</i>	<i>Upper</i>				
<i>Hallux length cont.</i>	Walk_loose ~ BHBK_loose	-1.743	10.459	1.577	-4.923	1.437	-1.106	-0.040	43	0.275
	Walk_firm ~ BHBK_firm	-0.600	9.967	1.439	-3.495	2.294	-0.417	0.290	47	0.678
Hallux length	Walk_loose ~ Walk_firm	-4.198	10.256	1.041	-6.265	-2.131	-4.031	0.601	96	<0.001
	Fast Walk_loose ~ Fast Walk_firm	-7.819	11.851	1.263	-10.330	-5.308	-6.189	0.418	87	<0.001
	Jog_loose ~ Jog_firm	-12.031	21.141	2.752	-17.540	-6.522	-4.371	0.096	58	<0.001
	Fast Walk_loose ~ Jog_loose	2.047	13.460	1.815	-1.591	5.686	1.128	-0.396	54	0.264
	Fast Walk_firm ~ Jog_firm	-2.223	18.859	2.722	-7.700	3.253	-0.817	0.114	47	0.418
	BHBK_loose ~ BHBK_firm	-4.848	11.286	1.536	-7.928	-1.767	-3.157	0.281	53	0.003
	Walk_loose ~ BHBK_loose	-1.050	9.173	1.383	-3.839	1.739	-0.76	0.416	43	0.452
	Walk_firm ~ BHBK_firm	0.032	10.374	1.497	-2.980	3.045	0.022	0.335	47	0.983

Total track length

Intra-track length was greater by only $0.39\% \pm 6.57$ ($P=0.187$, $SE=1.369$) for tracks created on the less compliant substrate. However, if speed is considered as a covariate then track length was always identified to be greater on the firmer substrate (maximum increase: $2.70\% \pm 6.14$) rather than the looser substrate (maximum increase: $0.68\% \pm 5.82$) (Table 3.3). A greater length of the tracks produced in the firmer substrate is most likely in response to the boundaries of the track collapsing after track creation when the material is looser. Strong positive correlations were established for foot length discrepancies between all substrate and speed variables (Table 3.3; Figure 3.9a). Consequently, it will be possible to ‘correct’ an increase in track length when substrate and/or speed is altered.

Long axis of the foot

The long axis of the foot was similarly affected by speed and movement. The measurement difference between substrates was $1.131\% \pm 4.946$ ($P=0.396$, $SE=1.357$). If speed is introduced as a covariate then the length of the long axis was found to be slightly more variable on the firm substrate ($-0.64\% \pm 7.48$) in comparison to the looser substrate ($-0.47\% \pm 5.94$) (Table 3.3). Strong positive correlations were established for the long axis of the foot discrepancies between the variables (Table 3.3; Figure 3.9b). Consequently, it will be possible to ‘correct’ an increase in the long axis of the foot when substrate and/or speed is altered in future studies.

Hallux length

Hallux length was identified to be considerably disparate between tracks produced on the two different substrates ($-10.96\% \pm 29.14$) ($P \leq 0.001$, $SE=1.041$). If speed is introduced as a covariate, hallux length was detected to be grossly variable between individuals when tracks were created on the loose ($-11.23\% \pm 27.18$) and firm substrates ($-5.43\% \pm 31.95$) (Table 3.3). Although track length was identified to be somewhat consistently changing between individuals as variables differed, hallux length was detected to be inconsistently changing between individuals. This suggests that outline shape may be more accurately extracted from a track than the internal proportions. Poor correlations – often negative associations – were established for hallux length discrepancies between factors (Table 3.3; Figure 3.9c). It will be negligible to ‘correct’ for an increase/decrease in hallux length when substrate and/or speed is altered.

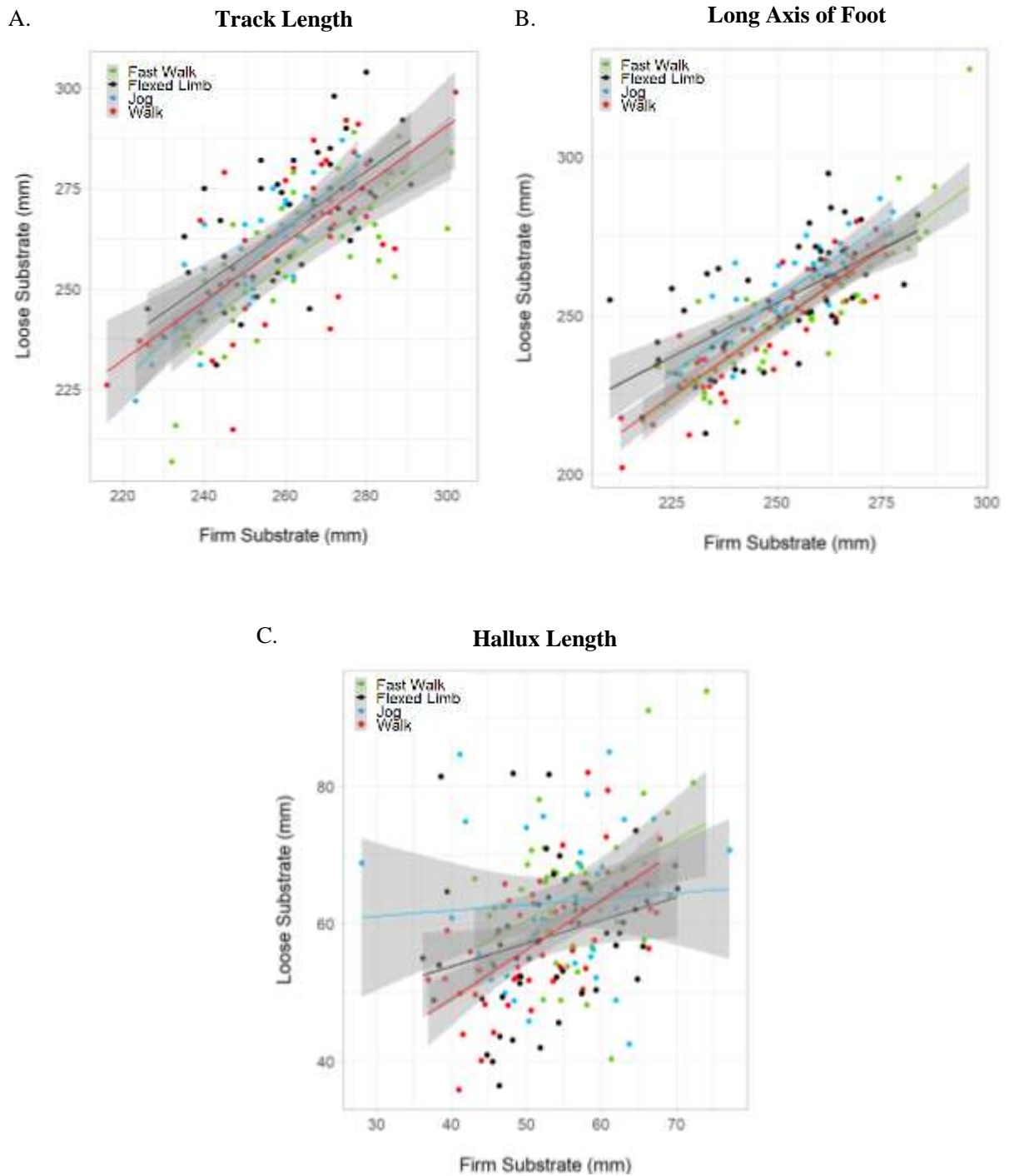


Figure 3.9. Regression of track length (A), the long axis of the foot (B) and hallucal length (C) from tracks produced on the firm substrate against those produced on the loose substrate, grouped according to motion.

Table 3.4. The reported percentage change in each of the length (A) and width (B) measurements (n=100 participants). Positive value indicates that the linear measurement generally increased between each variable (e.g., the foot became longer). Negative value indicates that the linear measurement generally decreased between each variable (e.g., the heel tapered). Dimensions were not always consistently measured, as discussed in text. M.S.E values are sorted from minimum (dark green) to maximum (red) to reflect the differences in intra-trackway dimensions.

A.	Foot Length		Long Axis		Hallux Length	
	M.S.E	Variance	M.S.E	Variance	M.S.E	Variance
Walk_loose ~ Walk_firm	0.778	0.102% ± 3.571	0.916	1.131% ± 4.003	3.787	-11.414% ± 16.548
Fast Walk_loose~ Fast Walk_firm	0.620	0.385% ± 2.977	1.030	0.906% ± 4.946	3.645	-16.080% ± 17.512
Jog_loose ~ Jog_firm	0.727	-2.671% ± 3.092	0.762	-2.630% ± 3.153	6.851	-10.964% ± 29.141
Walk_loose ~ Fast Walk_loose	0.905	-2.144% ± 4.442	1.211	-1.198% ± 5.941	5.539	-11.229% ± 27.178
Walk_firm ~ Fast Walk_firm	1.126	-0.436% ± 4.492	1.521	-0.642% ± 6.644	3.197	-6.024% ± 13.967
Fast Walk_loose ~ Jog_loose	1.407	-0.679% ± 5.819	1.310	-0.465% ± 5.416	5.198	-11.980% ± 21.496
Fast Walk_firm ~ Jog_firm	1.529	2.695% ± 6.136	1.868	-2.172% ± 4.479	7.961	-5.430% ± 31.950
BHBK_loose ~ BHBK_firm	1.751	-0.265% ± 6.807	2.140	-4.424% ± 8.317	7.083	-3.849% ± 27.533
Walk_loose ~ BHBK_loose	0.969	-0.736% ± 3.768	1.725	-1.460% ± 6.705	4.976	-0.308% ± 19.344
Walk_firm ~ BHBK_firm	1.721	-3.249% ± 6.689	1.645	-4.401% ± 6.395	6.182	-2.027% ± 24.030

Forefoot width

Forefoot width was considerably disparate between the two substrates ($-0.39\% \pm 29.44$) ($P \leq 0.001$, $SE = 1.397$). If speed is introduced as a covariate then forefoot width becomes increasingly variable amongst individuals on both the loose ($-16.76\% \pm 45.95$) and the firm ($0.07\% \pm 14.04$) substrates (Table 3.3). Both substrate typology and speed have thus been cumulatively identified to drastically affect track shape production. This gross discrepancy in forefoot width per individual ranged from an increase of 48.20% to a decrease of -42.07% in width, emphasizing that forefoot width is inconsistent between different substrates and at variable speeds. Negative correlations were established between forefoot width measurements from each of the substrates with speed introduced as a covariate (Table 3.5). Cumulatively, these results suggest that forefoot width does not change linearly on the looser substrate if speed is increased (Figure 3.10a) and that it will not be possible to ‘correct’ for an increase/decrease in width when speed is altered on a less compliant substrate. However, a strong positive association was established for tracks produced from various speeds/motions on the firm substrate. Consequently, changes in forefoot width can be ‘corrected’ when speed influences forefoot width on a compliant material (e.g., if the forefoot becomes wider when jogging rather than walking).

Heel width

Heel width was found to be considerably different between tracks produced on the two substrates ($-1.46\% \pm 16.83$). However, upon inspection of the dataset it was identified that three individuals (3% of participants) displayed a significant change in heel width ($>28\%$ change) when walking across the two different trackways. If these participants are removed from the dataset, heel width was identified to be variable between the substrates by $-4.90\% \pm 7.68$ ($P \leq 0.001$, $SE = 1.016$). If speed is introduced as a covariate then heel width was found to be grossly variable on the soft substrate ($-5.72\% \pm 49.95$) in comparison to the firm substrate ($0.068\% \pm 14.041$). If the same individuals are removed from the sample, heel width was found to be somewhat less variable on the loose substrate ($0.65\% \pm 12.73$) and the firm substrate ($-4.15\% \pm 12.46$) (Table 3.3). Width was regressed and grouped according to motion (Figure 3.10b). Heel width was detected to be non-linear between the variables. Poor correlations – often negative associations (e.g., tracks produced on the two different substrates at a fast walking speed) – were established (Table 3.5; Figure 3.10b). Consequently, it will not be possible to ‘correct’ for an

increase/decrease in heel width when substrate and/or speed is altered. This finding supports previous research into variable heel dimensions during track formation (Hatala et al. 2018).

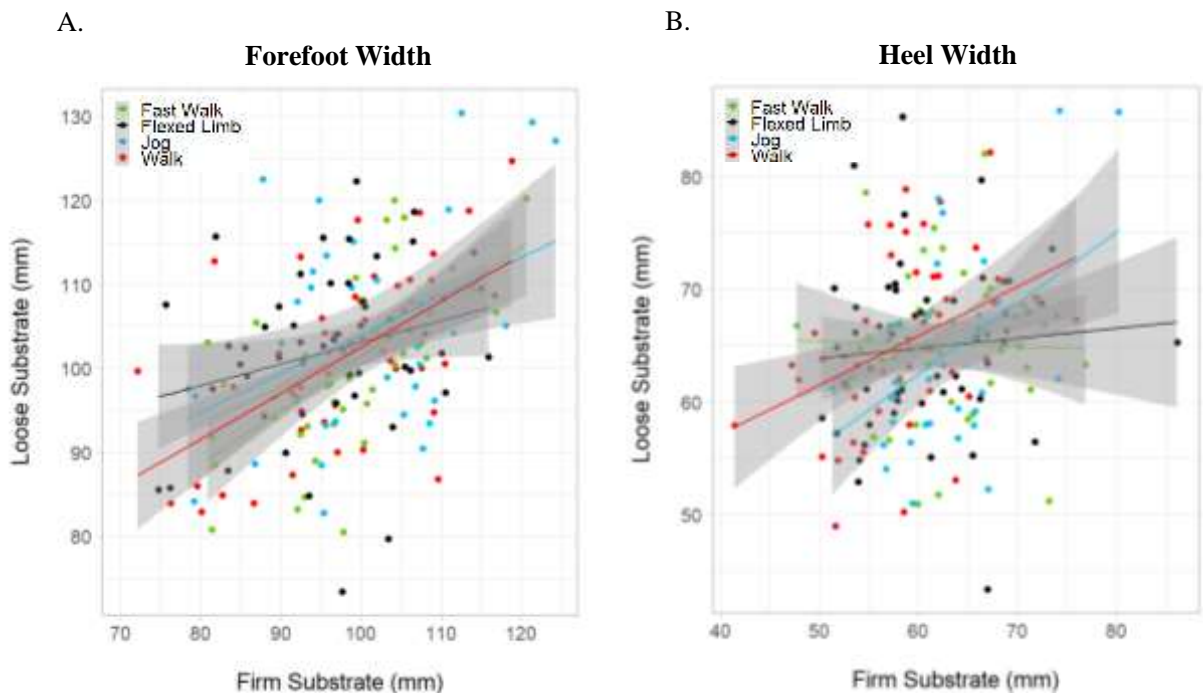


Figure 3.10. Regression of forefoot width (A) and heel width (B) from tracks produced on the firm substrate against those produced on the loose substrate, grouped according to motion.

Walking with a flexed limb (BHBK)

All track dimensions were different between those produced with an erect-hip erect-knee (EHEK) and those with a BHBK (Table 3.4; 3.5). Total track length and the long axis of the foot were both found to be comparably greater on the loose substrate. Hallux length, forefoot width and heel width were all found to be substantially disparate per participant when traversing across a less compliant substrate, as represented by the total group variance (Table 3.4; 3.5).

Table 3.5. The reported percentage change in each of the length (A) and width (B) measurements (n=100 participants). Positive value indicates that the linear measurement generally increased between each variable (e.g., the foot became longer). Negative value indicates that the linear measurement generally decreased between each variable (e.g., the heel tapered). Dimensions were not always consistently measured, as discussed in text. M.S.E values sorted from minimum (dark green) to maximum (red) to reflect the differences in intra-trackway dimensions.

	Forefoot Width		Heel Width	
	M.S.E	Variance	M.S.E	Variance
Walk_loose ~ Walk_firm	3.067	-0.387% ± 13.399	3.627	-11.601% ± 15.847
Fast Walk_loose~ Fast Walk_firm	2.121	-5.250% ± 9.996	3.503	-1.868% ± 16.872
Jog_loose ~ Jog_firm	2.663	-4.051% ± 11.321	2.480	-1.457% ± 10.550
Walk_loose ~ Fast Walk_loose	2.891	-1.507% ± 11.239	4.006	-1.623% ± 16.566
Walk_firm ~ Fast Walk_firm	2.328	0.068% ± 10.170	3.953	-10.544% ± 17.721
Fast Walk_loose ~ Jog_loose	4.748	-0.992% ± 18.457	3.882	-1.574% ± 15.091
Fast Walk_firm ~ Jog_firm	3.499	-6.615% ± 14.041	2.506	-0.229% ± 10.056
BHBK_loose ~ BHBK_firm	2.980	-5.717% ± 14.620	3.858	-10.706% ± 18.962
Walk_loose ~ BHBK_loose	2.991	1.515% ± 11.238	3.519	1.346% ± 13.678
Walk_firm ~ BHBK_firm	2.375	-0.472% ± 9.231	3.714	-3.964% ± 14.438

Corrected track measurements

Foot length, the long axis of the foot and the majority of forefoot width dimensions were all determined to be changing in a linear manner when the underlying substrate was changed, grouped according to motion (Figure 3.9; 3.10). Heel width and hallux length were more variable, with linear trends neglecting to be positively established for these variables. As track dimensions are used to inform on the biometrics and kinematics of the track-maker (e.g., Bennett and Morse 2014) then variable measurements are problematic (e.g., an increase in foot length of just 15 mm when walking at an increased speed on a softer substrate would predict an individual's stature as 177 cm, whereas in reality stature would be 167 cm). To reduce the error introduced by speed and substrate in linear measurements, correction factors for track length using each participants' foot length (measured during the trials using the osteometric boards) were created for each substrate and motion (Table 3.6). If the correction factors are used to correct the foot length of each track, then length discrepancy was reduced to within a <13.2 mm standard deviation. Only foot length was calculated during the data collection for each participant. Consequently, it is not possible to calculate a correction factor for any other measurement relative to foot metrics explored in this chapter.

Bi-lateral asymmetry was non-significantly variable ($t=-1.819$; $MSE=0.272$; $P=0.72$) within individuals, despite asymmetry being identified for 52.50% of participants. As foot length asymmetry will likely be unknown in fossil hominins, then correction factors were calculated and reported for the left foot only.

Table 3.6. Correction factor to be applied to tracks produced on firm and loose substrates to predict actual foot length of the track-makers (n=100 participants). Only foot length was calculated during the trials for each participant. Consequently, it is not possible to calculate a correction factor for any other measurement explored in this chapter.

	Correction Factor	
Walk_loose	$0.666(x) + 82.480$	± 12.319
Walk_firm	$0.609(x) + 96.596$	± 11.911
Fast Walk_loose	$0.581(x) + 103.123$	± 11.283
Fast Walk_firm	$0.613(x) + 93.855$	± 13.188
Jog_loose	$0.775(x) + 54.932$	± 11.069
Jog_firm	$0.822(x) + 46.744$	± 11.483
BHBK_loose	$0.570(x) + 101.543$	± 9.165
BHBK_firm	$0.641(x) + 85.211$	± 10.334

3.3.3 Biometric Predictions

Stature prediction

Actual foot length – as measured during the trials using an osteometric board– was regressed against stature to confirm that length is positively associated with stature for the current population. A strong positive correlation was established in females ($R^2=0.806$; $t=12.765$; $P\leq 0.001$) and males ($R^2=0.420$; $t=8.985$; $P\leq 0.001$), signifying that stature can be reliably predicted from track length (Figure 3.11). However, the correlation between stature and foot length in males was lower than other studies (e.g., Krishan et al. 2007; Kanchan et al. 2013). This is likely due to the recruited population, rather than a poor relationship existing between these variables. Nevertheless, a significant correlation was established, and this will be used as a basis for predicting stature from experimental footprints.

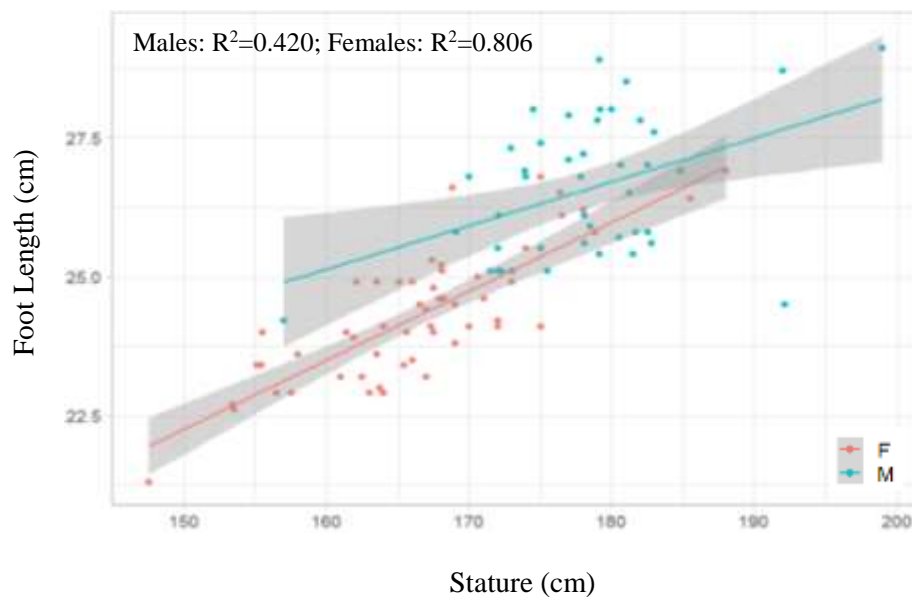


Figure 3.11. Regression of stature to total foot length. A positive relationship between the two variables was established.

To test the validity of the correction factors, stature was predicted for all participants using Robbin's Ratio (1984) and Martin's Ratio (1914) for track measurements and the corrected measurements. Results demonstrate that if non-corrected dimensions are used to predict stature from tracks then Martin's ratio produces a more accurately predicted

value (Table 3.7; Figure 3.12; 3.13). Similarly, if the corrected measurements are used to predict stature then Martin's ratio is always identified as producing the least amount of error. Although there is a small increase in the mean percentage error of stature prediction if the corrected measurements are used for stature prediction rather than the actual track dimension (error ranges from 0.03% to 4.50%), the standard error of the corrected values is always identified to be reduced for the corrected values compared to the non-corrected values (Table 3.7). The standard error (a measure of accuracy between the predicted stature value and true stature) for Martin's ratio was also lower than that of Robbin's ratio across all variables. This indicates that Martin's ratio is a more accurate method of predicting stature than Robbin's ratio.

If the corrected factors are applied to each track length measurement belonging to the different substrates at various speeds, the error of Robbin's ratio is not significantly improved (e.g., the error margin for stature prediction using Robbin's ratio is +0.06% when using the corrected measurements, and the discrepancy in error is 6.27% when using Robbin's ratio to predict stature rather than Martin's ratio), signifying that this method of stature prediction is non-applicable for this population in comparison to using Martin's ratio (Table 3.7; Figure 3.12; 3.13).

Small errors in stature prediction are always expected, as demonstrated by the prediction of stature using foot length measured during the trials. Martin's ratio predicted stature - to within $-0.96\% \pm 3.22$, whereas Robbin's ratio was only accurate to within $6.11\% \pm 3.55$ mean error.

Predicted stature results presented in Table 3.7 and visualized in Figures 3.12 and 3.13 demonstrate that Martin's ratio should be used to predict stature from tracks, preferably using corrected linear measurements. The results are visualized in the Bland-Altman graphs (Bland and Altman 1995), whereby the differences and limits of agreement (henceforth, LoA) of the predicted stature values from true stature are all reported within a 95% confidence interval from each walk, fast walk and jog on the loose and the firm substrate. Results are summarised below.

Stature prediction based on tracks produced on the firm substrate when walking

Stature prediction from tracks produced by walking on a firm substrate demonstrate under-predicted stature values for individuals <1600 mm tall (upper LoA= 187.680) and over-predicted stature values for individuals >1850 mm tall (lower LoA = -189.820,)

(Figure 3.12a). The mean difference between using the non-corrected track measurements (Figure 3.12a) and the corrected track measurements (Figure 3.12b) is minute: the difference in mean predicted values are 0.048 (Bias=-1.070 \pm 74.937) for the non-corrected length measurements and 0.066 (Bias=0.850 \pm 59.106) for the corrected length measurements.

There is less over-prediction of stature (upper LoA = 149.725) and, generally, less under-prediction of stature (lower LoA = -148.026) if the corrected track measurements are used to predict stature. However, stature prediction for three individuals are not within the LoAs. These predicted stature values are comparable to the stature prediction using the non-corrected measured values. Consequently, it was determined that the corrected track measurements should be used to predict stature for tracks formed in a firm substrate at a walking speed (Table 3.7).

Stature prediction based on tracks produced on the firm substrate when walking fast

All predicted stature values from the non-corrected measurements of tracks produced by a fast walk on the firm substrate fall within the 95% confidence interval, indicating that all measurements are reliably predicted (upper LoA = 248.018; lower LoA = -273.523) (Figure 3.12c). Despite all predicted measurements falling within the confidence interval, there was a large dispersal of predicted points between the upper and lower limits of agreement.

If the corrected foot length values are used to predict stature from tracks produced on the firm substrate during a fast walk, the hypothesized mean difference between stature and predicted stature is increased (Figure 3.12d) from -0.544 (Bias=-12.724 \pm 19.233) for the non-corrected track length measurements to 2.060 (Bias=34.846 \pm 73.523) for the corrected track length measurements. Predicted values are less dispersed when the corrected measurements are used to predict stature (upper LoA = 178.951; lower LoA = -157.612). However, there is a trend for the corrected track measurements to over-predict stature, but this issue also exists when the non-corrected measurements are used for stature prediction. Disregarding the one outlier present on the graph (Figure 3.12d), the successful removal of under-predicted values that exceeded ~55 mm from the mean when using the corrected track lengths indicates that the corrected measurements should be used to predict stature for tracks formed in a firm substrate at a fast walking speed (Table 3.7). Further assessment is required to determine if over-predicted stature values can be rectified.

Stature prediction based on tracks produced on the firm substrate when jogging

All predicted stature values from the non-corrected measurements of tracks produced by a jog on the firm substrate fall within the 95% confidence interval, indicating that all measurements are reliably predicted (upper LoA = 166.428; lower LoA = -216.923) (Figure 3.12e). Despite this, the spread of data between the upper and lower LoA was large.

If the corrected foot length values are used to predict stature from tracks produced on the firm substrate during a jog, the hypothesized mean difference between stature and predicted stature is increased from -1.480 (Bias=-25.25 \pm 69.109) for the non-corrected track length measurements to 2.200 (Bias=37.722 \pm 67.928) for the corrected track length measurements (Figure 3.12f). Predicted values are less dispersed when the corrected measurements are used to predict stature (upper LoA = 170.860; lower LoA = -147.687). Although under-predicted values exceeding 100 mm disparity were rectified by computing stature prediction from the corrected track measurements, this comes at the expense of an increase in over-predicted values. This is also apparent by a stark increase in the mean difference between stature and predicted stature. Because the majority of predicted values are closer to the hypothesized mean (0), the non-corrected measurements should be used to predict stature for tracks formed in a firm substrate at a jogging speed (Table 3.7).

Stature prediction based on tracks produced on the loose substrate when walking

Stature prediction from tracks produced by walking on a loose substrate demonstrate under-predicted stature values for three individuals which exceeds 100 mm disparity (upper LoA = 201.783; lower LoA = -186.966) (Figure 3.13a). No variable (e.g., body mass index, stature, sex, or habitual activity) explains why these three individuals in particular exceed the LoAs.

If the corrected foot length values are used to predict stature, the mean difference between stature and predicted stature is reduced (Figure 3.13b) from 0.464 (Bias=-7.408 \pm 74.255) for the non-corrected track length measurements to -0.005 (Bias=-2.351 \pm 91.786) for the corrected track length measurements. Despite the mean difference suggesting that the corrected track measurements are preferable for predicting stature, there is a gross increase in under-predicted values (upper LoA = 177.250; lower LoA = -242.916).

Generally, predicted stature values are less dispersed if the corrected track measurements are used for stature prediction, but there is trend for under-predicting stature by ~200 mm in taller individuals. Consequently, it was determined that the corrected track measurements should be used to predict stature for tracks formed in a loose substrate at a walking speed. Although, the non-corrected measurements should be used to predicted stature from tracks that exceed ~277 mm in length.

Stature prediction based on tracks produced on the loose substrate when walking fast

All predicted stature values from the non-corrected measurements (upper LoA = 164.816; lower LoA = -260.527) (Figure 3.13c) and corrected measurements (upper LoA = 177.242; lower LoA = -198.257) (Figure 3.13c) of tracks produced by a fast walk on the loose substrate fall within the 95% confidence interval, indicating that all measurements are reliably predicted using either method. The mean difference between each of the methods is minute: the difference in mean predicted values are -0.670 (Bias=-14.395 \pm 91.434) for the non-corrected track length measurements and -0.415 (Bias=-10.507 \pm 95.791) for the corrected track length measurements. Using the corrected track lengths for tracks produced on a loose substrate at a fast walking speed does not improve the stark dispersal of predicted values (Figure 3.13d). Consequently, the non-corrected track length measurements should be used for stature prediction when tracks are produced in a loose substrate (Table 3.7).

Stature prediction based on tracks produced on the loose substrate when jogging

All predicted stature values (with the exception of one outlier) from the non-corrected measurements of tracks produced by a jog on the loose substrate fall within the 95% confidence interval (upper LoA = 166.632; lower LoA = -228.922) (Figure 3.13e).

If the corrected foot length values are used to predict stature from tracks produced on the firm substrate during a fast walk, the mean difference between stature and predicted stature was increased (Figure 3.13f) from 0.129 (Bias=2.029 \pm 83.971) for the non-corrected track length measurements to 1.452 (Bias=25.832 \pm 75.818) for the corrected track length measurements. Predicted values are less dispersed when the corrected measurements are used to predict stature (upper LoA = 174.434; lower LoA = -182.714). Stature prediction was thus improved by using the corrected track length measurements for tracks formed in a loose substrate at a jogging speed (Table 3.7).

Table 3.7. Percentage errors of the predicted stature ranges using the actual track lengths as measured from the 3D models, and the corrected measurements using the correction factors from Table 3.7 (n=100 participants). ‘Actual’ values indicate stature predictions using the track dimensions. ‘Pred.’ values indicate stature predictions using the corrected track dimensions. Percentage errors of the stature values predicted from the measured foot length during the trials is reported in italics. Mean errors range from small (dark green) to large (red).

		Loose substrate				Firm Substrate			
		Mean% Error	Min.	Max.	Std. Dev	Mean% Error	Min.	Max.	Std. Dev
Walk	Actual Robbin’s ratio	7.440%	-4.377%	18.560%	± 5.339	7.460%	-7.695%	20.322%	± 5.467
	Pred. Robbin’s ratio	7.495%	-4.226%	18.735%	± 4.692	8.460%	-0.405%	17.423%	± 4.348
	Actual Martin’s ratio	0.278%	-13.846%	12.301%	± 5.102	0.296%	-10.751%	10.656%	± 4.983
	Pred. Martin’s ratio	1.229%	-7.045%	9.595%	± 4.057	0.329%	-10.611%	10.820%	± 4.379
Fast Walk	Actual Robbin’s ratio	7.312%	-3.670%	17.151%	± 5.913	7.652%	-8.723%	17.781%	± 6.325
	Pred. Robbin’s ratio	7.923%	-3.071%	16.641%	± 5.365	4.230%	-9.623%	11.002%	± 5.365
	Actual Martin’s ratio	0.158%	-10.110%	9.341%	± 5.519	0.450%	-14.808%	9.929%	± 5.903
	Pred. Martin’s ratio	-2.654%	-15.648%	3.602%	± 4.146	0.733%	-9.533%	8.865%	± 5.007
Jog	Actual Robbin’s ratio	7.130%	-1.078%	19.062%	± 5.098	4.893%	-2.065%	13.177%	± 4.084
	Pred. Robbin’s ratio	5.701%	0.562%	15.971%	± 4.596	5.065%	-2.069%	12.581%	± 3.489
	Actual Martin’s ratio	-2.010%	-8.594%	5.632%	± 3.812	-0.012%	-7.673%	11.126%	± 4.758
	Pred. Martin’s ratio	1.572%	-4.389%	9.991%	± 3.978	-1.346%	-6.142%	8.240%	± 4.290
BHBK	Actual Robbin’s ratio	10.220%	-0.332%	24.327%	± 5.506	8.028%	-0.047%	13.690%	± 4.021
	Pred. Robbin’s ratio	5.065%	-2.096%	12.850%	± 3.489	5.700%	0.563%	15.972%	± 4.596
	Actual Martin’s ratio	0.826%	-6.710%	6.111%	± 5.139	2.872%	-6.977%	16.035%	± 5.139
	Pred. Martin’s ratio	-1.939%	-8.598%	5.075%	± 3.257	-1.631%	-9.727%	7.869%	± 4.010
<i>Stature</i>	<i>Robbin’s Ratio</i>	<i>6.110%</i>	<i>0.422%</i>	<i>14.461%</i>	<i>± 3.454</i>				
	<i>Martin’s Ratio</i>	<i>-0.964%</i>	<i>-6.703%</i>	<i>6.830%</i>	<i>± 3.223</i>				

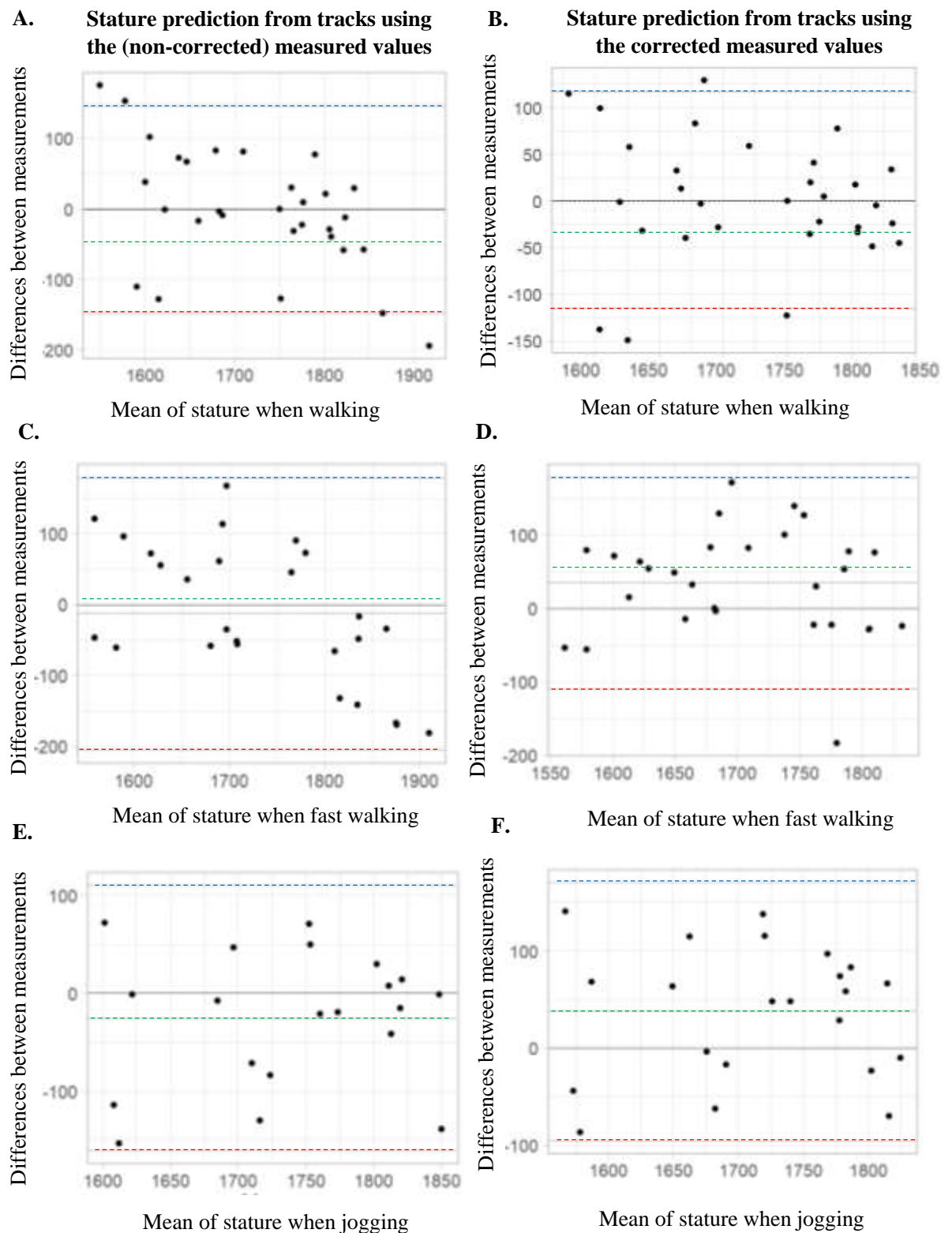


Figure 3.12. Bland-Altman graphs displaying the differences of mean stature prediction from track length on the firm substrate using the non-corrected track lengths (A, C and E) and the corrected track lengths (B, D and F) when walking (A and B), fast walking (C and D) and jogging (E and F). Upper (blue dotted line), lower (red dotted line) and the mean (green dotted line) of differences in predicted stature values are reported within a 95% confidence. The hypothesized mean (0) is indicated by the grey dotted line.

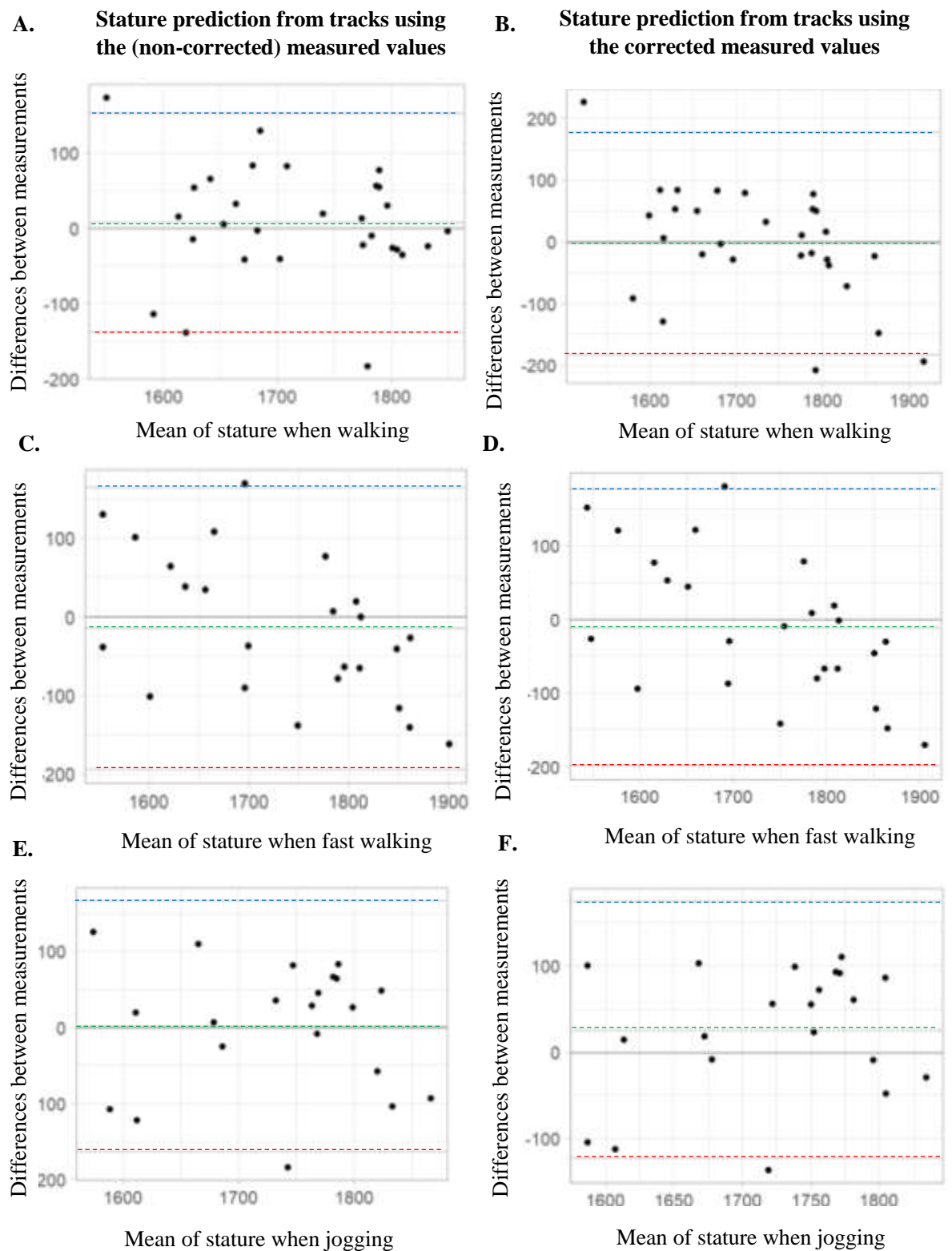


Figure 3.13. Bland-Altman graphs displaying the differences of mean stature prediction from track length on the loose substrate using the non-corrected track lengths (A, C and E) and the corrected track lengths (B, D and F) when walking (A and B), fast walking (C and D) and jogging (E and F). Upper (blue dotted line), lower (red dotted line) and the mean (green dotted line) of differences in predicted stature values are reported within a 95% confidence. The hypothesized mean (0) is indicated by the grey dotted line.

Age and sex predictions

Using the protocol adapted by Altamura et al. (2018), age and sex were successfully predicted for 55% – 60% (right and left foot, respectively) of participants when using the recorded foot length during the trials. The threshold for successfully predicting age and sex from the experimental tracks was set at 55%.

Age and sex were successfully predicted for 58.3% of tracks produced on the firm substrate and for 54.2% of tracks produced on the loose substrate using the corrected linear measurements of walking. The relationship between age/sex with foot length was found to be strongly determined when walking (adj. $R^2=0.667$; $t=4.476$; $P\leq 0.001$), thus allowing age and sex to be positively correlated with total foot length.

Age and sex predictions were only successfully predicted for 44.4% of tracks on the firm substrate and for 59.3% of tracks on the loose substrate when a fast walk was employed. Despite a poor success rate for the tracks on the firm substrate, the relationship between age/sex with foot length was determined to be strongly associated when fast walking (adj. $R^2=0.565$; $t=5.557$; $P\leq 0.001$).

Age and sex were successfully predicted for 60% of tracks produced on both the firm and loose substrates using the corrected linear measurements when a jog was employed. A strong positive relationship between age/sex with foot length was detected (adj. $R^2=0.788$; $t=1.653$; $P\leq 0.001$). This indicates that relative age and sex may be predicted from tracks which are determined to have been created whilst jogging.

Mass predictions

Numerous multivariate methods have been previously employed to predict body mass from track dimensions (e.g., Bennett and Morse 2014). To test the validity of these methods for the current population, body mass was regressed against foot length, as measured during the trials using an osteometric boards (Figure 3.14). Mass was positively associated with foot length for females ($R^2=0.581$; $t=5.200$; $P\leq 0.001$), but poorly correlated in males ($R^2=0.279$; $t=1.900$; $P=0.063$). Mass may have a stronger association with other foot dimensions, but unfortunately these measurements were not collected during the experiments. However, as mass had a strong relationship with foot length in females then the corrected track dimensions were regressed against body mass, with statistical relationships supported by Pearson's Correlation Coefficients (Table 3.8).

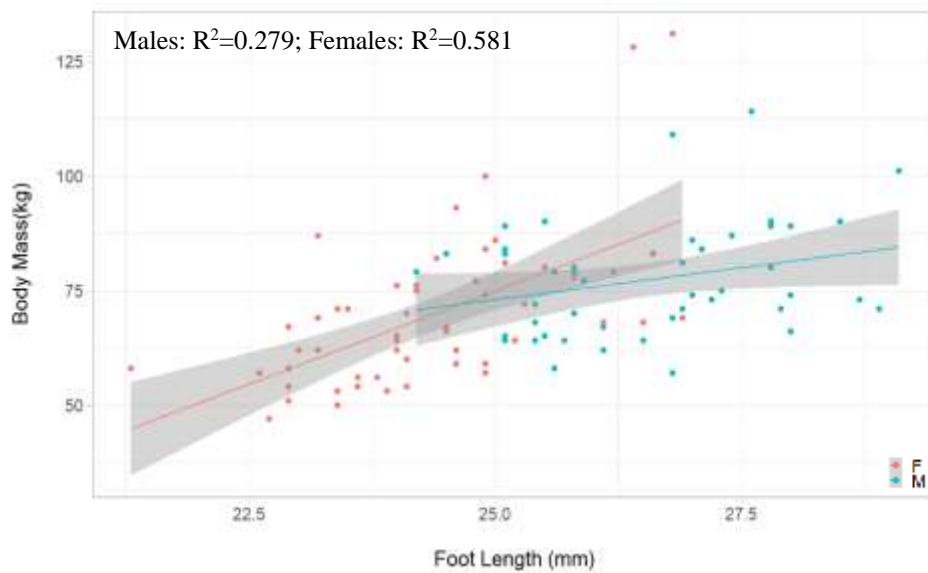


Figure 3.14. Regression of foot length (right foot used as an example) with body mass.

Table 3.8. Results of the Pearson's correlation which tested for association(s) between mass and track dimensions.

	Females				Males			
	DF	R ²	<i>t</i>	P	DF	R ²	<i>t</i>	P
Foot Length	53	0.422	3.39	0.001	43	0.255	1.73	0.091
Long Axis of Foot	53	0.074	0.538	0.593	43	-0.137	-0.909	0.369
Hallux Length	53	0.313	2.402	0.020	43	-0.176	-1.17	0.248
Forefoot Width	53	0.090	0.660	0.512	43	-0.078	-0.514	0.610
Heel Width	53	0.328	2.53	0.015	43	-0.240	-1.62	0.113

A strong positive association between mass and foot length ($R^2=3.39$; $P=0.001$), hallux length ($R^2=0.313$; $P=0.020$) and heel width ($R^2=0.328$; $P=0.015$) was detected in females, but all other track dimensions demonstrated a non-significant association with mass. No track dimensions were associated with body mass in males in this study.

A multivariate regression was computed using foot length and heel width to predict body mass for each individual from footprint dimensions. These dimensions were selected because they were previously detected to be strongly associated with body mass (Figure 3.15). Hallux length was omitted from the multivariate regression as the inclusion of this

variable over-emphasized mass prediction by ~ 30% in all participants (n=100). Because hallucal length is variable dependent on substrate typology and motion, the exclusion of this variable for mass prediction was justified. Body mass was predicted for grouped males and females using the following equation based on the assumption that sex will be non-determinable in fossil tracks:

Body Mass (Kg)

$$= -34.381 + 0.169 * (\text{measured heel width}) + 0.381 * (\text{measured track length}) \\ \pm 6.235$$

Body mass was successfully predicted for 43.53% ($t=1.682$; $P=0.096$) of males and females ($MSE=0.120\% \pm 16.974$); yet, the range of predicted values was quite dispersed (maximum over-estimation value = 41.69%; maximum under-estimation value = 62.360%). The body mass of one female was 47.00 Kg. The predicted body mass for this individual based upon track dimensions was 76.32 Kg, a disparity of +62.36%. The predicted mass value provides a body mass index of 32.4. If this multivariate equation using track dimensions had been used to predict the biometrics of this woman then she would have been classed as grossly over-weight.

Because poor correlation coefficients were identified with an obvious sex bias in conjunction with poor estimation of body mass from track dimensions (Table 3.7; Figure 3.15), multivariate assumptions to predict body mass from tracks for this sample are not possible.

Hip height

A regression was computed to determine if hip height could be positively calculated from track dimensions using measurements extracted from each participant during the trials (n=100). A strong correlation was determined between stature and hip height (grouped results: adj. $R^2=0.615$; $t=5.889$; $P\leq 0.001$) (Figure 3.16a). This strong association indicates that total foot length and predicted stature can be used to positively predict hip height from tracks. Foot length was regressed against hip height, with numerous outliers identified and weaker associations than that of stature to hip height (Figure 3.16b; Table 3.9).

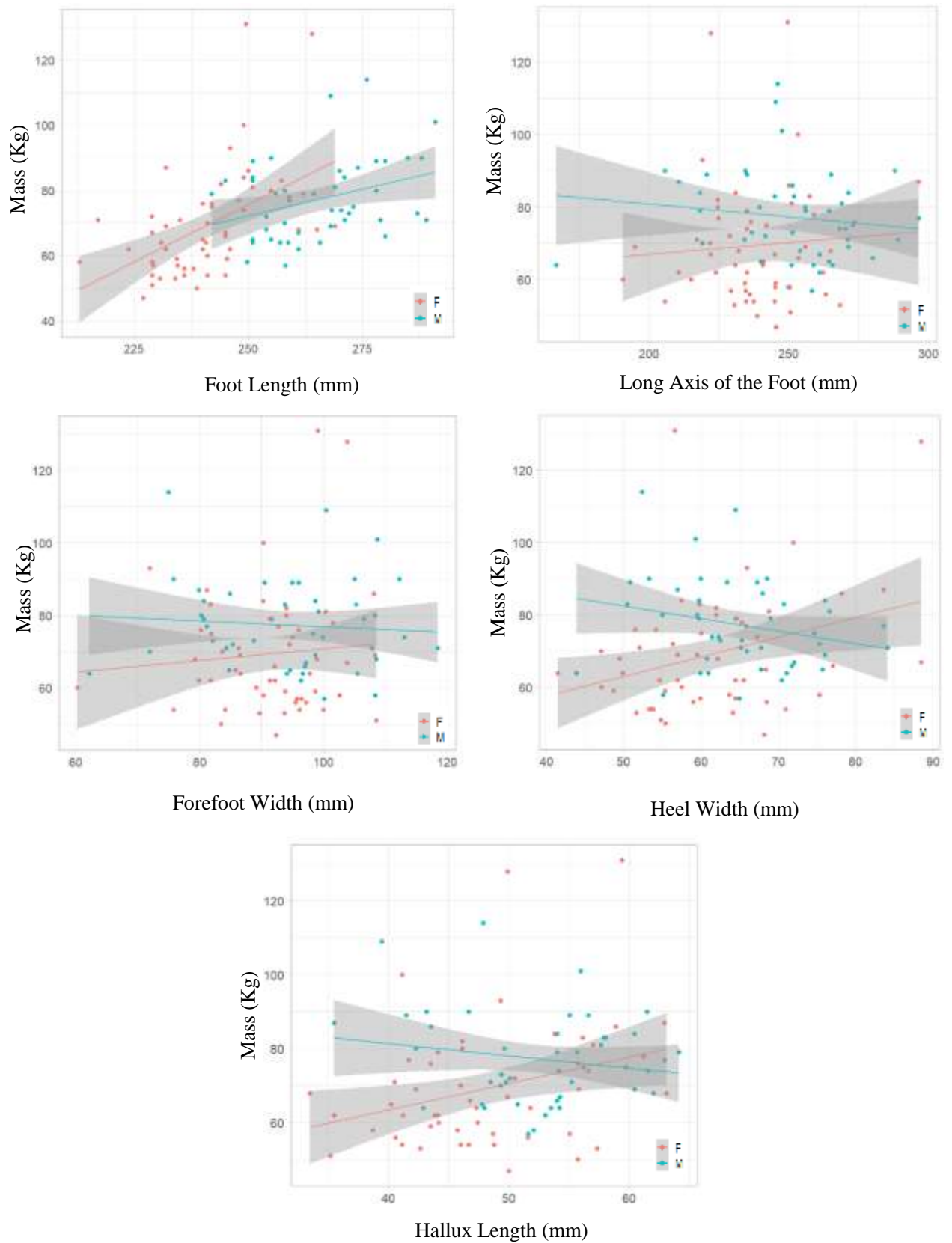
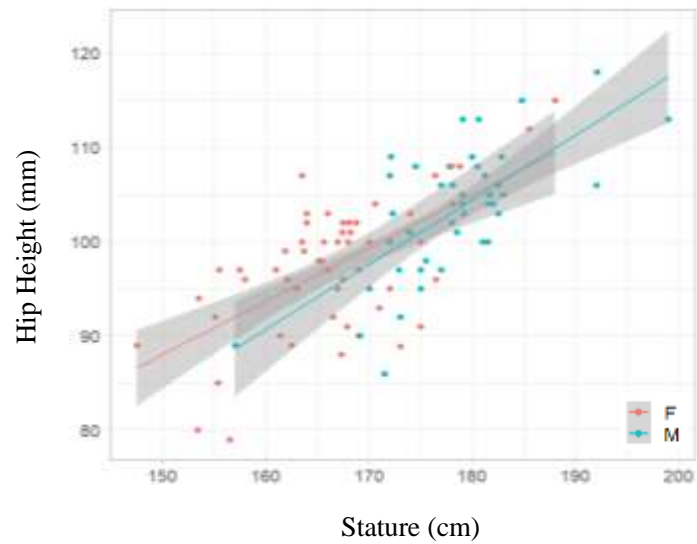


Figure 3.15. Regression of all linear measurements against mass to identify positive correlations between the variables. All measurements from the corrected measurements.

A.



B.

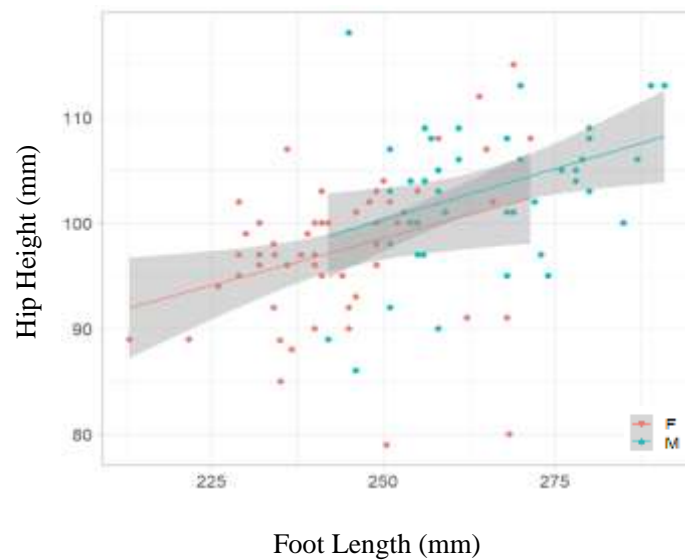


Figure 3.16. Regression of stature to hip height and foot length to hip height of known measurements (n=100 participants).

Table 3.9. Results of the Pearson's correlation to test for association between hip height and foot length. Positive P values are in bold.

	Females				Males			
	DF	R ²	t	P	DF	R ²	t	P
Foot Length	53	0.325	2.50	0.016	43	0.362	2.54	0.015

The relationship between foot length and hip height has been extensively explored (e.g., Raichlen et al. 2008), and positively detected in the current study (grouped results: $R^2=0.555$; $t=4.138$; $P<=0.001$). However, numerous outliers existed within the current sample suggesting that previous models of hip height prediction are not applicable to the current sample tested. Consequently, this method was refined by computing a GLM to explore the relationship between total foot length and hip height, with mass introduced as a nested effect (association demonstrated in Figure 3.15). Hip height was predicted for all tracks using the following equation as developed from known measurements:

Hip Height (mm)

$$= 0.203(x) + 54.639 \pm 7.117$$

Results indicate that if the relationship between foot length and known hip height is utilised to predict relative hip height without the introduction of mass as a nested effect, the mean standard error (MSE=9.230) of predicted values was moderately low, but poorly correlated ($R^2=0.359$; $P<=0.001$). If mass is introduced to correct the predicted values, the standard error of predicted values was greater (MSE=12.550), but hip height and foot length were strongly associated ($R^2=0.601$; $P<=0.001$).

Upon inspection of each predicted hip height value it was determined that for all participants (both groups from the pilot and biomechanical trials were included; $n=100$) hip height could be predicted to within 4 mm by using at least one of the methods (with or without mass as a nested effect). The accuracy for each method to reliably predict hip height was identified to be equal.

However, a sex bias in hip height prediction was detected. By incorporating mass, hip height was correctly predicted for 55% of female participants (Table 3.9). By removing mass as a nested effect hip height was correctly predicted for 57% of female participants. This suggests that neither model is optimally suited for hip height prediction. However, a small standard error for both methods suggests that relative hip height can be predicted from tracks as demonstrated by the successful prediction of hip height to within 4 mm for all participants (Table 3.9).

Table 3.10. Percentage errors of the predicted hip height prediction ranges using the corrected track lengths (mm) with males and females grouped. ‘With mass’ represents values that were predicted using mass as a nested effect in the linear model. ‘Without mass’ represents values that were predicted by a regression of foot length (mm) to hip height (mm). Std. Dev provided as %.

			Loose substrate				Firm Substrate			
			Mean% Error	Min.	Max.	Std. Dev	Mean% Error	Min.	Max.	Std. Dev
Males	Walk	<i>With mass</i>	2.802%	-1.916%	6.863%	± 2.400	3.853%	-1.532%	10.343%	± 3.599
		<i>Without mass</i>	-1.089%	-5.921%	5.191%	± 3.060	0.161%	-5.412%	7.216%	± 4.147
	Fast Walk	<i>With mass</i>	3.831%	-3.496%	10.549%	± 4.029	1.438%	-4.481%	6.626%	± 3.345
		<i>Without mass</i>	-0.339%	-8.016%	7.489%	± 4.477	-3.195%	-9.321%	2.582%	± 3.842
	Jog	<i>With mass</i>	1.471%	-3.143%	6.675%	± 3.080	3.617%	-0.228%	8.421%	± 2.868
		<i>Without mass</i>	-2.812%	-7.548%	4.784%	± 3.798	-0.008%	-5.521%	6.917%	± 3.732
	BHBK	<i>With mass</i>	0.352%	-3.607%	4.257%	± 2.772	1.511%	-4.007%	4.254%	± 2.644
		<i>Without mass</i>	-4.164%	-8.860%	2.873%	± 3.493	-2.878%	-9.504%	3.661%	± 3.452
Females	Walk	<i>With mass</i>	6.467%	-0.004%	15.805%	± 3.990	6.509%	1.788%	16.155%	± 3.955
		<i>Without mass</i>	0.068%	-8.381%	9.175%	± 4.228	0.124%	-6.007%	9.639%	± 4.054
	Fast Walk	<i>With mass</i>	5.636%	0.795%	14.566%	± 3.880	4.810%	-1.833%	13.066%	± 3.405
		<i>Without mass</i>	-0.770%	-6.682%	7.533%	± 4.040	-1.814%	-7.474%	5.545%	± 3.067
	Jog	<i>With mass</i>	5.926%	-1.791%	14.933%	± 4.923	6.847%	-1.000%	15.007%	± 4.506
		<i>Without mass</i>	-0.465%	-7.418%	8.020%	± 4.786	0.834%	-6.369%	8.117%	± 4.303
	BHBK	<i>With mass</i>	6.027%	-1.153%	14.112%	± 4.012	5.632%	-0.560%	13.408%	± 3.633
		<i>Without mass</i>	-0.514%	-6.573%	6.932%	± 3.879	-1.038%	-5.786%	5.999%	± 3.361

3.3.4 Lower limb kinematics

To explore whether locomotory behaviour was also reflected in topographical morphology, 3D motion capture systems were employed to record a variety of motions. Kinematics of the hip, knee and ankle were quantified and compared to patterns of morphology. Results are summarised below¹.

Kinematics of the hip

Hip flexion in females was significantly increased from 26.64° (\bar{x}) on the hard ground (the controlled walk) to 30.91° (\bar{x}) on the firm substrate ($P=0.017$; $F=5.744$), and was further increased to 33.91° (\bar{x}) on the loose substrate ($P=0.018$; $F=5.703$). Flexion was non-significantly variable between the loose and firm substrates when walking in males and females ($P\geq 0.05$, $F=0.569$ ♂; $P\geq 0.05$, $F=2.509$ ♀) (Table 3.11; 3.12). Hip flexion in males remained consistent between all trackways when walking (Table 3.11; 3.12).

Both males and females have greater hip flexion on a looser substrate when speed was increased to a fast walk ($\bar{x}=38.03^\circ$) ($P=0.025$, $F=4.486$ ♂; $P=0.029$, $F=5.385$ ♀) and a jog ($\bar{x}=44.51^\circ$) ($P\leq 0.001$, $F=13.396$ ♂; $P=0.031$, $F=5.148$ ♀). Peak hip flexion during the stance phase was up to 5° greater when fast walking, and ~12 – 15° greater when jogging (Figure 3.17; Table 3.11).

Hip extension remained constant between the different substrates at all speeds in males and females as reported by the Student's t -test ($P\geq 0.05$) (Table 3.11). However, hip extension in females was altered to accommodate changes in substrate when changing the underlying substrate from the hard ground ($\bar{x}=-14.46^\circ$) to the firm ($\bar{x}=-12.04^\circ$) ($P\leq 0.001$; $F=20.580$) and loose substrate ($\bar{x}=-11.55^\circ$) ($P\leq 0.001$; $F=42.954$). Hip extension was only slightly variable in males between walking on the hard ground and a firm substrate ($P=0.035$; $F=4.462$) but remained consistent when walking on the loose substrate ($P\geq 0.05$; $F=3.968$) (Table 3.12).

No differences were found in hip flexion or extension between the different substrates at any speed in males nor females for the BHBK movement as reported by the Student's t -test ($P\geq 0.05$) (Figure 3.18; Table 3.11).

¹ Both the left and right leg produced similar results, with no statistically significant bi-lateral asymmetry in lower limb movement determined ($P=0.912$). Statistical and graphical results presented here belong to the left leg.

Kinematics of the knee

Knee flexion was significantly smaller on the hard ground ($\bar{x}=65.55^\circ$) than on the firm ($\bar{x}=68.29^\circ$) ($P\leq 0.001$, $F=99.111$ ♂; $P\leq 0.001$, $F=35.625$ ♀) and loose substrates ($\bar{x}=72.04^\circ$) ($P\leq 0.001$, $F=16.659$ ♂; $P\leq 0.001$, $F=36.731$ ♀) (Table 3.12).

Knee flexion was significantly greater on the looser substrate than the firm one when walking ($P=0.023$, $F=5.421$ ♂; $P\leq 0.001$, $F=42.941$ ♀), fast walking ($P=0.035$, $F=4.510$ ♂; $P\leq 0.001$, $F=36.675$ ♀) and jogging ($P=0.020$, $F=5.557$ ♂; $P\leq 0.001$, $F=39.573$ ♀). Peak knee flexion during the swing phase was up to 8° greater when walking quickly, and $\sim 20^\circ$ greater when jogging in some individuals (Figure 3.17; Table 3.11).

Both males and females exhibited no significant change in knee extension between movement on the hard ground and the firm substrate ($P\geq 0.05$; Table 3.11). Yet, knee extension was significantly increased between movement on the hard ground ($\bar{x}=-0.15^\circ$) and the firm substrate ($\bar{x}=0.56^\circ$) ($P=0.006$, $F=7.562$ ♂; $P\leq 0.001$, $F=25.720$ ♀). Knee extension was non-significantly variable ($P\geq 0.05$; Table 3.11) between each substrate when walking, fast walking and jogging in males and females.

Knee flexion was significantly increased when walking on the looser substrate during a BHBK movement ($P\leq 0.001$, $F=8127$ ♂; $P=0.005$, $F=25.261$ ♀). Knee extension was also significantly increased to accommodate changes in substrate pliancy ($P=0.017$, $F=9.796$ ♂; $P=0.024$, $F=5.179$ ♀) (Figure 3.18; Table 3.11).

Kinematics of the ankle

There was no significant difference in dorsiflexion between each substrate (including the hard ground) when walking, fast walking and jogging in males and females ($P\geq 0.05$), as reported by the Student's *t*-test (Figure 3.17; Table 3.11; 3.12).

Plantarflexion was significantly smaller on the hard ground ($\bar{x}=-16.99^\circ$) than the firm ($\bar{x}=-18.86^\circ$) ($P=0.023$, $F=5.205$ ♂; $P\leq 0.001$, $F=1.322$ ♀) and loose substrates ($\bar{x}=-20.24^\circ$) ($P=0.003$, $F=9.277$ ♂; $P\leq 0.001$, $F=19.718$ ♀) (Table 3.11). Plantarflexion was significantly greater on the looser substrate than the firm one when walking ($P=0.007$; $F=7.622$ ♂; $P=0.004$, $F=8.694$ ♀) and fast walking ($P\leq 0.001$, $F=81.572$ ♂; $P=0.016$, $F=5.869$ ♀). Plantarflexion was $\sim 10^\circ$ greater on the looser substrate when speed is increased. When jogging, neither males nor females significantly increased their plantarflexion ranges to accommodate movement on a loose substrate ($P=0.765$, $F=0.802$ ♂; $P=0.346$, $F=0.913$ ♀).

Neither plantarflexion nor dorsiflexion were not found to be significantly increased when walking on the looser substrate during a BHBK movement in neither males nor females ($P \geq 0.05$), as reported by the Student's *t*-test (Figure 3.18; Table 3.11; 3.12).

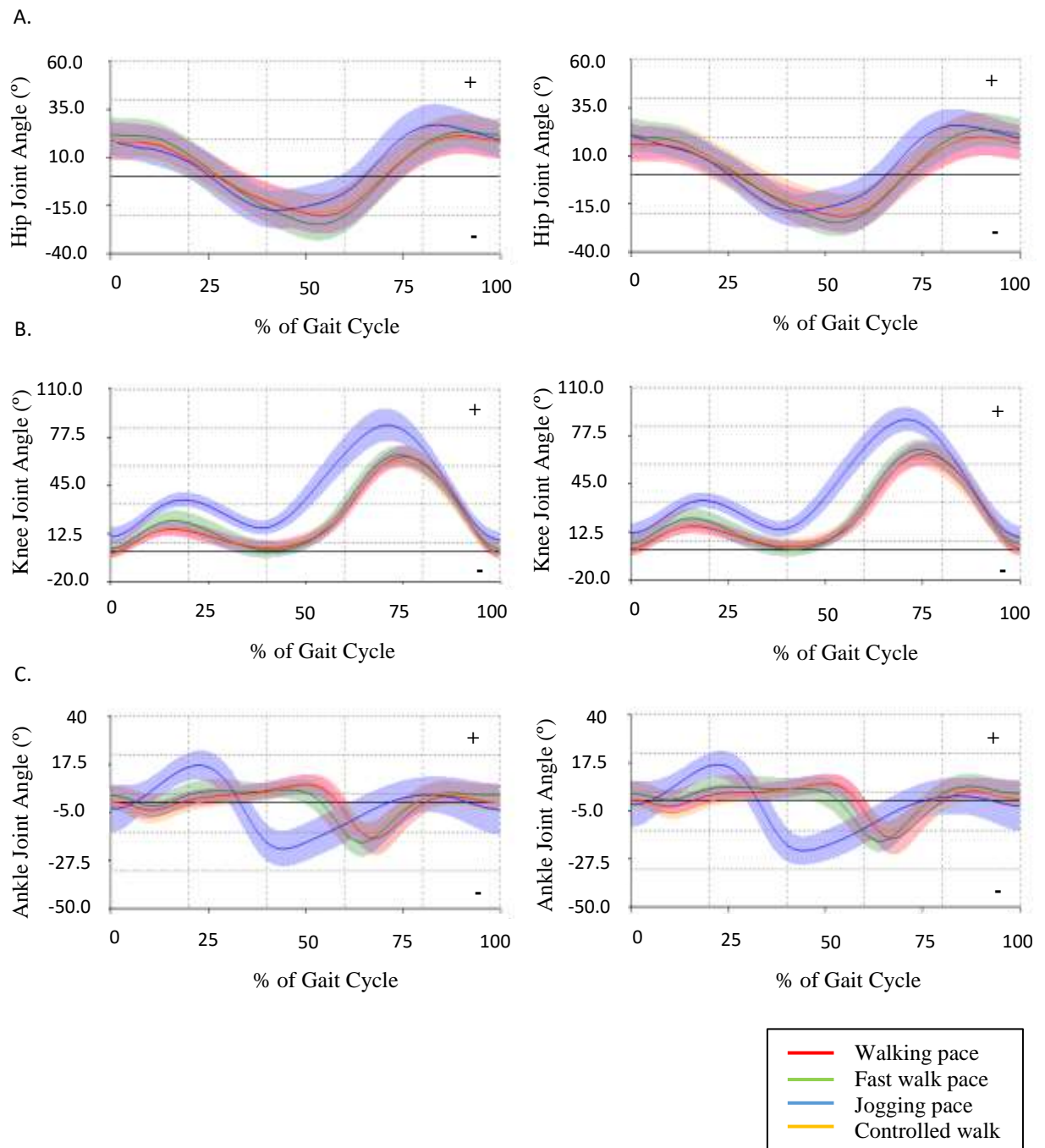


Figure 3.17. Extension and flexion of the hip (A) and knee (B), and ankle joint angles (C) during traversing on the firm (left) and loose (right) substrates in males ($n=20$). Solid lines represent group means and dotted lines indicate the standard deviation of each grouped variable. + represents flexion (hip and knee) and dorsiflexion. – represents extension (hip and knee) and plantarflexion.

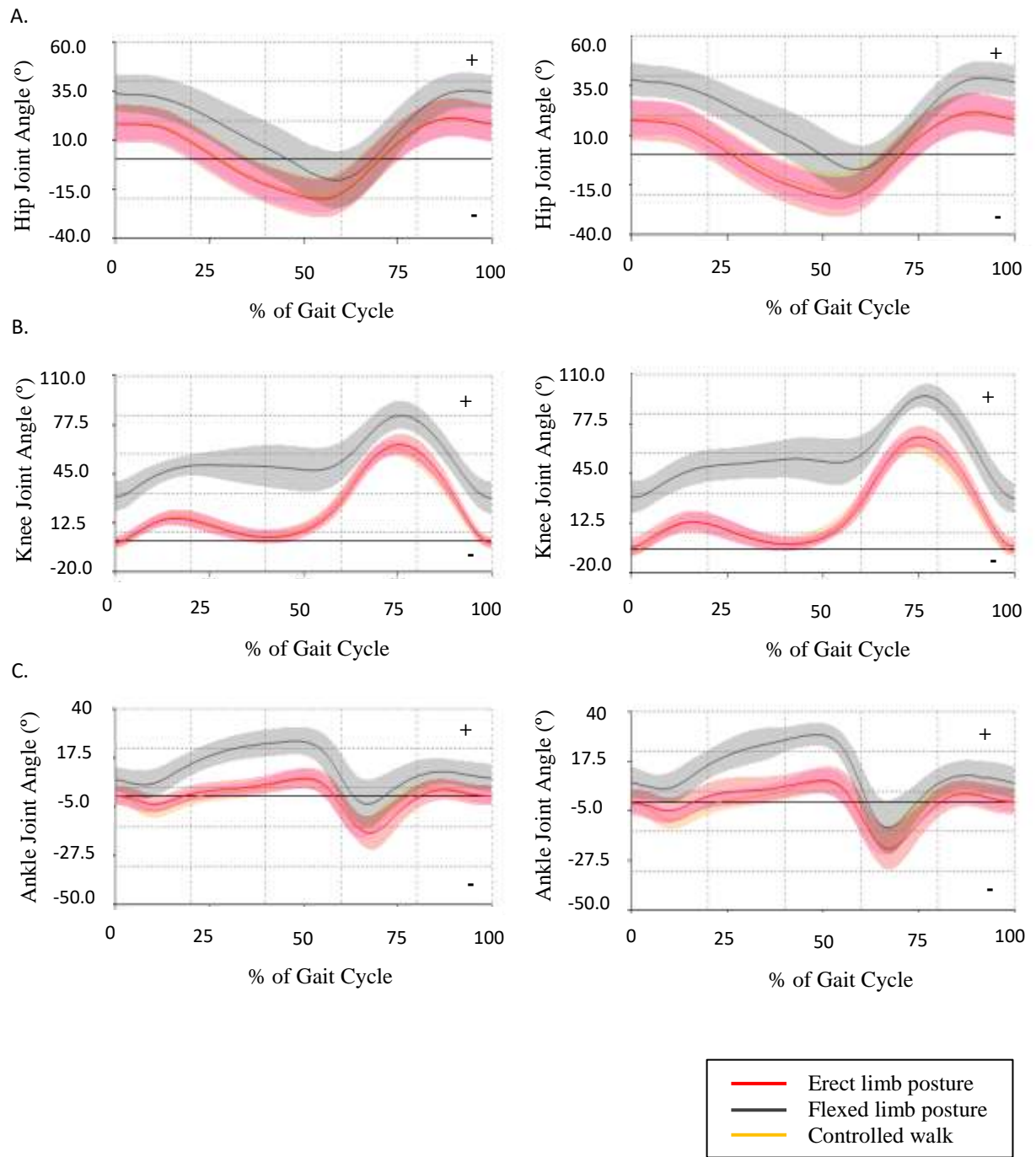


Figure 3.18. Extension and flexion of the hip (A) and knee (B) and ankle (C) joint angles with various limb postures on the firm (left) and loose (right) substrates in males. + represents flexion (hip and knee) and dorsiflexion. – represents extension (hip and knee) and plantarflexion.

Table 3.11. Results of the one-way ANOVA computed on peak flexion/extension of the knee and hip and peak dorsiflexion/plantarflexion of the ankle to identify any disparity in lower limb kinematics across the loose and firm substrates.

		Females					Males				
		DF	SS	MS	F	P	DF	SS	MS	F	P
Hip Flexion	Walk	1	141.934	141.934	2.509	0.115	1	29.208	29.208	0.327	0.569
	Fast Walk	1	303.474	303.474	4.847	0.029	1	425.534	425.534	5.386	0.025
	Jog	1	1246.545	1246.545	13.296	<0.001	1	152.823	152.823	5.148	0.031
	BHBK	1	1.290	1.290	0.012	0.913	1	163.909	163.909	2.083	0.152
Hip Extension	Walk	1	25.287	25.287	0.780	0.401	1	8.826	8.826	0.102	0.760
	Fast Walk	1	0.002	0.002	0.00009	0.992	1	33.923	33.923	0.514	0.474
	Jog	1	53.940	53.940	2.381	0.126	1	56.128	56.127	0.658	0.419
	BHBK	1	0.135	0.135	0.0005	0.982	1	55.934	55.934	0.279	0.598
Knee flexion	Walk	1	822.756	822.756	42.941	<0.001	1	229.141	229.141	5.241	0.023
	Fast Walk	1	751.852	751.852	36.675	<0.001	1	162.483	162.483	4.510	0.035
	Jog	1	2926.716	2926.716	39.573	<0.001	1	574.592	574.592	5.557	0.020
	BHBK	1	1231.761	1231.761	25.261	<0.001	1	514.702	514.702	8.127	0.005
Knee Extension	Walk	1	7.728	7.728	4.468	0.052	1	0.745	0.745	0.070	0.792
	Fast Walk	1	38.873	38.873	3.312	0.071	1	20.330	20.330	0.927	0.337
	Jog	1	248.331	248.331	7.351	0.007	1	46.585	46.585	2.749	0.100

Table 3.11 cont. Results of the one-way ANOVA computed on peak flexion/extension of the knee and hip and peak dorsiflexion/plantarflexion of the ankle to identify any disparity in lower limb kinematics across the loose and firm substrates.

		Males					Females				
		DF	SS	MS	F	P	DF	SS	MS	F	P
<i>Knee extension cont.</i>	BHBK	1	367.692	367.692	5.179	0.024	1	23.922	23.922	9.796	0.017
Ankle Dorsiflexion	Walk	1	141.934	141.934	2.508	0.115	1	29.210	29.210	0.326	0.569
	Fast Walk	1	555.705	555.705	6.597	0.051	1	9.842	9.842	1.461	0.230
	Jog	1	1246.545	1246.545	13.296	<0.001	1	21.543	21.543	2.538	0.115
Ankle Plantarflexion	BHBK	1	1.290	1.290	0.012	0.914	1	27.299	27.299	2.126	0.149
	Walk	1	448.866	448.866	8.694	0.004	1	242.374	242.374	7.622	0.007
	Fast Walk	1	141.884	141.884	5.869	0.017	1	103.776	103.776	81.574	<0.001
	Jog	1	10.623	10.623	0.913	0.360	1	27.382	27.382	0.803	0.373
	BHBK	1	22.517	22.517	0.517	0.475	1	128.418	128.418	1.513	0.221

Table 3.12. Results of the one-way ANOVA computed on peak flexion/extension of the knee and hip and peak dorsiflexion/plantarflexion of the ankle to identify any disparity in lower limb kinematics across the loose and firm substrates with that of the hard ground (controlled walk).

		Females					Males				
		DF	SS	MS	F	P	DF	SS	MS	F	P
Hip Flexion	Control ~ Firm	1	615.434	615.434	5.744	0.017	1	125.286	125.286	1.427	0.233
	Control ~ Loose	1	564.980	564.980	5.703	0.018	1	200.525	200.525	2.273	0.133
Hip Extension	Control ~ Firm	1	1909.114	1909.114	20.580	<0.001	1	380.099	380.099	4.462	0.035
	Control ~ Loose	1	3521.396	3521.396	42.954	<0.001	1	344.636	344.636	3.698	0.056
Knee flexion	Control ~ Firm	1	2718.393	2718.393	99.111	<0.001	1	616.213	616.213	16.659	<0.001
	Control ~ Loose	1	784.112	784.112	35.625	<0.001	1	994.267	994.267	36.731	<0.001
Knee Extension	Control ~ Firm	1	51.326	51.326	2.515	0.114	1	35.448	35.448	2.585	0.109
	Control ~ Loose	1	161.143	161.143	7.562	0.006	1	398.486	398.486	25.720	<0.001
Ankle Dorsiflexion	Control ~ Firm	1	9.449	9.449	0.598	0.440	1	9.427	9.427	0.562	0.454
	Control ~ Loose	1	0.196	0.196	0.013	0.910	1	13.873	13.873	0.776	0.379
Ankle Plantarflexion	Control ~ Firm	1	364.338	364.338	5.205	0.023	1	531.553	531.553	14.322	<0.001
	Control ~ Loose	1	701.980	701.980	9.277	0.003	1	735.107	735.107	19.718	<0.001

3.3.5 Locomotory behaviour reflected in track morphology

All registered tracks were visually examined for patterns of morphology to establish if lower limb kinematics were identifiable from track shapes. Track depth maps, which were used for qualitative visualization of morphological features, identified three key variations in morphology: (1) the midfoot shapes were over-represented on the looser substrate corresponding to increased posterior sediment displacement during the later stance phase; (2) there were variable depth distributions across each track as speed and substrate pliancy were both increased; and (3) lateral digit morphology was under-represented with increasing speed to the extent that it may be argued the impression of the digits were “lost”, particularly on the firmer substrate (Figure 3.19). Depth distribution during walking on both substrates was quite uniform across the track. This uniformity in depth was absent – particularly on the firmer substrate – as speed was increased.

As knee flexion increased (e.g., by an increase in speed or by movement on a less compliant substrate) the impression underneath the midfoot was higher. Plantarflexion was increased on the less compliant substrate when walking and fast walking, indicating that plantarflexion likely accounts for the increased sediment displacement on the loose substrate in the midfoot region. As the foot moved into the plantarflexed position in later stance and toe-off, stance was prolonged (as assessed from the 3D motion capture software which recorded real time movement at a rate of 250 Hz) to allow the foot to gain traction with the underlying sediment to provide leverage for toe-off. Consequently, material was posteriorly displaced from the forefoot to the midfoot region to accommodate the distal foot’s further penetration into the sediment (this accounts for generally deeper forefoot regions on the looser substrate than that of the firm substrate).

Generally, the volume of material (e.g., the shape and size, not just the height) representing the midfoot arch was greater when moving at increased speeds. An increase in speed utilizes greater hip flexion, corresponding to the tracks displaying greater volumes of sediment in the midfoot impression. Due to the sediment displacement caused by an increase in plantarflexion, it was not possible to ascertain if this assumption is reflective between the substrates; it was only possible to state that the volume of the midfoot impression changed on the same substrate with increased speed.

Tracks produced on each substrate when jogging are starkly different than those from walking and fast walking; there are variable depth distributions, midfoot shapes and

height, and distal foot morphology. Neither plantarflexion nor dorsiflexion were found to be significantly variable between substrates when jogging, indicating that distinguished track shape production was not associated with changes in the ankle. Alternatively, both hip and knee flexion were significantly altered to accommodate changes in substrate mechanics, suggesting that the hip and knee are more likely to be associated with changes in track shape than the ankle during a jogging pace.

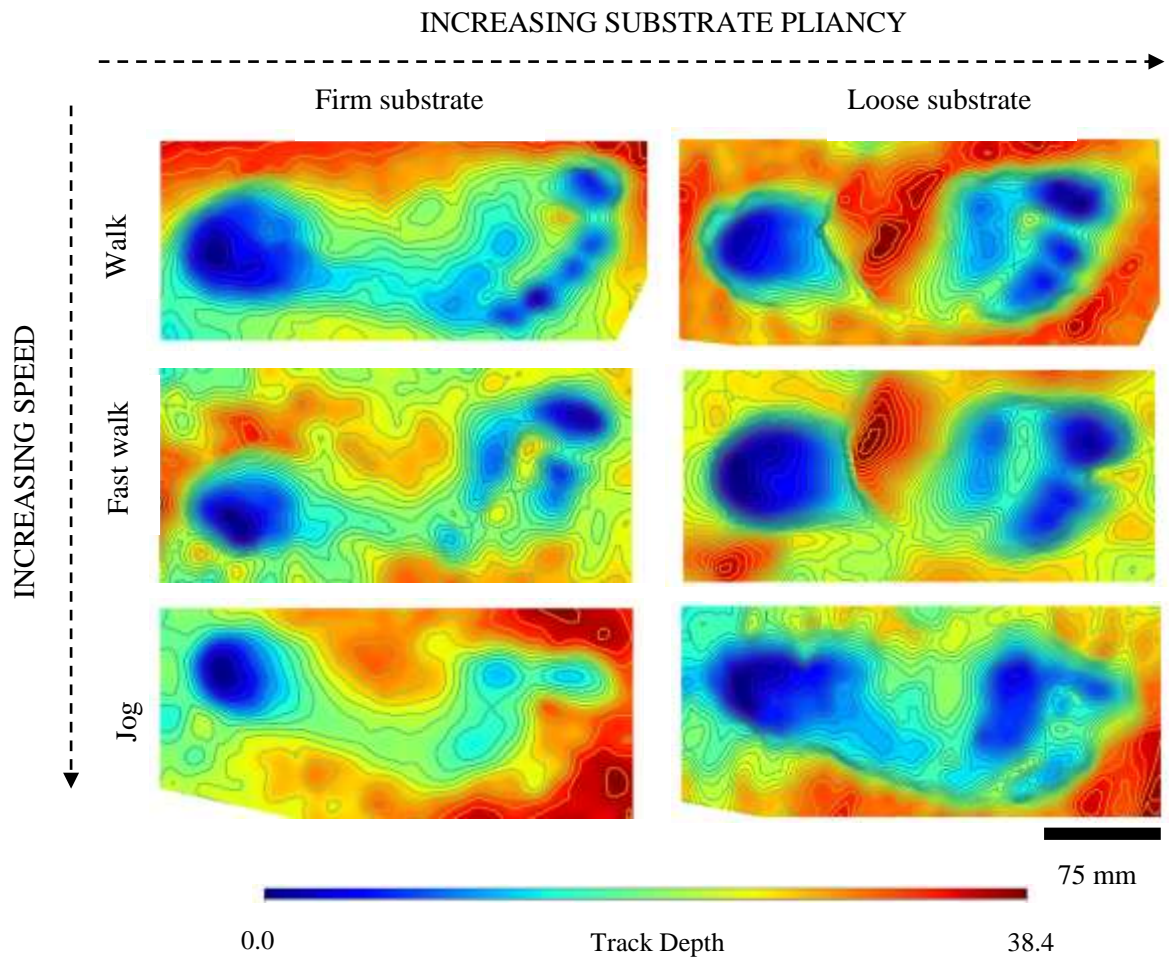


Figure 3.19. Track depth maps between the two different substrates in one male individual showing how track morphology changed with an increase in speed and with an increase in substrate pliancy.

It is evident that changes in lower limb mechanics produce morphological patterns in tracks for the current population (n=100). In sum, increased plantarflexion produced greater sediment displacement, which could be misconstrued as a higher arch. Knee flexion accounted for the majority of lower limb changes to accommodate movement on different substrates. Because knee kinematics dominated lower limb variability, it is a fair

assumption to state that knee flexion is likely associated with all patterns of morphological variability in tracks. Importantly, a pattern of increasing arch prominence was always established when knee flexion was greater between any two variables (e.g., movement on different substrates or by changing speed). Greater hip flexion generally changed the volume of the midfoot representation as speed was increased.

Because arch height was visually identified to be more prominent on the loose substrate than the firm one and, additionally, with changes in speed, arch height for all averaged tracks was quantified (Figure 3.20; Table 3.13). Midfoot height was identified to be significantly higher on the loose substrate than that of the firm substrate when walking ($P=0.026$; $t=2.316$) and when walking with a flexed limb ($P=0.007$; $t=2.832$) (Table 3.14). Midfoot height was not identified to be significantly disparate between any other variables ($P \geq 0.05$), signifying that changes in speed did not influence arch height. However, upon inspection of the range of data, arch height was much more variable on the loose substrate than the firm, and both the standard error and standard deviations in addition to the data ranges were always greater on the less compliant substrate, signifying that arch height could be more variably shaped on this substrate (Table 3.13). However, because the absolute height was mostly non-significantly distinguished between each variable (Table 3.14), midfoot impressions were not too sensitive to changes in substrate mechanics.

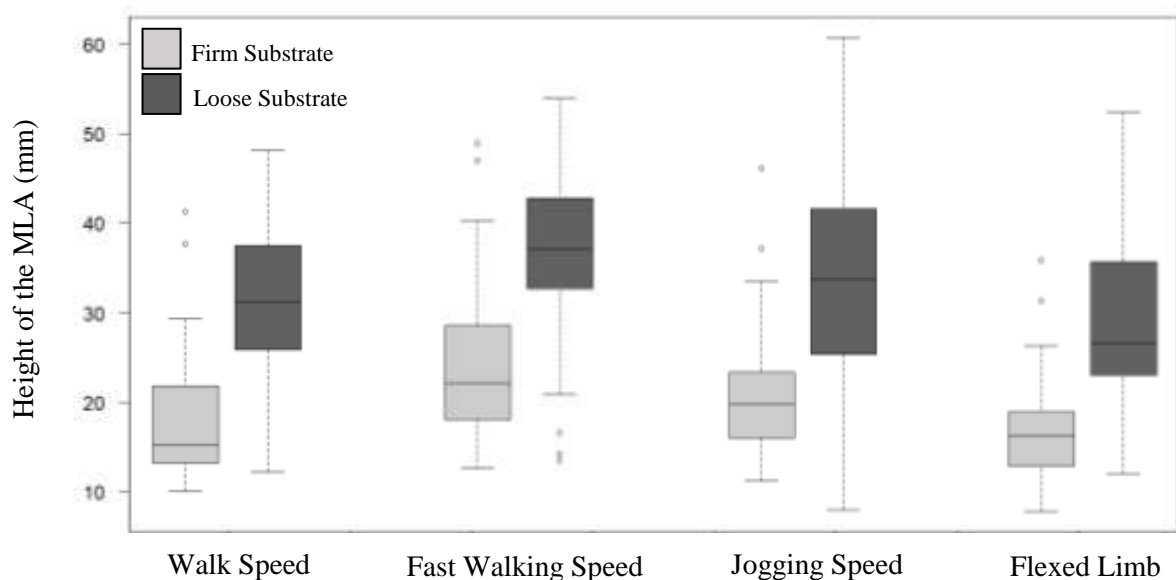


Figure 3.20. Boxplot of arch height as measured from 3D averaged tracks and grouped according to speed and substrate ($n=20$; a reduced dataset was used due to many of the participants keeping their foot in a dorsiflexed position, described in Section 3.2.4).

Table 3.13. The descriptive statistics for arch height on both substrates across each of the motions included in this study (n=20).

		Mean	Std. Dev	Std. Error	Range	
					Minimum	Maximum
Walk	Firm Substrate	17.351	6.603	0.943	9.800	41.040
	Loose Substrate	31.644	8.366	1.261	12.000	47.940
Fast Walk	Firm Substrate	23.614	8.238	1.132	12.010	48.220
	Loose Substrate	36.293	9.313	1.420	12.880	53.290
Jog	Firm Substrate	20.944	7.065	1.053	11.400	46.322
	Loose Substrate	32.574	12.101	2.045	8.145	60.900
BHBK	Firm Substrate	16.542	5.390	0.770	7.750	35.770
	Loose Substrate	30.442	10.506	1.516	12.000	52.300

Table 3.14. Results of the two-tailed student's *t*-test computed on the height of the midfoot impression between the loose and firm substrates to identify any disparity in arch height across the different motions.

	DF	R ²	<i>t</i>	P
Walk_loose ~ Walk_firm	37	0.357	2.316	0.026
Fast Walk_loose ~ Fast Walk_firm	37	-0.114	-0.698	0.490
Jog_loose ~ Jog_firm	37	0.195	1.126	0.269
Walk_loose ~ Fast Walk_loose	37	0.164	0.831	0.414
Walk_firm ~ Fast Walk_firm	37	0.049	0.279	0.782
Walk_firm ~ Jog_firm	37	0.184	0.991	0.330
Walk_loose ~ Jog_loose	37	0.022	0.112	0.912
BHBK_loose ~ BHBK_firm	38	0.417	2.832	0.007
Walk_loose ~ BHBK_loose	31	0.111	0.625	0.537
Walk_firm ~ BHBK_firm	30	0.082	0.448	0.658

To explore why (1) arch height was generally higher on the loose substrate than the firm, and (2) data ranges were more variable on the looser substrate, a Pearson's correlation and a MANOVA were computed using arch height from each condition (e.g., from a walk on a loose substrate in each individual) to test for relationships between absolute values of arch height with that of lower limb motions (hip, knee and ankle) at each speed/limb posture. Assumptions that arch height was associated with changes in the lower limb were not supported as all results were determined to be non-significant (P values ranged from 0.85-0.95; R^2 was always below 0.02; t -value was ~ 0 for all variables). The lack of relationship between arch heights with that of any lower limb variable signifies that arch height may be associated with other variables that were unaccounted for in the current study (e.g., modular movement within the foot).

Although arch height was mostly non-differentiated between variables with the exclusion of walking speeds (Table 3.13), inspections of the depth maps identified morphological changes in the midfoot region (Figure 3.19). To identify any potential shape disparity between tracks created at different speeds across substrates of varying compliance, mesh comparisons were computed on a small selection of tracks ($n=15$ participants). A scalar field was created relative to the absolute depth of each track, whereby red represents an increase and blue represents a decrease in track depth (Figure 3.21).

The majority of morphological differences were established in the midfoot region. The distribution of material representing the arch impression were more dispersed on the looser substrates. This gives the indication of a more prominent midfoot, despite the maximum absolute height being mostly consistent (Table 3.14). Although arch heights were determined to be slightly greater on the looser substrate than the firm one (Figure 3.19), a qualitative approach of the current comparative population would suggest that the shape of the midfoot impression was grossly different between the two substrates in height (Figure 3.20), which is a misidentification of functional morphology. By combining mesh comparisons with a quantitative analysis, the midfoot impression has instead been characterised as increasing in volume which is a more accurate conclusion of arch shape. By combining methods, patterns of morphology can be more clearly established (e.g., midfoot prominence is greater with increases in speed and substrate pliancy), which are summarised below.

Morphological disparity between tracks during several speeds

The volume of the arch impression on the different substrates during walking was greater on the less compliant substrate (Figure 3.21a). During fast walking and jogging, arch height was greater not just medially, but also laterally. This shape change in fast walking tracks may be due to increased posterior sediment displacement during toe-off (Figure 3.19). The volume of arch height in the tracks created with a flexed limb was greater medially, but remains consistently distributed on the lateral side of the tracks.

Morphological disparity on the same substrates at different speeds

If speed was increased from a walk to a fast walk, the volume of the midfoot impression increases on both the firm and the loose substrates (Figure 3.21b). However, it was difficult to establish this exact pattern on the looser substrate owing to the posterior displacement of sediment that warps true reflections of the midfoot shape. If speed was increased from a walk to a jog, the volume of the midfoot increases on the firm substrate, but decreases on the loose substrate. This decrease was related to the sediment displacement on the looser substrates, which was not present during the jogging trials.

Morphological disparity on the same substrates with different limb postures

If limb posture was changed to reflect a BHBK gait, the volume of the midfoot impression was less prominent on both the firm and the loose substrates both medially and laterally (Figure 3.21c). Consequently, the prominence of the arch impression was reduced, despite the absolute height of the arch being comparable to tracks produced with an EHEK on both substrates (Figure 3.20).

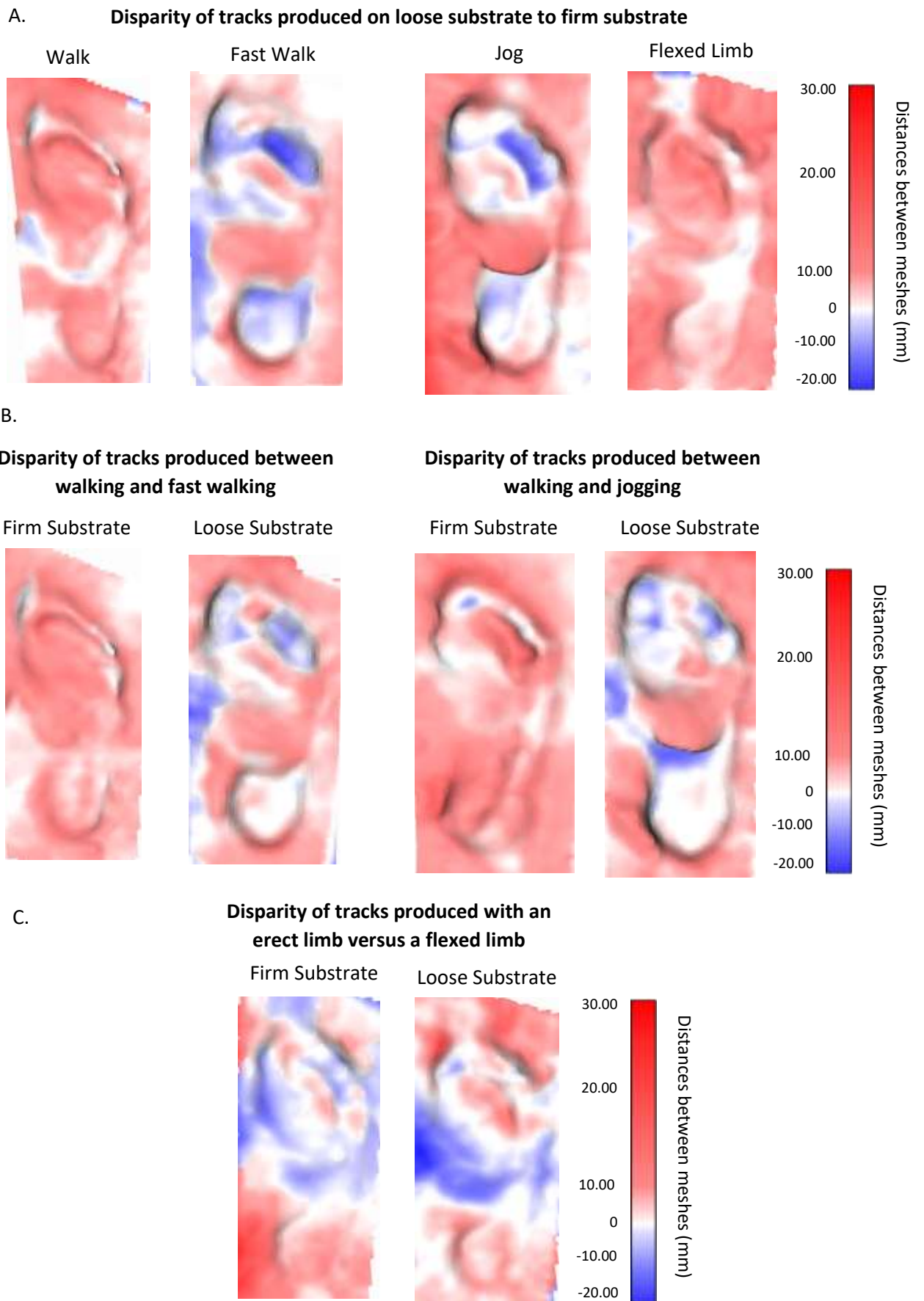


Figure 3.21. Mesh comparisons of tracks produced across a range of variables.

Associations between activity and track morphology

This study actively sought to recruit a variety of active and inactive participants (e.g., sedentary individuals, or those whom engage in daily active sport/exercise). Individuals were ranked from one to three based upon the level of activity they participated in weekly (n=100 participants). A rank of one identified mostly sedentary individuals. A rank of two identified individuals that engaged in some form of activity once or twice a week. A rank of three identified individuals whom engaged in almost daily sporting or exercise activities, particularly activities which utilised the lower limb, such as marathon training or limb strength conditioning.

Tracks produced from each ranked grouped were visually compared to establish any patterns of morphology between groups, such as an increased midfoot impression correlated to active movement (i.e., it was predicted that regular endurance runners may leave a greater midfoot impression than those who are more inactive). No patterns of morphology could be established between groups, indicating that activity does not influence track morphology. Additionally, limb flexion was not identified to be greater (when examining the same variables) between participants who engaged in different ranks of activity (n=40 participants). For example, one sedentary individual's knee flexion on the firm substrate during a walk was $\sim 72^\circ$. Whereas, an active participant's knee flexion was $\sim 77^\circ$. Because grouped knee flexion during walking on this substrate ranged from 60.153° to 79.571° , it is fair to state that regular activity cannot be reconstructed from track morphology.

Similarly, no morphological patterns were associated with habitual shoe-wear (e.g., the frequency of wearing high-heeled shoes).

3.3.6 The influence of a flexed limb posture on track morphology

To establish if limb posture could be identified from track morphology, a comparison between tracks created with a BHBK gait and those created with an EHEK gait was made. Two key variations in morphology were identified: (1) the volume of the midfoot region was under-represented on the firmer substrate; and (2) there were variable depth distributions across each track (Figure 3.22). Tracks created on the firmer substrate with a flexed limb produced very shallow tracks, with the complete loss of the midfoot impression. Only the hallux and 2nd digit left elongated depth maps typical of walking normally. On the looser substrate the depth distribution of the track was altered. There

was greater depth under the ball of the foot, less emphasis on each digit, and the depth of the heel was more uniformly spread than when moving with an EHEK gait.

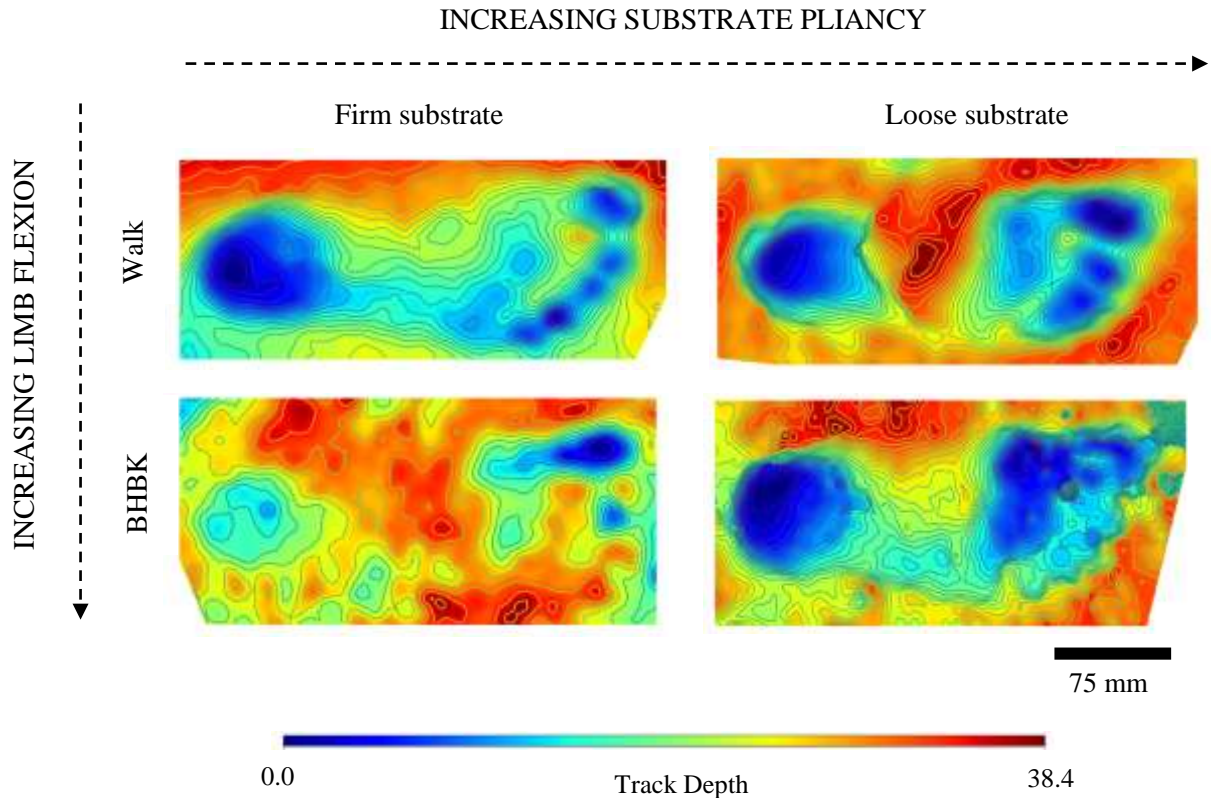


Figure 3.22. Track depth maps between the two different substrates in one male individual showing how track morphology changed with an increase in limb flexion and with an increase in substrate pliancy.

3.3.7 Variation in hallucal abduction across different substrates

Upon visual inspection of each registered track a pattern of increasing hallucal abduction with a BHBK was visually predicted. To test this prediction, hallucal angle was measured on all BHBK and EHEK tracks ($n=20$ participants). The angle of hallucal abduction was found to be significantly variable between tracks created with a BHBK compared with those created with an EHEK on the firm substrate ($t=3.720$; $P\leq 0.001$) and on the loose substrate ($t=3.446$; $P=0.002$) (Figure 3.23).

No significant relationship was determined between the angle of the hallux on the firm substrate with knee flexion ($R^2=0.294$; $P=0.073$) or hip flexion ($R^2=0.318$; $P=0.0519$). This affirms that limb flexion does not significantly alter hallucal abduction when walking on a compliant substrate. Both hip flexion ($R^2=0.421$; $P=0.009$) and knee flexion

($R^2=0.344$; $P=0.035$) were found to be weakly positively associated with the increasing angle of hallux abduction on the loose substrate. Lower limb kinematics were determined to be weakly associated with a change in limb dynamics when walking on a less compliant substrate.

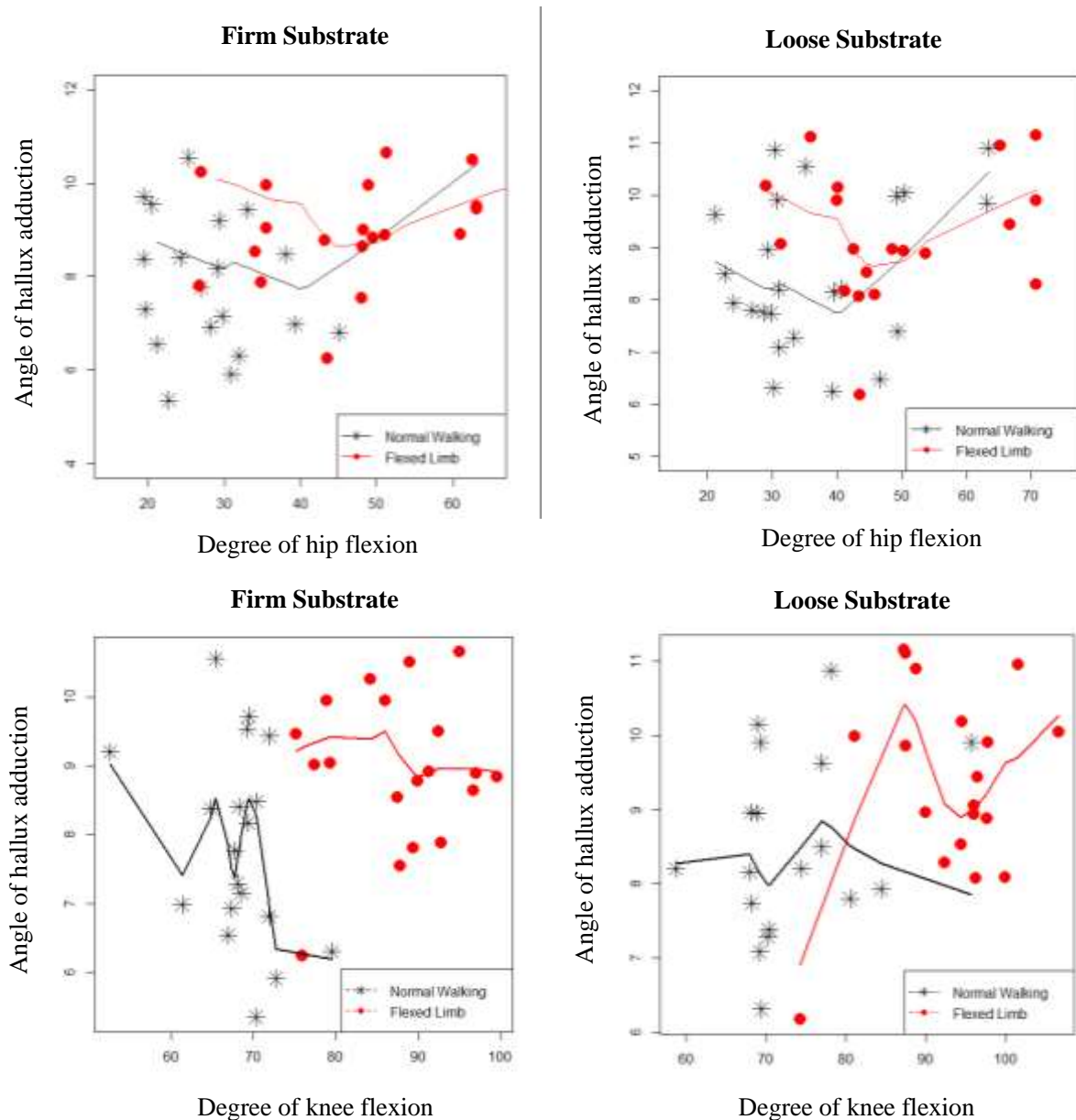


Figure 3.23. Graphical results of the GLM showing the association between hallux abduction with peak hip and knee flexion, and how this varies across each substrate.

3.4.0 Discussion

This study employed an experimental approach to determine if a footprint can be used to identify the track-maker's biometric information and locomotory behaviour. The main

aim was to investigate the effect of substrate on track morphology and the ability to predict biometric and biomechanical characteristics.

3.4.1 Can biometric information be accurately extracted from track dimensions?

Linear measurements from tracks are commonly used to infer biometric information about the track-maker, such as stature, body mass, sex and age (Bennett and Morse 2014). Variations in substrate mechanics can produce tracks that are both wider and longer, thus under- or over-estimating the biometrics of a track-maker (Morse et al. 2013). By taking simple linear measurements, this study aimed to assess the relationship between different movements across different substrates with track dimensions to establish if dimensions can be used to reliably identify the track-maker.

Track linear dimensions (lengths and widths) did not differ between substrates when walking at preferred speeds. Variations in track dimensions only occur once speed and/or limb flexion is increased, with track lengths being much more consistent between variables (e.g., movement across different types of substrates); whereas, track widths are more inconsistent. For example, a fast-paced walk will produce tracks which exhibit wider borders, in addition to displaying longer hallucal impressions when the tracks are created on a less compliant substrate. Once a participant is jogging then all linear measurements produced during different trackway conditions are disparate. Overall, it was established that track dimensions were more consistent on the firmer substrate when speed is increased, than on the loose substrate when traversing at different speeds (e.g., from a walk to a jog).

Changes in track dimensions when walking conditions were altered (e.g., movement on a less compliant substrate) were hypothesized to produce inaccurate biometric information regarding the track-maker. This prediction was mostly upheld as mass could not be predicted using any of the linear regressions; and age and sex predictions using track length regressions (Ashton et al. 2014; Altamura et al. 2018) were only ~60% accurate for 'normal' walking conditions (that is, for the walk on the firm substrate for which joint angles were most similar to the controlled walk). The accuracy of age and sex predictions were reduced when walking conditions were changed.

It was possible to correct for a change in track length caused by moving on the different substrates and/or at several speeds. The validity of the correction factors was explored by computing stature predictions of each track using corrected track length. Generally, most

predicted stature values were successfully predicted to within expected error ranges (Abledu et al. 2015). While the corrected measurements did not improve mass, age or sex predictions, it did improve stature prediction, albeit with some outliers. The presence of outliers in the dataset is not cause for concern; outliers will always exist when predicting stature from foot/track length for any population, which is demonstrated by this study and others (Agnihotri et al. 2007; Dhaneria et al. 2016; Ibeabuchi et al. 2018; Kim et al. 2018). By successfully correcting track length measurements, the accuracy of predicted stature values was improved. However, it will only be possible to correct for a change in track length in fossil tracks if speed and substrate material properties can be approximated.

As footprint length could be successfully corrected, further multivariate methods should be explored to attempt to reconstruct other biometric information from track length, rather than using grossly variable track width dimensions.

The results presented here indicate that some biometric information can be reliably extracted with a small error margin from different substrate types only if the individual is walking at a comfortable speed (<1.45 m/s). If the corrected foot length values are used, the error margin is reduced and biometric information (although not mass) can be extracted from individuals whom exceed this speed, ultimately allowing for the track-maker's stature and hip height to be identified from tracks produced in deformable materials of varying pliancy.

Greater comprehension of the relationship between substrate mechanics, movement and track dimensions is required to improve predictions of body mass, age and sex.

3.4.2 Establishing shape patterns associated with kinematics in track morphology

This project aimed to not only establish if a track could be used to predict biometric information of the track-maker, but also to determine if functional morphology is reflected in tracks. The results supported the hypothesis that lower limb movement would be significantly disparate when traversing across different types of substrate of varying saturation. Joint angle ranges of the lower limb were greater when moving across a looser substrate and more-so with increasing speed, with the hip being much more constrained in movement than the lower limb. The knee and ankle appear to be more susceptible to significant kinematic changes, and thus have more influence on substrate navigation than the hip.

The range of motion in the hip in fossil hominins

Hip flexion in this study was only increased on the looser substrate when speed was increased to a fast walk or a jog. Hip extension remained constant across all motions and substrates, conclusive with previous studies that have established that the modern human hip is quite stable and constrained, regardless of the underlying substrate (Volshina and Ferris 2015). Contrastingly, the hip in bipedal extant non-human primates is highly mobile when walking bipedally (D'Août et al. 2002; Ogihara et al. 2011; Hammond 2013), suggesting that a more constrained hip joint evolved in hominins.

It is now questionable if ranges of motion of the hip are reflected in track morphology in fossil hominins. Anatomical assessments of hominin pelvic remains (Robinson 1972; Aiello and Dean 2002; Brunet et al. 2002; Galik et al. 2004; Lovejoy 2005; Lovejoy et al. 2009a; White et al. 2009), investigations into the last common ancestor of modern humans (Lovejoy et al. 2009b; Grabowski and Roseman 2015) and research into locomotion using comparative primate analogies (Sockol et al. 2007; Pontzer 2014; Pontzer et al. 2014; Pontzer 2017; O'Neill et al. 2018) have all demonstrated that flexion was likely greater in the early hominin pelvis/hip relative to AMHs. Furthermore, changes in hip extension which are associated with patterns of morphology were not recognised in the current sample. Consequently, the range of motion of the hip – when considered as a single factor (see below) – in fossil hominins cannot be identified from tracks.

The range of motion in the knee in fossil hominins

The knee was the dominant factor (i.e., the joint that was most changeable with substrate and speed) in this study for adapting to different speeds and substrates, signifying that knee flexion will instead be identifiable from tracks. Angular movement of the knee was ~8° greater when walking across a looser sediment. As knee morphology was likely quite variable in early hominins as demonstrated via previous anatomical assessments that identified a suite of primitive and derived features which would have aided bipedalism, but also permitted a range of other locomotory repertoires (DeSilva and Lesnik 2008; DeSilva 2009; Lovejoy et al. 2009; Turley et al. 2011; DeSilva and Gill 2013; Tallman 2013; Frelat et al. 2015), it is questionable if knee movement will be reflected in foot impressions across a range of substrates in fossil tracks.

The inclusion of exploring different limb postures in this study has offered an informed insight into this question. As track morphology was distinguishable between those

produced with a BHBK – which employed significantly greater hip and knee flexion – and those produced with an EHEK, it will be possible to establish that fossil tracks with a prominent midfoot – particularly at fast speeds – likely employed an extremely flexed knee during track creation, concurrent with an erect postural positioning of the trunk/pelvis, in contrast to the ranges of motion seen in stance in the current study. Ultimately, this can be linked to the ability to extend the hip, suggesting that hip extension may in fact be identifiable from track morphology. Even though hip extension was consistent between each of the variables tested in this study (substrate, speed and limb posture), the combined postural positioning of the hip with the ability to walk with an extremely flexed knee joint has demonstrated that functional morphology of the hip and knee is distinguishable from tracks via a prominent midfoot impression, which is identifiable in the Ileret, Kenya tracks (Bennett et al. 2009; Crompton et al. 2012) and in the Happisburgh, UK tracks (Ashton et al. 2014).

Alternatively, if the volume of the midfoot impression is deemed to be small/lacking and, particularly, if the impression is medially distributed and not extending to the centre of the track (e.g., if it does not extend past the long axis of the foot), it is likely that a flexed limb was employed during track creation – as has been contentiously argued for the Laetoli track-maker (Raichlen et al. 2008; Hatala et al. 2016a), and recently reconstructed in pelvic remains ascribed to australopithecines (Kozma et al. 2018).

Investigations into the endurance running capabilities of hominins is poorly assessed (Carrier 1984; Lieberman et al. 2006; Rolian et al. 2011; Pontzer 2017), with the consensus that prominent arches of the foot were necessary for efficient energy production during running in hominins (Ker et al. 1984). These features likely developed later in the *Homo* genus resulting in economical endurance running capabilities (Bramble and Lieberman 2004; Pontzer 2017). In the present study, jogging on the loose substrate increased knee flexion by $\sim 20^\circ$. An increase of $\sim 20^\circ$ will reduce the moment arms of the *quadriceps femoris* muscle group which cumulatively act to bring the knee joint back into an extended position. Consequently, jogging on a less compliant substrate would be unsustainable compared to jogging on a firm substrate due to decreased muscle moment arms (Hurley and Johnson 2008; Lieber and Burkholder 2008). Jogging/running speeds identified on softer substrates from fossil tracks would likely identify the track-maker as an efficient, habitual biped as the track-maker would likely have derived features of the hip and knee joints (e.g., Aiello and Dean 2002) to permit such movements.

Only one fossil trackway comprised of just two steps has been identified as belonging to a jogging/running speed: FU-TL at Ileret, Kenya (Dingwall et al. 2013). Additionally, speed estimates of the FLT1 trackway suggests that the track-maker was either walking swiftly or running slowly. Morphological reports do not exist for these trackways, so it is not currently possible to postulate on shape patterns in comparison to the experimental data within the current project.

The range of motion in the ankle in fossil hominins

Plantarflexion was identified to be significantly greater ($\sim 10^\circ$ increase) when speed was increased, or substrate pliancy was decreased. A $\sim 10^\circ$ increase in plantarflexion, which is quite a significant discrepancy between the firm and loose substrates, will reduce the moment arms of the *tibialis anterior* muscle and the extensor muscle group of the foot which both act to bring the foot back into a dorsiflexed position. Consequently, movement across a less compliant substrate will be more costly in the ankle joint, and will not be as sustainable as movement on a more pliant substrate.

This increase in plantarflexion was associated with a large ridge-shaped displacement of material in the midfoot section, as deposited during later-stance into the toe-off stage of the gait cycle. This displacement of material warped a true investigation of midfoot morphology, as arch volume was identified to be over-emphasised.

Such a large sediment displacement that is uniformly distributed from the medial to lateral side is representative of an effective toe-off propulsion (Schultz 1930; Elftman and Manter 1935; Ker et al. 1987) on a less compliant substrate. The morphology of the proximal phalanges (Latimer and Lovejoy 1990; Harcourt-Smith et al. 2015; Trinkaus and Patel 2016), the metatarsals (Ward et al. 2011; Vereecke et al. 2003; Lovejoy et al. 2009; Takahashi et al. 2017; Fernandez et al. 2016; Fernandez et al. 2018), the ratio of the proximal foot to the distal phalanges (Susman et al. 1984; Ward et al. 2012; Haile-Selassie et al. 2012; Pablos et al. 2015) and muscle architecture in the hominoid foot (Rolian et al. 2009; Oishi et al. 2018; Farris et al. 2019) have all been assessed in fossil hominins to reconstruct hyper-dorsiflexion capabilities of the metatarsophalangeal joints. Although the exact foot morphologies permitting toe-off in putative hominins and australopithecines is contentious (Holowka et al. 2017; DeSilva et al. 2018; Holowka and Lieberman 2018), derived features of the metatarsophalangeal joints would have permitted an effective toe-off advantage (Farris et al. 2019). This morphological

advantage is reflected in track shapes on a less compliant substrate via sediment displacement which extends mediolaterally across the track's midfoot section.

This ridge-like morphology can be identified in the Okote Member, Kenya tracks which have been assigned to *Homo erectus* (Hatala et al. 2017), the Gombore 11-2, Melka Kunture, Ethiopia tracks which have been assigned to *Homo heidelbergensis* (Altamura et al. 2018), and in the Happisburgh, UK tracks which have been tentatively ascribed to *Homo antecessor* (Ashton et al. 2014). Additionally, this ridge has also been identified in the tentatively assigned *Homo neanderthalensis* tracks from Le Rozel, Normandy (Duveau et al. in review). This distinct ridge-type morphology, which has been recognized in the current study to be associated with an effective toe-off, is present in some of these fossil tracks (Figure 3.24). This suggests that a modern human-like toe-off was present in early and late *Homo* species. One early hominin print (Gombore 11-2; P-02) displays a more pronounced ridge relative to the other prints, indicating that increased knee flexion in conjunction with greater plantarflexion was employed to permit effective toe-off on this particular substrate.

The ridge is quite distinct in the later *Homo neanderthalensis* tracks from Le Rozel (n~800) which were all created in a loose and easily deformable sandy sediment (Figure 3.24c). Generally, deeper tracks exhibited a more anteriorly positioned ridge, than those which were shallow. Changes in track depth in an area with intermixed prints suggests that the tracks were made at various times of the day, likely caused by changes in moisture content at the time of formation as the substrate dried (See: Section 4.3.3). A deeper track would have been created in a less pliant circumstance than that of the shallow track, as reflected in discrepancies in ridge positioning. By understanding the change in ridge-formation, is it possible to state that plantarflexion would have been greater during movement when moisture contents were higher.

An effective toe-off is associated with other morphological changes in the foot: an adducted hallux, which would have provided space for the derived plantar aponeurosis of the midfoot to develop (Elftman and Manter 1935) to permit the mediolateral weight transfer characteristic of modern human foot function (Aiello and Dean 2002; Hatala et al. 2016b). Consequently, a ridge-like shape reflects not just plantarflexion, but an integrated functional morphology of the foot, particularly on looser sediments.

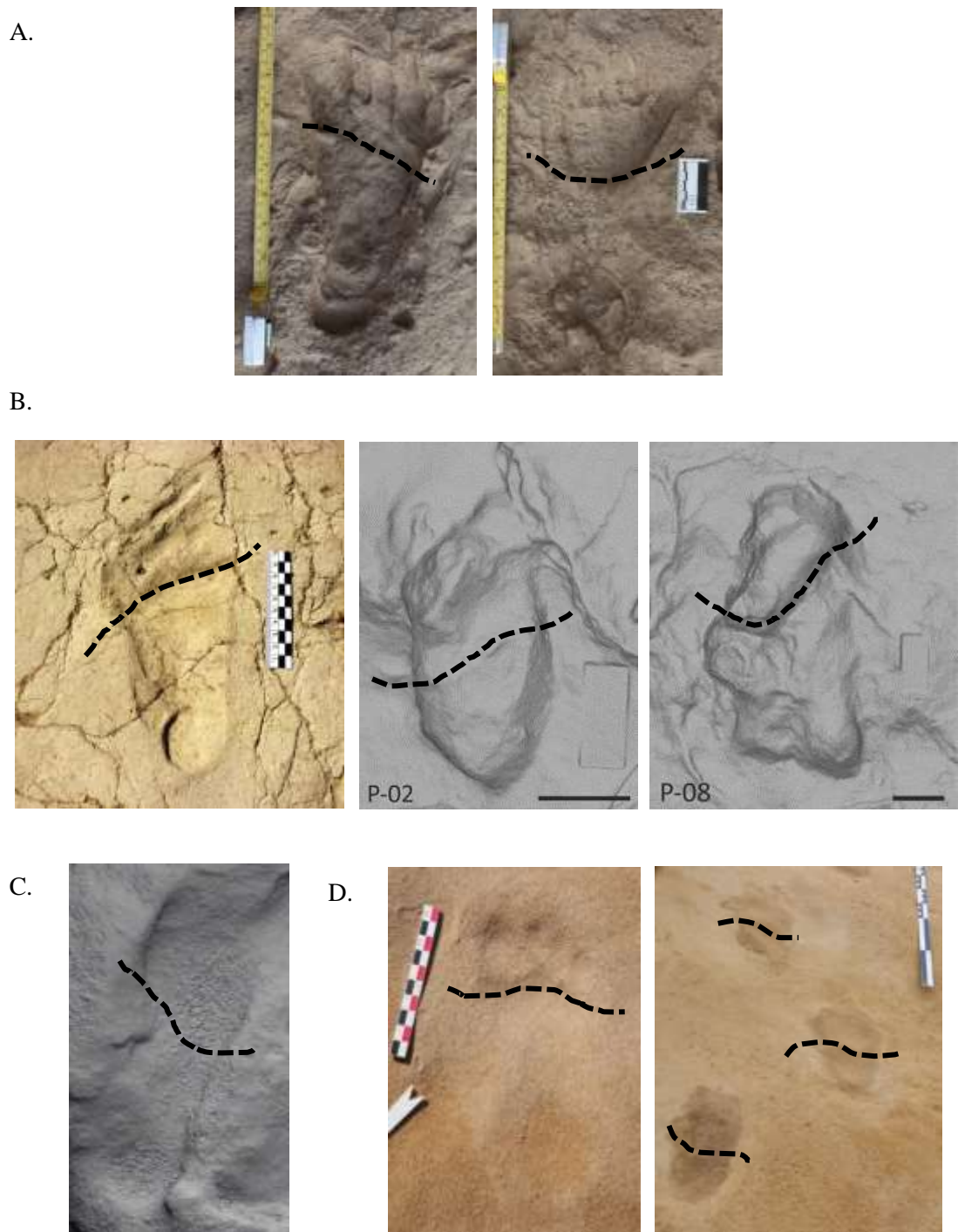


Figure 3.24. Examples of the (A) Okote Member (FU-H and FUTI-12), (B) the Gombore 11-2 tracks (P-01, P-02 and P-08), (C) the Happisburgh (Print 2), and (D) the Le Rozel tracks which all have a ridge in the forefoot region that extends mediolaterally across the track (emphasised by the black dotted line), signifying that an effective toe-off was utilised during locomotion on a less compliant substrate. Images from Okote Member were adapted with permission by K.G. Hatala. Images from Gombore 11-2 were adapted from Altamura et al. (2018). Photographs from Le Rozel have been used with permission by D. Cliquet.

Unfortunately, a 3D kinematic assessment of the metatarsophalangeal joints was not included as part of the original research questions. Future experiments exploring the relationship between kinematics, track morphology and substrate mechanics would benefit from analysing the dynamic movement within the foot from a 3D perspective, complimenting recent experimental research into hominin foot function (Holowka and Liebermann 2018).

In sum, increased plantarflexion on looser substrates was reflected in track shapes via a ridge-like morphology, possibly caused by hyper-dorsiflexion of the forefoot. Fossil tracks that exhibit this ridge were likely created by a track-maker whom had modern metatarsophalangeal joint and phalanx morphologies, and developed foot arches. This morphology is evident in fossil trackways as early as 1.5 Ma.

3.4.3 Revisiting the BHBK hypothesis

This study explored the relationship between increased lower limb flexion with track morphology across two different types of substrate. By exploring this relationship, it may be possible to address a critical question in human evolution of whether hominins walked with an EHEK or a BHBK posture. The results of the current study have determined that knee joint angles are significantly increased when walking across a softer substrate with a BHBK. The associated track production of this BHBK posture on the soft substrate is similar in morphology to those created with an EHEK posture on a firmer substrate.

Tracks produced with a BHBK on the loose substrate are similar in morphology to the Laetoli tracks, rather than those created with an EHEK (Figure 3.25). The main similarity includes the shape and prominence of the arches. Importantly, both the experimental track and the Laetoli tracks were created in soft and easily deformable substrates. Although it may be argued that making a direct comparison between these two substrates is problematic as the exact mechanical properties of each material likely differed, relative assumptions can be made. Based upon the morphologies observed in this study, the results presented here support recent studies that have claimed the Laetoli track-maker likely employed variable kinematics in the form of a more flexed limb rather than a fully erect posture (Hatala et al. 2016a; 2016b), which has also been suggested by more recent biomechanical explorations of hominin motion ranges in the lower spine and hip (O'Neill et al. 2018).

Importantly, limb flexion (in particular, knee flexion) was found to increase on the looser substrate regardless of limb posture (EHEK or BHBK). Based upon this finding, it is suggested that limb posture in hominins could have been dependent on substrate pliancy whereby a more flexed posture was employed for movement on a more deformable substrate (e.g., the Laetoli tracks), with an erect limb employed for movement on a more pliant material.

With a mosaic of skeletal features in the early hominin lower limb suited to a range of motions (Lovejoy 1979; Stern and Suman 1983; Susman et al. 1984; Lovejoy 1988; Susman and Stern 1991; Aiello and Dean 2002), it is a suitable to state that early hominins likely employed a range of motions, that may have ranged from an erect limb to a flexed limb as necessitated by substrate navigation.

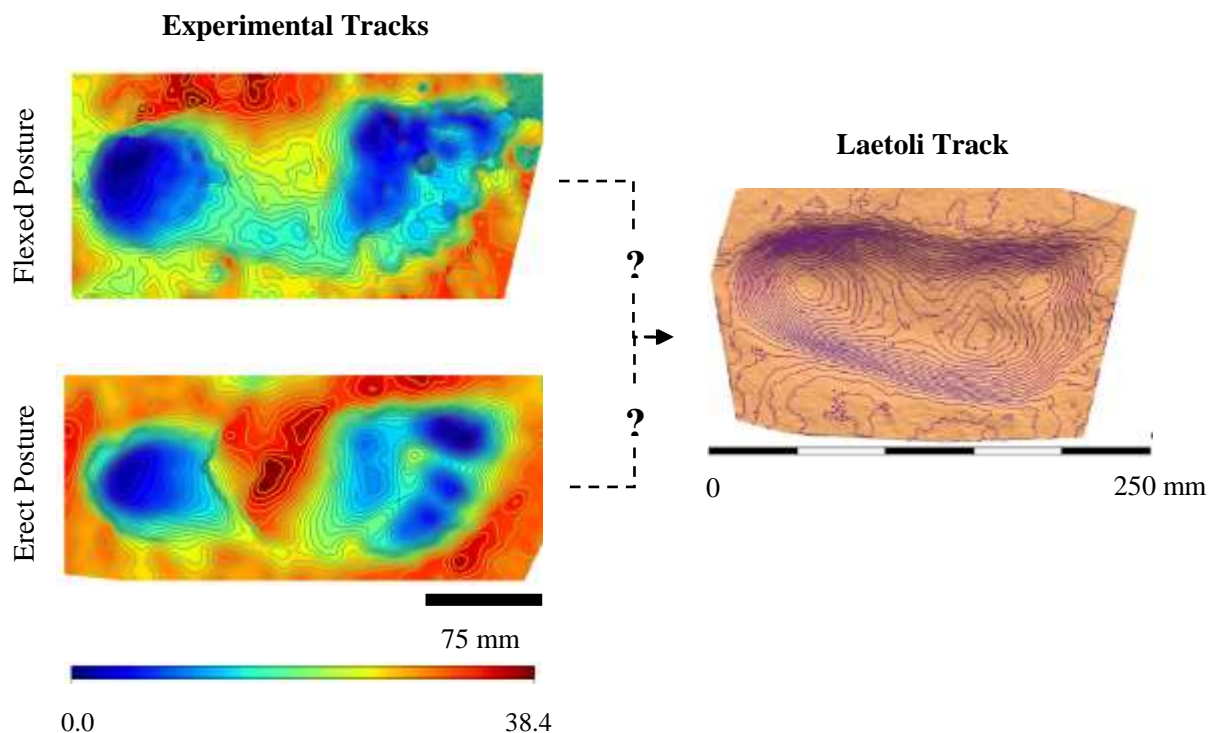


Figure 3.25. Comparison of the experimental tracks produced with a BHBK and an EHEK by the same individual on the looser substrate with that of the Laetoli track. The tracks created with an EHEK feature a very prominent medial longitudinal arch (MLA). This feature would likely undergo minimal degradation during diagenesis thereby likely reducing the height of the topographical features (Wiseman and De Groote 2018). Consequently, this prominence would likely be less pronounced after diagenesis. Regardless, this study still finds the Laetoli track most similar to that of the flexed posture. Image from Laetoli was adapted from Bennett et al. (2016).

Tracks created on the firm substrate with a BHBK have no midfoot impressions, with more evenly distributed depths across the track which is atypical to any other track production from this study. However, this morphology is somewhat similar to the archaic *Homo sapiens* fossil tracks from Langebaan, South Africa (Roberts and Berger 1997; Roberts 2008). Because the Langebaan tracks have been tentatively assigned to archaic humans (assignment based upon the geological age of the tracks and the poor taphonomy of the prints which some researchers have argued do not belong to any human species (e.g., Bennett and Morse 2014)), it is unlikely that a BHBK movement was employed during track creation. Alternatively, the tracks may belong to another unidentified hominin species (Helm et al. 2019), although this seems unlikely due to no contemporaneous species present in South Africa ~117 Ka who employed a flexed limb posture. The only known potentially alternative contender for the production of these tracks could be *Homo naledi* (Berger et al. 2015; Helm et al. 2019), yet the hindlimb (Marchi et al. 2017) and foot (Harcourt-Smith et al. 2015) of *Homo naledi* suggest an efficient biped. As only two potential prints were discovered in Langebaan, then extensive morphological comparisons cannot currently be established (Figure 3.26).

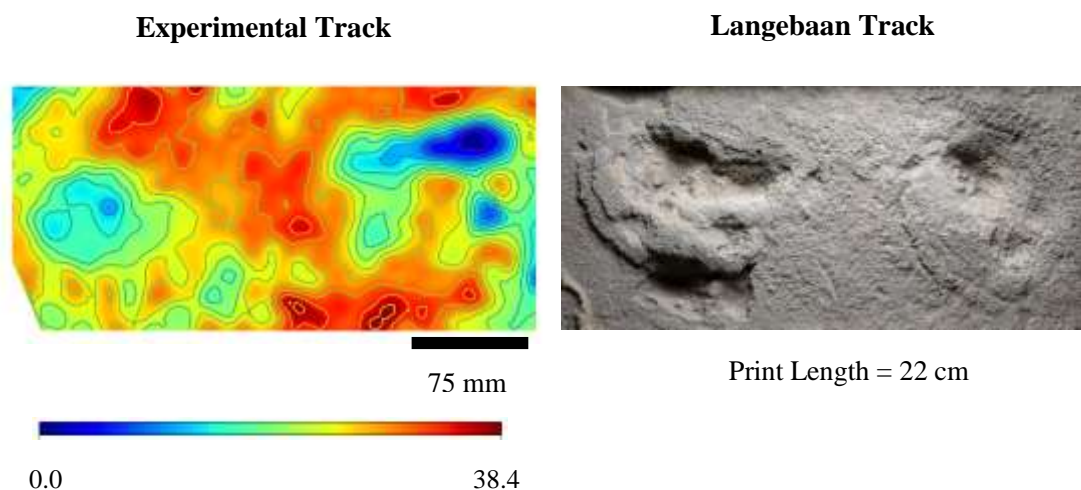


Figure 3.26. Comparison of the experimental tracks produced with a BHBK on a firm substrates with that of the Langebaan print. Both tracks exhibit a lack of midfoot impression with a clear definition of the hallux, but not the lateral digits. Photograph used with permission by the Iziko Museums, South Africa.

3.4.4 Revisiting the BHBK hypothesis: the dynamic movement of the foot

An unexpected result was observed: the angle of hallucal abduction was positively associated with increases in lower limb flexion. More specifically, the movement of the hip and knee were both found to be weakly associated with changes in hallucal abduction when moving across the looser substrate. However, no kinematic changes were observed to be correlated with changes across the firm substrate.

Changes in hallucal abduction during loading that also include supination and internal rotation have been medically acknowledged and reported (Ouzounian and Shereff 1989; Geng et al. 2015). However, this is the first study that has documented significant changes in hallucal abduction within an individual dependent on substrate use which is non-pathological. Increasing hallucal abduction may be explained by the way the foot has interacted with the underlying substrate. As a foot impacts the ground, the substrate will deform under the applied load as strain transfers to the surrounding materials, deforming the region around the applied load, leaving an impression of the foot (Morse et al. 2013). As limb flexion is increased then contact time during stance is positively increased as the assumed changes in force (not calculated within the current study) of the foot apply different pressures across the underlying substrate until traction of the material is achieved. If the material is looser then the foot will react appropriately to accommodate changes in the mechanical properties of the material compared to interaction with a more pliant substrate. Ultimately, greater limb flexion is achieved as the foot penetrates further into a looser substrate before traction is attained, explaining this increase in knee flexion.

However, no change was determined in the hip or the ankle movement. This suggests that the knee solely compensates for changes in substrate pliancy if a flexed posture is employed. A significant increase in the angle of hallucal abduction independent from ankle kinematics suggests that there is modular movement within the foot that is not associated with changes in the ankle. Due to the simple marker-set used the dynamic movement of the foot joints (e.g., the metatarsophalangeal and the mid-tarsal joints) observed in track morphology were unfortunately not captured using the 3D motion capture system.

Based upon the impression of increasing hallucal abduction it is possible to postulate that the first metatarsal is abducting (albeit, slightly as the range of abduction only increased by 3-5° per participant) to compensate for medial support during stance and toe-off. A more adducted first metatarsal is associated with the development of the midfoot arches which allow the foot to roll mediolaterally during walking for efficient weight transfer

(Elftman and Manter 1935). An adducted first metatarsal also stabilises the foot and supports the body's mass during later stance (Ker et al. 1987), whilst allowing flexion of the metatarsophalangeal joints during toe-off (Harcourt-Smith and Aiello 2004; Moore et al. 2011).

The abducted first metatarsal is likely explained by the lack of the foot's roll for efficient weight transfer. The morphology of the tracks produced in the firm substrate would also support this hypothesis. Within the track there is uniform depth distribution in the midfoot region. Importantly, there is little lateral impression of the midfoot, supporting the hypothesis that no foot roll was present. The morphology of the tracks produced in the looser substrate are more complex. A deep impression of the ball of the foot and a shallow impression of the lateral border indicates that no mediolateral roll was present when traversing across the looser substrate.

To compensate for a lack of weight transfer in the foot, the first metatarsal likely abducted to support the body's mass during later stance. Hallucal abduction likely became greater as knee flexion increased to compensate for movement across a less compliant substrate. With the first metatarsal in this position, the foot was no longer in an optimally suited position for adequate toe-off. The hallux likely applied greater load to the underlying substrate during toe-off to gain traction, resulting in the observed increase in hallux length as the sediment was posteriorly displaced.

Assuming that increasing hallucal abduction was the direct consequence of increased limb flexion, these results support recent studies that have claimed the Laetoli track-maker employed a more flexed limb than modern humans (Hatala et al. 2016a). As demonstrated by a comparative assessment of variable hallucal abduction angles in hominin fossil tracks in Section 4.3.1, the Laetoli tracks have a significantly greater angle of hallucal abduction than tracks that have been ascribed to *Homo* species. This greater angle of abduction observed may be the consequence of australopithecines employing a more flexed limb when traversing across the soft and deformable substrate present.

Future studies could assess the dynamic movement of the foot joints across various substrates to corroborate this finding which may address questions regarding the frequency of bipedal movement, rather than the ability of bipedalism.

3.5.0 Limitations and future directions

This study had several limitations. Primarily, this study only used one type of sand of varying moisture contents. Human movement across a wider range of substrates of various compaction, granular size and heterogeneous materials would likely demonstrate a greater repertoire of angular movement in the lower limb to accommodate these changes, similar to extant primates that accordingly change kinematics to optimise substrate deformation for efficient movement (Channon et al. 2011). Future studies could incorporate the use of increased materials to complement current results. In conjunction with additional materials, future studies should employ the use of electromyography signal capture to quantify muscle group powers in association with changing joint angles across various types of substrates. A comprehensive understanding of how locomotor costs are affected by limb posture across various substrates will not only be informative but will allow researchers to assess the relationship between form and function.

This study recruited participants from a shod population within the United Kingdom. Although great effort was taken to recruit participants of numerous ethnicities, this study is still limited by a small sample size ($n=100$ for track assessments, but only $n=40$ for combining track shapes with locomotion). Ranges of motion, the changes in hallux abduction and variable track morphology could vary per population. Future studies should target other populations, particularly unshod groups, for a direct comparison for fossil tracks.

Only one jogging speed was assessed per participant. Increased jogging/running/sprinting movements could have resulted in profound biomechanical alterations of the lower limb that are not apparent in the jogging pace present in the current study. However, the choice of preferred and sustainable running pace reflects behavioral locomotion accurately in fossil hominins based on the assumptions of the development of long-distance endurance running (Bramble and Lieberman 2004). Regardless, a high-speed movement could have informed on a more rounded locomotor repertoire in hominins.

This study actively recruited participants who partook in a range of activities, ranging from regular activity, to strength conditioning, to sedentary behavior. Whilst this offers a comprehensive overview of locomotion in trained and untrained personnel, it may be argued that recruiting only active individuals would have provided a greater insight into kinematics relative to hominin behavior, based on the assumption that it would be unlikely to find a sedentary hominin. However, this study recruited an array of individuals

to increase kinematic ranges to provide a more rounded overview of general limb movement. This provided a greater biomechanical model for evolutionary inferences whereby a range of motions could have been employed by early hominins, rather than extremely active bipedal movement.

Finally, very few postcranial skeletal remains have been discovered. Consequently, predicting early hominin ranges of motion from skeletal morphology is substantially hindered by small datasets that are not publically nor academically available for extensive analysis by other research teams (with the exception of the *Homo naledi* material). A lack of adequate postcranial data makes it difficult to predict biomechanics from skeletal material, resulting in the majority of studies addressing evolutionary locomotion to use mathematical models (e.g., Pontzer et al. 2009).

To circumvent this issue, numerous researchers use extant primates in an experimental setting to investigate locomotory behavior. However, this is fundamentally limited by the lack of appropriate analogues (D'Août et al. 2014). Many hominin species display a mosaic of anatomical skeletal morphologies, suggesting that these hominins likely employed a variety of locomotory behaviours, which may have ranged from terrestrial bipedalism to arboreal locomotion. No 'intermediatory' species exists today that could be used as an appropriate analogue for assessing past locomotion. Currently, using experimental methods to investigate movement between different materials is the most suitable model available. The results of the current study would be complemented by the incorporation of multi-body dynamics analysis on the small skeletal sample available to investigate the complete range of joint motion when the underlying substrate pliancy is changed. Subsequently, this could inform on the relationship between form and function of fossil tracks.

In lieu of a large sample of skeletal material, the most relevant data that exists is fossil tracks. Using an experimental approach, this study has demonstrated the key variables that affect track morphology. Importantly, the relationship between limb kinematics and track morphology have been explored offering insights into the functional morphology of fossil tracks which will be explored in further detail in the next chapter.

Chapter Four

Exploring patterns of shape affinities between fossil tracks

In the previous chapter it was determined that the shape of a human footprint is influenced by two factors: speed and substrate. Because shape patterns were associated with lower limb kinematics and substrate pliancy, it was hypothesised that these shape patterns would be recognisable in fossil tracks and, if so, these patterns could be quantified and statistically compared in a selection of tracks from what are assumed to be from different species. This hypothesis was directly addressed in the current chapter. Here, track shape patterns were assessed via landmark-based geometric morphometric techniques. First, the applicability of using 2D and 3D landmarks were assessed using a modern human sample. As 2D landmarks were established to most successfully synthesise the outline of a footprint, then a selection of fossil tracks from the Pliocene, Pleistocene and Holocene were collected and 2D geometric morphometric methods were applied. The successful application of shape-space assessments permitted morphological affinities between fossil tracks to be identified, which is currently being revised after submission to the Journal of Human Evolution. Importantly, this was the first study to comparatively assess the Happisburgh, UK footprints with other hominin prints.

This chapter forms the basis of one manuscript that is currently being revised:

Wiseman, A. L. A., Stringer, C. B., Ashton, N. M., Bennett, M. R., Hatala, K. G., Duffy, S., O'Brien, T., De Groote, I. *In Review*. The morphological affinity of the early Pleistocene footprints from Happisburgh, England with other tracks of Pliocene, Pleistocene and Holocene age. *Journal of Human Evolution*.

This chapter was presented at the following conferences:

Wiseman, A. L. A., Stringer, C. B., Hatala, K. G., Ashton, N. M., O'Brien, T., Duffy, S., De Groote, I. 2017. A 2D geometric morphometric approach to analysing the functional morphology of the hominin foot from the Pliocene to the Holocene. *British Association for Biological Anthropology and Osteoarchaeology 18th Annual Conference*. Liverpool, UK.

Wiseman, A. L. A., Stringer, C. B., Hatala, K. G., Ashton, N. M., O'Brien, T., Duffy, S., De Groote, I. 2017. Functional morphology of the hominin foot based upon the early Pleistocene footprints from Happisburgh, England. *European Society for the Study of Human Evolution 6th Annual Meeting*, Leiden. The Netherlands.

4.0 Abstract

Fossilised hominin tracks provide one of the most direct sources of evidence of locomotor behaviour and allow inferences of other biological data such as height and mass. Many recent comparative analyses of hominin tracks have employed 3D analytical methods to assess their morphological affinities with tracks from other locations and/or time periods. However, environmental conditions can sometimes preclude 3D digital capture, as was the case at Happisburgh, UK in 2013. With a loss of reliable 3D reconstructions of the Happisburgh prints, other avenues of morphological assessment must be sought. Consequently, a 2D geometric morphometric approach was used to investigate the evolutionary context of the Happisburgh prints. The sample used here consists of hominin tracks from nine localities that span a broad temporal range from the Pliocene to late Holocene.

Results show disparity in track shape between prints assessed to the Pliocene (presumably *Australopithecus afarensis*) and Pleistocene (*Homo* sp.) and Holocene (*Homo sapiens*) hominins. Three distinct morphological differences are apparent between time samples: changes in adduction of the hallux, changes in the prominence and position of the medial longitudinal arch impression, and apparent changes in foot proportions.

An approach using 2D geometric morphometric methods established that the Happisburgh tracks are morphologically similar to other presumed *Homo* tracks, and differ from the Laetoli footprints. The probable functional implications of these results fit well with previous comparative analyses of hominin tracks at other sites.

4.1.0 Introduction

Digitisation of fossil material has advanced scientific research and permitted the flexibility and availability of working with digital material by numerous research teams (Belvedere et al. 2011; Falkingham 2012; Falkingham et al. 2018). This is particularly pertinent for fossil track sites where excavation can be damaging and where tracks are susceptible to erosional processes (Bates et al. 2008; Wiseman and De Groote 2018; Zimmer et al. 2018). The resulting 3D modelled tracks have been utilised in a range of biometric, biomechanical and behavioural analyses (Breihaupt et al. 2004; Remondino et al. 2010; Bennett et al. 2013; Bennett et al. 2016a; Falkingham et al. 2018).

Yet, despite numerous novel attempts using a variety of experimental designs, the relationship between track shape, depth and sediment deformation remains poorly understood (Milan and Bromley 2006; D'Août et al. 2010; Bates et al. 2013b; Hatala et al. 2013), regardless of the acknowledgement that track shape production is associated with substrate displacement during movement (Gatesy 2003; Milan and Bromley 2008; Morse et al. 2013; Bennett and Morse 2014; Razzolini et al. 2014). This relationship was explored extensively in Chapter Three where it was established that substrate pliancy influenced track morphologies. Although shape patterns as produced in different substrates were successfully identified correlative to a number of variables (e.g., lower limb posture), the relationship of track depth with that of any variable was unresolved.

Comprehensive between-group assessments of fossil trackways have never been conducted due to this poor comprehension of substrate influence (Morse et al. 2013; Bennett and Morse 2014). Although track depths can provide information regarding locomotion (e.g., deeper prints will generally display a ridge-like appearance if an effective toe-off was present; Chapter Three), other methods of comparative track assessment must be explored to permit a greater comprehension of the relationship between depth, locomotion and substrate deformity to be established.

An alternative method is a 2D geometric morphometric (GM) approach that quantifies only the outline shape of a print, exclusive of the internal proportions which have variable depths. By utilising 2D methods for the comparative assessment of track morphology, depth dimensionality as a variable will be removed, thereby resulting in fewer measurements but also circumventing the issue of (1) having inconsistent track depths, or (2) poor depth resolution within tracks which may weight shape disparity results. By employing 2D methods, only the outline shape is quantitatively compared exclusive of

the influence of depth, whereby it may then be possible to compare prints that were produced in different substrates. If successful, a quantitative comparative shape assessment of fossil tracks will be possible.

In this chapter, the effects of substrate and speed variability on fossil track shape formation will be statistically assessed using GM methods. If GM methods can successfully synthesise the outline shape of a track, then comparative shape assessments can be conducted to explore shape patterns within fossil tracks, and will permit the Happisburgh tracks to be comparatively assessed with other fossil tracks for the first time.

4.1.1 Chapter aims and objectives

The overall aim of this chapter was to quantitatively assess track shape production across several types of substrates and motions and compare fossil tracks. Additionally, the effect that the ‘third dimension’ factor has on statistical assessments (e.g., Cardini et al. 2014) of track morphology was tested by comparing 2D and 3D GM shape-spaces. After identifying the best method for track comparisons (2D or 3D) using a modern human sample, shape affinities/disparities were statistically compared between fossil tracks.

The following objectives were addressed:

- iv. To determine if experimental track shapes will be statistically variable as identified via the application of GM methods when created in different substrates and from several types of movement across a given substrate.
- v. To determine if experimental track morphology is consistent enough within an individual to correctly identify them as the track-maker if substrate and/or speed/limb posture is altered.
- vi. To synthesise the outline shape in fossil tracks and to statistically compare outline shapes between fossil groups.
- vii. To identify any shape affinities of the Happisburgh, UK prints with those of other hominin tracks belonging to the Pliocene, Pleistocene and Holocene.

4.2.1 Protocol and experimental design

Prior to testing for shape affinities/disparities between fossil tracks, shapes were explored between individuals from the experimental trials, as discussed in Chapter Three. All data pertaining to the following study was recorded in the Biomechanics Laboratory in the Tom Reilly Building, Liverpool John Moores University. Ethical approval was granted

by the Liverpool John Moores University Research Ethics Committee (REC: 16/NSP/041).

During the pilot testing documented in Chapter Three, 60 adult participants were recruited (18 – 68 years old; 35 females and 25 males) from the Liverpool John Moores University staff and student population (Appendix E). Biometric information of each participant was recorded (Appendix D). Track production was documented in Section 3.2.1. Photogrammetry was documented in Section 3.2.3.

Conditions included in assessments

The aim of this preliminary study was to determine the applicability of GM methods for synthesising fossil tracks. Because all fossil tracks were made in a variety of substrates (see: Section 4.2; Table 4.2), the inclusion of both substrate typologies from the experimental trials into this preceding shape-space assessment (Section 4.4) will provide a rounded view of track creation. Importantly, if prints belonging to the same person are differentiated by substrate pliancy, it will not be possible nor recommended to statistically compare fossil tracks because the major disparity in fossil tracks will be due to substrate characteristics, rather than differences between assumed species (e.g., foot anatomies or kinematics).

All conditions were included in the following assessments (a walk, a fast walk, a run and a bent-hip bent-knee (BHBK)) because very often it is unknown or difficult to predict the speed of the track-maker. For example, the prints at Happisburgh were a mixture of hollows whereby it was not possible to discern trackways, or to make any inferences if any of the prints were made by the same individual. Consequently, it was not possible to predict speed from any of the prints based upon current methods of speed prediction (Vaughan and Blaszczyk 2008; Dingwall et al. 2013). The Happisburgh prints could have been made while walking, fast walking, or jogging. By incorporating all speeds from the experimental trials into shape-space assessments, it will be possible to determine if a track-maker can be identified from an impression regardless of speed, or if prints are variable within a person.

Similarly, tracks associated with both the erect limb and flexed limb postures within a single individual were included. Because limb posture remains questionable in the Laetoli track-maker (e.g., Hatala et al. 2016a; Bennett et al. 2016a), the incorporation of as many

conditions as possible that lead to track creation will determine if a track-maker is identifiable from track morphology.

‘Averaged’ tracks were previously created per condition for the assessments in Chapter Three (Section 3.2.8). To remove nuanced morphological features introducing additional shape variability into the shape-space analyses in this chapter, ‘averaged’ tracks were utilised here. One ‘averaged’ track is a representation of ~9 tracks within one trackway belonging to each condition. In total, this provided eight prints per individual: one print for each motion across the two different substrates.

4.2.2 Geometric morphometric analyses of the tracks

Size was explored extensively in Section 3.3.1. As such, the current chapter focuses primarily on shape disparity between tracks via the application of GM methods. Two sets of shape-space assessments were computed, each using a different method of landmark classification: 2D and 3D geometrically-defined type II landmarks (Bookstein 1990). These methods were applied to address the following hypotheses regarding shape differences:

- H₀ Footprint morphology cannot be used to identify the track-maker.
- H₁ The speed and posture of the lower limb (e.g., a flexed limb or an erect limb) during movement will affect footprint shape.
- H₂ Substrate pliancy will affect track shape.
- H₃ 2D landmarks can be used to synthesise the outline shape of a track to circumvent the issue of unreliable depth dimensionality.

Reliability test of 2D and 3D landmark selection

Reliability tests were conducted to determine the replicability of landmark placement onto footprint structures, which typically lack anatomically-defined points. Instead, all landmarks within a print are geometrically-defined. Geometrically-defined type II landmarks (Bookstein 1991) were placed onto each experimental track.

Intra-track landmark reliability tests were carried out to test the replicability of placing 3D type II landmarks on one single track. One ‘averaged’ track was randomly chosen to be landmarked over a period of ten days in Avizo (v.9.0.1 FEI, Oregon, USA). A total of 12 landmarks were initially chosen to simply represent track outline shape but to exclude the internal morphology. A lack of landmarks placed inside the track (e.g., to represent

heel and forefoot depth as seen in Figure 4.1) omits internal depth patterns influencing shape assessments.

Intra-track landmark reliability tests consisted of a Generalised Procrustes Analysis (GPA) which was computed in R (R Core Team 2017) to test for consistency in landmark digitisation (Slice 2005). The Procrustes distances between each landmark consensus with the mean landmark configuration were calculated (Dryden and Mardia 1998). To test for inter-landmark inconsistency (that is, to test the distance between each individual landmark placement from its consensus), the distances between each repetition within the shape-space (Kendall 1984) were averaged. This process provided the estimated error within a 95% confidence interval for inter-landmark placement. Mean values (Procrustes distances) over 0.05 specified that the distance between a landmark and the overall consensus was high and, thus, a landmark was non-replicable and should be removed from the dataset (Profico et al. 2017). All mean values lower than 0.05 indicated good repeatability in landmark placement (Zelditch et al. 2012).

The landmark that represented the most convex point on the lateral side of the forefoot had a Procrustes distance >0.05 ($\bar{x}=0.21$) from the mean Procrustes configuration during these initial tests, indicating this landmark could not be reliably placed (Figure 4.1; landmark highlight in red). The landmark was therefore removed from the dataset. The reliability tests were recomputed with the remaining 11 landmarks. The mean Procrustes distance from the consensus was 0.03 ± 0.02 . Considering all landmarks individually, all Procrustes distances were <0.05 , thus each landmark was consistently and reliably placed (Figure 4.1). This signifies that intra-observer error in repeatability of landmark placement was low, and that the landmark configuration is suitable for the subsequent analyses.

It should be noted that the average distance for two of the landmarks to their consensus were approaching the 0.05 threshold ($\bar{x}=0.04$ for LM7; $\bar{x}=0.041$ for LM8) (highlighted in yellow on Figure 4.1). These landmarks represent the medial midfoot – this region is less geometrically-defined than others (e.g., the tip of each digit). Despite this, the Procrustes distances were <0.05 , the threshold employed to decide if a landmark is reliably placed (Zelditch et al. 2012; Profico et al. 2017). Consequently, the landmarks were deemed to be replicable, but there is the small possibility that any variability determined in subsequent analyses associated with these two landmarks could be observer error, rather than intra- or inter-group differences (Dryden and Mardia 1998).

Reliability tests were also computed to test the replicability of placing 11 2D geometrically-defined type II landmarks which were identical to those selected for the 3D assessment. The Procrustes distance for each landmark consensus was <0.05 ($\bar{x}=0.02\pm0.01$). With the removal of the third dimension, the error in landmark placement was slightly reduced in comparison to placing 3D landmarks ($\bar{x}=0.03\pm0.02$). All 2D landmarks were found to be consistently and reliably placed using TPSDig 2.0 (Rohlf 2004).

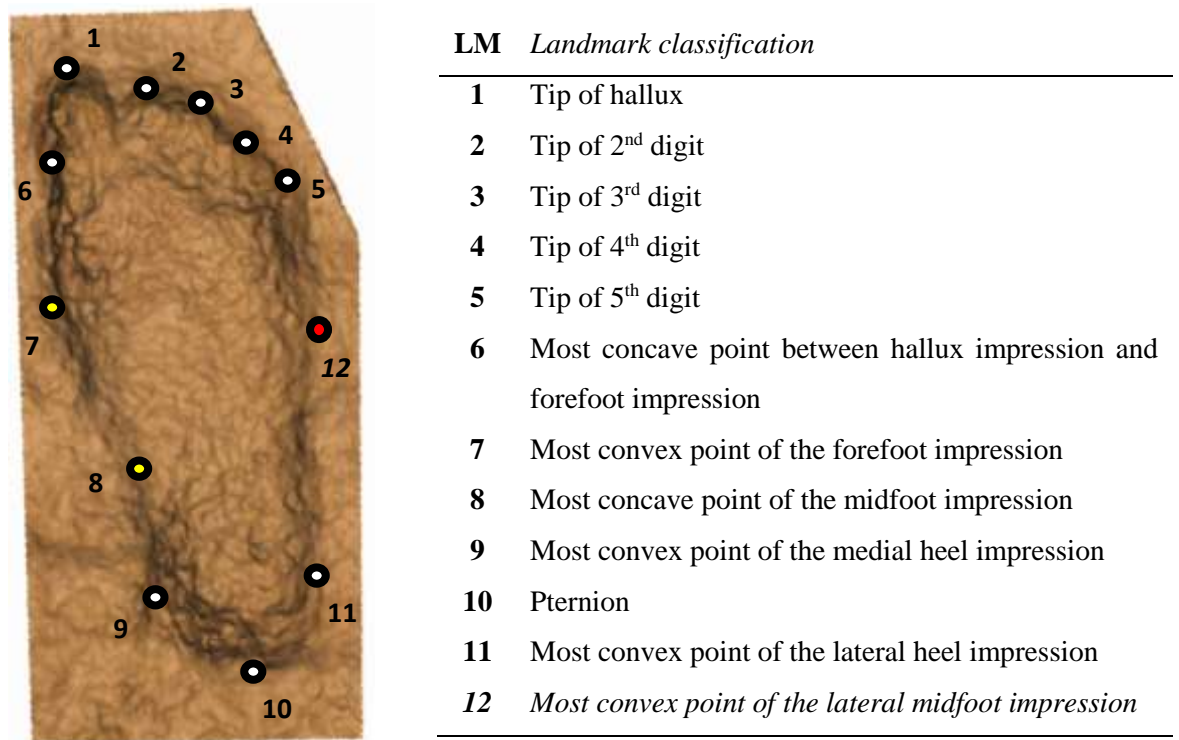


Figure 4.1. Twelve landmarks were chosen to represent the outline shape of each experimental track. Landmark selection was identical between the 2D and 3D assessments. Landmark in red (LM12) is the omitted landmark, which was identified to be non-replicable. Landmarks in yellow (LM7 and LM8) are most variable but repeatable (see: Section 4.2.2).

Statistical analyses

Eleven 2D and 3D geometrically-defined landmarks were found to be reliably placed and suitable for footprint assessments. Following on from the reliability tests, 2D and 3D landmarks were placed onto each averaged track belonging to a particular condition in Avizo (3D configurations) and TPSDig (2D configurations). This provided eight

landmark configurations per individual, incorporating all conditions tested during track creation: four different motions (a walk, a fast walk, a jog and a BHBK gait) across two different substrates of varying compliancy.

Categorical variables were created for each 2D and 3D landmark configuration associated with each condition (e.g., a walk on a loose substrate) to assist in assessing the causes of shape change. By adopting the use of categorical variables in the dataset, information about the tracks – such as the influence of substrate pliancy on outline shape – were included in the analyses. Their inclusion in the dataset assigns each configuration of landmarks to a group, allowing for groups to be statistically compared. For example, group one contains two variables: the loose and firm substrates. This group was then statistically compared with the second group whereby the configurations were assigned a variable according to the type of motion used to produce the tracks: a walk, a fast walk, a run or a BHBK gait. Subsequently, it was possible to determine if substrate and/or motion resulted in significant changes to track shape. Finally, to determine if results were influenced by inter-specific grouping, all data pertaining to a single participant were assigned a unique number, thereby incorporating information regarding height, weight, sex, activity and age into all statistical assessments.

All the following GM methods were computed separately for the 2D and 3D landmark configurations, but the methodology was identical for each configuration. A GPA was performed on each set of landmark configurations, from which shape variables were extracted (Gower 1975; Rohlf and Slice 1990; Adams et al. 2013). Shape variation was assessed using a Principle Components Analysis (PCA) (Bookstein 1991). Shape changes were visualised by non-affine partial warp grids (Rohlf and Slice 1990). An ANOVA using 1000 permutations was computed to assess the relative amount of shape variation between tracks produced on different substrates and between different motions (Dryden and Mardia 1998). Results were supported by a pairwise test that determined which variable(s) influenced shape variation (Zelditch et al. 2012). All analyses were computed in R packages (R Core Team 2017): *geomorph* (Adams and Otárola-Castillo 2013) and *morpho* (Schlager 2017).

4.3.1 Results

Both 3D and 2D methods produced comparable results. Graphical results presented here belong to the 3D methods only.

3D landmark configurations

To identify the prevalence of observer-error, the Pairwise Procrustes distances within Kendall's shape space (Kendall 1984) were extracted from the repeatability tests and compared with the Pairwise Procrustes distances from a sub-sample of the mean landmark configurations belonging to three randomly selected individuals. If considering the grouped differences (repeats versus the grouped individuals), Pairwise Procrustes distances were large between grouped specimens ($\bar{x}=0.10$) but were reduced for the repeated landmark placements ($\bar{x}=0.02$). As the distances were greater for the grouped samples, observer-error should be low (Figure 4.2).

All conditions were included here to determine if the Pairwise Procrustes distances were smaller between the same individual's footprints created at different speeds/limb postures than the Pairwise Procrustes distances between two different individuals. Small Procrustes distances (0.01-0.09) were identified within the same individual across different substrates when the tracks were created from a walk or a fast walk. Larger Procrustes distances (0.10-0.19) were associated with two variables: within the same individual moving across different substrates when jogging or employing a BHBK limb; and between participants (e.g., the distances between two different individuals when walking or fast walking) (Figure 4.2).

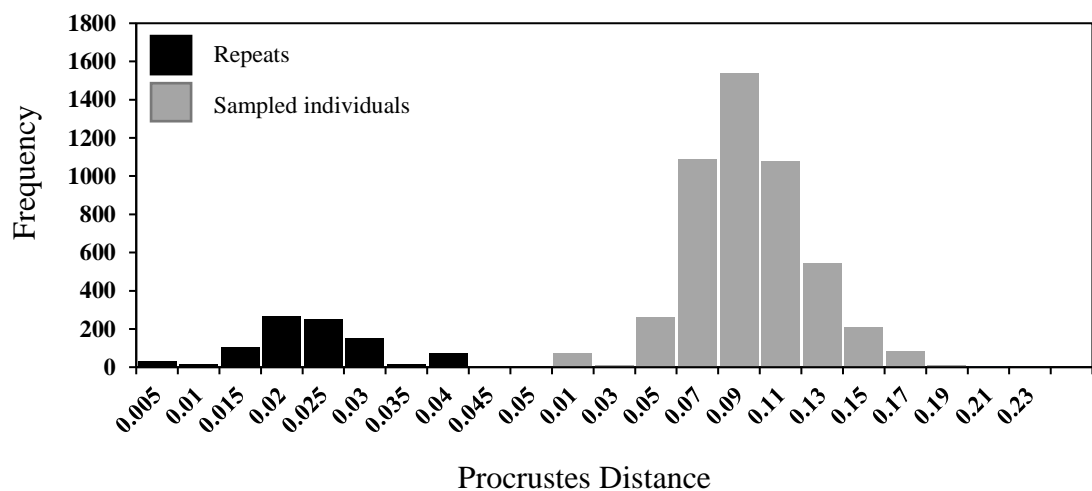


Figure 4.2. Histogram of the frequency of Pairwise Procrustes distances in the repeats (reliability tests) and a sub-sample of three randomly selected individuals ($n=8$ configurations per participant). As the Pairwise Procrustes distances were greater in the sampled individuals than that of the repeats, observer-error should be minimal. Additionally, the Pairwise Procrustes distances were identified to be smaller within the same individual than between individuals.

A PCA was computed to plot the Procrustes shape variables along their Principal Components (PC) axes. All individuals and their associated conditions that led to track creation were incorporated (e.g., a walk on a loose substrate). The PCA of all track shape variables produced an intermix of positive and negative PC scores along all PC loadings (100% of variance). There was no clear division of shape variables along any PC axis, suggesting that track shapes are somewhat consistent within this sample of AMHs across all conditions (e.g., substrate typology, speed and limb posture).

To explore these shape variables, a MANOVA was computed between the PC scores that explain 100% of total shape variance and their associated categorical variables (Table 4.1). The MANOVA revealed that shape variability is influenced by two factors: by each participant and lower limb motion. Inter-trackway differences (that is, the shape variables between each individual) accounted for 30.10% of total shape variance ($P=0.001$; $F=2.379$) (Table 4.1). The null hypothesis (H_0) is rejected, as individual participants can be identified from 3D track outline shapes, despite the PCA producing an overlap of PC scores along each PC axis (Figure 4.2). This suggests that shape variability within this sample of anatomically modern shod humans is explained by a suite of factors, not just by the individual.

The other factor identified by the MANOVA that influenced shape variability within the sample was lower limb motion ($P=0.011$; $F=1.881$) (Table 4.1). This confirms H_1 which stated that lower limb movement will affect track shape production, not only between several speeds (walk, fast walk and a jog), but also between different limb postures (erect and flexed limbs).

The results of this study have indicated that substrate does not significantly affect the outline shape of a track ($F=1.127$; $P=0.142$) (Table 4.1), as demonstrated by a MANOVA and supported by a mixture of loadings along all PC axes. Alternatively, Morse et al. (2013) argued that track shapes and metrics were differentiated within an individual based upon substrate material properties. Here, only the outline shape has been quantified, with size (metrics) and internal shape being excluded from assessments, explaining the discrepancy in results between the current study and the conclusions of Morse et al. (2013).

Here, substrate accounted for just 1% of total shape variance when only the outline shape was quantified. This indicates that the outline shape of a track is not sensitive to significant morphological changes when the tracks are created in different substrates. In

Chapter Three it was demonstrated that the internal proportions of a track are susceptible to shape changes when the underlying substrate is changed. Here, it has been established that the outline shape of a track is consistent within an individual regardless of the underlying substrate. Therefore, the null hypothesis regarding substrate influence on track shape production (H_2) can be rejected as the substrate pliancy did not affect track shape.

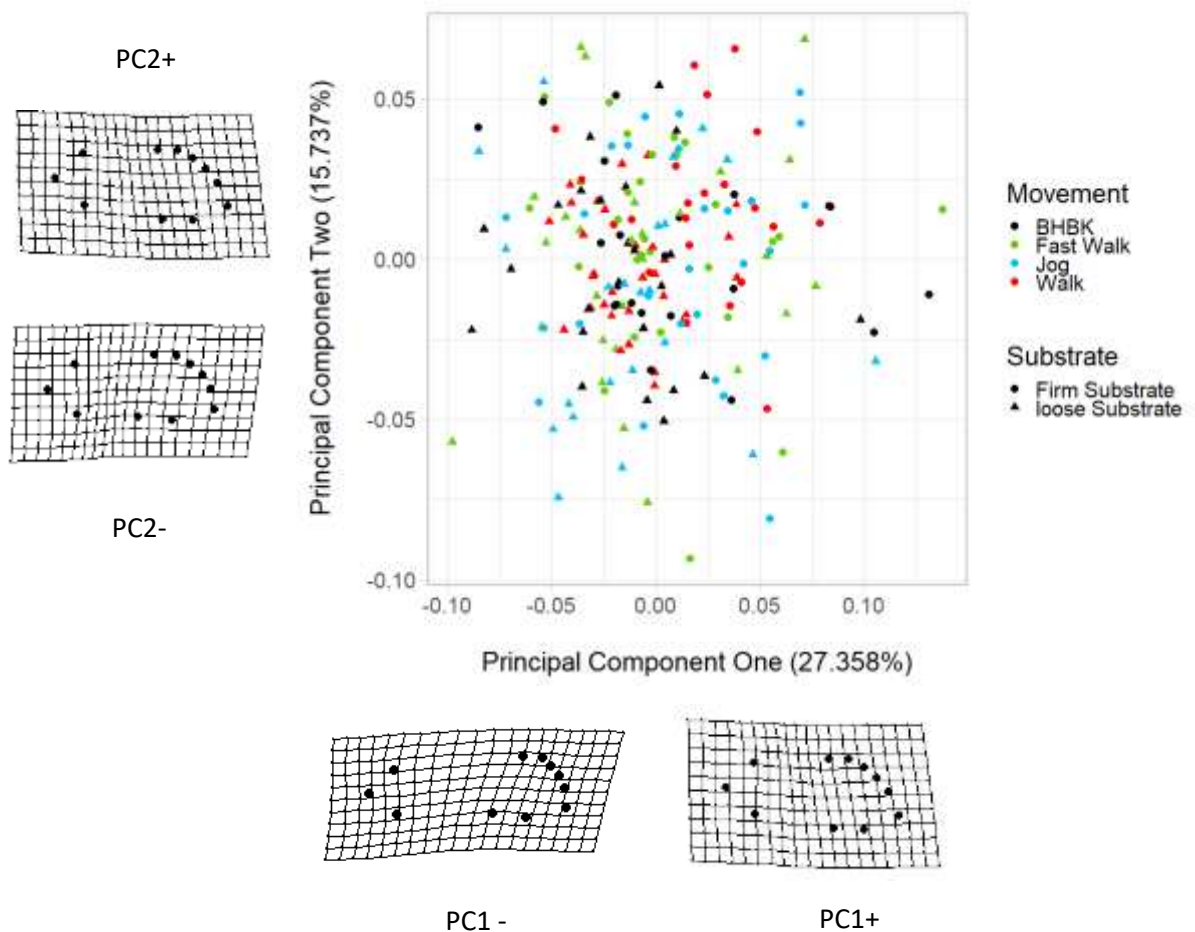


Figure 4.3. PCA graph illustrates shape change between different participants ($n=60$), grouped according to substrate typology and motion. Warp grids display the maximum and minimum relative shape changes along PC1 and PC2.

Table 4.1. Results of the MANOVA, with trackway introduced as a random effect to explore the relationship between three categorical variables (motion, substrate and log-centroid size (CS)) with shape. A separate MANOVA was also computed to establish if track shapes created by the same individual are similar or dissimilar to those made by another individual – this can be found in italics at the bottom of the table.

	Df	SS	MS	R ²	F	P
Motion	48	0.005	0.111	0.028	1.881	0.011
Substrate	48	0.006	0.005	0.010	1.127	0.142
Size	48	0.043	0.043	0.036	7.474	0.001
<i>Person</i>	<i>31</i>	<i>0.366</i>	<i>0.012</i>	<i>0.301</i>	<i>2.379</i>	<i>0.001</i>

2D landmark configurations

The PCA of track shape as represented by 2D landmarks produced comparable results to the PCA conducted using 3D landmark configurations. The PCA of all shape variables produced a mix of positive and negative PC scores along all PC loadings (100% of variance). There was no clear division of shape variables along any PC axis (PC1 to PC27). Numerous factors were included in the PCA (substrate and motion), which also included a variety of body proportions and ethnicities within the sampled population. Track outlines are similar within the entire sample, suggesting that GM methods cannot be used to identify the track-maker within a population (e.g., a species) because there is so much consistency in track shapes.

To explore these shape variables in more detail, a MANOVA was computed between the PC scores that explain 100% of total shape variance and their associated categorical variables. The MANOVA revealed that shape variability is influenced by speed and limb posture ($P=0.014$; $F=2.310$) and by the individual person ($P=0.001$; $F=7.315$), similar to the results of the 3D configurations. H_0 is rejected, because tracks belonging to individual participants are statistically disparate, as identifiable from 2D track outline shape, despite the PCA producing an intermix of shape variables along each PC loading. The discrepancy between the PCA and MANOVA may be explained by the chosen landmark configuration. Certain landmarks (such as those representing total track length; e.g., the tip of the hallux to the pternion) may be driving statistical variability, whilst other

landmarks could remain static between track shapes within the population. Consequently, simple linear measurements may be more likely to identify the track-maker within a population than outline shape.

No relationship was established between substrate pliancy ($F=0.516$; $P=0.818$) with track shape. The lack of association between substrate typology with that of track shapes are emphasised via the production of a P value approaching 1. Therefore, the null hypothesis regarding substrate influence on track shape production (H_2) can be rejected as substrate pliancy did not affect track shape.

4.3.2 The applicability of using 2D landmark configurations to quantify track shape

3D landmark configurations are most commonly employed in ichnology studies to explore shape patterns of a set of tracks (e.g., Bennett et al. 2016b; Gierlinski et al. 2017). The current study wanted to establish if the outline shape of a track can be used to identify the track-maker, exclusive of the internal impression. The application of 3D configurations determined that the outline shape of a track can successfully identify the track-maker, and that GM methods are suitable for exploring track shapes.

Both the 2D and 3D landmark configurations produced comparable and consistent results whereby track shapes were significantly disparate when produced by different individuals employing a range of speeds and limb postures. By repeating the 3D analyses with 2D configurations it was possible to establish that 2D methods can successfully synthesise track outline shapes.

Although individuals were identifiable from the GM analyses, the known morphological disparity in the foot between different hominin species (Aiello and Dean 2002; Ward et al. 2002; Lovejoy et al. 2009; Harcourt-Smith et al. 2015; Trinkaus and Patel 2016; Fernandez et al. 2016; Fernandez et al. 2018) suggests that variation in track shape between species will surpass that of intra-track variability amongst a population/species.

Conversely, the GM methods identified shape patterns associated with variable speeds and limb postures. Therefore, fossil trackways created from different speeds (e.g., a walk versus a jog) should not be statistically compared if speed is a known factor from fossil tracks. Within these analyses different limb postures were used to create experimental trackways (e.g., a flexed limb and an erect limb). Different limb postures produced diverse track morphologies, suggesting that it is probable that the same shape patterns can

be characterised in fossil tracks. Additionally, discrepancies in track sizes when created in different substrates at increased speeds were identified (see: Section 3.3.1). The results presented here capture these discrepancies, signifying that size should be considered as a variable during fossil track assessments. Because the methods produced similar results, depth can be confidently removed as a variable when comparing tracks from different places and/or species. Additionally, as substrate did not influence shape, GM methods can be reliably utilised for the comparison of fossil tracks that were created in a range of substrates.

Overall, by assessing a collection of experimental tracks, this preceding GM assessment has demonstrated that both 2D and 3D GM methods are comparable when just the outline shape of a print is synthesised. A subsequent quantitative comparative shape assessment of fossil tracks (e.g., the Laetoli, Ileret, Happisburgh and/or other fossil tracks) can be confidently computed via the application of 2D landmarks which will only capture outline shape and not the internal proportions that are susceptible to variable depths.

4.4.0 The morphological affinity of the early Pleistocene tracks from Happisburgh, England with other tracks of Pliocene, Pleistocene and Holocene age

Fossilised trackways which are known from the Pliocene, Pleistocene and Holocene (Bennett and Morse 2014), and contentiously from the Miocene (Gierlinski et al. 2017; Crompton 2017; Meldrum and Sarmiento 2018), can provide evidence of locomotor behaviour, and offer avenues for other biological inferences (Webb 2007; Webb et al. 2007; Tuttle 2008; Vaughan et al. 2008; Bennett et al. 2009; D'Août et al. 2010; Crompton et al. 2012; Morse et al. 2013; Bennett and Morse 2014; Masao et al. 2016; Hatala et al. 2016b; Hatala et al. 2016c; Bennett et al. 2016a; Raichlen and Gordon 2017). The advancement of 3D modelling for fossil track material has been pivotal in pioneering a revolution in the study of fossilised tracks (Remondino et al. 2010; Falkingham 2012; Bennett et al. 2016b; Falkingham et al. 2018). However, the digital 3D capture of tracks can be challenging in poor weather conditions where tracks are exposed for only a brief period (Wiseman and De Groote 2018).

This was the case at Happisburgh, UK. Marine erosion at Happisburgh in May 2013 exposed a sediment bed that contained 152 small (c.50 mm-320 mm) hollows, 49 of which were identified as potentially hominin tracks. Of these, only 12 were included in the original analyses when the discovery was first announced due to the severe erosion of

many of the prints (Ashton et al. 2014). High quality 3D data was, unfortunately, not captured prior to the loss of the prints to marine erosion (Ashton et al. 2014), resulting in modelled prints with unreliable depth dimensionality. This has led to the necessary exclusion of the Happisburgh tracks from many of the recent studies that have applied 3D analyses of hominin tracks to study locomotor evolution in hominins (e.g., Hatala et al. 2016a; Bennett et al. 2016a).

Here, the Happisburgh tracks were evaluated in a broader comparative context by applying a 2D GM approach based on track photographs to capture only the outline shape, exclusive of the internal structure of the prints. This builds on the work of Berge et al. (2006) and Bennett et al. (2009), who also used 2D GM approaches in comparative analyses of hominin tracks. By employing 2D methods depth dimensionality is removed, thereby resulting in fewer measurement variables but also circumventing the problems of poor depth resolution in 3D representations of the Happisburgh tracks (Figure 4.4)

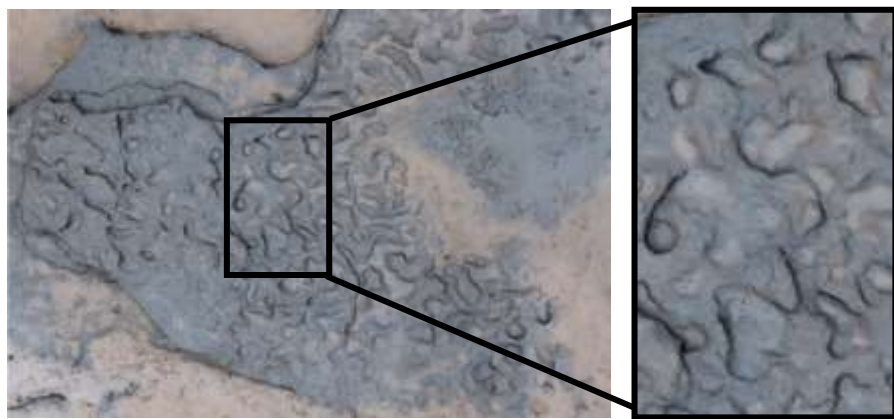


Figure 4.4. Poor resolution 3D models from Happisburgh, which were created rapidly during poor weather conditions, prior to marine erosion.

The aims of this study were to (1) compare the Happisburgh tracks with Pliocene, Pleistocene and Holocene tracks; and (2) evaluate the results of comparative analyses in functional and evolutionary contexts. Whilst exploring these aims, a number of predictions were addressed:

- i. Although the preliminary shape-space assessment determined an overlay of Procrustes shape scores with a modern population, the known morphological disparity in the foot between different hominin species (Aiello and Dean 2002; Ward et al. 2002; Lovejoy et al. 2009; Harcourt-Smith et al. 2015; Trinkaus

and Patel 2016; Fernandez et al. 2016; Fernandez et al. 2018) suggests that variation in track shape between different assumed species (i.e., the track-makers from each fossil locality) will surpass that of intra-track variability amongst a population/species. As such, it is predicted that track shapes will be different between species.

- ii. It is predicted that the midfoot impression will be more prominent in the tracks ascribed to AMHs than those belonging to australopithecines. With a more adducted hallux (Prediction iii), the hominin foot would have been better-suited to support the longitudinal arches of the foot (Elftman and Manter 1935), which would have permitted an efficient mediolateral weight transfer that is characteristic of modern humans (Harcourt-Smith 2002).
- iii. Concurrent with theories that the hominin foot lost prehensile capabilities due to a decrease in the angle of hallucal adduction that restricted hallucal opposability (e.g., Clarke and Tobias 1995; McHenry and Jones 2006; Bennett et al. 2009), the angle of hallucal adduction as represented in a track will be greater in tracks ascribed to *Homo* species than those of australopithecines.
- iv. It is predicted that foot proportions will differ between hominin track sites, which may imply different patterns in foot function across the taxa responsible for these tracks (e.g., Keith 1929; Aiello and Dean 2002).
- v. Contemporaneous with the geological age of the Happisburgh tracks, it is predicted that the early Pleistocene hominin tracks from Happisburgh will share a morphological affinity with other Pleistocene hominin tracks (Ileret, Kenya), as represented in both the shape-space assessments and by comparing track measurements.

4.4.1 Data acquisition

To compare the morphologies of the Happisburgh tracks with those of other hominin tracks, 2D data were collected from sites ranging from the Pliocene to the late Holocene (Table 4.2). Numerous trackways were excluded based on a number of criteria that might adversely affect the ability to confidently identify homologous landmarks on track outlines: camera parallax issues during data capture, walking speed, outline definition, and/or substrate typology.

Across all sites, this led to a total sample size of 274 tracks that provided well-preserved track outlines from which it was possible to obtain measurements and define homologous

geometric landmarks. Only small group samples were usable from the geologically oldest sites: Laetoli, Ileret and Happisburgh. Most of the sample (n=218) belongs to AMHs.

Orthogonal photographs were collected from published or archival records or photographed during excavation (Figure 4.5). Images were inspected for viewing angle to ensure that the track was centred in the photograph and that the camera position was sufficient to avoid parallax distortion (e.g., photographs that appeared to visually show the print captured at an angle were excluded, e.g., Figure 4.5b). This precaution may however not be necessary since Mullin and Taylor (2002) have shown that slight distortions in images are not necessarily a problem in most GM analyses. Despite this, data collection was conservative and, consequently, photographs that were not orthogonal or potentially suffered from parallax were excluded from this study. All inclusion/exclusion of photographs were completed visually, assuming the accuracy of Mullin and Taylor (2002).

Only trackways that were identified as belonging to a “walking speed” (classified as speeds below 1.5 m/s) were included in this study. Qualitative categorization was based upon the gait classifications of Jordan and Newell (2008), whereby any speed above ~1.6 m/s is classed as a fast-paced walk and speeds above ~1.9 m/s are classed as running. Speed was calculated using the method developed by Dingwall et al. (2013) for the Walvis Bay trackways based on published stride and foot length values (Morse et al. 2013), and for the Formby Point trackways collected in 2016/17 during field excavations. Speed was not calculated for the Happisburgh prints as associating singular tracks into trackways was confounded by a mix of superimposed hollows in the sediment bed (Ashton et al. 2014). Published speed estimates were used for Laetoli Site G and Site S trackways (Masao et al. 2016) and for the Ileret sample (Dingwall et al. 2013).

In most cases particularly deep trackways were omitted. Trackway morphology has been previously demonstrated to be influenced by depth correlative with substrate typology (Bates et al. 2013b). Bates et al. (2013b) established a threshold of >20 mm for deep prints and <20 mm for shallower prints. This threshold was applied in the current study for prints of known depth using published values and those calculated for the Formby Point trackways following the protocol outlined in Section 2.2.4. All Happisburgh tracks were included because depth remained unknown due to unreliable 3D mesh creation. If variability is established between all groups with that of the Happisburgh tracks, then the inclusion of all sampled Happisburgh tracks irrespective of depth should be identified as a potential factor driving statistical variance.

In the case of tracks for which 3D data were available rather than 2D photographs, an orthogonal image was created of the track and exported as a 2D image in Meshlab (Cignoni et al. 2008). Scale was checked using multiple measurements (track length, the long axis of the foot, forefoot width and heel width) in the extracted data to confirm that the images were consistent with the scale of published values of the Laetoli track lengths and were consistent with the publically available 3D models of the scaled Namibian tracks. Because scale was found to be identical in the extracted 2D images from 3D models, it was assumed that these images could be confidently used as comparable samples in this subsequent analyses.



Figure 4.5. (Ai) A selection of 2D images of fossilised tracks used within the current study. * indicates that track was not included in any statistical analyses, but linear measurements were collected. ^Δ Examples of 2D images extracted from 3D models. (B) An example of camera parallax, leading to the photograph's exclusion from the study.

Table 4.2. List of fossilised footprints used in this study. Fossils marked by an asterisk (*) were not included in the GM analyses or statistical analyses due to a small sample size.

Footprint locality	Geological Age	Substrate	Substrate description	Inferred species	<i>n</i>
Laetoli, Tanzania	Pliocene (~3.66Ma)	Volcanic ash	Partially lithified; natrocarbonatite ash;	<i>Australopithecus afarensis</i> (Leakey	
• Site S			fine to medium-grained sand.	and Hay 1979; White and Suwa	10
• Site G				1987; Masao et al. 2016)	17
Ileret, Kenya	Pleistocene	Fluvial-	Unlithified; fine-grained silt and fine sand	<i>Homo erectus</i> (Bennett et al. 2009;	
• FwJj14E	(1.5Ma)	Lacustrine		Hatala et al. 2017)	12
Happisburgh, UK	Pleistocene (950-850Ka)	Fluvial	Unlithified; laminated silts	<i>Homo antecessor</i> (Ashton et al. 2014)	14
Terra Amata, France	Pleistocene (380Ka)	Cave/Coastal	Coastal	<i>Homo heidelbergensis/Homo neanderthalensis</i> (DeLumley 1966)	1*
Langebaan, South Africa	Pleistocene (~117Ka)	Coastal Aeolianite	Lithified; calcareous and cemented with carbonate.	Early <i>Homo sapiens</i> (Roberts and Berger 1997)	2*
Vârtoș Cave, Romania	Pleistocene (>62Ka)	Cave	Calcareous sediment with desiccated calcite deposits	<i>Homo neanderthalensis</i> (Bogdan et al. 2005)	1*
Formby Point, UK	Holocene (~7-3Ka)	Coastal (sandy-silt)	Unlithified; medium to coarse grained sandy-silts. Cemented with salt.	<i>Homo sapiens</i> (Roberts 2009)	72
Walvis Bay, Namibia	Holocene (1.5-0.5Ka)	Fluvial	Unlithified ; fine-grained sand/silt/clay with partial cement of salt	<i>Homo sapiens</i> (Bennett et al. 2010)	146
Total number of footprints included in study:					274

By omitting deep trackways, intra-group variability should be constrained and the application of 2D landmark configurations which synthesise the outline shape of a track will be appropriate for cross-site comparisons. Finally, exclusion/inclusion of a particular track was often aided by loss of homology during landmark placement (e.g., damage to a region of a track or poor definition would result in that track's exclusion from the study). Tracks lacking clear outlines were excluded, such as those that exhibited the 'loss' of one part of a print due to supposed erosion (Wiseman and De Groote 2018). Only tracks with a clear outlined impression of all track aspects were included.

Only the G1 trackway from Laetoli Site G was used in this study. The G2/3 trackways were excluded as the overlay/trampling of these trackways would probably introduce noise error within the Laetoli sample, despite novel attempts to extract the G3 trackway by Bennett et al. (2016a).

Track-maker age was estimated using modern growth curves of the foot derived from the WHO (de Onis 2006) as employed by Ashton et al. (2014) for the prediction of relative age of the Happisburgh track-makers using 2D measurements, and refined for the Gombore II-2, Ethiopia trackways (Altamura et al. 2018). Although defining track-maker age is problematic due to ontogeny remaining unknown in hominin species (e.g., the inferred species for the creation of each fossilised trackway), relative age was predicted for all tracks incorporated into this study using the method defined by Altamura et al. (2018). It is acknowledged that slight error may be present as (1) skeletal maturity may have been reached earlier in some hominin species thus warping age predictions; (2) the boundary between sub-adult and adult is poorly defined, as an adult female could produce a similar track to a sub-adult male; and (3) the extent of hominin skeletal dimorphism requires further exploration.

4.4.2 Geometric morphometric analyses

To assess variation in track morphology across Pliocene, Pleistocene and Holocene samples, changes in outline shape were explored between-groups by applying GM techniques (Bookstein 1991; Slice 2005). All tracks within a trackway belonging to a single individual were included in these analyses. Because there are multiple tracks per individual, some individuals will be more heavily weighted in statistical assessments than others. Despite the use of 'averaged' tracks in Chapter Three, this method is not applicable for fossil tracks as it can remove nuanced morphological features and can warp a true reflection of track shape (Belvedere et al. 2018). Even if the mean track was used

per fossil trackway, the statistical weighting issue will still be paramount as it is uncertain which species made which prints, or which tracks produced at the same site may have been made by the same person, but at different times of the day (e.g., it was evident from the excavations at Formby Point in 2016/17 that the tracks were made at various times of the day; some of the prints were much more deeply pressed – the deepest prints were excluded from this study – than others, probably owing to changes in moisture content at the time of track formation). Consequently, all statistical analyses have incorporated ‘trackway’ (i.e., all tracks pertaining to a singular trackway) as a random effect to address this issue directly.

While it is acknowledged that intra-group variability will probably exist (e.g., speed and substrate covariates), the landmark dataset was kept as simple as possible, capturing homologous outline shape that could be identified across the entire sample, rather than to provide an in depth comparative outline shape (e.g., many tracks lack clear toe impressions resulting in a loss of complex forefoot comparative analyses).

Reliability tests of landmark placement were conducted to ensure that landmarks could be consistently identified within and across samples. Landmarks were placed over a period of ten days on three randomly selected tracks: one track each from Laetoli, Happisburgh and Formby Point. It was assumed that the greatest variance may be introduced by incorporating tracks from Laetoli and/or Happisburgh as these tracks were visually the least defined in comparison to the clear outlines in many of the Formby Point tracks.

Landmark reliability tests consisted of a GPA computed in R (R Core Team 2017) to test for consistency in landmark digitisation (Slice 2005). The Procrustes distances between each landmark consensus with the mean landmark configuration were calculated (Dryden and Mardia 1998). The distances between each repetition were averaged. This process provided the error estimate for inter-landmark placement. Mean values (Procrustes distances) over 0.05 specified that the distance between a landmark and the overall consensus was high and that a landmark was non-replicable (Profico et al. 2017). All mean values lower than 0.05 indicate good repeatability in landmark placement (Zelditch et al. 2012).

Through this process, landmarks found to be non-replicable between specimens were removed (e.g., the deviation from the landmark consensus was >0.05). Three landmarks were subsequently removed (these landmarks synthesised the lateral midfoot) and the

replicability tests were recomputed using the remaining 16 landmarks. The mean Procrustes distance from the consensus was 0.03 ± 0.01 . Considering all landmarks individually, all Procrustes distances were <0.05 , thus each landmark was consistently and reliably placed (Figure 4.6). This signifies that intra-observer error in repeatability of landmark placement was low, and that the landmark configuration is suitable for the subsequent analyses. This process resulted in the selection of 16 type II landmarks that all had a Procrustes distance <0.05 . These landmarks captured the outline shape of each track (Figure 4.6) and were digitised on all 274 prints within the sample using TPSDig 2.0 (Rohlf 2004). To circumvent the issue of asymmetry, all left landmark configurations were mirrored (Dryden and Mardia 1998; Mardia et al. 2000).

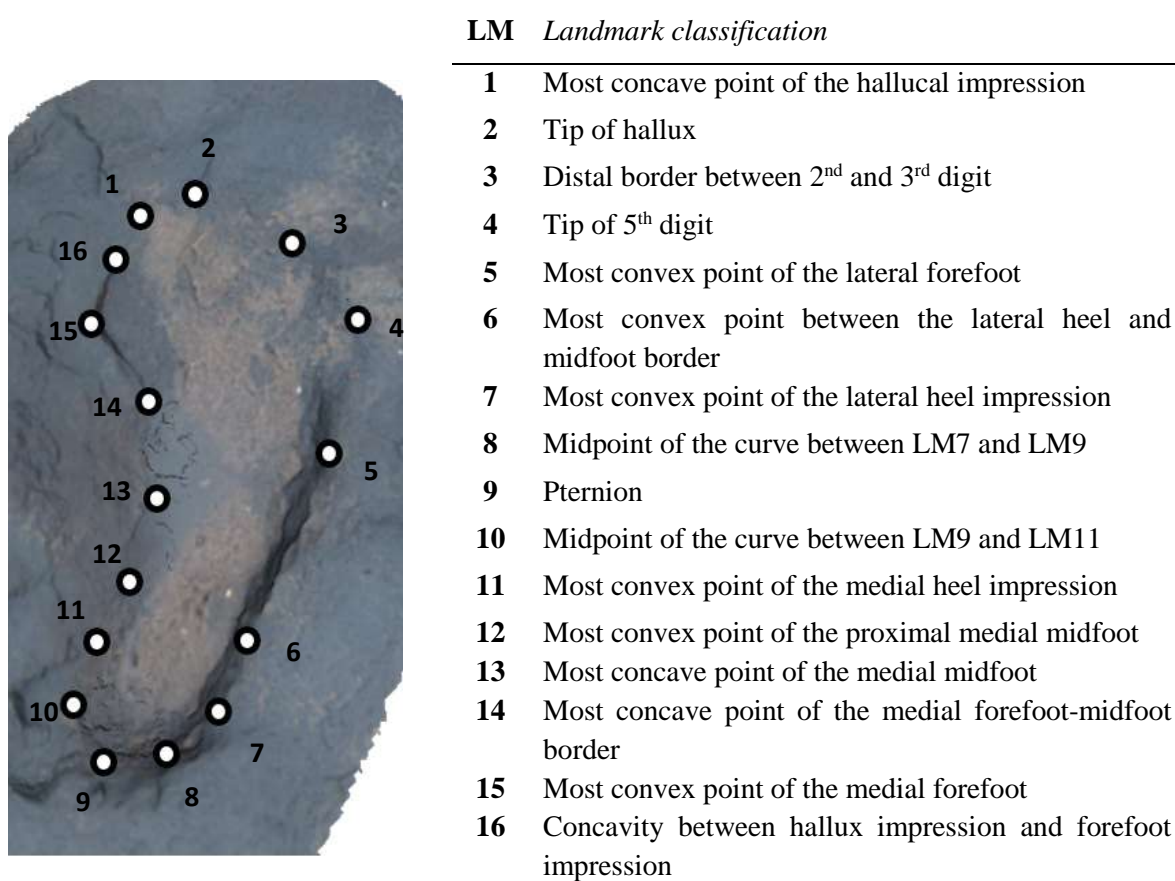


Figure 4.6. Landmarks used within the current study. Sixteen landmarks were used in the study. Specimens that were found to have very prominent foot slippage were excluded from the dataset. These individuals were found to be outliers in the analyses and were deemed unreliable to be included in the current study due to a warping of true shape.

All landmark configurations (n=274) were superimposed using a GPA, which translates and rotates a landmark configuration to a common origin, whilst scaling to log-transformed unit-CS (Gower 1975). Shape variation was assessed using a between-groups PCA. This methodology allows the number of variables to be higher than the number of observations (Mitteroecker and Bookstein 2011), which was particularly relevant for comparative analyses of the Laetoli, Ileret and Happisburgh samples. A nested MANOVA with a mixed effect was computed on the resulting shape scores using trackway number (Appendix F) as a random effect, and age and fossil location as fixed effects to determine the statistical significance of morphological variation among fossil localities. Analyses were computed in the geomorph (Adams and Otárola-Castillo 2013) and morpho (Schlager 2017) R packages (R Core Team 2017).

The effect of speed on track outline

Although the results in Section 4.3.1 demonstrated that speed (exclusive of jogging tracks, which were not included in this study) did not affect trackway outline shape, this study employed a conservative approach and computed a MANOVA using 1000 permutations to establish if the observed variance in track outline shape was associated with speed (m/s), or if variance was the result of different inferred species producing variable outline shapes. Trackway was introduced as a random effect on the 137 tracks from Laetoli, Ileret, Formby Point and Namibia for which speed estimations were possible. This was consciously computed for two reasons: (1) speed has been previously demonstrated to affect topographical morphology (e.g., Dingwall et al. 2013; McClymont et al. 2016); and (2) it remains unknown how speed may affect track production in other hominin species.

Adult track variation

The sample represents a mixture of juvenile and adult tracks. To explore ontogeny as a factor that may be driving shape disparity, size was introduced as a variable. CS was regressed against shape to examine the influence that ontogeny has on shape. Results were supported by a pairwise comparison test. Because statistical significance was identified between juvenile and adult tracks, all analyses were recomputed using only adult tracks, thus omitting ontogeny as a factor.

Substrate controls

A limiting factor of any ichnological study that compares tracks across multiple fossil sites is the probability that substrate variation will affect track morphological comparisons (Morse et al. 2013; Bennett and Morse 2014). To assess the influence of substrate variability, the Holocene tracks that represent the same species (*Homo sapiens*), but in different substrate contexts were sub-sampled: Formby Point (a coastal site) and Walvis Bay (a fluvial site). A PCA and a MANOVA were computed using just the Holocene samples to assess the influences of substrate and/or biometric variation on track morphology.

Additionally, the dataset was qualitatively sub-divided based on presumed substrate conditions: one sampled group contained relatively shallower tracks (Laetoli, shallow Namibian tracks and shallow Formby Point tracks), and the other group contained deeper tracks (Ileret, Happisburgh, deeper Namibian tracks and deeper Formby Point tracks). A PCA was computed on the separate landmark configurations to determine if shape variation was consistent when relative track depth (a qualitative proxy for substrate deformability) was considered as a confounding factor. Statistical variance was quantified using a MANOVA on the PC shape scores that account for 100% of variance.

4.4.3 Comparing linear track metrics

The angle of hallux abduction was measured for each track by calculating the angle between the long axis and an intersecting line crossing from the tip of the hallux impression through the deepest (mid-point) point within the hallux impression (Bennett et al. 2009).

Although experimental track dimensions were established to be significantly variable when walking speed was increased (Chapter Three), this study wanted to test the relative variance in fossil track dimensions between species. To test this, four linear measurements of each track were extracted in TPSDig 2.0 (Rohlf 2004): the tip of the hallux to the pternion (track length), the second digit to the pternion (the long axis), forefoot breadth, and heel breadth (Figure 4.7). Track length was used to predict stature using Martin's ratio of 15% (Martin 1914).

To test whether foot proportions changed from the Pliocene to the Holocene, the total length of the impressions for the hallux and the length of the distal toes in each track with clear toe impressions were computed (Figure 4.7). The proportion of distal track length to total track length was also calculated for each track. This permitted an assessment of

the internal proportions of the track which were otherwise excluded in the GM analyses to prevent these internal shapes influencing shape-space results. Because some samples within this dataset included juvenile tracks (Happisburgh, Formby Point and Walvis Bay) and it is known that foot proportions change during ontogeny (e.g., Davenport 1932), tracks attributed to juveniles were excluded from these analyses.

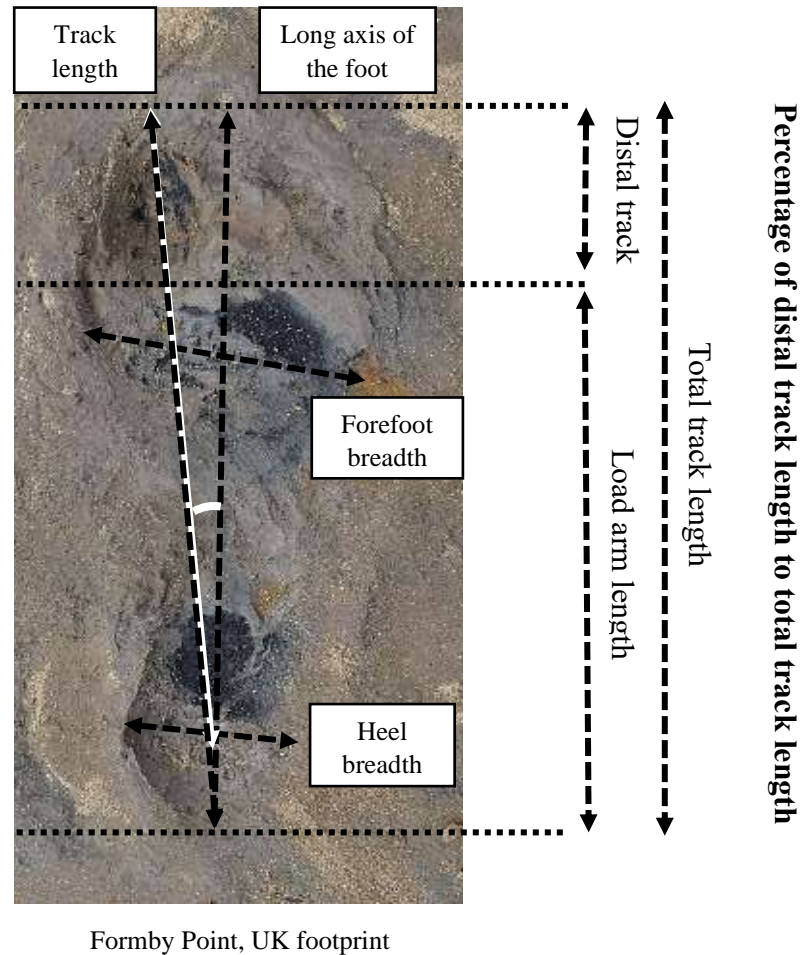


Figure 4.7. Four linear dimensions (mm) of each track (dashed black lines). Solid white line indicates the intersecting line between the tip of the hallux and the long axis of the foot. The angle between this intersecting line and the long axis was used to calculate the angle of hallux abduction in each print. Foot proportions were determined by calculating the percentage of the distal foot to the total track length.

4.4.4 Results

Track shape results

To test the prediction that track shape varies between fossil localities, GM methods were applied on landmark configurations that synthesise the outline shape of a selection of

fossil prints assumedly belonging to different hominin species. A PCA was performed using Procrustes-fitted landmarks across all samples of hominin tracks (Figure 4.8). All categorical variables were primarily treated as independent observations (e.g., different inferred species and the inclusion of several substrates) to identify which factor(s) explains the majority of shape change.

Variation along PC1 was characterised by a separation of negative PC scores for the Laetoli tracks and positive PC scores for the Ileret tracks. Positive and negative scores exist for all other hominin track samples. Track outline shape between each fossil group explains 11.74% of the total variance ($P \leq 0.001$, $F=8.255$), as determined by a MANOVA. Multiple factors, aside from the fact that this study sampled tracks from multiple hominin taxa, could explain this mix of PC scores. For example, each site includes a different mixture of tracks produced by infant, juvenile and adult individuals, and the locations of these sites imply that eco-geographical differences (the samples represent boreal, temperate and warm-climate populations) in body proportions may influence variation in track morphology. However, relative age (e.g., juvenile or adult) of the track-maker was identified to explain just 1.78% of total shape variability ($P=0.002$, $F=2.503$), as determined by a MANOVA (Table 4.3).

Maximum and minimum shape corresponding to PC1 were visualised as shape deformation graphs within the morphospace (Bookstein 1989). Shape change along PC1 can be explained by three variables: increasing adduction of the hallux, the anteroposterior displacement of the medial longitudinal arch (MLA) and a reduction in heel width (Figure 4.8). On the other hand, PC2 seems related to the prominence of the MLA impression. Interestingly, scores along the PC2 axis overlapped for the Laetoli tracks and the Holocene infant/juvenile tracks.

The axis of PC3 appears to highlight the morphological disparity between AMHs (majority distributed as PC3+ scores) and all other hominins (PC3- scores) (Figure 4.9). Shape change along PC3 can be explained by the prominence of the MLA impression, with PC4 explaining once more the change in the MLA but also hallucal adduction. Evidently, changes in the midfoot region accounts for much of the shape variance present within this sample (PC1 to PC11; 87.24%).

Table 4.3. Results of the nested MANOVA with trackway introduced as a random effect. Significant P values are in bold.

	Df	SS	MS	R ²	F	Z	P
Fossil Locality	4	0.581	0.142	0.117	8.255	8.424	<0.001
Age of track-maker	4	0.088	0.044	0.018	2.503	3.317	0.002
<i>Residuals</i>	236	4.151	0.018	0.839			
<i>Total</i>	244	4.820					

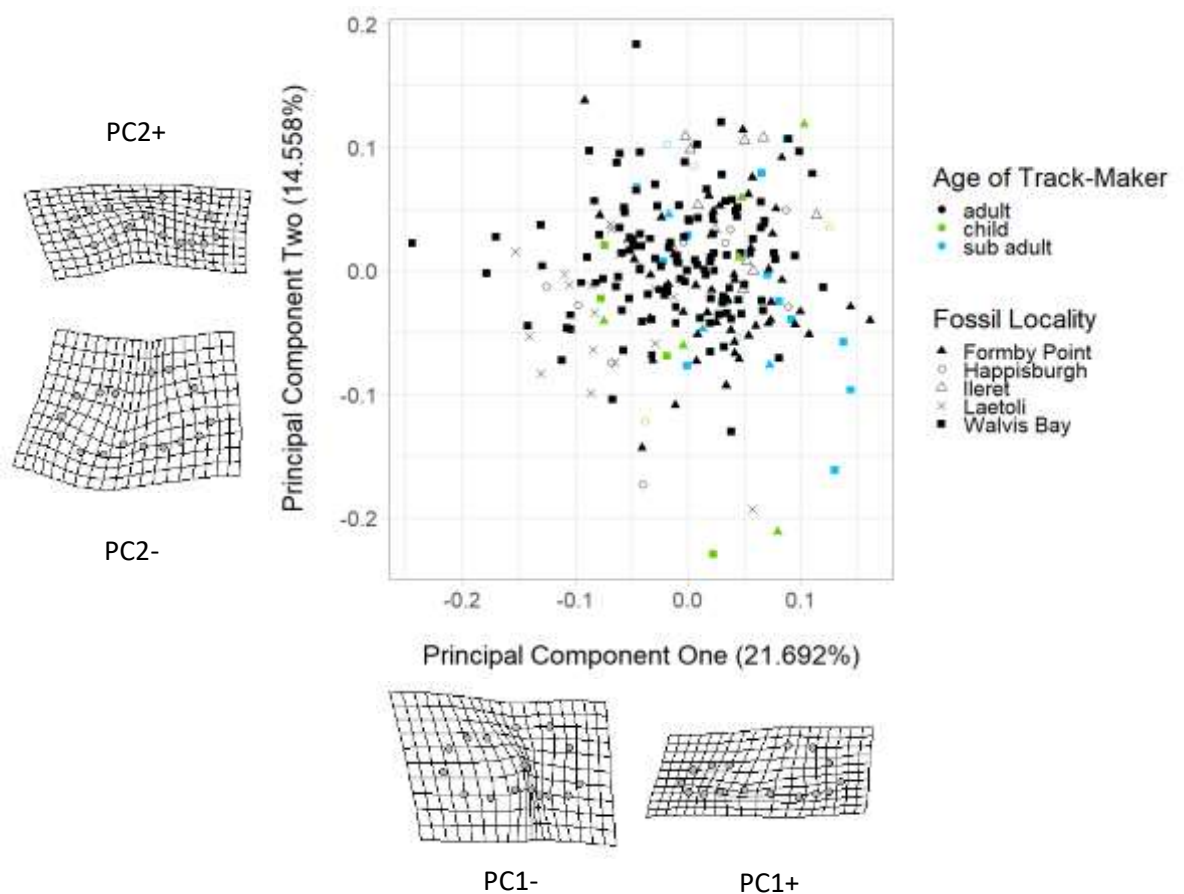


Figure 4.8. Graphical results of the PCA plotting PC1 against PC2 scores. Due to a confounding mix of data points in this graph, interpretations were aided by a MANOVA which was computed on all landmark configurations. Generally, there is similarity in footprint shapes between footprints belonging to different assumed species. General shape trends along PC1 and PC2 were interpreted from the TPS grids.

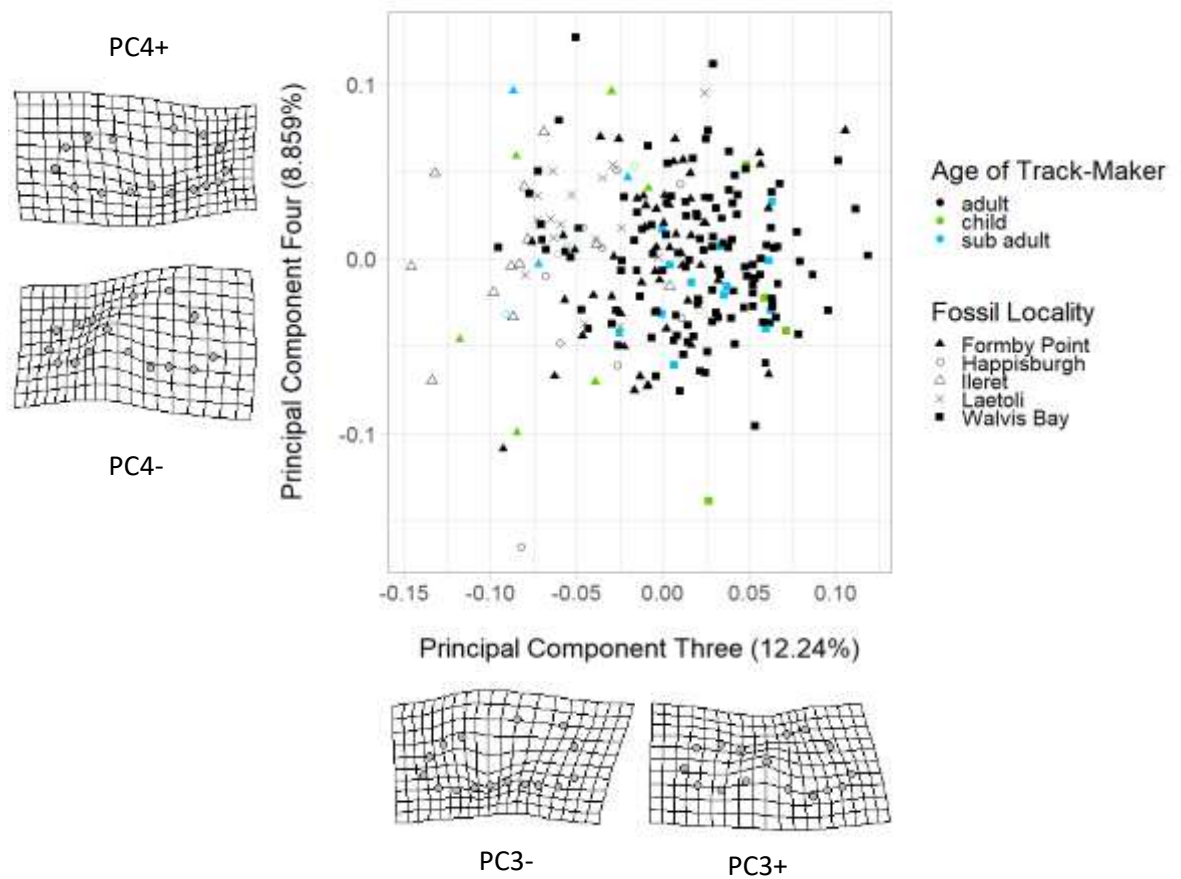


Figure 4.9. Graphical results of the PCA plotting PC3 against PC4 scores. All Laetoli, Ileret and Happisburgh footprints were characterised by PC3- shape scores. The majority of Holocene footprints were characterised by PC3+ shape scores. The division of these shape scores along PC3 aided morphological interpretations of shape affinities/disparities between the assumed species present at each fossil site.

The influence of speed on track shape

As the midfoot impression accounted for much of the shape change between tracks, it remained unknown as to which factor(s) explained this change. To determine if track morphology was affected by walking speed (m/s) across the fossil samples (excluding the Happisburgh population), speed was introduced as a covariate and a MANOVA that accounted for 100% of shape variance was computed to establish the influence that speed may have on track outline alongside two other factors: fossil locality and track-maker age. Statistical significance was identified between tracks produced at various speeds ($P=0.010$; $F=8.191$), although the relationship between speed and shape was determined to be poorly correlated ($R^2=0.175$) (Table 4.4). Nevertheless, the effect that speed may

have on outline shape should not be ignored as it does explain 17.50% of total shape variance within this sample, whereas the difference between fossils representing different assumed species explains only 15.21% of the total variance. Cumulatively, these results suggest that other factors which are not assessed here (e.g., biometrics, foot anatomies and phylogeny) are likely the major cause(s) of shape differentiation between these sampled groups. One such variable may be ontogeny.

Table 4.4. Results of the influence of speed on track outline shape, as reported by a MANOVA with trackway introduced as a random effect. n=137 tracks for which speed predictions were possible. Significant P values are in bold.

	Df	SS	MS	R ²	F	Z	P
Speed	4	0.488	0.122	0.175	8.191	8.347	0.010
Fossil Locality	4	0.424	0.106	0.152	7.119	8.961	<0.001
<i>Residuals</i>	<i>126</i>	<i>1.876</i>	<i>0.015</i>	<i>0.673</i>			
<i>Total</i>	<i>134</i>	<i>2.788</i>					

Adult track variation

Outline shape variance was significantly dependent on speed and fossil locality (Table 4.3). However, the sample includes both juvenile and adult tracks (classification was based upon the methods defined by Altamura et al. (2018); described in Section 4.4.1). To determine if this established shape difference could be due to the effect of ontogenetic differences present within the sample, size (log-CS) was introduced as a variable. A MANOVA was computed between-groups (track-maker age and fossil locality) using all PC scores (100% of shape variance) and log-CS. Child and adult tracks within each fossil locality were found to be statistically significantly variable (P=0.002; $z=6.238$ between the Formby Point child and adult tracks. P=0.002; $z=2.859$ between the Walvis Bay child and adult tracks. P=0.032; $z=2.368$ between the Happisburgh child and adult tracks) (see: Appendix G for Effect Sizes Table). The contrasts in the z values reported here (grouped: $P \leq 0.001$; $z \geq 2$) have demonstrated that the greatest morphological disparities revealed by the GM analyses separate the infant/juvenile from all adult specimens (Holocene and Pleistocene). Ontogeny is thus the principle factor in morphological disparity.

To support this, pairwise comparisons of log-CS to shape (PC scores) were computed. Results indicated that there are no significant differences between the adult tracks from the Pliocene, Pleistocene or Holocene ($P \geq 0.05$; $z \geq 1$ between all groups, within a 95% confidence interval). This suggests that morphology remained similar between hominin adult groups, despite eco-geographical and temporal differences, and variability in substrate typologies. Alongside these differences, there was a wide range of anatomy in the *Homo* foot (De Silva et al. 2018), so it is quite surprising to find such similarity between the *Homo* tracks. Such poor levels of significance are probably explained by a stark contrast in sample size (Cohen 1988; Collyer et al. 2015) and are difficult to measure due to comparatively small sample sizes (e.g., in the Ileret and Happisburgh samples) with those of the larger Holocene samples (Walvis Bay and Formby Point).

Because shape variance was dominated by the presence of infant and juvenile prints in the dataset, an additional PCA and MANOVA using only the adult specimens (now characterised as dependent observations) were computed, so as to reduce the number of confounding variables (Table 4.5). The results of the PCA indicate that there was broad similarity between all tracks, with only minute variations identifiable. Speed explains 17.11% of the total variance ($P=0.001$) in outline shape. Eco-geographical and temporal differences between each fossil locality explains 16.12% of the total variance in the adult tracks, although an overlay of Procrustes scores makes it difficult to clearly distinguish shape differences between different inferred species. This suggests that unaccounted-for, non-independent factors, such as changes in foot anatomies, likely explains any major variability in hominin tracks.

Table 4.5. Results of the influence of speed on track outline shape in the adult sample, as reported by a MANOVA with trackway introduced as a random effect. Significant P values are in bold.

	Df	SS	MS	R ²	F	Z	P
Speed	4	0.577	0.144	0.171	8.090	8.584	0.001
Fossil Locality	4	0.544	0.136	0.161	7.631	9.367	0.001
<i>Residuals</i>	<i>126</i>	<i>2.246</i>	<i>0.018</i>	<i>0.668</i>			
<i>Total</i>	<i>134</i>	<i>3.367</i>					

The effect of substrate on track outline in fossil samples

To examine the extent to which substrate may influence the variations observed in the outline shapes of tracks, a PCA and a MANOVA were also computed on the two Holocene track samples from Formby Point and Walvis Bay which were produced on different substrates. The PCA results demonstrate a mixture of Holocene PC- and PC+ scores ($R^2=0.016$; $F=3.121$; $P=0.005$), indicating that substrate only accounts for 1.61% of morphological variation between these two localities. Rather, other factors, such as biometric variation, are more influential factors in the variance of track outline shapes.

This compliments the results in Section 4.3.1 where it was determined that the outline shape between experimental tracks are consistent when produced in substrates of varying compliancy. Levels of significance identified in the fossil tracks (despite substrate explaining just 1.61% of the total variance) suggests that different materials (e.g., fluvial deposits) respond differently to footprint creation than the experimental prints, and that substrate does have a small influence on outline shape.

To test the effect of substrate on fossil track shapes composed in a larger variety of sediments (e.g., natrocarbonatite ash and sandy deposits), a final PCA and MANOVA were computed using track samples which represent the deeper and shallower ends of the spectrum (Figure 4.10). Results were found to be similar to the PCA inclusive of all track data (see: Figure 4.8): the geologically oldest tracks show little intra-group variability along PC1, represented by strong negative characterisation along PC1 in both the deep tracks ($R^2=0.123$; $F=4.836$; $P\leq 0.001$) and the shallow tracks ($R^2=0.108$; $F=8.396$; $P\leq 0.001$). The Holocene tracks have a mix of PC scores, with a broad overlap of the Happisburgh scores. Differences in inferred species account for 70.27% of the total variance in the deep tracks and 76.34% for shallow tracks. This signifies that the majority of shape variation is influenced by the track-maker and not by depth. Some consideration should still be given to substrate as despite depth being non-influential, this study sampled seven different substrate typologies which will likely introduce some error into these analyses. Regardless, outline shape can be consistently extracted from track morphologies permitting a comparative assessment of hominin tracks.

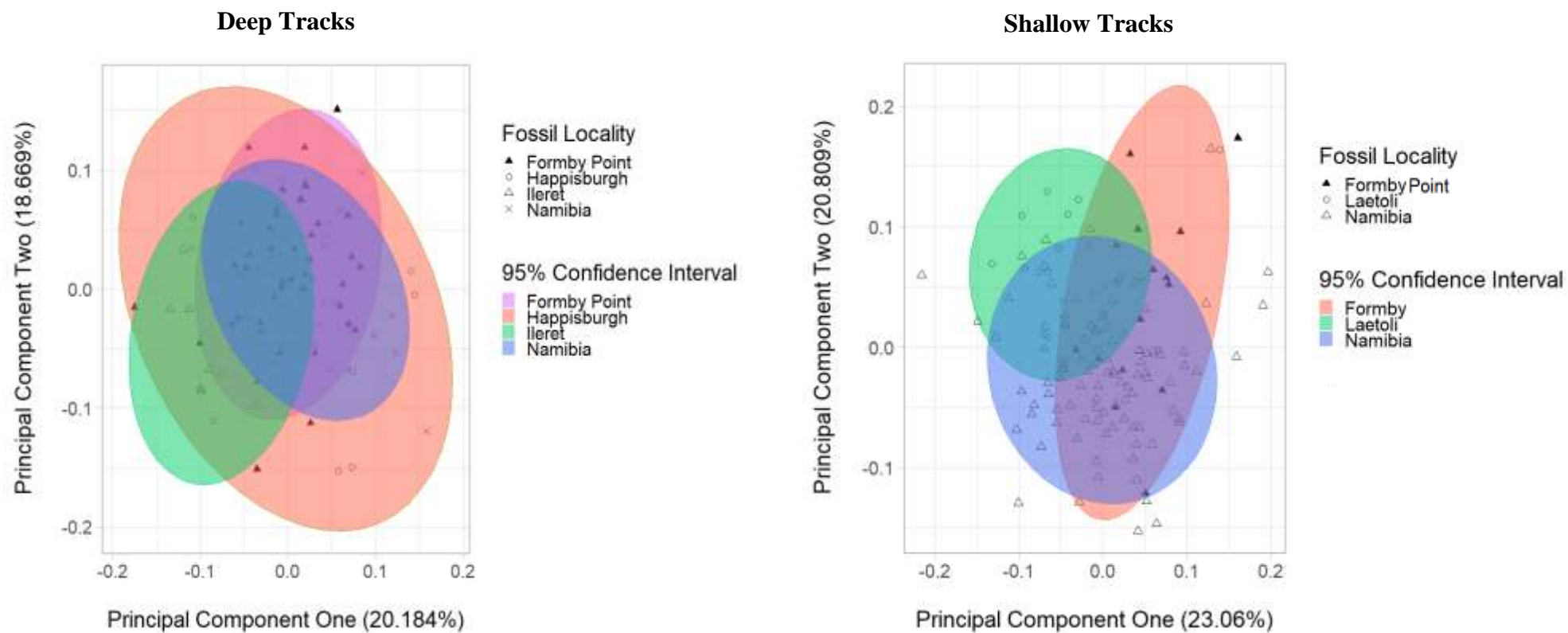


Figure 4.10. PCA computed separately on samples of relatively deeper and shallower tracks.

Comparing linear track measurements

To evaluate changes in foot/track size from the Pliocene to the Holocene, four linear length and breadth measurements were computed and compared (Table 4.6). Results from the one-way ANOVA and Games-Howell post-hoc tests demonstrated that track lengths and lengths of the long axes significantly increased from the Pliocene to the Pleistocene, despite high variation within the Laetoli sample. After this point, a trend, albeit non-significant, was identified for decreasing track lengths over time when simply assessing the median values of each sample (Table 4.6; Figure 4.11), consistent with previous comparative assessments (Kim et al. 2008). Forefoot and heel breadth were found to remain static across hominin prints from the Pliocene to the Holocene, except for variability in heel breadth dimensions between Holocene populations. Because track lengths increased between the Pliocene to the early Pleistocene samples, so did stature predictions (Table 4.7).

Comparisons of hallux abduction angles revealed a trend for a significant reduction in hallucal abduction ($P \leq 0.001$, $F=275.563$ between all groups) from the Pleistocene to the Holocene (Table 4.9; Figure 4.12).

Table 4.6. Mean measurements (mm) and mean predicted stature (mm) of each individual. As determining which track belongs to a certain individual in the Happisburgh hominins is subjective, the group means are reported for inferred child, sub-adult and adult prints. Individual tracks not belonging to a trackway from Ileret, Formby Point and Walvis Bay are not reported here. Group means provided from Group One and Group Two from Walvis Bay are provided (Bennett et al. 2014).

	Track ID	Length	Stature	2nd digit to heel	Heel breadth	Forefoot breadth
Laetoli	M9-S1	256.71	1711.67	247.02	65.46	101.85
	L8-S1	261.02	1740.13	262.32	78.75	103.25
	G1	173.93	1159.54	165.26	46.08	73.44
	TP2-S1	271.01	1806.73	272.11	82.00	99.45
Ileret	FUT1A	261.06	1740.39	259.45	48.08	82.79
	FUT2	283.98	1893.17	274.02	57.20	93.96
Happisburgh	Child mean	150.02	1000.11	150.40	31.34	63.15
	Adult mean	217.72	1451.49	208.90	49.09	77.34
Terra Amata	Single print	242.66	1617.75	250.13	53.78	83.34
Vârtop Cave	Single					
	Print	222.25	1481.17	210.68	77.20	113.72
Langebaan	1	220.00	1466.67	/	62.96	89.42
	2	220.50	1470.00	/	/	/
Formby Point	1	113.87	759.12	106.11	41.89	76.20
	2	250.78	1671.85	241.21	58.79	88.73
	3	204.67	1364.47	198.72	50.97	72.25
	4	274.86	1832.41	263.94	46.45	88.50
	5	230.15	1534.33	210.35	45.34	82.55
	6	207.03	1380.17	192.46	40.96	64.97
	7	259.54	1730.26	230.36	51.33	87.34
	8	235.52	1570.11	217.77	34.27	76.39
	9	260.74	1738.26	251.92	47.72	86.53
	10	278.96	1859.73	255.96	47.79	102.99
Walvis Bay	Group One	172.89	1490.85	158.92	42.16	61.12
	Group Two	204.94	1366.27	189.08	45.12	62.40
	Trail One	255.25	1678.58	238.11	62.33	88.75
	Trail Two	229.43	1529.56	212.67	52.44	75.14

Table 4.7. Results of the ANOVA and Games-Howell Test. Table displays the between-groups variability of linear measurements of the track and stature. Both df1 (between-groups) and df2 (within-groups) are reported. Levels of significance are reported within a 95% confidence level. Significant P values are in bold.

One-way ANOVA					Games-Howell Test			
Measurement (mm)	df1	df2	f	P	<i>Between-groups variability</i>		Std. error (mm)	P
Foot length	4	220	18.4	<0.001	Laetoli	Ileret	13.26	<0.001
						Happisburgh	26.09	0.997
						Formby Point	9.21	<0.001
						Walvis Bay	7.78	0.009
					Ileret	Happisburgh	27.23	0.126
						Formby Point	12.06	0.169
						Walvis Bay	11.01	0.005
					Happisburgh	Formby Point	25.50	0.476
						Walvis Bay	25.02	0.900
					Formby Point	Walvis Bay	5.50	0.002
Stature	4	220	19.266	<0.001	Laetoli	Ileret	88.38	<0.001
						Happisburgh	173.93	0.997
						Formby Point	61.14	<0.001
						Walvis Bay	51.89	0.009

Table 4.8 cont. Results of the ANOVA and Games-Howell Test. Table displays the between-groups variability of linear measurements of the track and stature. Both df1 (between-groups) and df2 (within-groups) are reported. Levels of significance are reported within a 95% confidence level. * indicates statistically significant variability between-groups.

	One-way ANOVA				Games-Howell Test			
Measurement (mm)	df1	df2	f	P	<i>Between-groups variability</i>		Std. error (mm)	P
					Ileret	Happisburgh	181.52	0.126
						Formby Point	80.22	0.203
						Walvis Bay	73.41	0.005
					Happisburgh	Formby Point	169.93	0.449
						Walvis Bay	166.82	0.900
						Formby Point	36.28	0.001
Long axis of foot	4	220	18.008	< 0.001	Laetoli	Ileret	14.50	< 0.001
						Happisburgh	27.46	0.993
						Formby Point	9.61	< 0.001
						Walvis Bay	8.47	0.033
					Ileret	Happisburgh	28.80	0.105
						Formby Point	12.95	0.026
						Walvis Bay	12.13	0.0028

Table 4.8 cont. Results of the ANOVA and Games-Howell Test. Table displays the between-groups variability of linear measurements of the track and stature. Both df1 (between-groups) and df2 (within-groups) are reported. Levels of significance are reported within a 95% confidence level. * indicates statistically significant variability between-groups.

	One-way ANOVA				Games-Howell Test			
Measurement (mm)	df1	df2	f	P	<i>Between-groups variability</i>		Std. error (mm)	P
					Happisburgh	Formby Point	26.67	0.690
						Walvis Bay	26.28	0.970
					Formby Point	Walvis Bay	5.40	0.006
Forefoot breadth	4	220	2.489	0.044	Laetoli	Ileret	6.76	0.327
						Happisburgh	12.85	1.000
						Formby Point	4.12	0.323
						Walvis Bay	3.91	0.998
					Ileret	Happisburgh	13.61	0.863
						Formby Point	6.08	0.909
						Walvis Bay	5.95	0.309
					Happisburgh	Formby Point	12.51	0.964
						Walvis Bay	12.44	1.000
					Formby Point	Walvis Bay	2.57	0.065

Table 4.8 cont. Results of the ANOVA and Games-Howell Test. Table displays the between-groups variability of linear measurements of the track and stature. Both df1 (between-groups) and df2 (within-groups) are reported. Levels of significance are reported within a 95% confidence level. * indicates statistically significant variability between-groups.

	One-way ANOVA				Games-Howell Test			
Measurement (mm)	df1	df2	f	P	<i>Between-groups variability</i>		Std. error (mm)	P
Heel breadth	4	220	3.82	0.005	Laetoli	Ileret	5.32	0.990
						Happisburgh	7.11	0.969
						Formby Point	2.93	0.715
						Walvis Bay	2.69	0.728
					Ileret	Happisburgh	8.15	0.915
						Formby Point	4.95	0.728
						Walvis Bay	4.81	1.000
					Happisburgh	Formby Point	6.83	1.000
						Walvis Bay	6.73	0.780
					Formby Point	Walvis Bay	1.85	0.002

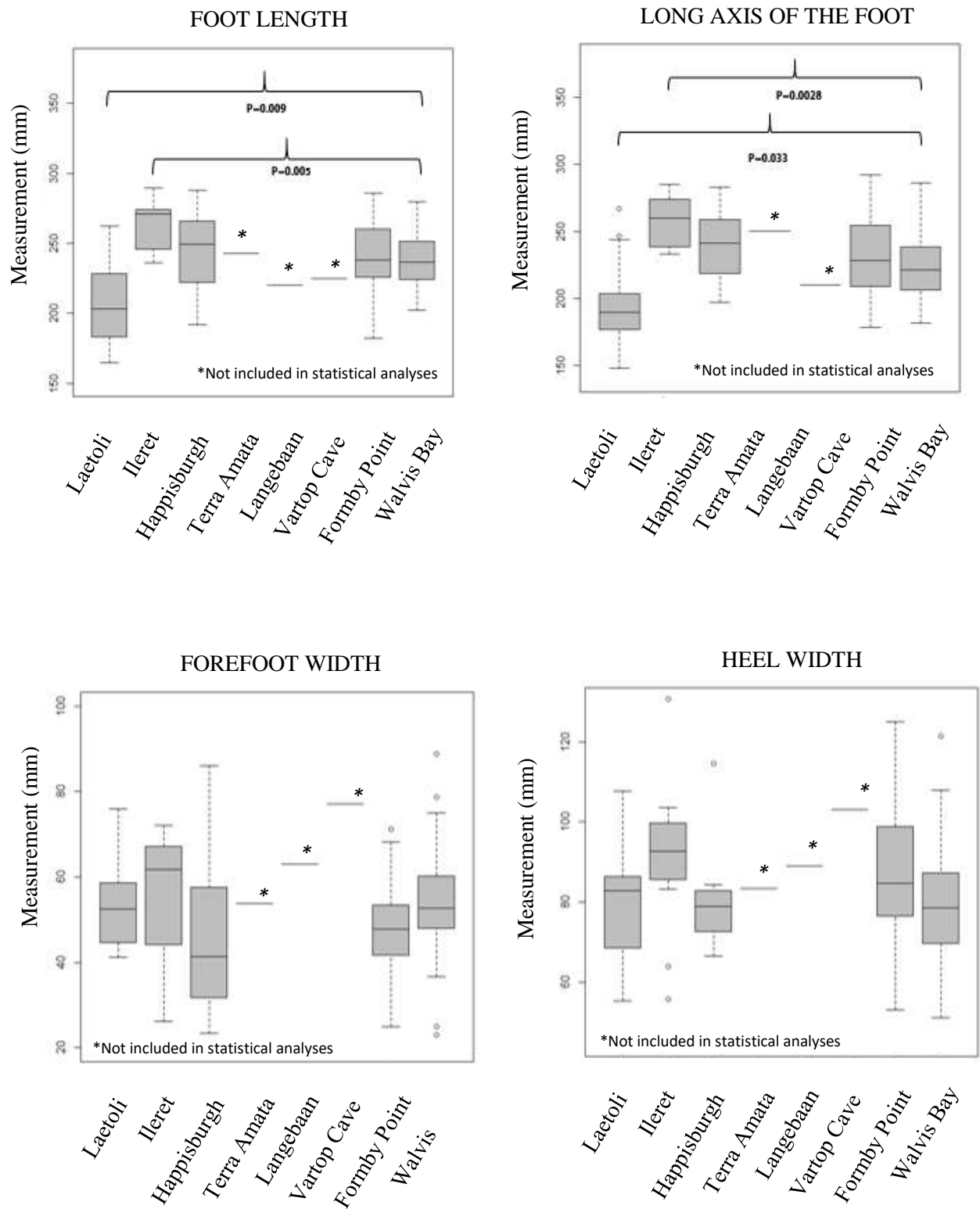


Figure 4.11. Variability between various fossil localities in adult track linear measurements (mm). Infant and juvenile tracks are excluded from graphical representations of changing foot proportions. P-values from the one-way ANOVA are displayed only for statistically significant measurements between sample-sets. * represents fossil tracks which were not included in statistical analyses.

Table 4.8. Results of the ANOVA and Games-Howell Test for hallux abduction. Table displays the between-groups variability of hallux abduction angles. Both df1 (between-groups) and df2 (within-groups) are reported. Levels of significance are reported within a 95% confidence level. Significant P values are in bold.

One-way ANOVA				Games-Howell Test			
df1	df2	f	P	<i>between-groups variability</i>		Std. error (°)	P
4	189	275.563	<0.001	Laetoli	Ileret	1.44	0.035
					Happisburgh	1.31	<0.001
					Formby Point	1.17	<0.001
					Walvis Bay	1.15	<0.001
				Ileret	Happisburgh	1.09	0.023
					Formby Point	0.93	<0.001
					Walvis Bay	0.90	<0.001
				Happisburgh	Formby Point	0.69	<0.001
					Walvis Bay	0.66	<0.001
				Formby Point	Walvis Bay	0.31	<0.001

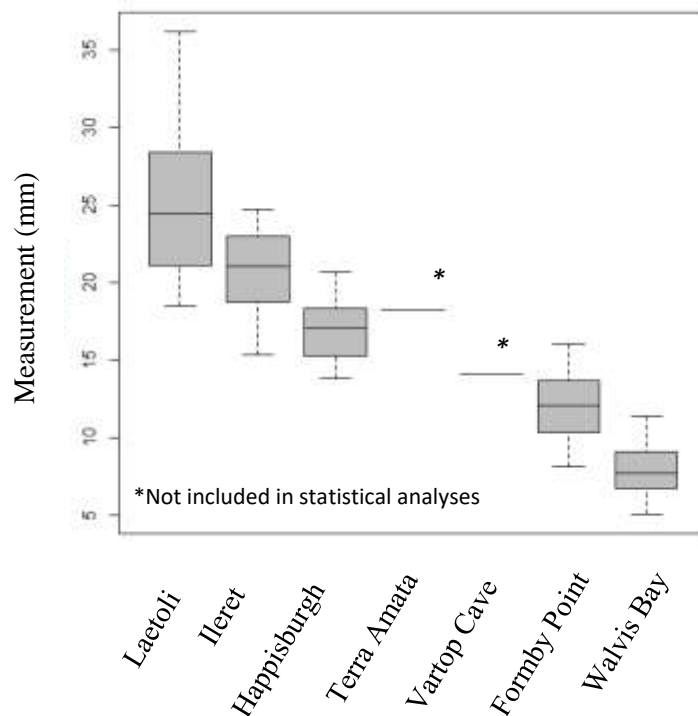


Figure 4.12. Boxplot of the angle of hallux abduction (°) from the earliest track discovery through to the late Holocene. Hallux abduction angle between all groups was found to be significantly variable, with a clear linear trend for a reduction in the degree of angle abduction, from the Pliocene through to the Holocene (Table 4.8).

Foot proportions

To explore comparative foot proportions between each set of tracks, digit lengths were calculated for each track and then the ratio of distal track to total track length was calculated to examine load arm lengths (e.g., to establish functional morphology of the track for an effective toe-off). Results indicate a 30.15% mean reduction in relative length of the hallux between the Laetoli and Ileret hominins (Table 4.9). There was a 4.42% reduction in hallux length established between the Ileret and Happisburgh individuals. Hallux length changed by ~-0.51 to ~2.62% between the Happisburgh individuals and AMHs. The latter is likely caused by substrate variability (see: Chapter Three), rather than a percentage increase or decrease in length.

Table 4.9. Changing proportions of the hallux compared to total track length. Only adult specimens were included in this analysis. Mean values per group are reported here.

Mean % change in hallux length to total track length				
	Laetoli	Ileret	Happisburgh	Formby Point
Ileret	-30.15			
Happisburgh	-24.39	4.42		
Formby Point	-21.13	6.93	2.62	
Walvis bay	-30.23	-0.07	-4.69	-7.51

Synchronous with a reduction in the length of the distal foot, it was determined that the ratio of toe lengths (hallux and second digit) to total track length decreased from the Pliocene to the early Pleistocene (Table 4.10; Figure 4.13). The hallux to total track length ratio was found to reduce as much as 30.15% between the Laetoli and early Pleistocene hominins, and the second digit to total track length ratio was found to reduce as much as 26.24%. The ratio of toe length to total track length experienced very little variability thereafter, with miniscule changes being the probable result of the interactions of the foot with the underlying substrate as determined in Chapter Three, rather than an effective change in lever mechanics. The mean percentage of digit length to track length is found to be within modern human ranges (Keith 1929) from the early Pleistocene, resulting in modern human-like foot proportions from the first appearance of trackways attributable to the genus *Homo*.

Table 4.10. Changing proportions of digit length compared to total track length. Only adult specimens were included in this analysis. Mean values per group are reported here.

Mean % change in 2 nd digit length to total foot length				
	Laetoli	Ileret	Happisburgh	Formby Point
Ileret	-26.24			
Happisburgh	-12.96	10.52		
Formby Point	-26.79	-0.43	-12.24	
Walvis bay	-30.09	-3.05	-15.17	-2.60

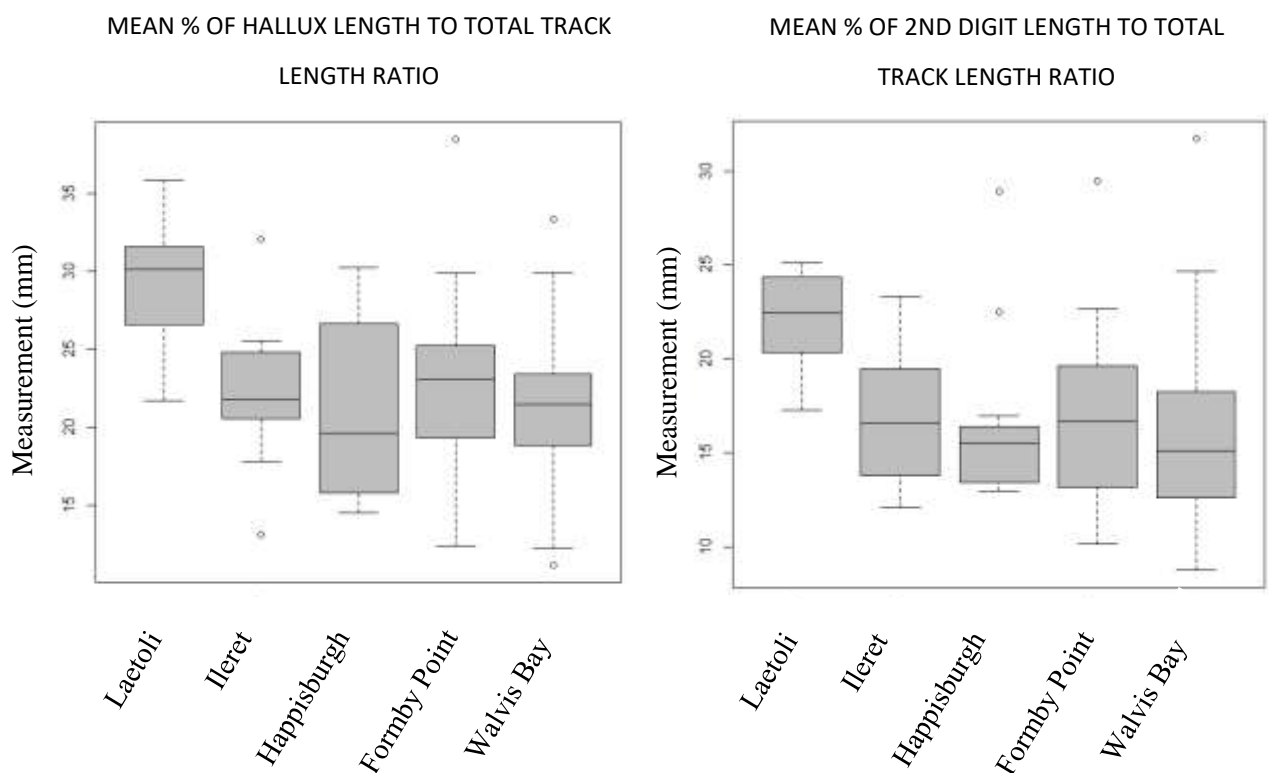


Figure 4.13. Boxplots illustrating the variability in foot proportions (distal track length to total track length) between fossil localities.

4.5.1 Discussion

The first objective of this study was to determine if GM methods could be used to characterise shape patterns of a track. It was determined that track shapes within an individual were consistent when speed was increased from a walk to a fast walk, and when the underlying substrate was changed. Although there was so much overlap in

Procrustes scores which hindered the identification of individual track-makers in the preliminary assessments, the known morphological disparity in the foot between different hominin species (Aiello and Dean 2002; Ward et al. 2002; Lovejoy et al. 2009; Harcourt-Smith et al. 2015; Trinkaus and Patel 2016; Fernandez et al. 2016; Fernandez et al. 2018) implies that variation in track shape between species will surpass that of intra-track variability amongst a population/species. Because track shapes remained so consistent within an individual (e.g., outline shapes were not sensitive to changes in substrate pliancy), it was determined that GM methods could be used to successfully capture the outline shape of a selection of fossil tracks.

The second objective of this chapter was to determine if 2D landmark configurations could be used to capture the outline shape of a track. Both 2D and 3D landmark configurations produced comparable results in a large selection of experimental tracks which were created in different substrates and from several types of movement. Because both 2D and 3D landmark configurations were identified to be replicable and the subsequent results were comparable, it was determined that the ‘third dimension’ could be successfully removed as a factor when comparing the outline shape of a track between different groups (i.e., 2D landmark configurations could be used to capture the shape of a track). It was of particular importance to remove the third dimension from shape-space assessments for the inclusion of the Happisburgh tracks within a comparative sample due to unreliable depth dimensionality in the 3D models. 2D landmark configurations were used to synthesise the outline shape of fossil tracks from the Pliocene, Pleistocene and Holocene. GM methods were thus reliably used to synthesise the outline shape of fossil tracks, concurrent with the work of Berge et al. (2006) and Bennett et al. (2009).

Shape affinities and disparities were identified between each set of fossilised tracks, which are discussed in detail below. Importantly, this was the first study to assess the shape of the Happisburgh tracks.

Disparities and affinities in hominin track shapes

It was predicted that track shapes would be different between species. Differences in track shapes were identified between the geologically oldest tracks (Laetoli) with Pleistocene tracks ascribed to *Homo* species, indicating that there may be differences in form and function between genera. Although morphological disparity was established between australopithecines and *Homo* species, no shape differences as reflected in track outline

shapes were identifiable between *Homo* groups. Given the wide range of anatomy in the *Homo* foot (Aiello and Dean 2002; De Silva et al. 2018), it is quite surprising to find such similarity between the *Homo* prints as determined via the application of 2D GM methods. As this study only assessed outline morphology, perhaps the internal structures of a print will instead reflect these anatomical disparities that are otherwise lacking in track outlines. Therefore, this study also calculated foot proportions from tracks by taking simple linear measurements. A combined shape-space and linear measurement approach permitted the assessment of both outline shapes and internal proportions to be cumulatively analysed, thus providing a more rounded view of changing track shapes from the Pliocene to the Holocene. The potential relationship between form and function is discussed below.

Trends in foot functional morphology inferred from comparative analyses

It was predicted that these analyses would infer that the midfoot impression became more prominent from the Pliocene to the Holocene. This morphological change would have occurred in conjunction with a more adducted hallux. With a more adducted first metatarsal, the early Pleistocene foot would have been better-suited to support the longitudinal arches of the foot (Elftman and Manter 1935), allowing for the mediolateral weight transfer that is characteristic of modern human foot function (Aiello and Dean 2002; Hatala et al. 2016a). This prediction was supported within the current sample. It was determined that the shapes of hominin tracks imply an increasingly prominent and more posteriorly positioned MLA from the Pliocene to the late Holocene.

However, it should be noted that the extent to which tracks reflect longitudinal arch morphology might be highly dependent on substrate properties (e.g., Meldrum 2004; Bennett et al. 2016a), and can also be deformable within an individual even if the underlying substrate is consistent (Bates et al. 2013a; Pataky et al. 2013; McClymont et al. 2016). Similarly, the midfoot impression (height and volume) was identified to be reliant on substrate pliancy in a large sample of modern shod humans (n=100), with softer substrates producing more prominently impressed midfoot regions (Chapter Three). Even though outline shape was identified to be consistent regardless of the underlying substrate in experimental tracks, the trend for changing midfoot shapes in fossil material should be cautiously interpreted due to the size of the fossil sample-set. Regardless, the fossil record is small, and researchers must work with the limited material available. As such, inferences may be made here that midfoot morphology does change from the Pliocene to

the Holocene, supported by the results presented here that show a clear linear trend, consistent with previous interpretations suggesting that morphology of the midfoot region differs between hominin genera (Meldrum 2007; Meldrum et al. 2011; Hatala et al. 2016a). These results based upon footprint impressions reflect changing hominin skeletal foot anatomy from the Pliocene to the Holocene (e.g., Aiello and Dean 2002; Ward et al. 2011; Harcourt-Smith et al. 2015; Pablos et al. 2015; Holowka et al. 2017; De Silva et al. 2018; Holowka and Liebermann 2018). Hominin foot anatomy and foot impressions are complimentary, suggesting that foot anatomy can be inferred from footprint shapes.

In conjunction with a more prominent MLA, it was predicted that the comparative shape analyses would reveal a trend of decreasing hallucal abduction from the Pliocene to the early Pleistocene. This prediction was fully supported. The results of the PCA (supported by shape deformation grids) indicated a pattern for increasing hallucal adduction from the Pliocene to the Holocene, which was also determined by measuring and comparing the angle of hallucal abduction within all fossil tracks. Although the Ileret and Happpisburgh tracks suggested greater angles of hallucal abduction than AMHs, they were still more adducted than the hallucal impressions of the Laetoli tracks. A vast range of hallucal abduction in the Laetoli population infers the potential ability to abduct the hallux, despite bipedal behaviour. This suggests the possibility of other locomotory or behavioural activities e.g., climbing ability (De Silva 2009).

Although the internal structures of a footprint were not synthesised by the landmark configurations, internal track proportions were statistically compared by calculating the ratio of the distal track relative to the proximal track. It was predicted that foot proportions would vary across hominin track sites, which may imply different patterns in foot function across the taxa responsible for these tracks. In the modern human foot, the distal foot constitutes ~18% of the total foot length, whereas in chimpanzees (a habitual quadruped) the distal foot accounts for ~35% of total foot length (Keith 1929; Aiello and Dean 2002). By having a smaller ratio of phalanx to foot length, humans increase the load arm of the foot relative to chimpanzees, thereby increasing the mechanical efficiency of plantarflexion during bipedality.

This prediction was fully supported by the current sample. Relative toe lengths were found to be within modern human ranges for all Pleistocene and Holocene tracks. These tracks also reflect a more adducted hallux and perhaps a more prominent MLA (the latter was reflected in the GM assessments). The Laetoli tracks, on the other hand, are characterised by relatively longer toe impressions, in addition to a more abducted hallucal

impression and perhaps a less prominent MLA (the latter was reflected in the GM assessments). These shape differences were also identified in the shape comparisons of the tracks. It was established that the Laetoli tracks were differentiated from the Pleistocene hominin tracks (although some overlap in shape scores were identified). The differences in landmarks associated with shape change along the first PC axis corresponded to an antero-posterior displacement of the midfoot impression and a change in the angle of the hallux relative to the long axis. Assuming that the prominence of the MLA and a change in hallucal abduction reflect functional capabilities (Harcourt-Smith and Aiello 2004; Sellers et al. 2005; Bates et al. 2013a; Holowka et al. 2017), together these results of comparative analyses (linear measurement tests and the GM methods) hint at possible functional differences between the feet of the Laetoli track-makers and *Homo* track-makers (Bennett et al. 2009; Hatala et al. 2016a).

The results from this study corroborate other methodologies (e.g., qualitative and 3D morphometry) employed for comparative assessments that have identified the Laetoli tracks as morphologically distinct from those of *Homo* species (Meldrum 2007; Meldrum et al. 2011; Hatala et al. 2016a). Despite the limitations of analysing tracks in two dimensions, the results here provide interesting conclusions that morphology remains relatively consistent between *Homo* species, and that there are slight differences between australopithecines and *Homo*. These conclusions compliment other studies that have identified this disparity, resulting in the adoption of two distinct ichnotaxa: *Praehominipes* and *Hominipes* (Meldrum et al. 2011; Lockley et al. 2016).

The morphological affinity of the Happisburgh tracks

It was predicted that the early Pleistocene hominin tracks from Happisburgh would share a morphological affinity with other Pleistocene hominin tracks. This study determined that track morphology within the genus *Homo* was broadly uniform over a wide temporal and geographical range which is consistent with previous comparative studies (Kim et al. 2008). Consistent with the geological ages and phylogenies of Pleistocene and Holocene groups (Strait et al. 2014), the Happisburgh tracks were found to share closer affinities with these groups than to the Pliocene tracks, despite some inter-group variability most likely related to differences in substrate conditions.

To this end, it is possible that this result in some way reflects that locomotor activity has probably remained relatively consistent within the genus *Homo* since the Pleistocene. However, inference on kinematic affinity/disparity between-groups should be cautious,

as extracting kinematic data from track morphology has previously been demonstrated to be problematic (D'Août et al. 2010; Bates et al. 2013b; Hatala et al. 2013; Pataky et al. 2013), despite broad shape patterns identified in Chapter Three. Further exploration into the complex relationships between foot motion and substrate mechanics is necessary before drawing comprehensive functional conclusions of fossil tracks. For now, it is only appropriate to make broad inferences between form and function.

The highly variable shapes observed in the AMH samples is probably the result of higher within-group variability in age, sex, body mass and/or stature (the minimum number of individuals is much higher within these samples than in other the Pliocene or Pleistocene groups, which will be weighting statistical results (Cohen 1988)), or slight differences in substrate. For example, within a single track from Walvis Bay there exists significant variability in morphology owing to the track spanning four different substrate typologies (Morse et al. 2013). The deeper track types typically belong to wetter, softer and less-conformable substrates. To avoid the issue of track morphology becoming heavily influenced by depth, tracks made in these substrate types were omitted from this study, owing to the fact that shape is known to be influenced by depth (Bates et al. 2013b). It is acknowledged that choosing which tracks are “deep” is subjective and does not entirely remove the issue of substrate potentially affecting outline morphology, but the results in Section 4.3.1 demonstrate that outline shape is not significantly affected by the pliancy or moisture content of a substrate.

Limitations of substrate

Within this study, 274 tracks from nine different fossil localities, spanning the Pliocene to the Holocene were analysed. Consequently, the results presented should be interpreted with some caution; within the dataset, there exists variability in substrates, ranging from fluvial-lacustrine at Ileret to natrocarbonatite ash at Laetoli. Within these ranges of substrates, there exists a large variance in material properties, water content and heterogeneity of the materials. Variability in material properties translates into disparity of substrate deformation that occurs when a foot strikes the ground, affecting the morphology of the print that is left behind (Morse et al. 2013; Bennett and Morse 2014). However, most sites incorporated in this study – with the exception of the Laetoli trackways – were created in similarly soft substrates, based on qualitative between-site comparisons of trackway depths and topographies.

The limitations introduced by substrate inconsistencies are acknowledged, but the generally limited knowledge of exactly how substrate variability influences track shapes precludes the researcher from accommodating substrate differences in these analyses. This study deals solely with 2D outline shapes, effectively removing the third dimension of depth, which has been identified as the dimension most influenced by substrate properties (Morse et al. 2013; Bates et al. 2013b). By analysing only 2D track outlines, this study has attempted to minimise the effects of substrate between-group comparisons.

4.5.2 Concluding remarks

The dataset used within the current study includes hominin trackways that have been attributed to six distinct hominin species within two genera, spanning from the Pliocene to the Holocene. Even across such a broad sample of time and space, general aspects of track morphology are found to be remarkably consistent. However, between-sample differences were identified in three morphological aspects of the tracks. These differences are related to the prominence and position of the medial midfoot impression, the abduction angle of the hallux impression, and the length of the forefoot relative to the rest of the track. Generally, comparing sites across time from the Pliocene to the Holocene, the MLA is more prominent, the hallux is less adducted, and the forefoot is relatively shorter in more recent track samples.

Importantly, this is the first study to specifically examine the morphology of the Happisburgh tracks within such a broad comparative context. The Happisburgh tracks are found to be morphologically similar to other early Pleistocene and Holocene hominin tracks consistent with the geological age of the site, yet distinct from the Pliocene tracks from Laetoli.

Chapter Five

General discussion

Bipedalism is recognised as an adaptation that shaped human evolution (e.g., Darwin 1871), but the evolutionary patterns of emerging bipedalism remain contentiously debated. Numerous researchers have debated the locomotion of early hominins, but addressing this question based on skeletal anatomy has proved difficult due to the combinations of primitive and derived anatomical features of the early hominin skeleton (e.g., Aiello and Dean 2002). The discovery of fossil footprints attributed to early hominins, such as those at Laetoli, Tanzania dated to ~3.66 Ma (Leakey and Hay 1979), have offered an interesting insight into the debates regarding the emergence of bipedal behaviour, whilst also providing a direct representation of the interactions between form and function in the track-maker (Tuttle 1987). In lieu of skeletal material, fossil footprints are thus the most direct representation of locomotion available (Alexander 1976; Gatesy et al. 1999; Raichlen et al. 2008), whilst also representing a direct impression of the interaction between soft and hard tissues of the foot (Day and Wickens 1980; Crompton et al. 2012).

Hominin tracks have been previously used to reconstruct both the locomotory behaviour of hominins and to characterise track-maker biometrics (Bennett and Morse 2014). Despite functional interpretations of fossil trackways gained from a multitude of experimental research avenues (D'Août et al. 2010; Bennett et al. 2016a; Hatala et al. 2016a; Raichlen and Gordon 2017), the relationship between the conditions that lead to track creation (e.g., foot anatomies, biometrics and lower limb kinematics) with that of substrate deformity are only recently beginning to be understood (Gatesy and Falkingham 2017; Hatala et al. 2018).

In this project, the ability to identify the track-makers' biometrics and locomotory behaviour were explored by examining modern human movement across several types of substrates and speeds using a larger sample size than that of previous studies (e.g., Hatala et al. 2016a; Hatala et al. 2018). Additionally, the current project incorporated a wide range of variables to directly explore track form and function. Numerous morphological patterns were identified in the experimental prints, offering insights into the functional morphology of tracks that were then visually examined in a selection of fossil footprints.

However, it was only possible to extensively examine these shape patterns from 3D models after successfully determining the best method for digitally reconstructing the trackways. Fossil material is susceptible to erosion (Wiseman and De Groote 2018; Zimmer et al. 2018), but also to damage by the excavator, as was documented during fieldwork at Formby Point in 2016/2017. Numerous methods of photogrammetry were employed to circumvent delays in recording that can lead to erosion and further damage (Chapter Two). Despite attempts to utilise Unmanned Aerial Vehicle (UAV) technology to not only remove the excavator from the locality but to also rapidly record an area of interest, inaccurate reconstructions of track topography were produced. Although UAV technology produced unreliable reconstructions, UAVs remain a technological solution when sites may be at immediate risk of destruction. Although the produced models may not have precise depth dimensionality, it is better to have a record of these footprints without risking further damage to the fossil interface via the excavator or jeopardising their complete destruction. If circumstances permit longer data capture periods, then it is recognised that the best method for recording fossil tracks would be to use a handheld DSLR camera following a circular/oval path.

This method was used in Chapter Three to record a large selection of experimental trackways, permitting many of the research objectives to be addressed. However, this recording method was employed in an indoor environment where a number of factors could be controlled (e.g., lighting and time). This method will not always be possible for fossil localities. Often, time constraints can be a limiting factor, and even if this recording method is deployed (e.g., at Formby Point, UK), external factors cannot be controlled and photogrammetry can be rushed to record as much as possible before the sediments are destroyed (e.g., by an incoming tide in coastal locations).

This scenario was pertinent at Happisburgh, UK. The destruction of the Happisburgh tracks in 2013 (Ashton et al. 2014) highlighted the need for rapid recording to permit the digital preservation of fossil material (Bennett et al. 2013; Falkingham et al. 2018). The prints were recorded using a handheld DSLR camera, yet 3D models were later deemed to be of a low resolution, inhibiting a comprehensive morphological assessment of prints belonging to an Early Pleistocene hominin in north-western Europe.

Unfortunately, it is no longer possible to re-capture the Happisburgh prints, meaning that we must now work with the available data; e.g., 2D extracted images from 3D reconstructions. By examining the tracks in two-dimensions, the issue of unreliable depth is excluded, resulting in only the track outlines being examined. In Chapter Three it was

determined that track outline shapes are consistent within an individual regardless of the underlying substrate and/or speed. Consequently, in Chapter Four the outlines of fossil tracks were synthesised in shape-space assessments, permitting the morphological analysis of the Happisburgh prints for the first time within a comparative context with other fossil tracks.

5.1 Considerations for the functional interpretations of tracks

Perhaps the most interesting morphological feature identified in this study was the presence of a ridge-like shape produced on the softer sediment when walking. This feature was identified in the Ileret, Gombore II-2, Happisburgh and Le Rozel tracks, which were all made in easily deformable materials by *Homo* species (Bennett et al. 2009; Altamura et al. 2018; Duveau et al. in review). This ridge is representative of the ability to dorsiflex the forefoot and indicative of an effective toe-off in these Pleistocene hominins. Importantly, the presence of this ridge is reflective of the ability to navigate complex substrates, signifying that these hominins were capable of economical substrate navigation on a variety of sediments.

Other shape patterns were also identified using a modern human sample, such as the ability to slightly abduct the hallux to permit stability when traversing on looser sediments, and the deformity of the midfoot arches correlative with movement on different substrates and between different speeds. The latter was also identified in a recent study by Hatala et al. (2018). Evidently, track shapes are sensitive to a range of variables, supporting previous studies (e.g., D'Août et al. 2010; Morse et al. 2013; Hatala et al. 2018). This suggests that statistical comparisons of tracks are only possible if speed and substrate are considered and included as covariates, if possible. Statistical methods should be complimented by qualitative inspections, but it should be noted that these methods may be contradictory.

Professional trackers (animal and human) are able to correctly identify the track-maker's sex and if they were carrying items (such as a child) from a simple visual inspection of the print (Pastoors et al. 2016). It could be suggested that quantitative methods are not necessary due to the success of professional trackers. However, this study sought to explore ichnology from an evolutionary perspective. Both quantitative and qualitative methods are crucial within palaeoanthropology to characterise track-maker locomotory behaviour, but also biometrics. Because results can be contradictory, these methods should be combined to provide a rounded interpretation of the footprint. For example, this

project recognised that quantitative methods produced different results than that of qualitative methods for interpretations on the shape of the midfoot region from a collection of experimental tracks. Differences in speed and substrate pliancy both affected the shape of the midfoot arch impressions. The qualitative methods implied that the area changed in volume, with slight discrepancies in height. The quantitative methods indicated that arch height was significantly different between each substrate but remained consistent regardless of the speed or posture employed during trackway creation.

These findings have considerable implications for assessing fossil tracks, particularly with consideration of the results in Chapter Two. Here, it was demonstrated that experimental tracks were susceptible to significant degradation prior to fossilisation, thus affecting the topographical features of the prints. Landmark heights were reduced concurrent with weathering and exposure to natural elements. Post-exposure, fossilised tracks are vulnerable to erosion via a number of external factors. Considering that track shape/size can be changed both before and after fossilisation, interpretations based upon the topographical height of landmarks is questionable.

A prime example of this is the functional significance debate of the Laetoli footprints. Some researchers have argued that the Laetoli prints exhibit a less pronounced midfoot arch impression relative to modern humans (White and Suwa 1987; Bennett et al. 2009; Meldrum et al. 2011). This morphology has been used to deliberate the locomotory capabilities in the australopith foot (e.g., Stern and Susman 1983; Crompton et al. 2012). Yet, a loss in landmark height could impede upon track interpretations. Fortunately, the Laetoli footprints were uncovered during excavations (Leakey and Hay 1979), rather than exposed naturally like the Happisburgh prints (Ashton et al. 2014), thus minimising erosional processes prior to 3D data capture (Wiseman and De Groote 2018). However, the extent of degradation prior to the covering of these prints (the process that leads to fossilisation), will remain unknown. Changes in weather (e.g., rain or high wind speeds) could have reduced the height of the topographical structure of the Laetoli tracks before the fossilisation process began.

Consequently, it is questionable whether functional interpretations can be made from fossil footprints if the effects of degradation and/or erosion are unknown. Severe erosion occurred in the Happisburgh prints resulting in many of the prints being classified as ‘hollows’ due to the questionable ichnology. Despite this, it was still possible to extract the outline shape of many of the Happisburgh prints in Chapter Four which were excluded in the original publication (Ashton et al. 2014). These shapes, despite having undergone

significant erosion, were statistically comparable to other Pleistocene tracks, indicating that it is still possible to assess morphological patterns.

Therefore, there are two solutions to analysing the morphology of fossil tracks: (1) apply qualitative methods to prevent any losses in topographical heights hindering results; or (2) only quantify the outline form between tracks.

First solution: To circumvent the issue of degradation and/or erosion introducing error into comparative track assessments, a qualitative approach investigating functional morphology (e.g., of the midfoot) should be utilised rather than using depth/contour maps (e.g., Bennett et al. 2016a; Masao et al. 2016; Belvedere et al. 2018) or measuring the absolute height of the midfoot impression (Hatala et al. 2018).

For example, in Chapter Three mesh to mesh comparisons successfully characterised changes in the volume of the midfoot impression in the experimental trackways. A more voluminous midfoot impression that not only extends towards the lateral foot, but also antero-posteriorly will suggest a modern human-like anatomy if identified in fossil tracks. This anatomy can be accurately inferred from qualitative approaches that excludes the issue of a reduction in landmark heights, although only if consideration is given to changes in substrate pliancy and speed between samples.

Second solution: Otherwise, a 2D geometric morphometric approach can be employed to synthesise the outline shape of a track. This method quantifies shape affinities/disparities between tracks but circumvents the issue of depth hindering a comprehensive assessment. Chapter Four successfully employed 2D GM methods and identified shape patterns between different fossil localities, exclusive of the internal structures.

Alternatively, a combined approach: Statistical-based assessments of track shapes should be used in conjunction with morphological descriptions to provide a rounded interpretation of the relationship between form and function (Belvedere et al. 2018). This was accomplished in the current project: (1) Chapter Three provided a visual inspection and comparison of the internal structures of fossil tracks, offering an insight into the relationship between form and function; (2) the outline of a track was consistently impressed, signifying that track outlines will not inform on function, but rather just differences in anatomical/biometric shapes (e.g., increased hallual adduction); concluding in (3) Chapter Four which explored a statistical approach to comparing shapes between species.

The combined effort of these methods has presented an interesting insight into the form and function of track-makers, with a consideration of biometrics. One example is the erect postural positioning of the hip which was associated with a more voluminous midfoot impression. Another example was the identification of a ridge-like morphology that was associated with an effective toe-off. This morphology was visually recognised in tracks ascribed to *Homo* species in Chapter Three. In Chapter Four these tracks (although, not the Gombore II-2 or Le Rozel trackways) were quantified using GM methods and additionally by calculating the internal foot proportions. These combined results determined that foot proportions (associated with effective lever mechanics of the foot) are within modern human ranges from the first appearance of *Homo*, and that these foot proportions are disparate from tracks belonging to australopithecines.

The relationship between foot anatomy, lower limb kinematics and substrate deformation was extensively explored in this project using a range of substrates, speeds and limb postures, alongside a large population size. The combined results of this project will aid future interpretations of fossil tracks via the application of multiple methods of analysis.

5.2 From discovery to archive

As demonstrated, this project has addressed a timeline of events for the assessment of fossil tracks which spans from discovery to archive. In sum, after the exposure of fossil material, the prints must be recorded as quickly as possible before further damage can occur. After the high-resolution 3D reconstruction of fossil tracks, the tracks should be inspected for shape patterns which could inform on the biometrics and function of the lower limb that led to track creation.

By creating 3D models of the tracks, this provides the opportunity not only for the material to be digitally preserved, but for the data to become available through online repositories for future access by other research teams (Belvedere et al. 2018; Falkingham et al. 2018). Only by sharing data, can researchers gain a greater comprehension of the relationship between form and function in fossil tracks – as has been achieved in the current project by the accessibility to fossil tracks from nine different localities spanning from the Pliocene to the Holocene. Chapter Four would not have been possible without the free access to material, nor without my collaborators willingness to share fossil data. It is planned for 3D models of the Formby Point trackways collected during fieldwork for

this project to become digitally and freely available online in the future for other research teams to use.

Chapter Six

Conclusions

This project aimed to provide an insight into the relationship between track morphology with substrate mechanics, biometrics and lower limb movement via the characterisation of modern human movement across a range of different substrates. It was only possible to explore this relationship once sources of error (erosion) were identified, and after the successful identification of accurate methods of 3D modelling of trackways.

Track morphological patterns were identified in this project, which were correlated with particular types of lower limb movement, such as an effective toe-off on a looser substrate associated with a ridge-like pattern that extends mediolaterally across the track. These patterns were also identified in a selection of fossil tracks, implying a relationship exists between form and function. The patterns identified in this project compliment previous research by Hatala et al. (2018) whereby dynamic movement of the forefoot region (as an example) were correlated with the shapes of the midfoot impressions in a sample of experimental tracks.

6.1 Addressing research questions

As this project is multi-disciplinary, several research questions were addressed. A combination of analytical methods within controlled environments were adopted to address the overarching aims of this project: (1) the best practises for the successful reconstruction of 3D modelled trackways were identified, and (2) the relationship between track morphology with that of substrate mechanics, biometrics and lower limb movement was explored by combining 3D motion capture systems with qualitative assessments of track production.

To address the first aim, a combination of fossil trackways and experimental trackways were recorded every day to quantify the daily degradation/erosion of trackways via the application of 3D geometric morphometric techniques (Chapter Two). The results addressed the following research questions:

Does degradation affect footprint morphology prior to fossilisation?

And:

To what extent will erosional processes alter the shape and size of a footprint after exposure?

By combining experimental research with fieldwork, the extent by which degradation and erosion affects track morphology was statistically examined for the first time, building upon acknowledgements that tracks are highly susceptible to erosional processes (Demas and Agnew 2006; Dalton 2008; Marty et al. 2009; Bennett et al. 2009; Bennett et al. 2013). Shape and size were quantified to investigate changes both prior to fossilisation (experimental tracks) and after exposure (prehistoric tracks). Through this process, it was possible to identify the effects of erosion on track interpretation, particularly in softer sediments. Results indicated that weather action can result in significant morphological change to a track both prior to and after fossilisation. After fossilisation and exposure, a track will undergo considerable morphological change directly associated with weather and, in some cases (e.g., at Happisburgh, UK and Formby Point, UK), coastal activity. Consequently, there is the need for the rapid recording of fossil tracks which are located in highly erodible locations (Bennett et al. 2013; Zimmer et al. 2018).

Will predicted changes in shape and size as the direct consequence of either degradation and/or erosion alter biometric predictions of the track-maker?

Erosional processes significantly affected the shape and size of prehistoric and experimental tracks. Concurrent with these changes, it was questionable if biometric predictions were also affected. Biometric predictions (assessed using stature as an example) were significantly affected by minute changes in track dimensions. The error in biometric predictions increased daily, indicating that fossil tracks should be recorded as quickly as possible before further erosion may occur.

Currently, laser scanning and photogrammetry are the most commonly applied methods to record fossil trackways (Falkingham et al. 2018). Because these methods can be invasive (i.e., the excavator is often required to trample the sediment layer during data capture), non-destructive methods that can swiftly record an area of interest were explored

to circumvent issues in advertently destroying fossil material. The use of Unmanned Aerial Vehicles (UAV) formed the second research question of this project:

Can UAV technology be deployed to reconstruct fossil footprints via photogrammetry? And are the produced models of high enough resolution to allow reconstructions usable in ichnological studies?

A series of experiments using non-invasive and non-destructive methods tested the applicability of UAV technology to rapidly and accurately record tracks before further damage occurred, and to also digitally preserve the tracks before their destruction. Various flight paths, UAVs, camera types, and heights were incorporated in this study to identify the accuracy in minute depth reconstruction and subsequent 3D mesh creation (Chapter Two).

Results specified that currently UAV technology does not record fossil track data to the standards required by palaeoanthropologists. Rather, it is recommended to use a handheld DSLR camera following a circular/oval path. However, this may not always be appropriate. If tracks are at immediate risk of destruction (e.g., by the incoming tide) then a UAV can effectively record the area quickly. Although depth dimensionality will be unreliable, 2D images of the trackways will still be useful, as demonstrated in Chapter Four which assessed the use of 2D track outlines in a comparative context.

After successfully identifying the best practise for recording fossil footprints, it was possible to address the following research questions:

Are track dimensions of a single individual consistent when created in several types of substrates at different speeds and limb postures?

And:

Can track dimensions be used to accurately identify the track-maker's biometrics?

Experimental trackways were created in two different substrates (loose and firm) at several speeds (a walk, a fast walk and a jog) and limb postures (a flexed limb and an erect limb). Linear measurements of each averaged track were measured and statistically compared. Variations in track outline metrics were established. Several metrics resulted

in unreliable biometric predictions of the track-maker. This indicated that biometric information (mass, age and sex) cannot currently be reliably extracted from some tracks, particularly when the underlying substrate moisture content is increased and/or speed is altered (Chapter Three). However, stature was reliably predicted from track length after correction factors were applied to the tracks to correct for a change in linear measurements (e.g., tracks belonging to the same individual were generally longer when increasing a walking speed to a fast walk).

Although it was not always possible to identify the track-maker from track dimensions, it was questionable whether lower limb movement could instead be reconstructed from track shapes. This formed the next research question:

Are lower limb kinematics reflected in track shapes?

An experimental study that combined morphological assessments with that of 3D motion capture systems to record modern human movement across several substrates addressed the variability in track shapes and investigated if these shapes can be used to infer biometric and/or biomechanical information about the track-maker. Experimental trackways were created in substrates of differing compliance at varying speeds and limb postures.

Patterns of shape disparity were visually identified between experimental tracks, which were associated with changes in joint angle. Shape patterns included an effective toe-off producing a ridge-like form across the midfoot region, and a prominent midfoot-impression with an erect hip postural positioning. These shape variations were also identified in fossil material, permitting a potential insight into hominin locomotion as reflected in tracks.

Can limb posture be reconstructed from track shapes in a range of substrates?

A critical question in human evolution is whether early hominins (particularly australopithecines) walked with an erect limb or a flexed limb posture (Lovejoy 1979; Stern and Suman 1983; Susman et al. 1984). This project directly addressed this question by incorporating different limb postures into the biomechanical assessments. The volume of the midfoot impression and the angle of hallucal abduction were both identified to be associated with hip and knee flexion. Consequently, it was predicted that the Laetoli

track-maker may have walked with a more flexed limb than modern humans when moving across soft and deformable substrates, concurrent with the findings of Hatala et al. (2016a).

This study established that modern humans significantly alter limb kinematics to accommodate changes in substrate pliancy. It is appropriate to assume that early hominins would have adopted similar kinematic changes necessary for efficient substrate navigation. For future fossil trackway discoveries, it is recommended that the range of motion associated with the substrate typology of the proposed track-maker should be considered when assigning ichnotaxon (e.g., could this hominin have employed the necessary hip extension/plantarflexion to enable movement across a softer substrate?).

With shape patterns identified in Chapter Three, the final objective of this project was to characterise these patterns in a selection of fossil tracks. Unfortunately, due to poor resolution of 3D modelled tracks from Happisburgh, UK, it was not possible to explore shape patterns from 3D models. An alternative approach using 2D GM methods was proposed:

Can 2D geometric morphometrics be used to synthesise the functional morphology of tracks?

Using a selection of experimental trackways, 2D and 3D GM methods were computed and compared. Both methods produced similar results, indicating that 2D landmark configurations successfully captured the shape of a track.

Because internal print structures were associated with limb kinematics and were susceptible to substrate deformity, this study sought to exclude the internal shapes from comparative assessments, and to instead only synthesise the outline shape of fossil tracks (Chapter Four):

Can the outline shape (a representation of anatomy and biometrics) of fossil tracks be captured and statistically compared?

Track outlines were assessed in fossil tracks belonging to at least six different hominin species within two genera, dated to the Pliocene, Pleistocene and Holocene. The successful application of shape-space assessments permitted morphological affinities

between fossil tracks to be identified. Surprisingly, despite broad changes in the conditions (foot anatomy and substrates) that led to the production of these tracks, there was consistency in the track shapes between all *Homo* species. Consistency in shape was quite possibly related to the fact that quantitative methods only examined outline forms between tracks. The internal structure of the tracks may reflect both anatomical and kinematic differences between species but were not investigated here. These results addressed the final research question of this project:

Do the Happisburgh, UK tracks share any shape affinities with other Pliocene, Pleistocene and/or Holocene tracks?

The Happisburgh tracks were found to be morphologically similar to other early Pleistocene and Holocene hominin trackways consistent with the geological age of the site, yet distinct from the Pliocene tracks from Laetoli.

6.2 Overall conclusions

From this project as a whole, the main conclusion is that track morphologies are not consistent across a range of substrates when traversing at several speeds or limb postures. Even after a range of variables leading to track creation that will change the internal shape patterns (e.g., changes in speed during movement), the impressions are susceptible to degradation prior to fossilisation and then, additionally, erosional processes after exposure. Consequently, there are numerous considerations that must be made when examining fossil material. One such factor that can be controlled is 3D modelling.

This study identified several issues within 3D reconstructions of trackways, whereby camera angle, camera type, the height of the camera or even just the camera settings can all result in significant changes in model resolution, particularly in an outdoor environment where a number of variables cannot be controlled (e.g., lighting). The consequence is poor depth reconstruction, as was the case at Happisburgh, UK in 2013. However, this circumstance is rare and often 3D modelling is performed to a high standard (e.g., Masao et al. 2016).

Assuming that 3D models are accurately produced, a number of patterns in track morphologies can be identified, such as the ridge-like impression indicating an effective toe-off, and a prominent midfoot region suggesting an erect hip. If 3D models are

unreliable, then it is still possible to compare shapes with other fossil tracks by only quantifying the outline form – these can be extracted as a 2D image from a 3D model if orthogonal photographs are not available.

Although it was not possible to identify age, sex or mass for some tracks, it was possible to characterise the track-makers' locomotory behaviour by employing 3D motion capture systems. Form and function of tracks were successfully analysed, and a list of morphological features were identified within tracks that can be positively associated with lower limb movement. These include a ridge-like pattern that extends mediolaterally across the forefoot, the angle of hallucal adduction and the prominence of the midfoot impression. These patterns were visually identified in fossil tracks from Ileret, Engare Sero, Happisburgh and Le Rozel, signifying the importance of combining 3D kinematics with morphological studies.

Importantly, this was the first study to specifically examine the morphology of the Happisburgh tracks within such a broad comparative context. Although it was not possible to examine these prints from 3D models due to unreliable depth reconstructions, this study successfully recognised the consistency in track shapes between *Homo* species, and the disparity in track shapes between australopithecines and *Homo*.

6.3 Future directions

It is proposed that future studies exploring methods of track analysis be undertaken. These studies would benefit from including a wider range of UAVs, camera types, and different experimental set-ups to confirm the usefulness of UAV technology to record fossil tracks.

The results from Chapters Two and Three (variable footprint metrics were recognised) have considerable implications for a range of podiatry and forensic studies which rely upon the accuracy of biometric predictions to identify the track-maker (e.g., Reel et al. 2010; Davies et al. 2014; Krishan et al. 2015). Erosional processes were demonstrated to affect the size and shape of the prints, thus hindering biometric predictions. Likewise, changes in track dimensions were correlated with changes in speed and substrate pliancy. Future studies should incorporate a greater range of materials to advance forensic applications and to corroborate the validity of these methods when applied in forensic situations.

Although size and shape changes were identified which may hinder forensic applications, these morphological patterns in experimental track creation were associated with lower

limb movement and posture (Chapter Three). These changes are informative for palaeoanthropological studies. Further experiments should incorporate a wider range of sediment material, whilst also synthesising the movement of the foot, such as the flexibility of the metatarsophalangeal joint. A consideration of pelvic obliquity and trunk angle would complement the current findings by exploring the body's postural positioning during track creation in more detail. Future studies should also consider incorporating extant non-human primates to provide a comprehensive insight to limb movement and posture across a range of substrate (e.g., D'Août et al. 2014), ethics permitting.

After further biomechanical questions have been addressed, then the form and function of fossil tracks will be better understood. The comparative methods discussed in Chapter Four would be advanced by the incorporation of a larger sample spanning a wider temporal and geographical range. For example, tracks from Jeju Island, South Korea (Kim and Kim 2004), Willandra Lakes, Australia (Webb et al. 2006), Calvert Island, Canada (McLaren et al. 2018) and the contentious Miocene footprints from Crete (Gierlinksi et al. 2017) could all be incorporated into future studies to give a more rounded view of evolving track morphologies.

Finally, it is fully expected that further fossilised tracks will be discovered in the future. Recent excavations have uncovered Early Pleistocene tracks at Gombore 11-2, Ethiopia (Altamura et al. 2018), potential Late Pleistocene Neanderthal prints at Gibraltar, Iberian Peninsula (Muniz et al. 2019), and Late Pleistocene tracks at Le Rozel, France, which are yet unpublished. Excavations at Le Rozel have so far yielded ~800 Neanderthal tracks. These prints belong to a species which has so far not been statistically represented in any hominin track analysis, because complete trackways for this species did not exist until very recently. The inclusion of these new tracks in future comparative assessments will be an exciting avenue. As the sample size of hominin tracks continues to grow, further morphological analyses of fossil footprints will continue to offer a unique insight into the emergence of fully-upright bipedality during human evolution.

References

- Abledu, J. K., Abledu, G. K., Offei, E. B. & Antwi, E. M. (2015). Determination of sex from footprint dimensions in a Ghanaian population. *PLoS ONE*, *10*(10), e0138981.
- Achille, C., Adami, A., Chiarini, S., Cremonesi, S., Fassi, F., Fregonese, L. & Taffurelli, L. (2015). UAV-based photogrammetry and integrated technologies for architectural applications—methodological strategies for the after-quake survey of vertical structures in Mantua (Italy). *Sensors*, *15*, 15520-15539.
- Adams, D. C., Otárola-Castillo, E., & Paradis, E. (2013). geomorph: An r package for the collection and analysis of geometric morphometric shape data. *Methods in Ecology and Evolution*, *4*(4), 393-399.
- Adams, D. C., Rohlf, F. J. & Slice, D. (2013). A field comes of age: Geometric morphometrics in the 21st century. *Hystrix*, *21*, 7-14.
- Aiello, L. & Dean, C. (2002). An introduction to human evolutionary anatomy. *Elsevier Academic Press, The Netherlands*.
- Agisoft PhotoScan Professional v.1.3.4. Agisoft, St. Petersburg, Russia.
- Agnihotri, A. K., Purwar, B., Googoolye, K., Agnihotri, A. & Jeebun, N. (2007). Estimation of stature by foot length. *Journal of Forensic and Legal Medicine*, *14*(5), 279-283.
- Altamura, F., Bennett, M. R., D'Août, K., Gaudzinski-Windheuser, S., Melis, R. T., Reynolds, S. C., & Mussi, M. (2018). Archaeology and ichnology at Gombore II-2, Melka Kunture, Ethiopia: everyday life of a mixed-age hominin group 700,000 years ago. *Science Reports*, *8*(1), 2815.
- Ashton, N., Lewis, S. G., De Groote, I., Duffy, S. M., Bates, M., Bates, R., Hoare, P., Lewis, M., Parfitt, S. A., Peglar, S., Williams, C. & Stringer, C. (2014). Hominin footprints from early Pleistocene deposits at Happisburgh, UK. *PLoS One*, *9*(2), e88329.
- Atamturk, D. (2010). Estimation of sex from the dimensions of foot, footprint and shoe. *Journal of Biological and Clinical Anthropology*, *68*(1), 21-29.
- Avanzini, M., Mietto, P., Panarello, A., De Angelis, M., & Rolandi, G. (2008). The Devil's Trails: Middle Pleistocene Human Footprints Preserved in a Volcanoclastic Deposit of Southern Italy. *Ichnos*, *15*(3-4), 179-189.
- Avizo v.9.0.1 FEI, Oregon, USA.

- Bates, K. T. (2006). The application of Light Detection and Range (LIDAR) imaging to vertebrate ichnology and geoconservation. *M.Phil. Thesis, University of Manchester, Manchester, UK*.
- Bates, K. T., Avanzini, M., Belvedere, M., De Gasperi, M., Ferretti, P., Girardi, S., Remondino, F. & Tomasoni, R. (2008). Digital 3D modelling of dinosaur footprints by photogrammetry and laser scanning techniques: integrated approach at the Coste dell'Anglone tracksite (Lower Jurassic, Southern Alps, Northern Italy). *Geologica Acta*, 83, 303-315.
- Bates, K. T., Collins, D., Savage, R., McClymont, J., Webster, E., Pataky, T. C., D'Août, K., Sellers, W. I., Bennett, M. R. & Crompton, R. H. (2013a). The evolution of compliance in the human lateral mid-foot. *Proceedings of Biological Science*, 280(1769), 20131818.
- Bates, K. T., Savage, R., Pataky, T. C., Morse, S. A., Webster, E., Falkingham, P. L., Qian, R. Z., Bennett, M. R., McClymont, J. & Crompton, R. H. (2013b). Does footprint depth correlate with foot motion and pressure? *J R Soc Interface*, 10(83), 20130009.
- Behrensmeyer, A. K. and Laporte, L. F. (1981). Footprints of Pleistocene hominid in northern Kenya. *Nature*, 289, 167–169.
- Belvedere, M., Baucon, A., Furin, S., Mietto, P. & Muttoni, G. (2011). Sharing ichnological data: From the theoretical model to the development of ichnibase. *Journal of Vertebrate Paleontology*, 31, 69.
- Belvedere, M., Bennett, M. R., Marty, D., Budka, M., Reynolds, S. C., & Bakirov, R. (2018). Stat-tracks and mediotypes: powerful tools for modern ichnology based on 3D models. *PeerJ*, 6, e4247.
- Bemis, S. P., Micklethwaite, S., Turner, D., James, M. R., Akcis, S., Thiele, S. T. & Bangash, H. A. (2014). Ground-based and UAV-based photogrammetry: A multi-scale, high-resolution mapping tool for structural geology and palaeoseismology. *Journal of Structural Geology*, 69, 163-178.
- Bennett, M. R., Falkingham, P., Morse, S. A., Bates, K., & Crompton, R. H. (2013). Preserving the impossible: conservation of soft-sediment hominin footprint sites and strategies for three-dimensional digital data capture. *PLoS One*, 8(4), e60755.
- Bennett, M. R., Gonzalez, S., Huddart, D., Kirby, J., & Toole, E. (2010). Probable Neolithic footprints preserved in inter-tidal peat at Kenfig, South Wales (UK). *Proceedings of the Geologists' Association*, 121(1), 66-76.

- Bennett, M. R., Harris, J. W., Richmond, B. G., Braun, D. R., Mbua, E., Kiura, P., Olago, D., Kibunja, M., Omuombo, C., Behrensmeyer, A. K., Haddart, D. & Gonzalez, S. (2009). Early hominin foot morphology based on 1.5-million-year-old footprints from Ileret, Kenya. *Science*, 323(5918), 1197-1201.
- Bennett, M. R., & Morse, S. A. (2014). *Human Footprints: Fossilised Locomotion?* Springer, London.
- Bennett, M. R., Morse, S. A., Liutkus-Pierce, C., McClymont, J., Evans, M., Crompton, R. H., & Thackeray, F. J. (2014). Exceptional preservation of children's footprints from a Holocene footprint site in Namibia. *Journal of African Earth Sciences*, 97, 331-341.
- Bennett, M. R., Reynolds, S. C., Morse, S. A., & Budka, M. (2016a). Footprints and human evolution: Homeostasis in foot function? *Palaeogeography, Palaeoclimatology, Palaeoecology*, 461, 214-223.
- Bennett, M. R., Reynolds, S. C., Morse, S. A., & Budka, M. (2016b). Laetoli's lost tracks: 3D generated mean shape and missing footprints. *Science Reports*, 6, 21916.
- Berge, C., Penin, X., & Pellé, É. (2006). New interpretation of Laetoli footprints using an experimental approach and Procrustes analysis: Preliminary results. *Comptes Rendus Palevol*, 5(3-4), 561-569.
- Berger, L. R., Hawks, J., de Ruiter, D. J., Churchill, S. E., Schmid, P., Deleuzene, L. K., Kivell, T. L., Garvin, H. M., Williams, S. A., DeSilva, J. M., Skinner, M. M., Musiba, C. M., Cameron, N., Holliday, T. W., Harcourt-Smith, W., Ackermann, R. R., Bastir, M., Bogin, B., Bolter, D., Brophy, J., Cofran, Z. D., Congdon, K. A., Deane, A. S., Dembo, M., Drapeau, M., Elliott, M. C., Feuerriegel, E. M., Garcia-Martinez, D., Green, D. J., Gurtov, A., Irish, J. D., Kruger, A., Laird, M. F., Marchi, D., Meyer, M. R., Nalla, S., Negash, E. W., Orr, C. M., Radovicic, D., Schroeder, L., Scott, J. E., Throckmorton, Z., Tocheri, M. W., VanSickle, C., Walker, C. S., Wei, P. & Zipfel, B. (2015). *Homo naledi*, a new species of the genus *Homo* from the Dinaledi Chamber, South Africa. *eLIFE*, e09560.
- Bergstrom, K., Lawrence, A. B., Pelissero, A. J., Hammond, L. J., Maro, E., Bunn, H. T., & Musiba, C. M. (2019). High-resolution UAV map reveals erosional patterns and changing topography at Isimila, Tanzania. *AfricArXiv*, <https://doi.org/10.31730/osf.io/6myhn>.
- Bland, J. M. & Altman, D. G. (1986). Statistical methods for assessing agreement between two methods of clinical measurement. *Lancet*, i, 307-310.

- Bland, J. M. & Altman, D. G. (1995). Comparing methods of measurement: Why plotting difference against standard method is misleading. *The Lancet*, 346, 1085-1087.
- Bookstein, F. L. (1990). Introduction to methods for landmark data. In: Rohlf, F. J. & Bookstein, F. (eds.), *Proceedings of the Michigan Morphometrics Workshop, The University of Michigan Museum of Zoology, Special Publication 2*, 216-225.
- Bookstein, F. L. (1991) *Morphometric Tools for Landmark Data Geometric and Biology*. Cambridge University, Cambridge.
- Bramble, D. M. & Lieberman, D. E. (2004). Endurance running and the evolution of *Homo*. *Nature*, 432, 345-352.
- Breithaupt, B. H., Matthews, N. A. & Noble, T. A. (2004). An integrated approach to three-dimensional data collection at dinosaur tracksites in the Rocky Mountain West. *Ichnos*, 11, 11-26.
- Brown, F. H., Haileab, B. & McDougall, I. (2006). Sequence of tuffs between the KBS Tuff and the Chari Tuff in the Turkana Basin, Kenya and Ethiopia. *Journal of the Geological Society of London*, 163, 185-204.
- Brunet, M., Guy, F., Pilbeam, D., Mackaye, H. T., Likius, A., Ahounda, D., Beauvillian, A., Blondel, C., Bocherens, H., Boisserie, J., De Bonis, L., Coppens, Y., Dejax, J., Denys, C., Düringer, P., Eisenmann, V., Fanone, G., Fronty, P., Geraads, D., Lehmann, T., Lihoureau, F., Louchart, A., Mahamat, A., Merceron, G., Mouchelin, G., Otero, O., Campomanes, P. P., De Leon, M. P., Rage, J., Sapanet, M., Schuster, M., Sudre, M., Tassy, P., Valentin, X., Vignaud, P., Viriot, L., Zazzo, A. & Zollikofer, C. (2002). A new hominid from the Upper Miocene of Chad, Central Africa. *Nature* 418, 145–151.
- Budka, M., Bakirov, R., Deng, S., Falkingham, P., Reynolds, S. C. & Bennett, M. R. (2016). DigTrace Pro [Computer Software], Version 1.8.0. Bournemouth University.
- Bustos, D., Jakeway, J., Urban, T. M., Holliday, V. T., Fenerty, B., Raichlen, D. A., Budka, M., Reynolds, S. C., Allen, B. D., Lore, D. W., Santucci, V. L., Odess, D., Willey, P., McDonald, G. & Bennett, M. R. (2018). Footprints preserve terminal Pleistocene hunt? Human-sloth interactions in North America. *Science Advances*, 4(4), eaar7621.
- Campana, S. (2017). Drones in archaeology. State-of-the-art and future perspectives. *Archaeological Prospection*, 24(4), 275-296.
- Campbell, N. A. & Atchley, W. R. (1981). The geometry of canonical variate analysis. *Systematic Zoology*, 30(3), 268-280.

- Cappozzo, A., Della Croce, U., Leardini, A., & Chiari, L. (2005). Human movement analysis using stereophotogrammetry. Part 1: theoretical background. *Gait Posture*, 21(2), 186-196.
- Carbonell, E., de Castro B. J. M., Arsuaga, J. L., Allue, E. ... Bastir, M. (2005) An Early Pleistocene hominin mandible from Atapuerca-TD6, Spain. *Proceedings of the National Academy of Science*, 102, 5674–5678.
- Carbonell, E., Bermudez de Castro, J. M., Pares, J. M., Perez-Gonzalez, A., Cuenca-Bescos, G., Olle, A., Perez-Gonzalez, J., Rodriguez, X. P., Rosas, A., Rosell, J., Sala, R., Vallverdu, J. & Arsuaga, J. L. (2008). The first hominin of Europe. *Nature*, 452(7186), 465-469.
- Cardini, A. (2014). Missing the third dimension in geometric morphometrics: how to assess if 2D images really are a good proxy for 3D structures? *Hystrix, The Italian Journal of Mammology*, 25(2), 73-81.
- Carrier, D. R. (1984). The energetic paradox of human running and hominid evolution. *Current Anthropology*, 25(4), 483-495.
- Channon, A. J., Gunther, M. M., Crompton, R. H., D'Août, K., Preuschoft, H. & Vereecke, E. E. (2011). The effects of substrate compliance on the biomechanics of gibbon leaps. *Journal of Experimental Biology*, 214, 687-696.
- Catmull, E. (1974). A subdivision algorithm for computer display of curved surfaces. *PhD Thesis, University of Utah*.
- Charteris, J. (1981). Functional reconstruction of gait from Pliocene hominid footprints at Laetoli, northern Tanzania. *Nature*, 290, 496-498.
- Chiabrando, F., Nex, F., Piatti, D. & Rinaudo, F. (2011). UAV and RPV systems for photogrammetric surveys in archaeological areas: two tests in the Piedmont region (Italy). *Journal of Archaeological Science*, 38(3), 697-710.
- Cho, S. H., Park, J. M. & Kwon, O. Y. (2004). Gender differences in three dimensional gait analysis data from 98 healthy Korean adults. *Clinical biomechanics*, 19, 145–152.
- Cignoni, P., Callieri, M., Corsini, M., Dellepiane, M., Ganovelli, N. & Ranzuglia G. (2008). MeshLab: An Open-Source Mesh Processing Tool. *Sixth Eurographics Italian Chapter Conference*, 129-136.
- Clarke, R. J. (1979). Early homnininid footprints from Tanzania. *South African Journal of Science*, 75, 148-149.

- Clarke, R. J. & Tobias, P. V. (1995). Discovery of complete arm and hand of the 3.3 million-year-old *Australopithecus* skeleton from Sterkfontein. *South African Journal of Science*, 96, 477-480.
- Cliquet, D. (2016). Néandertal au Rozel. *Association historique de Surtainville*, 3, 1-61.
- CloudCompare v.2.10 OpenGL, 2018.
- Cohen, J. (1988). *Statistical Power Analysis for the Behavioural Sciences*. New Jersey: Erlbaum.
- Collyer, M. L., Sekora, D. J. & Adams, D. C. (2015). A method for analysis of phenotypic change for phenotypes described by high-dimensional data. *Heredity*, 115, 357–365.
- Cooke, S. B. & Terhune, C. E. (2014). Form, function and geometric morphometrics. *The Anatomical Record*, 298, 5-28.
- Cowell, R. W., Milles, A. & Roberts, G. (1993). Prehistoric footprints on Formby Point beach, Merseyside. In: Middleton, R. (eds.), *North West Wetlands Survey Annual Report*, 43-48.
- Crompton, R. H. (2017). Making the case for possible hominin footprints from the Late Miocene (c. 5.7 Ma) of Crete? *Proceedings of the Geologists' Association*, 128(5-6), 692-693.
- Crompton, R. H., Pataky, T. C., Savage, R., D'Août, K., Bennett, M. R., Day, M. H., Bates, K., Morse, S. & Sellers, W. I. (2012). Human-like external function of the foot, and fully upright gait, confirmed in the 3.66 million year old Laetoli hominin footprints by topographic statistics, experimental footprint-formation and computer simulation. *Journal of the Royal Society Interface*, 9(69), 707-719.
- Dalton, R. (2008). Fears for oldest human footprints. *Nature*, 451, 118.
- D'Août, K., Aerts, P., De Clercq, D., De Meester, K. & Van Elsacker, L. (2002). Segment and joint angles of the hind limb during bipedal and quadrupedal walking in the bonobo (*Pan paniscus*). *American Journal of Physical Anthropology*, 119, 37–51.
- D'Août, K., Aerts, P., & Berillon, G. (2014). Using primate models to study the evolution of human locomotion: concepts and cases. *Bmsap*, 26(3-4), 105-110.
- D'Août, K., Meert, L., Van Gheluwe, B., De Clercq, D., & Aerts, P. (2010). Experimentally generated footprints in sand: Analysis and consequences for the interpretation of fossil and forensic footprints. *American Journal of Physical Anthropology*, 141(4), 515-525.
- Darwin, C. R. (1871). *The Descent of Man and Selection in Relation to Sex*. J. Murray, London.

- Davenport, C. B. (1932). The growth of the human foot. *American Journal of Physical Anthropology*, 17(2), 167-211.
- Day, M. H., (1991). Bipedalism and fossilised footprints. *Origines de la Bipedie Chez les Hominides, Cahiers de Palaeoanthropologie, Editions du CNRS, Paris*, 199-213.
- Day, M. H. & Wickens, E. H. (1980). Laetoli Pliocene hominid footprints and bipedalism. *Nature*, 286, 385-387.
- Davies, C. M., Hackmann, L. & Black, S. M. (2014). The foot in forensic human identification - a review. *The Foot*, 24, 31-36.
- De Lumley, H. (1966) Les fouilles de Terra Amata à Nice. Premiers résultats. *Bulletin du Musée d'Anthropologie Préhistorique de Monaco*, 13, 29–51.
- de Onis. (2006). Assessment of differences in linear growth among populations in the WHO Multicentre Growth Reference Study. *Acta Paediatr.* 95, 56–65.
- De Silva, J. (2009). Revisiting the "midtarsal break". *American Journal of Physical Anthropology*, 141(2), 245-258.
- De Silva, J. & Lesnik, J. J. (2008). Brain size at birth throughout human evolution: a new method for estimating neonatal brain size in hominins. *Journal of Human Evolution*, 55, 1064-1074.
- De Silva, J. & Gill, S. V. (2013). Brief communications: a midtarsal (midfoot) break in the human foot. *American Journal of Physical Anthropology*, 151, 495-499.
- De Silva, J., McNutt, E., Benoit, J., & Zipfel, B. (2018). One small step: A review of Plio-Pleistocene hominin foot evolution. *American Journal of Physical Anthropology*.
- Dell'Unto, N., Landeschi, G., Apel, J. & Giulio, P. (2017). 4D recording at the trowel's edge: using three-dimensional simulation platforms to support field interpretation. *Journal of Archaeological Science: Reports*, 12, 632-645.
- Demas, M. & Agnew, N. (2006). Decision making for conservation of archaeological sites: the example of the Laetoli hominid trackway, Tanzania. *Of the Past, for the Future, Integrating Archaeology and Conservation Getty Conservation Institute Symposium Proceeding Publication of the 5th World Archaeological Congress*, 66-72.
- Dhaneria, V., Shrivastava, M., Mathur, R. K. & Goyat, S. (2016). Estimation of height from measurement of foot breadth and foot length in adult population of Rajasthan. *Indian Journal of Clinical Anatomy and Physiology*, 3(1), 78-82.
- Di Marco, R., Rossi, S., Castelli, E., Patane, F., Mazza, C. & Cappa, P. (2016). Effects of the calibration procedure on the metrological performances of

- stereophotogrammetric systems for human movement analysis. *Measurement*, 101, 265-271.
- Dingwall, H. L., Hatala, K. G., Wunderlich, R. E., & Richmond, B. G. (2013). Hominin stature, body mass, and walking speed estimates based on 1.5 million-year-old fossil footprints at Ileret, Kenya. *Journal of Human Evolution*, 64(6), 556-568.
- Domjanic, J., Fieder, M., Seidler, H. & Mitteroecker, P. (2013). Geometric morphometric footprint analysis of young women. *Journal of Foot and Ankle Research*, 6-27.
- Domjanic, J., Seidler, H., & Mitteroecker, P. (2015). A combined morphometric analysis of foot form and its association with sex, stature, and body mass. *American Journal of Physical Anthropology*, 157(4), 582-591.
- Dryden, I. L. & Mardia, K. V. (1998). *Statistical shape analysis*. Wiley, Chichester.
- Eisenbeiss, H. & Sauerbier, M. (2011). Investigation of UAV systems and flight modes for photogrammetric applications. *Photogrammetry Record*, 26, 400-421.
- Elftman, H. & Manter, J. (1935). Chimpanzee and human feet in bipedal walking. *American Journal of Physical Anthropology*, 20, 69-79.
- Evans, E. (2007). Kenfig peat shelf, Porthcawl, Bridgend: site visit. Glamorgan Gwent Archaeological Trust Report No. 2007/007, 1-10.
- Falkingham, P. L. (2012). Acquisition of high resolution 3D models using free, open-source, photogrammetric software. *Palaeontologia Electronica*, 15(1), 1-15.
- Falkingham, P. L. (2014). Interpreting ecology and behaviour from the vertebrate fossil track record. *Journal of Zoology*, 292(4), 222-228.
- Falkingham, P. L. (2016). Applying objective methods to subjective track outlines. In: Falkingham, P. L., Marty, D. & Richter, A. (eds.). *Dinosaur tracks: the next steps*. Indiana University Press.
- Falkingham, P. L., & Gatesy, S. M. (2014). The birth of a dinosaur footprint: subsurface 3D motion reconstruction and discrete element simulation reveal track ontogeny. *Proceedings of the National Academy of Science USA*, 111(51), 18279-18284.
- Falkingham, P. L., Hage, J., & Baker, M. (2014). Mitigating the Goldilocks effect: the effects of different substrate models on track formation potential. *Royal Society Open Science*, 1(3), 140225.
- Falkingham, P. L., Bates, K. T., Avanzini, M., Bennett, M., Bordy, E. M., Breithaupt, B. H., Castanera, D., Citton, P., Díaz-Martínez, I., Farlow, J. O., Fiorillo, A. R., Gatesy, S. M., Getty, P., Hatala, K. G., Hornung, J. J., Hyatt, J. A., Klein, H., Lallensack, J. N., Martin, A. J., Marty, D., Matthews, N. A., Meyer, C. A., Milàn, J., Minter, N. J., Razzolini, N. L., Romilio, A., Salisbury, S. W., Sciscio, L.,

- Tanaka, I., Wiseman, A. L. A., Xing, L. D. & Belvedere, M. (2018). A standard protocol for documenting modern and fossil ichnological data. *Palaeontology*, 61(4), 469-480.
- Farris, D. J., Kelly, L. A., Cresswell, A. G., & Lichtwark, G. A. (2019). The functional importance of human foot muscles for bipedal locomotion. *Proceedings of the National Academy of Science USA*.
- Feibel, C. S., Agnew, N., Latimer, B., Demas, B., Marshall, F., Waane, S. A. C & Schmid, P. (1995). The Laetoli hominid footprints - a preliminary report on the conservation and scientific restudy. *Evolutionary Anthropology*, 149-154.
- Felstead, N. J., Gonzalez, S., Huddart, D., Noble, S. R., Hoffmann, D. L., Metcalfe, S. E., Leng, M. J., Albert, B. M., Pike, A. W. G., Gonzalez-Gonzalez, A. & Jiménez-López, J. C. (2014). Holocene-aged human footprints from the Cuatrociénegas Basin, NE Mexico. *Journal of Archaeological Science*, 42, 250-259.
- Fernandez, P. J., Holowka, N. B., Demes, B. & Jungers, W. L. (2016). Form and function of the human and chimpanzee forefoot: implications for early hominin bipedalism. *Scientific Reports*, 6, 30532.
- Fernandez, P. J., Mongle, C. S., Leakey, L., Proctor, D. J., Orr, C. M., Patel, B. A., Almejica, S., Tocheri, M. W. & Jungers, W. L. (2018). Evolution and function of the hominin forefoot. *Proceedings of the National academy of Sciences of the United States of America*, 115(35), 8746-8751.
- Fernandez-Hernandez, J., Gonzalez-Aguilera, D., Rodriguez-Gonzalves, P. & Mancera-Taboada, J. (2015). Image-based modelling from unmanned aerial vehicle (UAV) photogrammetry: an effective, low-cost tool for archaeological applications. *Archaeometry*, 57(1), 128-145.
- Folz, E. (2000). La luminescence stimulée optiquement du quartz : développements méthodologiques et applications à la datation de séquences du Pléistocène supérieur du Nord-Ouest de la France. *Thèse de doctorat, Université de Paris 7*.
- Frelat, M. A., Shaw, C. N., Sukdeo, A., Hublin, J. J., Banazzi, S. Ryan, T. M. (2017). Evolution of the hominin knee and ankle. *Journal of Human Evolution*, 108, 147-160.
- Galik, K., Senut, B., Pickford, M., Gommery, D., Treil, J., Kuperavage, A. J. & Eckhardt, R. B. (2004). External and internal morphology of the BAR 1002'00 Orrorin tugenensis femur. *Science*, 305(5689), 1450-1453.

- Ganley, K. J. & Powers, C. M. (2005). Gait kinematics and kinetics of 7-year-old children: a comparison to adults using age-specific anthropometric data. *Gait Posture*, 21, 141-5.
- Gatesy, S. M. (2003). Direct and indirect track features: what sediment did a dinosaur touch? *Ichnos* 10, 91–98.
- Gatesy, S. M. & Falkingham, P. L. (2017). Neither bones nor feet: track morphological variation and "preservation quality". *Journal of Vertebrate Paleontology*, 37, e1314298.
- Gatesy, S. M., Middleton, K. M., Jenkins, F. A. & Shubin, N. H. (1999). Three-dimensional preservation of foot movements in Triassic theropod dinosaurs. *Nature*, 399, 141-144.
- Geng, X., Wang, C., Ma, X., Wang, X., Huang, J., Zhang C., Xu, J. & Yang, J. (2015). Mobility of the first metatarsal-cuneiform joint in patients with and without hallux valgus: in vivo three-dimensional analysis using computerized tomography scan. *Journal of Orthopaedic Surgery and Research*, 10, 140.
- Gierliński, G. D., Niedźwiedzki, G., Lockley, M. G., Athanassiou, A., Fassoulas, C., Dubicka, Z., Boczarowski, A., Bennett, M. R. & Ahlberg, P. E. (2017). Possible hominin footprints from the late Miocene (c. 5.7 Ma) of Crete? *Proceedings of the Geologists' Association*, 128, 697-710.
- GIM International (2014). Oblique airborne photogrammetry: properties, configurations and applications. Retrieved from: <https://www.gim-international.com/content/article/oblique-airborne-photogrammetry> [Accessed: 23/01/2019]
- Gonzalez, A., Huddart, D. & Roberts, G. (1997). Holocene development of the Sefton Coast: a multidisciplinary approach to understanding the archaeology. In: Sinclair, A., Slater, E. & Gowlett, J. (eds.), *Archaeological Science*, Oxbow Books, Oxford, 289-299.
- Gower, J. C. (1975). Generalized Procrustes Analysis. *Psychometrika*, 40, 33-50.
- Grabowski, M., Hatala, K. G., Jungers, W. L., & Richmond, B. G. (2015). Body mass estimates of hominin fossils and the evolution of human body size. *Journal of Human Evolution*, 85, 75-93.
- Grabowski, M. & Roseman, C. C. (2015). Complex and changing patterns of natural selection explain the evolution of the human hip. *Journal of Human Evolution*, 85, 94-110.

- Guerrieri, T. & Marsella, S. (2017). STORM project and the use of UAV to improve emergency management of disasters threatening cultural heritage. *"UAV & SAR: using drones in rescue operations"*, Rome, 29th March, 2017.
- Haile-Selassie, Y., Saylor, B. Z., Deino, A., Levin, N. E., Alene, M., & Latimer, B. M. (2012). A new hominin foot from Ethiopia shows multiple Pliocene bipedal adaptations. *Nature*, 483(7391), 565-569.
- Hammond, A. S. (2014). In vivo measurements of hip joint range of motion in suspensory and nonsuspensory anthropoids. *American Journal of Physical Anthropology*, 153(4), 417-434.
- Hatala, K. G., Demes, B., & Richmond, B. G. (2016a). Laetoli footprints reveal bipedal gait biomechanics different from those of modern humans and chimpanzees. *Proceedings of Biological Science*, 283, 1836.
- Hatala, K. G., Dingwall, H. L., Wunderlich, R. E., & Richmond, B. G. (2013). The relationship between plantar pressure and footprint shape. *Journal of Human Evolution*, 65(1), 21-28.
- Hatala, K. G., Roach, N. T., Ostrofsky, K. R., Wunderlich, R. E., Dingwall, H. L., Villmoare, B. A., Greem, D. J., Braun, D. R., Harris, J. W. K., Behrensmeyer, A. K. & Richmond, B. G. (2017). Hominin track assemblages from Okote Member deposits near Ileret, Kenya, and their implications for understanding fossil hominin paleobiology at 1.5 Ma. *Journal of Human Evolution*, 112, 93-104.
- Hatala, K. G., Roach, N. T., Ostrofsky, K. R., Wunderlich, R. E., Dingwall, H. L., Villmoare, B. A., Green, D. J., Harris, J. W. K., Braun, D. R. & Richmond, B. G. (2016c). Footprints reveal direct evidence of group behavior and locomotion in *Homo erectus*. *Science Reports*, 6, 28766.
- Hatala, K. G., Wunderlich, R. E., Dingwall, H. L., & Richmond, B. G. (2016b). Interpreting locomotor biomechanics from the morphology of human footprints. *Journal of Human Evolution*, 90, 38-48.
- Hatala, K. G., Perry, D. A. & Gatesy, S. M. (2018). A biplanar X-ray approach for studying the 3D dynamics of human track formation. *Journal of Human Evolution*, 121, 104-118.
- Harcourt-Smith, W. E. H. (2002). Form and function in the hominoid tarsal skeleton. *Ph.D Thesis, University College London, London, UK*.
- Harcourt-Smith, W. E. H. & Aiello, L. C. (2004). Fossils, feet and the evolution of human bipedal locomotion. *Journal of Anatomy*, 204(5), 403-416.

- Harcourt-Smith, W. E. H., Throckmorton, Z., Congdon, K. A., Zipfel, B., Deane, A. S., Drapeau, M. S. M., Churchill, S. E., Berger, L. R., DeSilva, J. M. (2015). The foot of *Homo naledi*. *Nature Communications*, 6, 8432.
- Helm, C. W., McCrea, R. T., Cawthra, H. C., Lockley, M. G., Cowling, R. M., Marean, C. W., Thesen, G. H. H., Pigeon, T. S. & Hattingh, S. (2018). A new Pleistocene hominin tracksite from Cape South Coast, South Africa. *Scientific Reports*, 8, 3772.
- Helm, C. W., Lockley, M. G., Cole, K., Noakes, T. D. & McCrea, R. T. (2019). Hominin tracks in southern Africa: A review and an approach to identification. *Palaeontologica Africana*, 53, 81-96.
- Holowka, N. B., & Lieberman, D. E. (2018). Rethinking the evolution of the human foot: insights from experimental research. *Journal of Experimental Biology*, 221(Pt 17).
- Holowka, N. B., O'Neill, M. C., Thompson, N. E., & Demes, B. (2017). Chimpanzee and human midfoot motion during bipedal walking and the evolution of the longitudinal arch of the foot. *Journal of Human Evolution*, 104, 23-31.
- Hrdlička, A. (1935). The Pueblos. With comparative data on the bulk of the tribes of the Southwest and northern Mexico, *American Journal of Physical Anthropology*, 20, 235–460.
- Huddart, D., Roberts, G., Gonzalez, S. (1999). Holocene human and animal footprints and their relationships with coastal environmental change, Formby Point, NW England, *Quaternary International* 55(1), 29-41.
- Hurd, W. J., Chmielewski, T. L., Axe, M. J., Davis, I. & Snyder-Mackler, L. (2004). Differences in normal and perturbed walking kinematics between male and female athletes. *Clinical Biomechanics*, 19(5), 465-472.
- Hurley, B. F. & Johnson, A. T. (2008). Factors affecting mechanical work in humans. In: Peterson, D. R., Bronzino, J. D. (eds.). *Biomechanics: Principles and applications*. Taylor and Francis Group, Florida.
- Ibeabuchi, M., Okubike, E. M., Olabiyi, O. A. & Nandi, M. E. (2018). Predictive equations and multiplication factors for stature estimation using foot dimensions of an adult Nigerian population. *Egyptian Journal of Forensic Sciences*, 8(63), 1-12.
- Jacobs, Z., Roberts, D. L. (2009) Last interglacial age for aeolian and marine deposits and the Nahoon fossil human footprints, southeast coast of South Africa. *Quaternary Geochronology* 4(2), 160–169.

- Jordan, K. & Newell, K. M. (2008). The structure of variability in human walking and running is speed-dependent. *Exercise and Sport Science Reviews*, 36(4), 200-204.
- Kanchan, T., Krishan, K., Geriani, D. & Khan, I. S. (2013). Estimation of stature from the width of static footprints - insight into an Indian model. *The Foot*, 23, 136-139.
- Kanchan, T., Krishan, K., Prusty, D. & Machado, M. (2014). Heel–Ball index: An analysis of footprint dimensions for determination of sex. *Egyptian Journal of Forensic Sciences*, 4, 29-33.
- Kanchan, T., Menezes R. G., Moudgil, R., Kaur, R., Kotian, M. S. & Garg, R. K. (2008). Stature estimation from foot dimensions. *Forensic Science International*, 179, 241.e1-241.e5.
- Keith, A. (1929). The history of the human foot and its bearing on orthopaedic practise. *The Journal of Bone and Joint Surgery*, 11, 10-32.
- Kendall, D. G. (1984). ‘Shape-manifolds, Procrustean metrics and complex projective spaces’, *Bulletin of the London Mathematical Society*, 16, 81–121.
- Ker, R. F., Bennett, M. B., Bibby, S. R., Kester, R. C., & Alexander, R. M. (1987). The spring in the arch of the human foot. *Nature*, 325(7000), 147-149.
- Kerrigan, D. C., Todd, M. K & Croce, U. D. (1998). Gender differences in joint biomechanics during walking: normative study in young adults. *American Journal of Physical Medicine & Rehabilitation*, 77(1), 2-7.
- Kim, J. L., Kim, K. S., Lockley, M. G. & Matthews, N. (2008). Hominid Ichnotaxonomy: An Exploration of a Neglected Discipline. *Ichnos*, 15(3-4), 126-139.
- Kim, J. L. & Kim, K. S. (2004). Hominid and other animals footprints from the Cenozoic Hamori Formation of Jeju Island. *Proceedings of the 2004 Spring Meeting of the Korean Earth Science Society*, 25–31.
- Kim, W., Kim, Y. M. & Yun, M. H. (2018). Estimation of stature from hand and foot dimensions in a Korean population. *Journal of Forensic and Legal Medicine*, 55, 87-92.
- Kinahan, J. (1996). Human and domestic animal tracks in an archaeological lagoon deposit on the coast of Namibia. *South African Archaeological Bulletin*, 51, 94–98.
- Klingenberg, C. P. & Monteiro, L. R. (2005). Distances and directions in multidimensional shape spaces: implications for morphometric applications. *Systematic Biology*, 54, 678-688.

- Kozma, E. E., Webb, N. M., Harcourt-Smith, W. H., Raichlen, D. A., D'Août, K., Brown, M. H., Finestone, E. M., Ross, S. R., Aerts, P. & Pontzer, H. (2018). Hip extensor mechanics and the evolution of walking and climbing capabilities in humans, apes, and fossil hominins. *Proceedings of the National Academy of Sciences of the United States of America*, 115(16), 4134-4139.
- Krishan, K. (2007). Individualizing characteristics of footprints in Gujjars of North India-forensic aspects. *Forensic Science International*, 169, 137-44.
- Krishan, K. (2008). Establishing correlation of footprints with body weight-forensic aspects. *Forensic Science International*, 179, 63-9.
- Krishan, K., Kanchan, T. & DiMaggio, J. A. (2015). Emergence of forensic podiatry - A novel sub-discipline of forensic sciences. *Forensic Science International*, 255, 16-27.
- Lague, D., Brodu, N. & Leroux, J. (2013). Accurate 3D comparison of complex topography with terrestrial laser scanner: application to the Rangitikei canyon (N-Z). *ISPRS Journal of Photogrammetry and Remote Sensing*, 82, 10-26.
- Lallensack, J. N., can Heteran, A. & Wings, O. (2016). Geometric morphometric analysis of intratrackway variability: a case study on theropod and ornithopod dinosaur trackways from Münchehagen (Lower Cretaceous, Germany). *PeerJ*, 4, e2059.
- Latimer, B. & Lovejoy, C. O. (1989). The calcaneus of *Australopithecus afarensis* and its implications for the evolution of bipedality. *American Journal Physical Anthropology*, 78, 369e386.
- Leakey, M. D. & Harris, J. M. (1987). Laetoli: A Pliocene site in Northern Tanzania. *Clarendon Press, Oxford*.
- Leakey, M. D. & Hay, R. L. (1979). 'Pliocene footprints in the Laetolil beds at Laetoli, northern Tanzania', *Nature*, 278, 317-323.
- Levine, D., Richards, J. & Whittle, M. W. (2002). *Whittle's gait analysis*. Elsevier Ltd., Fifth Edition.
- Lieber, R. L. & Burkholder, T. J. (2008). Musculoskeletal soft tissue mechanics. In: Peterson, D. R., Bronzino, J. D. (eds.). *Biomechanics: Principles and applications*. Taylor and Francis Group, Florida.
- Lieberman, D. E., Raichlen, D. A., Pontzer, H., Bramble, D. M. & Cutright-Smith, E. (2006). The human gluteus maximus and its role in running. *Journal of Experimental Biology*, 209, 2143-2155.

- Lieberman, D. E., Venkadesan, M., Werbel, W. A., Daoud, A. I., D'Andrea, S., Davis, I. S., Mang'Eni, O. R. & Pitsiladis, Y. (2010). Foot strike patterns and collision forces in habitually barefoot versus shod runners. *Nature*, 463(7280), 531-535.
- Lockley, M. & Hunt, A. P. (1995). *Dinosaur tracks and other fossil footprints of the western United States*. Comlumbia University Press, New York.
- Lockley, M., Roberts, G., & Kim, J. Y. (2008). In the footprints of our ancestors: An overview of the hominid track record. *Ichnos*, 15(3-4), 106-125.
- Lockley, M. G., Meldrum, D. J. & Kim, J. Y. (2016). Major events in hominin evolution. In: Mángano, L.A. Buatois (eds.), *The Trace-Fossil Record of Major Evolutionary Events in Geobiology*, 40, 411-448.
- Lovejoy, C. O. (1979). A reconstruction of the pelvis of A.L. 288-1 (Hadar Formation, Ethiopia). *American Journal of Physical Anthropology*, 50, 460.
- Lovejoy, C. O. (1988). Evolution of human walking. *Science America*, 259, 118–125.
- Lovejoy, C. O. (2005). The natural history of human gait and posture. *Gait Posture* 2, 95–112.
- Lovejoy, C. O., Latimer, B., Suwa, G., Asfaw, B., & White, T. D. (2009). Combining Prehension and Propulsion: The Foot of *Ardipithecus ramidus*. *Science*, 326(5949), 72e71-72e78.
- Lovejoy, C. O., Suwa, G., Spurlock, L., Asfaw, B., White, T. D. (2009b). The pelvis and femur of *Ardipithecus ramidus*: the emergence of upright walking. *Science*, 326, 71e1–6.
- Mallison, H. & Wings, O. (2014). Photogrammetry in paleontology - a pratical guide. *Journa of Paleontological Techniques*, 12, 1-31.
- Manning, P. L. (1999). Dinosaur track formation, preservation and interpretation: fossil and laboratory simulated dinosaur track studies. *Ph.D. dissertation, University of Sheffield, Sheffield, UK*.
- Mansouri, S.S., Karvelis, P., Georgoulas, G. & Nikolakopoulos, G. (2017). Remaining useful battery life prediction for UAVs based on machine learning, *IFAC-PapersOnLine* 50, 4727–4732.
- Marchi, D., Walker, C. D., Wei, P., Holliday, T. W., Churchill, S. E., Berger, L. R. & DeSilva, J. M. (2017). The thigh and leg of *Homo naledi*. *Journal of Human Evolution*, 104, 174-204.
- Mardia, K.V., Bookstein, K. V. & Moreton, I. J. (2000). Statistical assessment of bilateral symmetry of shapes. *Biometrika*. 87, 285-300.
- Martin R (1914) *Lehrbuch der Anthropologie* 2. Jena, Fischer.

- Marty, D., Strasser, A., & Meyer, C. A. (2009). Formation and Taphonomy of Human Footprints in Microbial Mats of Present-Day Tidal-flat Environments: Implications for the Study of Fossil Footprints. *Ichnos*, 16(1-2), 127-142.
- Masao, F. T., Ichumbaki, E. B., Cherin, M., Barili, A., Boschian, G., Iurino, D. A., Menconero, S., Moggi-Cecchi, J. & Manzi, G. (2016). New footprints from Laetoli (Tanzania) provide evidence for marked body size variation in early hominins. *Elife*, 5.
- Milan, J. (2006). Variations in the morphology of emu (*Dromaius novaehollandiae*) tracks reflecting differences in walking pattern and substrate consistency: ichnotaxonomic implications. *Palaeontology*, 49, 405-420.
- McDougall, I. & Brown, F. H. (2006). Precise $^{40}\text{Ar}/^{39}\text{Ar}$ geochronology for the upper Koobi Fora Formation, Turkana Basin, northern Kenya. *Journal of the Geological Society of London*, 163, 205-220.
- McHenry, H. M. & Jones, A. L. (2006). Hallucial convergence in early hominids. *Journal of Human Evolution*, 50(5), 534-539.
- McLaren, D., Fedje, D., Mackie, Q., Gauvreau, A. & Cohen, J. (2018). Terminal Pleistocene epoch human footprints from the Pacific coast of Canada. *PLoS ONE*, 13(3), e0193522.
- McClymont, J., Pataky, T. C., Crompton, R. H., Savage, R., & Bates, K. T. (2016). The nature of functional variability in plantar pressure during a range of controlled walking speeds. *Royal Society for Open Science*, 3(8), 160369.
- Meldrum, D. J. (2007). Renewed perspective on the Laetoli trackways: The earliest hominid footprints. *New Mexico Museum of Natural History and Science Bulletin*, 42, 233–239.
- Meldrum, D. J., Lockley, M. G., Lucas, S. G., & Musiba, C. (2011). Ichnotaxonomy of the Laetoli trackways: The earliest hominin footprints. *Journal of African Earth Sciences*, 60(1-2), 1-12.
- Meldrum, D. J. & Sarmiento, E. (2018). Comments on possible Miocene hominin footprints. *Proceedings of the Geologists' Association*, 129(4), 577-580.
- Mercier, N., Martin, L., Kreutzer, S., Moineau, V., & Cliquet, D. (2017). Dating the palaeolithic footprints of 'Le Rozel' (Normandy, France). *Quaternary Geochronology*, 49, 271-277.
- Mietto, P., Avanzini, M. & Rolandi, G. (2003). Human footprints in a Pleistocene volcanic ash. *Nature*, 422, 133.

- Milan, J. & Bromley, R. G. (2006). True tracks, undertracks and eroded tracks, experimental work with tetrapod tracks in laboratory and field. *Palaeogeography, Palaeoclimate, Palaeoecology*, 231(2), 253-264.
- Mitteroecker, P. & Bookstein, F. (2011). Linear discrimination, ordination, and the visualization of selection gradients in modern morphometrics. *Evolutionary Biology*, 38, 100-114.
- Moore, K. L., Agur, A. M. R. & Dalley, A. F. (2011). *Essential Clinical Anatomy*. Fifth Edition, Lippencott Williams & Wilkins, Philadelphia.
- Morse, S. A., Bennett, M. R., Gonzalez, S., & Huddart, D. (2010). Techniques for verifying human footprints: reappraisal of pre-Clovis footprints in Central Mexico. *Quaternary Science Reviews*, 29(19-20), 2571-2578.
- Morse, S. A., Bennett, M. R., Liutkus-Pierce, C., Thackeray, F., McClymont, J., Savage, R., & Crompton, R. H. (2013). Holocene footprints in Namibia: the influence of substrate on footprint variability. *American Journal of Physical Anthropology*, 151(2), 265-279.
- Mozas-Calvache, A. T., Perez-Garcia, J. L., Cardenal-Escarcena, F. J., Malta-Castro, E. & Delgado-Garcia, J. (2012). Method for photogrammetric surveying of archaeological sites with light aerial platforms. *Journal of Archaeological Science*, 39, (2), 521-530.
- Mullin, S. K. & Taylor, P. J. (2002). The effects of parallax on geometric morphometric data. *Computers in Biology and Medicine*, 32, 455-464.
- Muniz, F., Caceres, L. M., Rodriguez-Vidal, J., de Carvalho, C. N., Belo, J., Finlayson, C., Finlayson, S., Izquierdo, T., Abad, M., Jimenez-Espejo, F. J., Sugisaki, S., Gomez, P. & Ruiz, F. (2019). Following the last Neanderthals: mammal tracks in Late Pleistocene coastal dunes of Gibraltar (S Iberian Peninsula). *Quaternary Science Reviews. In Press, Corrected Proof, Available online 31 January 2019*.
- Nakamura, M. J. J. (2009). Hominid footprints in recent volcanic ash: new interpretations from Hawaii volcanoes National Park. *Ichnos*, 16, 118-123.
- Nex, F. & Remondino, F. (2013). UAV for 3D mapping applications: A review. *Applied Geomatics*, 6, 1-15.
- Nikolakopoulos, K., Soura, K., Koukouvelas, I. K. & Agyropoulos, N. G. (2017). UAV vs classical aerial photogrammetry for archaeological sites. *Journal of Archaeological Science: Reports*, 14, 758-773.
- Ogihara, N., Aoi, S., Sugimoto, Y., Tsuchiya, K. & Nakatsukasa, M. (2011). Forward dynamic similarity of bipedal walking in the Japanese macaque: investigation of

- causal relationships among limb kinematics, speed, and energetics of bipedal locomotion in a nonhuman primate. *American Journal of Physical Anthropology*, 145(4), 568-580.
- Oishi, M., Ogihara, N., Shimizu, D., Kikuchi, Y., Endo, H., Une, Y., Soeta, S., Amasaki, H. & Ichihara, N. (2018). Multivariate analysis of variations in intrinsic foot musculature among hominoids. *Journal of Anatomy*, 232(5), 812-832.
- Olsen, M. J., Johnstone, E., Kuester, F., Driscoll, N. & Ashford, A. A. (2011). New automated point-cloud alignment for ground-based light detection and ranging data of long coastal sections. *Journal of Surveying Engineering*, 137(1), 14-25.
- Onac, B. P., Viehmann, I., Lundberg, J., Lauritzen, S. E., Stringer, C. & Popitã, V. (2005). U-Th ages constraining the Neanderthal footprint at Vârtope Cave, Romania. *Quaternary Science Reviews*, 24, 1151–1157.
- Ouzounian, T.J. & Shereff, M. J. (1989). In vitro determination of midfoot motion. *Foot Ankle International*, 10, 140–6.
- O'Neill, M. C., Demes, B., Thompson, N. E. & Umberger, B. R. (2018). Three-dimensional kinematics and the origin of the hominin walking stride. *Journal of the Royal Society Interface*, 15(145), 20180205.
- Oxnard, C.E. & O'Higgins, P. (2009). 'Biology clearly needs morphometrics? Does morphometrics need biology?', *Biological Theory* 4(1), 84-97.
- Pablos, A., Lorenzo, C., Martinez, I., Bermudez de Castro, J. M., Martinon-Torres, M., Carbonell, E., & Arsuaga, J. L. (2012). New foot remains from the Gran Dolina-TD6 Early Pleistocene site (Sierra de Atapuerca, Burgos, Spain). *Journal of Human Evolution*, 63(4), 610-623.
- Pajares, G. (2015). Overview and current status of remote sensing applications based on unmanned aerial vehicles (UAVS). *Photogrammetric Engineering and Remote Sensing ASPRS*, 81 (4), 281-329.
- Panarello, A., Mazzardo, L. & Mietto, P. (2018). The devil's touch: A first dataset from what could be the oldest human handprint ever found (central-southern Italy). *Alpine and Mediterranean Quaternary*, 31, 37-47.
- Pastors, A., Lenssen-Erz, T., Breuckmann, B., Cique, T., Kxunta, U., Rieke-Zapp, D. & Thao, T. 2016. Experience based reading of Pleistocene human footprints in Pech-Merle. *Quaternary International*, 430, 155-162.
- Pataky, T. C. & Goulermas, J. Y. (2008). Pedobarographic statistical parametric mapping (pSPM): a pixel-level approach to foot pressure image analysis. *Journal of Biomechanics*, 41, 2136–2143.

- Pataky, T. C., Savage, R., Bates, K. T., Sellers, W. I., & Crompton, R. H. (2013). Short-term step-to-step correlation in plantar pressure distributions during treadmill walking, and implications for footprint trail analysis. *Gait Posture*, 38(4), 1054-1057.
- Pix4Dmapper v.4.327 Pix4D, Lausanne, Switzerland.
- Pontzer, H. (2015). Energy expenditure in humans and other primates: a new synthesis. *Annual Review of Anthropology*, 44, 169–187.
- Pontzer, H. (2017). Economy and Endurance in Human Evolution. *Current Biology*, 27(12), R613-R621.
- Pontzer, H., Raichlen, D. A., & Rodman, P. S. (2014). Bipedal and quadrupedal locomotion in chimpanzees. *Journal of Human Evolution*, 66, 64–82.
- Poulakakis, N., Lymberakis, P., Valakos, E., Zouros, E. & Mylonas, M. (2005). Phylogenetic relationships and biogeography of Balkan Podarcis species by Bayesian and Maximum Likelihood Analyses of Mitochondrial DNA Sequences. *Molecular Phylogenetics and Evolution*, 37, 845-857.
- Preusser, F., Degering, D., Fuchs, M., Hilgers, A., Kadereit, A., Klasen, N., Krbetschek, M.R., Richter, D., Spencer, J. Q. G. (2008). Luminescence dating: basics, methods and applications. *Quaternary Science Journal*, 57, 95–149.
- Profico, A., Piras, P., Buzi, C., Di Vincenzo, F., Lattarini, F., Melchionna, M., Veneziano, A., Raia, P. & Manzi, G. (2017). The evolution of cranial base and face in Cercopithecoidea and Hominoidea: Modularity and morphological integration. *American Journal of Primatology*, e227221.
- Qualysis, AB, Gothenburg, Sweden.
- Qualysis Motion Camera System, Oqus Cameras, Qualysis AB, Gothenburg, Sweden.
- R Core Team, (2017). R: A Language and Environment for Statistical Computing. *R Foundation for Statistical Computing, Vienna, Austria*. <https://r-project.org>.
- Raichlen, D. A., & Gordon, A. D. (2017). Interpretation of footprints from Site S confirms human-like bipedal biomechanics in Laetoli hominins. *Journal of Human Evolution*, 107, 134-138.
- Raichlen, D. A., Gordon, A. D., Harcourt-Smith, W. E., Foster, A. D., & Haas, W. R. (2010). Laetoli footprints preserve earliest direct evidence of human-like bipedal biomechanics. *PLoS One*, 5(3), e9769.
- Raichlen, D. A., Pontzer, H., & Shapiro, L. J. (2013). A new look at the Dynamic Similarity Hypothesis: the importance of swing phase. *Biology Open*, 2(10), 1032-1036.

- Raichlen, D. A., Pontzer, H., & Sockol, M. D. (2008). The Laetoli footprints and early hominin locomotor kinematics. *Journal of Human Evolution*, 54(1), 112-117.
- Razzolini, N. L., Vila, B., Castanera, D., Falkingham, P. L., Barco, J. L., Canudo, J. I., Manning, P. L. & Galobart, A. (2014). Intra-trackway morphological variations due to substrate consistency: the El Frontal dinosaur tracksite (Lower Cretaceous, Spain). *PLoS One*, 9(4), e93708.
- Reel, S., Rouse, S., Vernon, W. & Doherty, P. (2010). Reliability of two-dimensional footprint measurement approach. *Science & Justice*, 50(3), 113-118.
- Remondino, R., Rizzi, A., Girardi, S., Petti, F. M. & Avanzini, M. (2010). 3D ichnology - recovering digital 3D models of dinosaur footprints. *The Photogrammetry Record*, 25(131), 266-282.
- Richmond, B. G., Hatala, K. G., Behrensmeyer, A. K., Bobe, A., Braun, D.R., Dingwall, H. L., Green, D. J., Kiura, P., Villmoare, B. A., Wunderlich R. E. & Harris, J. W. K. (2013). Hominin size, stature, and behavior based on 1.5-million-year-old footprints from Ileret, Kenya. *PaleoAnthropology*, A32.
- Rinaudo, F., Chiabrando, R., Lingua, A. & Spano, A. (2012). Archaeological site monitoring: UAV photogrammetry can be an answer. *International Archives of the Photogrammetry, Remote Sensing and Spatial Information Sciences, Volume XXXIX-B5, XXII ISPRS Congress, 25 August – 01 September 2012, Melbourne, Australia*.
- Roach, N. T., Hatala, K. G., Ostrofsky, F. R., Villmoare, B., Reeves, J. S., R., Braun, Harris, J. W. K., Behrensmeyer, & Richmond, B. G. (2016). Pleistocene footprints show intensive use of lake margin habitats by *Homo erectus* groups. *Science Reports*, 6, 26374.
- Robinson, J. T. (1972). Early Hominid Posture and Locomotion. *University of Chicago Press, Chicago and London*
- Robbins, L. M. (1985). Footprints: collection, analysis, and interpretation. *CC Thomas, Springfield*.
- Roberts, D. L. (2008). Last Interglacial Hominid and Associated Vertebrate Fossil Trackways in Coastal Eolianites, South Africa. *Ichnos*, 15(3-4), 190-207.
- Roberts, D. L. & Berger, L. R. (1997). Later interglacial (c. 117 kyr) human footprints from South Africa. *South African Journal of Science* 93, 349-350.
- Roberts, G. (2009). Ephemeral, Subfossil Mammalian, Avian and Hominid Footprints within Flandrian Sediment Exposures at Formby Point, Sefton Coast, North West England. *Ichnos*, 16(1-2), 33-48.

- Roberts, G., Gonzalez, S., Huddart, D., (1996). 'Intertidal Holocene footprints and their archaeological significance', *Antiquity* 70(269), 647-651.
- Robinson, M. A. & Vanrenterghem, J. (2012). An evaluation of anatomical and functional knee axis definition in the context of side-cutting. *Journal of Biomechanics*, 45(11), 1941-1946.
- Rohlf, F. J. (2003). Bias and error in estimates of mean shape in geometric morphometrics. *Journal of Human Evolution*, 44, 665-683.
- Rohlf, F. J. & Slice, D. E., (1990). 'Extensions of the Procrustes method for the optimal superimposition of landmarks', *Systematic Zoology*, 39, 40–59.
- Rolian, C., Lieberman, D. E., Hamill, J., Scott, J. W. & Werbel, W. (2009). Walking, running and the evolution of short toes in humans. *Journal of Experimental Biology*, 212, 713-721.
- Rolian, C., Lieberman, D. E. & Zermeno, J. P. (2011). Hand biomechanics during simulated stone tool use. *Journal Human Evolution*, 61, 26-41.
- Schlager, S. (2017). morpho and Rvcg - shape analysis in R. In: Zheng, G., Li, S. & Szekely, G. (eds.). *Statistical Shape and Deformation Analysis*. Academic Press, London.
- Schmid, P. (2004). 'Functional interpretation of Laetoli footprints' in Meldrum, D. J. and Hilton (ed), *From Biped and Strider: The Emergence of Modern Human Walking, Running and Resource Transport*. Springer US, New York.
- Schultz, A. H. (1930). The skeleton of the trunk and limbs of higher primates. *Human Biology*, 2, 303–43.
- Scuvée F. & Vérague J. (1984). *Paléolithique supérieur en Normandie occidentale: l'abri-sous-roche de la pointe du Rozel (Manche)*. LITTUS-C.E.H.P, Cherbourg.
- Sellers, W. I., Cain, G. M., Wang, W. & Crompton, R. H. (2005). Stride lengths, speed and energy costs in walking of *Australopithecus afarensis*: using evolutionary robotics to predict locomotion of early human ancestors. *Journal of the Royal Society Interface*, 2(5), 431-441.
- Slice, D., E. (ed.) (2005). *Modern Morphometrics in Physical Anthropology*. Kluwer Academic/Plenum, New York.
- Smith, N. G., Passone, L., al-Farhan, S. M. & Levy, T. E. (2014). Drones in Archaeology: Integrated Data Capture, Processing, and Dissemination in the al-Ula Valley, Saudi Arabia. *Near Eastern Archaeology*, 77(3), 176-181.

- Sockol, M. D., Raichlen, D. A. & Pontzer, H. (2007). Chimpanzee locomotor energetics and the origin of human bipedalism. *Proceedings of the National Academy of Sciences of the United States of America*, 104(30), 12265-12269.
- Stavlas, P., Grivas, T. B., Michas, C., Vasiliadis, E., & Polyzois, V. (2005). The evolution of foot morphology in children between 6 and 17 years of age: a cross-sectional study based on footprints in a Mediterranean population. *Journal of Foot & Ankle Surgery*, 44(6), 424-428.
- Stern, J. T. & Susman, R. L. (1983). The locomotor anatomy of *Australopithecus afarensis*. *American Journal of Physical Anthropology* 60(3), 279–317.
- Stern, J. T. & Susman, R. L. (1991). “Total morphological pattern” versus the “magic trait”: conflicting approaches to the study of early hominid bipedalism. In: Coppens, Y., Senut, B. (eds.), *Origine(s) de la bipédie chez les hominides. Cah. Paleoanthropol. 99e112 (CNRS, Paris)*.
- Strait, D., Grine, F. E. & Fleagle, J. G. (2015). Analysing hominin phylogeny: cladistic approach. In: Henke, W. & Tattersall, I. (eds.). *Handbook of Paleoanthropology, Springer-Verlag, Berlin Heidelberg*.
- Stoetzel, E., Koehler, H., Cliquet, D., Seveque, N. & Auguste, P. (2016). New data on Late Pleistocene small vertebrates from northern France, *Comptes Rendus Palevol*, 15(6), 681-695.
- Susman, R. L., Stern, J. T. & Jungers, W. L. (1984). Arboreality and bipedality in the Hadar hominins. *Folia Primatologica*, 43(2), 113-156.
- Takahashi, K. Z., Worster, K. & Bruening, D. A. (2017). Energy neutral: The human foot and ankle subsections combine to produce near zero net mechanical work during walking. *Science Reports*, 7, 15404.
- Tallman, M. (2013). Forelimb to hindlimb shape covariation in extant hominoids and Plio-Pleistocene hominins. *Anatomical Records*, 296, 290–304.
- Tamrat, E., Thouveny, N., Taieb, M. & Brugal, J. P. (2014). Magnetostratigraphic study of the Melka Kunture archaeological site (Ethiopia) and its chronological implications. *Quaternary International*, 343, 5–16.
- Tocheri, M. W., Solhan, C. R., Orr, C. M., Femiani, J., Frohlich, B., Groves, C. P., Harcourt-Smith, W. E., Richmond, B. G., Shoelson, B. & Jungers, W. L. (2011). Ecological divergence and medial cuneiform morphology in gorillas. *Journal of Human Evolution*, 60, 171–184.

- Trinkaus, E., & Patel, B. A. (2016). An Early Pleistocene human pedal phalanx from Swartkrans, SKX 16699, and the antiquity of the human lateral forefoot. *Comptes Rendus Palevol*, 15(8), 978-987.
- Turley, K., Guthrie, E. H. & Frost, S. R. (2011). Geometric morphometric analysis of tibial shape and presentation among catarrhine taxa. *Anatomical Records*, 294, 217–230.
- Tuttle, R. H. (1985). Ape footprints and Laetoli impressions: A response to the SUNY claims. In: Tobias, P. V. (eds.). *Hominid Evolution: Past, Present, and Future. Taung Diamond Jubilee International Symposium*. New York.
- Tuttle, R. H. (1987). ‘Kinesiological inferences and evolutionary implications from Laetoli bipedal trails G-1, G-2/3’, in Leakey, M., D. and Harris, J., (eds.), *Laetoli A Pliocene site in northern Tanzania*, 503–523. Clarendon Press, Oxford.
- Tuttle, R. H. (2008). Footprint Clues in Hominid Evolution and Forensics: Lessons and Limitations. *Ichnos*, 15(3-4), 158-165.
- Tuttle, R. H., Webb, D., Weidi, E. & Baksh, M. (1990). Further progress on the Laetoli trails. *Journal of Archaeological Science*, 17, 347–362.
- Tuttle, R. H., Webb, D. M. & Baksh, M. (1991). Laetoli toes and *Australopithecus afarensis*. *Human Evolution* 6(3), 193-200.
- van Hinsbergen, D. J. & Meulenkamp, J. E. (2006). Neogene supradetachment basin development on Crete (Greece) during exhumation of the South Aegean core complex, *Basin Research*, 18, 103-124.
- Van Vliet-Lanoë, B., Cliquet, D., Auguste, P., Folz, E., Keen, D., Schwenninger J., Merceir, N., Alix, P., Roupin, Y., Meurisse, M. & Seignac, H. (2006). L’abri sous-roche du Rozel (France, Manche): un habitat de la phase récente du Paléolithique moyen dans son contexte géomorphologique. *Quaternaire* 17(3), 207-258.
- Vanrenterghem, J., Gormley, D., Robinson, M. A. & Lees, A. (2010). Solutions for representing the whole-body centre of mass in side-cutting manoeuvres based on data that is typically available for lower limb kinematics. *Gait and Posture*, 31(4), 517-521.
- Vaughan, C. L. & Blaszczyk, M. B. (2008). ‘Dynamic similarity predicts gait parameters for *Homo floresiensis* and the *Laetoli* hominins’, *American Journal of Human Biology* 20(3), 312-316.
- Vereecke, E., D’Août, K., De Clercq, D., van Elsacker, L. Aerts, P. (2003). Dynamic plantar pressure distribution during terrestrial locomotion of bonobos (*Pan paniscus*). *American Journal of Physical Anthropology*, 120, 373–383.

Visual3D v.5.02.30, C-Motion Inc., Germantown, USA.

- Voloshina, A. S. & Ferris, D. P. (2015). Biomechanics and energetics of running on uneven terrain. *Journal of Experimental Biology*, 218, 711-719.
- Ward, C. V. (2002). Interpreting the posture and locomotion of *Australopithecus afarensis*: Where do we stand? *American Journal of Physical Anthropology*, 119, 185e215.
- Ward, C. V., Kimbel, W. H. & Johanson, D. C. (2011). Complete fourth metatarsal and arches in the foot of *Australopithecus afarensis*. *Science*, 331(6018), 750-753.
- Watson, P. J., Kennedy, M. C., Willey, P., Robbins, L. & Wilson, R. (2005) Prehistoric footprints in Jaguar Cave, Tennessee. *Journal of Field Archaeology*, 30, 25–43.
- Webb, S., Cupper, M. L., & Robins, R. (2006). Pleistocene human footprints from the Willandra Lakes, Southeastern Australia. *Journal of Human Evolution*, 50(4), 405-413.
- Webb, S. (2007). Further research of the Willandra Lakes fossil footprint site, southeastern Australia. *Journal of Human Evolution*, 52, 711-715.
- Westoby, M. J., Brasington, J., Glasser, N. F., Hambrey, M. J. & Reynolds, J. M. (2012). 'Structure-from-Motion' photogrammetry: a low-cost, effective tool for geoscience applications. *Geomorphology*, 179, 300–314.
- White, T. D. (1980). Evolutionary implications of Pliocene hominid footprints. *Science*, 208, 175-176.
- White, T. D. & Suwa, G. (1987). Hominid footprints at Laetoli: facts and interpretations. *American Journal of Physical Anthropology*, 72, 485-514.
- White, T. D., Asfwa, B., Beyene, Y., Haile-Selassie, Y., Lovejoy, C. O. & Suwa, G. (2009). *Ardipithecus ramidus* and the paleobiology of early hominids. *Science*, 326, 75–86.
- Wiseman, A. L. A., & De Groote, E. (2018). A three-dimensional geometric morphometric study of coastal erosion and its implications for biological profiling of fossilised footprints from Formby Point, Merseyside. *Journal of Archaeological Science: Reports*, 17, 93-102.
- Wood, B. & Richmond, B. G. (2000). Human evolution: taxonomy and paleobiology. *Journal of Anatomy*, 196, 19-60.
- Zelditch, M. L., Swiderski, D. L., Sheets, H. D., Fink, D. L., (2004). *Geometric Morphometrics for Biologists: A Primer*. Elsevier Academic Press, London.
- Zimmer, B., Liutkus-Pierce, C., Marshall, S. T., Hatala, K. G., Metallo, A., & Rossi, V. (2018). Using differential structure-from-motion photogrammetry to quantify

erosion at the Engare Sero footprint site, Tanzania. *Quaternary Science Reviews*, 198, 226-241.



Contents lists available at ScienceDirect

Journal of Archaeological Science: Reports

journal homepage: www.elsevier.com/locate/jasrep

A three-dimensional geometric morphometric study of the effects of erosion on the morphologies of modern and prehistoric footprints[☆]

Ashleigh L.A. Wiseman^a, Isabelle De Groote^a Research Centre in Evolutionary Anthropology and Palaeontology, Liverpool John Moores University, United Kingdom

ARTICLE INFO

Keywords:

Fossilised footprints
Geometric morphometrics
Erosion
Photogrammetry
3D modelling

ABSTRACT

Introduction: Fossilised footprints have been discovered all over the world and can provide information regarding the foot size and subsequent body size estimates of the track makers or an insight into the kinematics of the foot/lower limb. After exposure, these fossils rapidly erode. It is predicted that footprint morphology is compromised after creation, prior to fossilisation and that erosion after exposure will affect the morphology of a footprint after exposure. To date, no studies have assessed if degradation prior to fossilisation and/or after fossilisation, and subsequent exposure, affects the morphology of the print, thereby affecting any measurements taken. This study aims to quantify these pre- and post-erosional processes.

Materials and methods: A set of experimentally generated footprints were created to test the effects of degradation of footprint morphology prior to fossilisation. In addition, Holocene footprints were recorded at Fomby Point, Sefton, UK. In just over a week tidal action had completely eroded the Holocene beds. Photogrammetry was applied to the experimental human footprints and a selection of Holocene human and animal footprints. Three-dimensional Geometric Morphometric methods were utilised to estimate differences in shape and size.

Results: Results from the experimental footprints indicate that weather action affects the size and shape of a footprint prior to fossilisation. When the weather was dry, footprint shape and size showed little difference for two weeks, but rainfall caused significant changes. The Holocene footprints show that after fossilisation and exposure to coastal erosion, footprint rigidity is highly compromised. The human footprint borders progressively recede, increasing length and width each day. Footprint depth, often used to inform upon speed and kinematics, varied considerably in one week. Some regions becoming shallower, others increasing in depth. Similar results were found for the animal footprints, but with less significant changes in shape and size determined.

Conclusion: Observed significant differences in measurements result in problems for predicting stature, mass, sex, and kinematic analyses. This warrants caution when making interpretations from fossilised footprints. Rapid recording of fossilised prints from first exposure and assessing pre-fossilisation processes are necessities when recording footprint surfaces.

1. Introduction

Fossilised hominin footprint localities have been discovered across Africa, Eurasia, Australia and the Americas (Leakey and Hay, 1979; Behrensmeyer and Laporte, 1981; Roberts and Berger, 1997; Miletto et al., 2003; Watson et al., 2005; Webb, 2007; Bennett et al., 2009; Roberts, 2009; Moore et al., 2013; Felstead et al., 2014; Ashton et al., 2014; Masao et al., 2016). In lieu of skeletal material, fossil footprints can be used to infer body dimensions of the track makers (Bennett and Morrie, 2014). Numerous fossil and forensic-based studies have been conducted that have attempted to find a correlation between footprint

measurements (e.g.; forefoot breadth, heel breadth, length, toe extremity length, etc.) and body dimensions, such as stature, body mass, hip height, sex and age (Krishan, 2006; Kanchan et al., 2008; Avanzini et al., 2008; Bennett et al., 2009; Dingwall et al., 2013; Domjanec et al., 2015; Hatala et al., 2016a).

For example, stature is often predicted using the length of the foot by applying Martin's ratio of 0.15 (Martin, 1914). Dependent on substrate material properties, these measurements extracted from a single trackway belonging to a single individual can vary substantially. Stature and mass predictions from just one trackway from Walvis Bay, Namibia have estimated that the individual ranged from 1.35 m to

[☆] Conflicts of interest: None.

[☆] Corresponding author at: Liverpool John Moores University, Byrom Street, Liverpool L3 3AF, United Kingdom.

E-mail addresses: A.L.Wiseman@liverpool.ac.uk (A.L.A. Wiseman), I.DeGroote@liverpool.ac.uk (I. De Groote).

<https://doi.org/10.1016/j.jasrep.2017.10.044>

Received 12 June 2017; Received in revised form 12 October 2017; Accepted 28 October 2017

Available online 07 November 2017

2352-409X/ © 2017 Elsevier Ltd. All rights reserved.

1.73 m tall, with the individual being either malnourished or clinically obese (Bennett and Morse, 2014). Evidently, slight variations in a trackway results in grossly variable biometric predictions.

In other locations, such as at Laetoli, Tanzania and Ileret, Kenya, the substrate material properties are much more uniform across a trackway, and biometric data that is extracted is much less variable (Bennett et al., 2009). Less variable measurements have resulted in numerous studies utilising these measurements to predict not only biometric data, but also kinematic data (Schmid, 2004; Berge et al., 2006; Vaughan and Blaszczyk, 2008; Raichlen et al., 2008; Raichlen et al., 2010; Crompton et al., 2011; Bates et al., 2013; Dingwall et al., 2013; Bennett et al., 2016; Hatala et al., 2016b; Masan et al., 2016; Raichlen and Gordon, 2017). These studies have allowed palaeoanthropologists to assess evolutionary trends in bipedal locomotion and body proportions.

It has been previously demonstrated that footprints are susceptible to taphonomic changes prior to diagenesis as the result of a number of variables; weather conditions, changes in surface hydrology or bioturbation (Marty et al., 2009; Bennett and Morse, 2014). After the footprints have undergone diagenesis, and have either become exposed or excavated a number of variables can lead to the footprints becoming eroded, thus affecting footprint shape (Bennett et al., 2013). As with any archaeological material, once the fossils are uncovered and exposed to the elements they will begin to erode, with softer, lithified sediments being more susceptible to erosion (Bennett et al., 2013). It must be acknowledged that weather action, such as wind or rain, may affect the size and shape of a footprint in a similar manner that slight variations in substrate typology may affect a footprint (Marty et al., 2009; Bennett et al., 2013).

No studies to date have quantified the effects of degradation on morphology, and how this can affect measurements taken from a footprint. The current study aims to quantitatively assess the effects of taphonomy and erosion on footprint morphology through the assessment of experimental and Holocene footprints. New discoveries of human trackways at Formby Point, Merseyside has offered a unique opportunity to record a set of Holocene footprints as they rapidly erode.

This study proposes that footprints are at risk of significant morphological change which will alter body size predictions at two stages. The first stage is immediately after footprint creation. The second stage is post-excavation. It is predicted that a delay in events leading to excavation and recording could result in changes in shape and size of a footprint, particularly in easily deformable softer sediments that are more susceptible to morphological changes (Bennett et al., 2006).

We use a selection of experimentally generated footprints to assess changes in footprint morphology prior to fossilisation. Holocene human and animal footprints discovered along the Sefton Coast were also assessed to determine if there is any changes in shape or size per day after exposure. It is predicted that the longer a footprint is exposed then there will be a significant change in shape and size of the print. Shape change is predicted to affect measurements of the foot used to inform upon body size estimates. An improvement on understanding the effects of erosion on morphology will improve the ability to accurately assess body size estimates from future footprint sites.

1.1. Geological and archaeological context

Formby Point is located along the Sefton Coast in Merseyside, England and is characterised by silty, fine-grained sands and peat sediments, and sand dunes (Roberts et al., 1996) preserved in unlithified, soft sediments (Roberts, 2009; Bennett and Morse, 2014). Encroaching coastlines have led to the exposure of numerous ancient sediments since the 1970s, many of which contain over 145 Holocene human trackways and animal footprints along a 4 km stretch of this coastline (Huddart et al., 1999; Roberts, 2009). The Formby Point sediments are similar to other fossilised sediment beds at Terra Amata, a site containing a Neanderthal footprints (De Lumley, 1966).

Carbon and optically stimulated luminescence (OSL) dating of the previously excavated sediments have yielded dates from 6650 ± 700 OSL BP – 3575 ± 45 ^{14}C BP (Roberts, 2009). The latter date was obtained by dating roots that overlay the Holocene beds, indicating a *terminus ante quem* for the beds (Roberts et al., 1996; Huddart et al., 1999; Roberts, 2009), confirming a Mesolithic age. These beds offer an interesting insight into human activity of the Late Mesolithic-Early Neolithic transition along the Sefton Coast.

In June 2016 three human trackways were exposed due to wave erosion at Formby Point immersed in over 700 animal footprints. Auroch, roe and red deer, crane bird, wolf/dog, and beaver footprints have been identified (Roberts et al., 1996; A. Burns 2017, pers. comm.). The interaction of many animal and human prints offer a glimpse into Mesolithic human activity, and even offer a unique opportunity to assess the gait dynamics of an extinct species of cattle, although this is not the focus of the current study.

The Holocene sediment layer was excavated by staff and students of The University of Manchester. Unfortunately, the bed was destroyed in just under two weeks after exposure due to the destructive nature of the high tide. Twice a day the sediment layer was completely immersed by high tide, with the prints only reappearing with low tide. Visually, it was possible to see the daily erosion of the footprints as the direct result of wave action (Fig. 1). The sediment bed was unlithified and despite efforts to prevent human and animal interference with the footprints, tidal action still led to the destruction of the footprint bed quite rapidly due to the bed being composed of soft, easily deformable silts. Such a rapid degradation of the footprints that was noticeable by the naked eye is hypothesised to have resulted in significant morphological change. Importantly, we expect that linear measurements of the foot will have changed on a daily basis. As previously discussed, these linear measurements are used to predict an individual's biometric information. Changes in these measurements are expected to produce highly variable predictions regarding body size estimations.

Holocene footprints have previously been exposed along the Sefton Coast (Roberts, 2009), with fossilised footprints appearing at other coastal sites in the UK, such as at Happisburgh, Suffolk (Ashton et al., 2014). These beds containing unlithified footprints were also destroyed rapidly due to tidal action in a matter of weeks. If our study is successful in determining that morphological changes are paramount in coastal locations, particularly with footprints that are unlithified, then the biometric data that has been previously published from these sites, such as at Happisburgh (Ashton et al., 2014), is questionable. The sediments are variable between Formby Point and Happisburgh, but it is a fair assumption that two soft, unlithified sediment beds would have reacted similarly when exposed to the same variables: vigorous tidal action and poor weather conditions. Both of these beds deformed and were destroyed rapidly. It is expected that both sites also experienced changes in footprint morphology coinciding with the rapid destruction of the beds.

The rapid erosion of the footprints at Formby Point have offered a unique opportunity to quantitatively assess the effects of daily degradation on footprint morphology. If the current study is successful in determining that footprints undergo daily morphological changes, then our results will have considerable implications for future studies that assess footprint discoveries from coastal locations.

2. Materials

2.1. Experimental set-up

A selection of experimental footprints were created in homogenous fine-grained sand composed of rounded to sub-angular particles measuring $\sim 0.06\text{--}0.7$ mm in diameter with $\sim 20\%$ saturation at a 40 mm depth (Fig. 2). Previous experiments have determined that this is the optimal saturation for footprint definition, whereby sand composition has no significant effect on morphology after saturation (D'Août et al.,

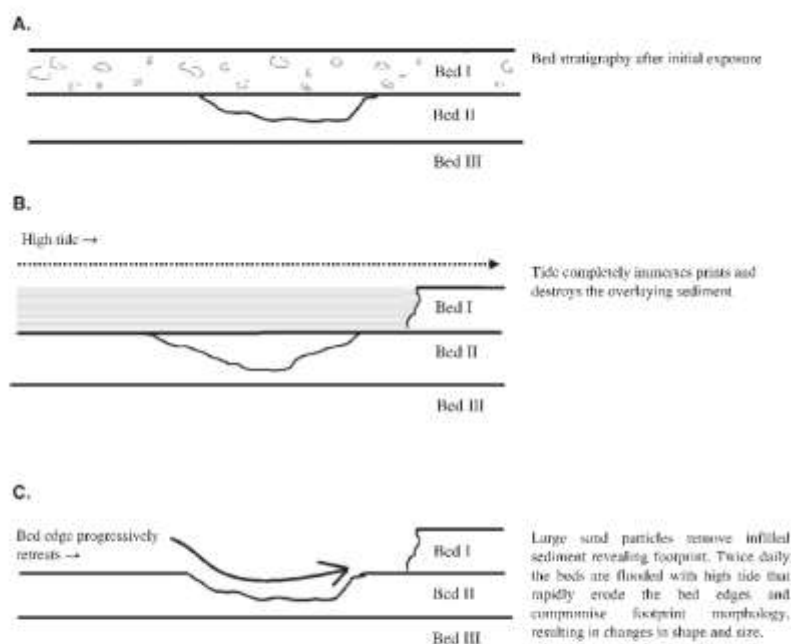


Fig. 1. Diagram explaining the destructive nature of the high tide. Twice a day the beds were flooded by high tide which resulted in damage to the bed edges and the loss of ~60 cm of the west-facing bed daily. Large sand particles and water eroded the footprint edges resulting in changes in shape and size.

2010; Crompton et al., 2011). The footprints were created inside a container with a drainage system in place. The base of the tray allowed any rainwater that saturated through the overlying sediment to drain through to the ground to prevent the tray from flooding. Netting was placed over the footprints to prevent animal interference, but still allowed wind and rain to penetrate through.

The experimental prints were placed outdoors in an open area in Liverpool, Merseyside during winter. During the first 14 days the weather was dry with low wind speeds and near-freezing temperatures. There was rain and medium-to-high wind speeds during the remaining six days of the experiment. Rain resulted in small dents across the sediment to form. Footprint features progressively eroded in the final days of the experiment.

These experimental footprints were not created in a material that reflect any sediments belonging to fossilised beds containing footprints.

We have deliberately chosen a homogenous material of uniform particle distribution and water content. The rationale for using this material is to demonstrate that footprints are susceptible to morphological change prior to becoming covered with overlying material, a process that often leads to fossilisation (Morse et al., 2013). By using this homogenous material, we have avoided the problem of attempting to replicate sediments from Formby Point, Ilcort or Lactoll, etc. Any un lithified material (e.g., volcanic ash, fluvial or lacustrine deposits composed of silt, sand or clay of varying material properties) is expected to behave in a similar manner as the container of sand; it is expected that there will be morphological change as the direct result of weathering or coastal action. If a material can be deformed to produce a footprint with anatomical features, then the material is certainly capable of deforming as the result of weather action in the period before the material becomes covered by overlying sediment. This must



Fig. 2. Set-up of the experimentally generated footprints on the first day of the experiment. Netting was placed over the prints each day to prevent animal interference. Photographs were taken with a camera mounted to a tripod.

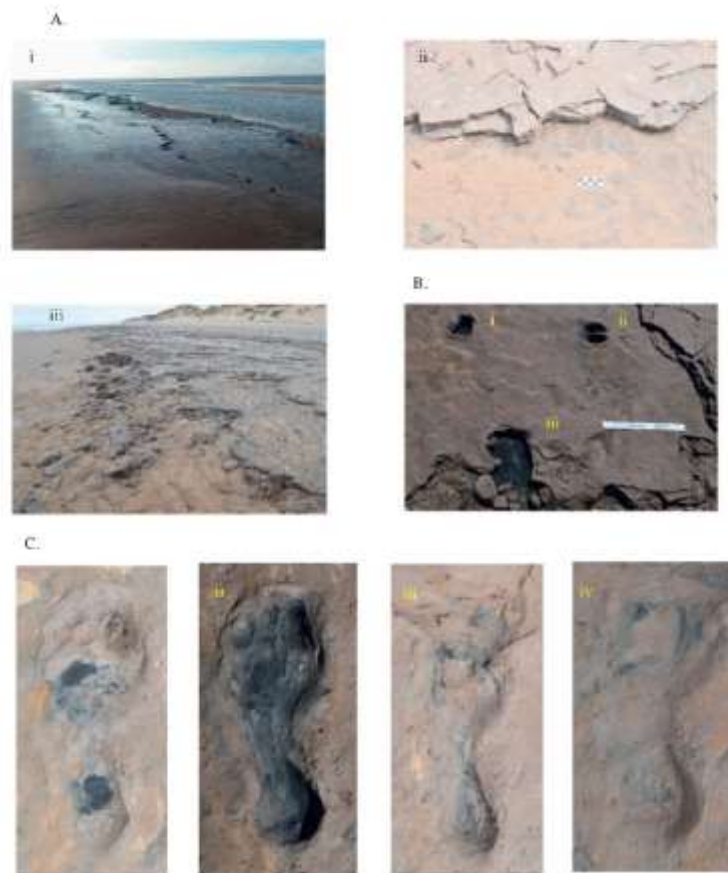


Fig. 3. (A) High tide completely immersed the bed each day. (i) shows the incoming high tide that later reached on average 8 m high. Overlying beds were rapidly removed by the tide, revealing lower beds below (ii). After repeated tidal immersion, the fossilised beds were destroyed. (iii) shows the bed after just one week. Around 5 m of the west-facing bed was lost in just one week. (B) Photograph of the selected animal prints on the second day. (i) and (ii) belong to roe deer. (iii) belongs to auroch. Note the fragmented posterior region of the auroch print. (C) Photographs of the human print during the four days of recording, with (i) belonging to day one and (iv) belonging to day four.

remain an important consideration when analysing fossilised footprints: any information extracted from the footprints can only be classed as relative information about the track-maker.

2.2. Holocene footprint data collection

Three human trackways were discovered at Formby Point containing a total of seventeen complete human footprints of definite ichnology. Due to daily time constraints of the incoming high tide, only one human footprint was recorded daily and used for this study. It was the longest surviving print. Others were initially selected in addition, but were rapidly destroyed after just a few days warranting their removal from the dataset. One auroch and two roe deer footprints were also selected (Fig. 3). The auroch prints offer a unique opportunity to assess the gait dynamics of an extinct species of cattle.

Due to a combination of excavation limitations and bad weather the human footprint was only recorded on four days out of a possible 7 days, and the animal prints were recorded on a total of five days. On the seventh day the section of bed containing the human print had completely degraded. The animal prints were destroyed the following day.

A DSLR D3300 Nikon camera with a macro 60 mm lens of fixed zoom was used to photograph each footprint each day. Due to sporadic

weather conditions (a mix of cloud cover and bright sunlight) camera settings were consistently altered to accommodate weather. The first model of the animal prints were made using a GoPro Hero4 due to time constraints of the incoming high tide.

3. Methodology

Photogrammetry was applied to create 3D models of each footprint daily on the licensed software Pix4D. Weather conditions during the experiments were consistent with heavy cloud cover. Conditions at Formby Point were mostly very bright, with the ground quite wet, which has reduced the resolution for two models. All photographs were taken during dry periods of the day. Model editing was completed using Avizo 9.0.

Footprint length was calculated by measuring the distance between the most distal point of the hallux and the most inferior point of the pterion. Length was then used to predict stature using Martin's ratio of 0.15, which has repeatedly been found to positively predict stature in modern habitually unshod populations (Martin, 1914; Hrdlička, 1935; Dingwall et al., 2013), and has been previously applied at fossilised sediment localities such as Laetoli (Tuttle, 1967) and Happisburgh (Ashton et al., 2014).

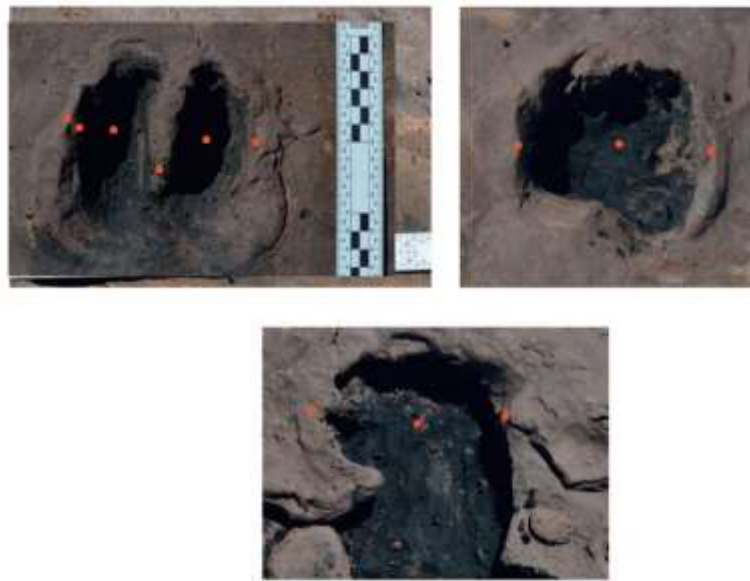


Fig. 4. Landmark datasets for the human prints and animal prints. A lack of homologous landmarks in the animal dataset has resulted in a reduced landmark dataset.

3.1. Geometric morphometrics

Geometric morphometrics (GM) is a suite of statistical methods employed to measure and compare patterns of similarity and differences in many objects through the process of datum acquisition, processing, analysis and visualisation of geometric information (Bookstein, 1991; Slice, 2005). These methods allow for morphological changes to be quantified from the statistical application of landmarks (Oxnard and O'Higgins, 2009). These techniques will be applied in the current study to determine if shape/size change occurs between daily models, and if this is the direct result of coastal erosion. All analyses were computed in R, and two R packages: morpho (Schlager, 2017) and geomorph (Adams and Otárola-Castillo, 2012).

A total of 44 models were landmarked, representing the experimental prints and Holocene human print. A further 15 models were landmarked, representing the animal prints. A total of 20 type II landmarks were used for the human dataset and a total of 10 landmarks were used for the animal dataset (five for the first roe deer print, three for second, and three for the auroch print). All landmarks were found to be homologous between each daily model. Landmarks were digitised on 3D ply surfaces in Avizo 9.0 (Fig. 4).

Prior to any geometric morphometric applications, the depth of four landmarks were calculated for all experimental and Holocene human prints: the medial and lateral forefoot region at the deepest points, and the medial and lateral heel at the deepest points. The depth of these landmarks are expected to change, corresponding to increased degradation of the footprint. The landmarks that synthesised the most concave points on the medial and lateral heel and forefoot were used to calculate the linear distance across these regions. Depths were thus measured using simple trigonometry for all human prints.

A General Procrustes Analysis (GPA) was performed, which translates and rotates each homologous landmark to the origin, whilst scaling to unit-centroid size (Zelditch et al., 2004). These configurations are all aligned to a single reference specimen, representing the mean shape. The resulting Procrustes coordinates compose the shape of each specimen within Kendall's shape space (Kendall, 1984).

Shape variation was then assessed using a Principle Components Analysis (PCA), which is a non-parametric statistical technique used to examine the relationship between a set of variables by calculating the maximum distance between each individual landmark (Zelditch et al., 2004). Each principle component (PC) was examined to determine shape variability. Shape change was visualised by non-affine partial warp grids called thin plate splines (TPS). These grids allow for the visual representation of relative shape deformation and display landmark transformation which maps a set of GPA-aligned configuration of landmarks between a set of structures, with the grid lines representing the relative amount of bending energy between each landmark (Rohlf and Slice, 1990). TPS grids were not created for the animal prints due to a reduced landmark dataset.

An ANOVA was computed to assess the relative amount of shape variation per day. Categorical variables were created for each landmark configuration to assist in assessing the cause of shape change. By adopting the use of categorical variables in the dataset, information about the footprints – such as the sudden appearance of holes in the surface as the direct result of rain – can be included in the analyses. Their inclusion in the dataset assigns each configuration of landmarks to a group, allowing for groups to be statistically compared. For example, group one contains two variables: the presence or absence of raindrops. This group can then be statistically compared with the second group whereby the configurations have been assigned a variable stating if the footprint has experienced a reduction in height of the landmarks relative to landmark height on day one. Subsequently, it will be possible to determine if rain action has resulted in the reduction of landmark height, and if these variables have cumulatively resulted in changes to the shape and size of a footprint.

Two categorical variables were developed for the experimental prints. The first describes the presence of rain drops in the bed that left small dents in the sediment towards the end of the experiment. The second describes the reduction in height of several landmarks in the forefoot region, corresponding to degradation. Two categorical variables were created for the animal prints: the presence/absence of toe ridges in the roe deer and the severe erosion of the posterior border of

Table 1

The depth of the Holocene human footprint at five separate locations taken from each model. Measurements are in mm. See Supporting Information 1 for experimental print measurements.

	Model one	Model two	Model three	Model four
Depth of hallux	15.34486	14.28583	2.656838	1.894133
Depth of 2nd to 5th metatarsals	19.20728	12.09233	11.39823	11.32415
Depth of 1st metatarsal	11.54897	8.409708	10.03207	13.9389
Depth of midfoot	6.422628	6.452933	8.009055	5.766013
Depth of heel	12.11445	16.10337	17.66635	18.48052

the auroch footprint.

Two categorical variables have been established for the Holocene human dataset: the grade of footprint degradation and depth. Two grades have been established for degradation: the presence and absence of the forefoot region. Footprint depth was measured at five separate points across the foot (Table 1). Two grades were established for depth based upon the significant reduction in hallux depth relative to an increasing heel depth. This is split between the first two days and the final two days for the Holocene print.

Finally, the relationship between footprint degradation and size was assessed by regressing log-centroid size (CS) to the first PC. Levels of significance were computed by permutation tests to a 95% confidence level, using 1000 permutations which tests the sampling distributions. Finally, morphological disparity tests were computed which performs a pairwise comparison between groups.

4. Results

4.1. Morphological change prior to fossilisation

Foot length was calculated for each model (S1), with stature being predicted using Martin's ratio (Martin, 1914). Different statures were produced for the models representing the final two days of the experiment, with foot length increasing as much as 6.016%.

PCA of the experimental prints over a period of 20 days revealed that shape variance can be explained by the first two PCs that account for > 84% of total variance (Fig. 5a). The first two axes (PC1 and PC2) can be cumulatively summarised as accounting for the observations previously accounted for in the creation of the categorical variables: the reduction in height of the toe ridges (identified in PC2) and the appearance of numerous holes as the direct result of rain/weather (identified in PC1). The maximum (PC1+) and minimum (PC1-) shape difference indicates that changes in foot length are associated with poor weather conditions, with an increased distance between anterior and posterior landmarks as ridges become shallower and less convex. As expected, weather action has cumulatively resulted in changes in shape/size of the footprint (according to PC1) and changes in footprint depth (according to PC2). This is characterised by the strong separation of negative PC scores for the final two days of the experiment and positive PC scores for the first 18 days of the experiment. The least displacement for both the experimental and Holocene prints occurs in the heel region, with shape remaining almost static with increasing erosion.

To analyse if degradation affects size, shape variability (assessed by using PC1) was regressed against log-CS for all footprints (Fig. 6). Results indicate that size is significantly affected by degradation in the final two days of the experiment and that the null hypothesis can be rejected, and that there is a statistically significant difference in shape and size between the models, as shown by a one-way ANOVA. This is corroborated by the change in length and the change in foot width for the right foot as the direct result of rain. Shape change has a significantly strong association with log-CS ($R^2 = 0.57524$; $P = 0.002$), that has a weak positive correlation with weather action

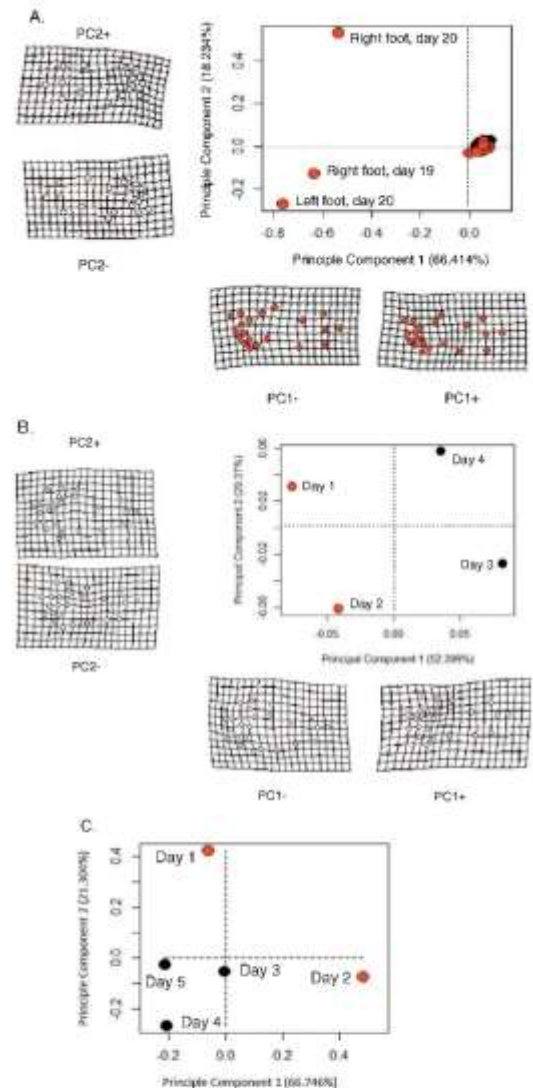


Fig. 5. A. This PCA graph illustrates the shape change in the experimental footprints ($n = 44$). Projection of each of the experimental prints on PC1 and PC2. Red dots represent the presence of rain damage which increased in the final two days of the experiment. Black dots represent the experiments before weather damage. B. This PCA graph illustrates the shape change in Holocene human footprint ($n = 4$). Red dots represent the presence of the footprint. Warp grids display the maximum and minimum relative shape changes along each PC axis. Black dots represent the severe degradation of the footprint. C. This PCA graph illustrates the shape change in Holocene animal footprints ($n = 5$). Red dots represent the first two days of recording. Black dots represent the last two days of recording when the auroch print became severely degraded. (For interpretation of the references to colour in this figure legend, the reader is referred to the web version of this article.)

($R^2 = 0.22281$; $P = 0.002$).

A morphological disparity test found that shape change is only significantly affected by weather in the final six days of the experiment with the severe degradation of the toe ridges ($P = 0.004$) and the

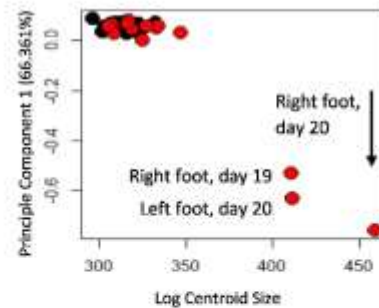


Fig. 6. Linear regression establishing the positive relationship between centroid size and shape of the experimental prints, as explained by PC1. Red dots represent the presence of rain damage, which increased in the final two days of the experiment. Black dots represent the experiments before weather damage, which are clustered in the graph. Initial weather damage does not cause significant change until the final days of the experiment after prolonged exposure. (For interpretation of the references to colour in this figure legend, the reader is referred to the web version of this article.)

increased presence of raindrops ($P = 0.002$). No statistically significant shape/size change occurred in the first fourteen days of the experiment when weather remained dry. The null hypothesis can be rejected as there is a significant association between weather and shape change, as supported by a Pairwise test.

4.2. Morphological change after exposure/excavation

Upon visual inspection it was clear that all of the Holocene footprints selected displayed the collapse of key features of the footprints. The human footprint suffered severe degradation in the forefoot, the roe deer prints lost toe ridges, and the auroch print, which was located on the edge of the sediment bed, progressively lost the posterior region of the footprint each day alongside the erosion of the bed edge. If the bed had been discovered during the final two days of exposure then it is questionable whether the footprints would have been identified as human or animal, as the hollows that remained resembled bed damage, rather than footprints.

Foot length was calculated (S1). As expected, four different foot length measurements were generated, although the variance between day one and day two is only 3.8 mm and is not deemed significant. Measurements from the final two days are quite different. The tip of the hallux is still easily distinguishable in the day three model, although the ridge is much less prominent. In day four a more inferior point has been identified as the tip of the hallux, although this is roughly one centimetre shorter than the first two days, and two centimetres shorter than the third day. Evidently, a large margin of error exists in determining footprint extremities after prolonged exposure.

Stature was then predicted using Martin's ratio. Different statures were produced in accordance with varying foot length, with the percentage increase in foot length increasing as much as 6.21% with erosion.

PCA of the Holocene human print revealed that shape variance can be explained by the first two axes that account for > 81% of total variance (Table 2). The first axis can be surmised as describing the significant degradation of the forefoot region and the collapse of ridges between the 2nd to 5th metatarsals that are prominent in the first two days only – these observations were previously identified during the creation of the categorical variables, and have thus informed on the major shape change of the Holocene footprint. The forefoot region becomes flat (supported by a loss of depth, as discussed in Section 2.3), with no clear identifiable structures, with two exceptions: the hallux and the ridge surrounding the extremity of the 5th toe. This is characterised by the strong separation of individual PC scores, represented

Table 2

Relative wraps analysis of all footprints showing the first four principle components for the Holocene human print, the first five for the animal prints and the first 11 for the experimental prints, accounting for over 95% of variance.

PC	Singular value	% Explained variance	Cumulative variance
Fossilised human print			
1	0.07182	0.52399	0.52399
2	0.05377	0.29370	0.81769
3	0.04237	0.18231	1
4	6.266E-17	0	1
Animal prints			
1	0.08068	0.66746	0.66746
2	0.04558	0.21304	0.88050
3	0.02975	0.09079	0.97128
4	0.01673	0.02872	1
5	5.848E-17	0	1
Experimental prints			
1	0.1932	0.6636	0.6636
2	0.1013	0.1822	0.8458
3	0.06836	0.08304	0.92883
4	0.03668	0.02391	0.95274
5	0.02638	0.01237	0.96510
6	0.02009	0.00171	0.97227
7	0.01599	0.00454	0.97681
8	0.01400	0.00348	0.98030
9	0.01231	0.00269	0.98299
10	0.01096	0.00241	0.98540
11	0.0106	0.0020	0.9874

by negative PC scores for the first two days and positive PC scores for the final two days that the footprint was recorded. This division can be emphasised by the dotted line along the PC1 axis (Fig. 5b).

Variation along the second PC described changes in depth of the footprint as a whole. The hallux is seen to be decreasing in depth relative to the heel which increases depth. The depth of the lateral foot (2nd to 5th metatarsals) is found to decrease. The region under the 1st metatarsal slightly decreases in depth during the first two days then increases in depth relative to the loss to the lateral border of the foot. The midfoot region (area lateral to the medial arch) remains almost static in depth, displaying the least amount of depth and shape variance across the footprint.

The shape differences depicted reveal that footprint shape can be warped into two different shapes, per the forefoot region. The maximum (PC1 +) and minimum (PC1 -) shape difference along PC1 indicates that the forefoot region becomes much more constricted as erosion increases, with a reduced height and a reduced amount of bending energy (PC1 -) between each landmark. A likely cause in this displacement may be the degradation of numerous distinguishable features in this region, and a reduction in the height of numerous landmarks. Similarly, the most obvious shape change along PC2 in the experimental prints occurs in the forefoot region, explaining a reduction in the height of the toe ridge landmarks as the ridges are slowly eroded.

The most obvious shape change along PC2 in the print would appear to be around the head of the metatarsals. This area seems to be wider between PC2 + and PC2 -, with the landmarks characterising the medial border of the foot being stretched relative to the lateral border of the foot. The lateral border of the foot becomes much less distinguishable during the last two days making this the likely cause in this displacement. The loss of the medial ridge may further explain this shape variance. This is further corroborated by the depth test which found this area lost considerable depth relative to the medial border of the foot.

A morphological disparity test found that shape change is significantly correlated with changes in size ($P = 0.0038$), with depth also significantly affected ($P = 0.00452$). CS is very weakly correlated to changes in depth ($R^2 = 0.00723$). A poor R^2 value may be explained by

a reduced dataset ($n = 4$). Regardless, the null hypothesis regarding depth cannot be rejected as a positive association could not be established. Similarly, a Pairwise test was computed to establish the amount of shape change relative to footprint depth. The null hypothesis cannot be rejected as the interaction between depth and shape/size was not found to be significant ($P > 0.05$).

4.3. Morphological change in the Holocene animal prints

Shape change of the animal prints can be explained by the first three PCs that account for > 97% of total variance (Fig. 5c). The first axis can be surmised as describing the degradation of the auroch footprint, which was discovered at the edge of Bed III. By the second day half of the print had completely disappeared, with the lateral and medial edges of the footprint progressively eroding until its complete disappearance on the fifth day. By the third day it is no longer identifiable as a print. The loss of identifiable features of this print has resulted in the strong separation of individual PC scores along the first axis, represented by negative PC scores for the first two days and positive PC scores for the last three days.

Shape change along the second axis can be surmised as describing relative changes in depth. With the loss of the toes the base of the print became less convex. This loss is more evident on the fifth day, represented by negative PC scores for the first two days and a positive PC score for the final day. Variation along the third and fourth axes cumulatively describe changes in the loss of toe ridges in the roe deer footprints. The ridge between the medial and lateral toes had completely vanished by the fourth day. The borders of one of the roe deer prints are no longer undercut, but are shallow and slanted. This results in a considerable lack of distinction of internal morphology.

5. Discussion

5.1. Taphonomic changes to footprint morphology prior to diagenesis

GM methods were applied to quantitatively assess the effects of erosion on footprint morphology and to assess if degradation affects body proportion estimates. One Holocene human footprint, two experimental human prints and three Holocene animal prints were chosen to be recorded daily ($n = 59$). This study was testing the hypothesis that footprint morphology will change in shape and size prior to fossilisation and after fossilisation and subsequent exposure. It was predicted that prolonged exposure will significantly affect measurements taken of the foot, thereby decreasing the accuracy of biological inferences.

It has been previously demonstrated that footprints undergo significant taphonomic processes prior to burial and diagenesis (Marty et al., 2009), that may alter the shape of a footprint thus affecting any inferences extracted, such as body proportion predictions (Bennett and Morse, 2014). However, to date no study has quantified morphological change due to taphonomic processes and how these changes may affect body proportion predictions.

The results from the current study have demonstrated that significant morphological change may occur in softer sediments prior to diagenesis, according to weather conditions. Shape and size will change significantly after rainy periods or high wind speeds. These shape/size changes have affected measurements taken of the foot (length has been used in this study as an example) thereby producing inaccurate predictions of stature. Although not the focus of this study, it can be assumed that other biological predictions will vary greatly if a footprint is exposed to adverse weather conditions prior to fossilisation. While the current study has only focused on weather action as a taphonomic variable, it is a fair assumption to say that other taphonomic processes such as bioturbation, will also affect footprint morphology.

The results of the current study have considerable implications for the human evolution fossil record: how accurate are previously

published body proportion estimates of fossil footprints? As previously stated, by analysing the morphology of a footprint numerous inferences can be made. For example, foot parameters (such as using foot length to predict stature and foot index to predict body mass) have been used in conjunction with contemporaneous skeletal data from north-western Europe dating to 950–850Kya to assign *Homo antecessor* as the maker of the footprints from Happisburgh (Ashton et al., 2014). Taphonomic processes, such as changes in surface hydrology or even bioturbation, after footprint creation may have affected the shape and size of these prints, thus altering taxon assignment and body proportion predictions. Similarly, taphonomic processes of the footprints from either Laetoli or Dieret may have resulted in the hominin body proportion estimates being under- or over-estimated.

It is suggested that sediment beds should be inspected for evidence of weather damage, particularly in softer lithified sediments, in future fossilised bed discoveries as the surface area may have been exposed for several days prior to fossilisation, with a potential loss of information. In particular, an archaeologist should inspect the sediment bed for rain drops.

5.2. Morphological changes to a human footprint after exposure/excavation

After a footprint has become covered by overlaying sediment and has begun the process of diagenesis, and subsequently exposed the print is susceptible to significant changes in shape and size, thereby affecting body size estimates. An example of how degradation can affect footprint inferences can be found in the high variance of predicted stature values presented in the current study. The first 3D model was created just under a week after the footprint was first exposed. The rapid degradation of the print after this point has significantly affected stature predictions. Shape change during the first two days is miniscule, and any analyses and subsequent results would not have produced drastically different results. As such, foot size and subsequent body size estimates can be reliably predicted in the first few days of exposure, assuming that minimal change occurred as a result of taphonomic processes prior to diagenesis. Prolonged exposure after excavation has significant implications for extracting reliable data. This problem is not unique to Formby Point, it was paramount during the excavations at Happisburgh. The Happisburgh footprints were also found on the coastline and were destroyed rapidly due to tidal action (Ashton et al., 2014). Any delay in recording the footprints may have resulted in stature and mass values that are not true representations of the Happisburgh hominins.

This has considerable implications for other footprint sites. The Ileret and Koobi Fora, Kenya footprints are the oldest footprints attributable to the genus *Homo* (Bennett et al., 2009), and are thus of great scientific importance. The sediment bed containing the footprints are composed of fine-grained silt and sands that are unlithified and highly erodible (Bennett et al., 2013). These sediments are quite comparable to the fine-grained sand and peaty sediments from Formby Point. Similarly, the Kenyan footprints are at threat of flooding and storm action (Bennett et al., 2013) – two variables that are somewhat comparable to the Formby Point sediment beds. With the exception of changes in water salinity (Formby Point is characterised by salt-water immersion and the threat of flooding at Kenya relates to non-saline lake inundation), the variables highlighted in the current study are applicable to the highly-erodible Kenyan footprints. Fortunately, the Kenyan tracks have been covered post-excavation in an attempt to geo-protect the footprints. However, if the footprints are exposed for excavation or geo-tourism during periods of stormy weather or flooding, then it is expected that the footprints will undergo significant morphological change that may affect our interpretation of the track-makers.

The Laetoli footprints which were formed in natrocarbonate ash (Leakey and Hay, 1979) are only partially lithified, resulting in these footprints being much more robust and firm than the unlithified footprints from Ileret (Bennett et al., 2013). It is expected that the Laetoli

sediments will be less-susceptible to morphological change as the direct result of wind or rain action, due to much firmer substrates. However, the threat of degradation as the direct result of exposure is not redundant. Despite being much more robust and composed of a different substrate than that of Formby Point, it is expected that constant or prolonged exposure will likely result in the partially lithified Laetoli prints undergoing morphological changes. It is expected that any material that is not fully lithified and preserved will undergo significant changes in shape and size due to a number of external factors. Care should be taken for the immediate preservation of footprints of high interest, such as footprints from Laetoli. Without preservation, a footprint will continue to be subjected to considerable morphological change, and eventually the footprint may be unrecognisable. This occurred with the human footprint at Formby Point. Due to the severe degradation in the forefoot region in the Holocene human print, it is questionable as to whether the print would have been declared human, if discovery was delayed. If it had been declared human, remarkable differences in footprint measurements would have been made. These measurements are used to determine body size estimates (age, sex, mass and stature). Any inferences or estimations that could be calculated from these measurements taken in the final few days would have changed drastically from those made from the first model.

Happisburgh is a prime example of severe degradation hampering ichnotaxonomy. Numerous hollows were excluded in the analyses of the Happisburgh footprints due to questionable ichnology; only 14 footprints out of a total of 152 could be definitively declared hominin (Ashton et al., 2014). These hollows could be remnants of hominin footprints whereby only the heel and border of the prints – the deepest regions that are preserved the longest – have survived, as has been observed at Formby Point (Fig. 7). Alternatively, the hollows could be eroded animal footprints. Tidal erosion and a delay in recording these footprints that potentially belong to an extinct *Homo* species may have resulted in a considerable loss of data.

The results from the current study are a prime example of how rapidly a footprint can degrade. Within two weeks the Holocene sediment bed had completely vanished. During this time, one of the human trackways had completely eroded, with only one very deep trackway remaining in situ. The footprint that formed the basis of this study lay towards the west of Bed II and was the first print to be immersed by high tide. By the end of the first week Bed II had completely eroded, revealing another sediment bed below. Bed III (towards the north) was the final bed to disappear. Severe erosion in Bed III by this point made 3D modelling impossible due to the numerous pockets of water that remained during low tide. The rapid degradation of these footprints have demonstrated the pivotal need for digital recording for the preservation and future scientific investigation of these fragile fossils.

5.3. Morphological changes in animal footprints after exposure/excavation

In the current study it was demonstrated that the Holocene animal footprints also experienced a significant change in shape and size as the direct consequence of weather action. The roe deer prints, which were deeply pressed, demonstrated no significant shape change or change in size (except for the toe ridge region). This implies that lightly pressed prints are more susceptible to degradation. Prolonged exposure will affect print definition and depth.

The complete loss of the posterior region of the auroch print from Formby Point further raises questions regarding ichnology. By the second day the print would have been identified as damage to the bed, rather than an extinct species of cattle. Although not the focus of the current study, the auroch trackways provide a unique opportunity to study the gait dynamics of an extinct animal that could have been lost if the Formby Point prints were not rapidly recorded. Similarly, the delayed excavation at Happisburgh resulted in numerous damaged prints – poor anatomical definition has resulted in many of the Happisburgh footprints not being assigned to any taxa (Ashton et al., 2014) – being



Fig. 7. Comparison of hollows from Happisburgh (top) and Formby Point (bottom). Many of the hollows that were disregarded by Ashton et al. (2014) that have questionable ichnology from Happisburgh could have been identified as hominin if a delay in recording had not occurred. The photograph from Formby was taken on the penultimate day of excavation. The red highlighted footprints were previously identified as human, but on this day appeared as oval hollows with no distinctive features. Photo credit: Photograph of Happisburgh sediment bed by Simon Purfin, May 2013. (For interpretation of the references to colour in this figure legend, the reader is referred to the web version of this article.)

unidentifiable and rightly excluded from analyses. However, the loss of this data may have resulted in a lost opportunity to identify an extinct species of animal present in Britain during MIS 21/25.

Fortunately, better preservation resulted in the identification of numerous animal hollows within the Laetoli tracks, representing a range of extinct Pliocene species within the canivora, equidae, suidae, and bovidae mammalian orders (Jenken and Hay, 1979). However, taphonomic and/or post-excavation erosion of these prints may have resulted in a warping of anatomical features. A loss of this data may have resulted in the incorrect ichnotaxonomy of the prints, or unreliable biological data of the species.

While rapid recording is recommended in order to extract the most reliable data, it must be acknowledged that taphonomic changes may

have occurred prior to diagenesis, resulting in a loss of reliable data. Prints that display poor anatomical features are concluded to be unreliable. Prints that are deeply pressed, with clear anatomical details will undergo insignificant morphological changes in the period immediately after exposure. It is expected that clearly defined footprints will be the most reliable to inform on the track makers.

5.4. Concluding remarks

By applying GM techniques it was possible to identify the effects of erosion on footprint interpretation, particularly in softer sediments. The use of statistical techniques created a fundamental tool for the evaluation of footprint erosion. Results have shown that weather action can result in significant morphological change to a footprint prior to and after fossilisation. If a surface is free from weather damage then it may be assumed that there has been no loss of reliable data prior to fossilisation. After fossilisation and exposure a footprint will undergo considerable morphological change directly associated with weather and coastal activity. Morphology was not found to be significantly affected in the first few days after initial exposure, necessitating the need for rapid recording to provide the most accurate results, particularly in highly erodible substrates. It is recommended that inferences made on footprints that have a questionable time frame of exposure should be treated with caution. By creating high resolution 3D models rapidly these fragile fossils have been digitally preserved for further analyses.

Supplementary data to this article can be found online at <https://doi.org/10.1016/j.jasrep.2017.10.044>.

Acknowledgements

The authors would like to thank the National Trust Formby and Natural England for access and permission to carry out research. We would also like to thank Simon Parfitt for use of an image taken at Happisburgh, Norfolk in May 2013.

References

- Adams, D.C., Ostroff-Castillo, E., 2012. Geomorph: an R package for the collection and analysis of geometric morphometric shape data. *Methods Ecol. Evol.* 4, 393–399.
- Adrian, K., Lewis, S.G., De Groote, I., Driffl, S.B., Bates, M., Bates, R., Hesse, P., Lewis, M., Parfitt, S.A., Peglar, S., Williams, S., Williams, C., Stringer, C., 2014. Hominid footprints from early Pleistocene deposits at Happisburgh, UK. *PLoS One* 9 (2), e88329.
- Atanasiu, M., Miermi, P., Pasanelli, A., De Angelis, M., Rolandi, G., 2008. The Devil's trail: middle Pleistocene human footprints preserved in volcanoclastic deposit of southern Italy. *Int. J. Plant Anim. Traces* 15 (3–4), 179–189.
- Bates, R.T., Savage, R., Pataky, T.C., Morse, S.A., Webster, E., Fillingham, P.L., Ren, L., Qian, Z., Collins, D., Bennett, M.R., McClymont, J., Crompton, R.H., 2013. Does footprint depth correlate with foot motion and pressure? *J. R. Soc. Interface* 10, 20130009.
- Behrensmeyer, A.K., Laporte, L.F., 1981. Footprints of a Pleistocene hominid in northern Kenya. *Nat. Lett.* 289, 167–169.
- Benazzi, M.R., Morse, S.A., 2014. Human Footprints: Footfall Locomotion? Springer International Publishing, London.
- Benazzi, M.R., Morse, S.A., Bates, K., Crompton, R.H., 2006. Preserving the impossible: conservation of soft-sediment hominid footprint sites and strategies for three-dimensional digital data capture. *PLoS One* 1 (4), e60755.
- Benazzi, M.R., Harris, J.W.K., Richmond, B.G., Braun, D., Moun, E., Kilar, D.D., Kibunjia, M., Ormanidis, C., Behrensmeyer, A.K., Haddad, G., 2009. Early Hominin foot morphology on 1.5-million-year-old footprints from Eret, Kenya. *Sci. Rep.* 3, 1197–1201.
- Benazzi, M.R., Fillingham, P., Morse, S.A., Bates, K., Crompton, R.H., 2013. Preserving the impossible: conservation of soft-sediment hominid footprint sites and strategies for three-dimensional digital data capture. *PLoS ONE* 8 (4), e60755.
- Benazzi, M.R., Reynolds, S.C., Morse, S.A., Bates, K., 2016. Lactol foot tracks: 3D generated mean shape and missing footprints. *Nat. Sci. Rep.* 6, 24916.
- Berge, M.R., Pénia, X., Pélle, E., 2006. New interpretation of Lactol footprints using experimental approach and Procrustes analysis: preliminary results. *C.R. Palevol* 5 (3–4), 561–569.
- Bookstein, F.L., 1991. Morphometric Tools for Landmark Data: Geometry and Biology. Cambridge University Press, New York.
- Crompton, R.H., Pataky, T.C., Savage, R., D'Adit, K., Benazzi, M.R., Day, M.H., Bates, K., Morse, S., Adfieri, W.L., 2011. Human-like external function of the foot, and fully

- upright gait, confirmed in the 3.66 million year old Lactol hominid footprints by topographic statistics, experimental footprint-formation and computer simulation. *J. R. Soc. Interface*. <https://doi.org/10.1098/rsif.2011.0258>.
- D'Août, K., Meert, L., Van Gheulen, B., De Groote, I., Aerts, P., 2010. Experimentally generated footprints in sand: analysis and consequences for the interpretation of fossil and forensic footprints. *Am. J. Phys. Anthropol.* 141 (4), 515–525.
- De Lortie, H., 1956. Les fouilles de Terra Amata à Nice. In: *Prémices études Bulletin du Musée d'Anthropologie Préhistorique de Monaco*. 15, pp. 29–51.
- Dingwall, H.L., Hatala, K.G., Wunderlich, R.E., Richmond, B.G., 2012. Hominin stature, body mass, and walking speed estimates based on 1.5 million-year-old fossil footprints of Eret, Kenya. *J. Hum. Evol.* 64, 556–566.
- Dumortier, J., Riedler, H., Mitteroecker, P., 2013. A combined morphometric analysis of foot form and its association with sex, stature, and body mass. *Am. J. Phys. Anthropol.* 157, 582–591.
- Feldman, N.J., González, S., Haddad, D., 2014. Holocene-aged human footprints from the Cienfuegos Basin, NE Mexico. *J. Archaeol. Sci.* 42, 250–259.
- Hatala, K.G., Dingwall, H.L., Wunderlich, R.E., Richmond, B.G., 2016a. The relationship between plantar pressure and footprint shape. *J. Hum. Evol.* 65, 21–28.
- Hatala, K.G., Wunderlich, R.E., Dingwall, H.L., Richmond, B.G., 2016b. Interpreting locomotor biomechanics from the morphology of human footprints. *J. Hum. Evol.* 90, 39–44.
- Holliday, A., 1995. The Puebloans. With comparative data on the bulk of the tribes of the southwest and northern Mexico. *Am. J. Phys. Anthropol.* 29, 235–460.
- Huddart, D., Roberts, G., González, S., 1999. Holocene human and animal footprints and their relationships with coastal environmental change, Purnby Point, NW England. *Quat. Int.* 55 (1), 29–41.
- Kamrin, T., Meserole, R.G., Moudgil, R., Kaur, R., Kaur, M.S., Garg, R.K., 2008. Stature estimation from foot dimensions. *Forensic Sci. Int.* 179, 241.e1–241.e5.
- Kendall, D.G., 1984. Shape-manifolds, procrustes metrics and complex projective spaces. *Bull. Lond. Math. Soc.* 16, 81–121.
- Krishna, K., 2006. Individualizing characteristics of footprints in Gujarat of North India – forensic aspects. *Forensic Sci. Int.* 169, 137–144.
- Lesley, M.D., Hay, R.L., 1970. Pliocene footprints in the Lactol beds at Lactol, northern Tanzania. *Nature* 226, 317–325.
- Martin, R., 1914. *Lehrbuch der Anthropologie* 2. Fischer, Jena.
- Marty, D., Serrano, A., Meyer, C.A., 2009. Formation and taphonomy of human footprints in mineral-rich soils of present-day tidal flat environments: implications for the study of fossil footprints. *ichnos* 16, 127–142.
- Mera, F.T., Ichimaki, E.B., Cheria, M.B.A., Boichian, G., Irujo, D.A., Menconeri, S., Maggi-Cecchi, G., 2016. New footprints from Lactol (Tanzania) provide evidence for marked body size variation in early hominins. *elife* 5, e19584.
- Miermi, P., Atanasiu, M., Rolandi, G., 2003. Paleontology: human footprints in Pleistocene volcanic ash. *Nature* 422, 123.
- Morse, S.A., Bennett, M.R., Lurkin-Pierce, C., Prockney, F., McClymont, J., Savage, R., Crompton, R.H., 2015. Holocene footprints in Namibia: the influence of substrate on footprint variability. *Am. J. Phys. Anthropol.* 157 (2), 265–278.
- Oxand, C.E., O'Higgins, P., 2009. Biology clearly needs Morphometrics? Does Morphometrics need biology? *Biol. Theory* 4 (1), 84–97.
- Rakulic, D.A., Gordon, A.D., 2017. Interpretation of footprints from Site 5 confirms human-like bipedal biomechanics in Lactol hominins. *J. Hum. Evol.* 107, 134–138.
- Rakulic, D.A., Gordon, A.D., Harcourt-Smith, W.E.H., Foster, A.D., Randall, W.M., Hart, J., 2008. Lactol footprints preserve earliest direct evidence of human-like bipedal biomechanics. *PLoS One* 3 (3), e2769.
- Rakulic, D.A., Gordon, A.D., Harcourt-Smith, W.E.H., Foster, A.D., Hart, W.R.J., 2010. Lactol footprints preserve earliest direct evidence of human-like bipedal biomechanics. *PLoS One* 5 (3), e9789.
- Roberts, G., 2009. Ephemeral, subfossil mammalian, avian and hominid footprints within Flandrian sediment exposures at Purnby Point, Suffolk Coast, North West England. *Int. J. Plant Anim. Traces* 16 (1–2), 33–48.
- Roberts, D., Berger, L.R., 1997. Last interglacial (c.11k kyr) human footprints from South Africa. *J. Afr. J. Sci.* 93, 349–350.
- Roberts, G., González, S., Huddart, D., 1996. Interim Holocene footprints and their archaeological significance. *Antiquity* 70 (269), 647–651.
- Rohlf, F.J., Slice, D.E., 1990. Extension of the Procrustes method for the optimal superimposition of landmarks. *Syst. Zool.* 39, 40–59.
- Schlager, S., 2017. Morpho and Rvcg – shape analysis in R. In: Zheng, G., Li, S., Székely, G. (Eds.), *Statistical Shape and Deformation Analysis*. Academic Press, pp. 217–256.
- Schmid, P., 2004. Functional interpretation of Lactol footprints. In: Maderne, D.J., Hilton (Eds.), *From Biped and Strider: The Emergence of Modern Human Walking, Running and Resource Transport*. Springer US, New York, pp. 49–62.
- Slice, D.E., 2005. *Modern Morphometrics in Physical Anthropology*. Elsevier Academic/Plenum.
- Tuttle, R., 1967. Kinesiological inferences and evolutionary implications from Lactol bipedal trails G-1, G-2/3. In: Lesley, M.D., Harris, J. (Eds.), *Lactol: A Pliocene Site in Northern Tanzania*. Clarendon Press, Oxford UK, pp. 503–523.
- Vaughan, C.L., Blazewicz, M.B., 2008. Dynamic similarity predicts gait parameter for Homo floresiensis and the Lactol hominid. *Am. J. Hum. Biol.* 20 (3), 312–316.
- Watson, P.J., Kennedy, M.C., Willey, P., Robbins, L., Wilson, R.C., 2005. Prehistoric footprints in Jaguar Cave, Tennessee. *J. Field Archaeol.* 30, 25–43.
- Webb, S., 2007. Further research of the Willandra Lakes fossil footprints site, southeastern Australia. *J. Hum. Evol.* 52, 711–715.
- Zelditch, M.L., Swidowski, D.L., Sheets, H.D., Pink, D.L., 2004. *Geometric Morphometrics for Biologists: A Primer*. Elsevier Academic Press, London.

Appendix B

Relative warps analysis of all tracks showing the first four principle components (PCs) for the Holocene human print, the first five PCs for the animal prints and the first 11 PCs for the experimental prints, accounting for over 98% of variance.

	PC	Singular value	% explained variance	Cumulative variance
<hr/>				
Fossilised human print				
	1	0.072	0.524	0.524
	2	0.054	0.294	0.818
	3	0.042	0.182	1.000
	4	0.000	0.000	1.000
Animal prints				
	1	0.081	0.667	0.667
	2	0.046	0.213	0.883
	3	0.030	0.091	0.971
	4	0.017	0.029	1.000
	5	0.000	0.000	1.000
Experimental prints				
	1	0.193	0.664	0.664
	2	0.101	0.182	0.846
	3	0.068	0.083	0.929
	4	0.037	0.024	0.953
	5	0.026	0.012	0.965
	6	0.020	0.002	0.972
	7	0.016	0.005	0.980
	8	0.014	0.003	0.983
	9	0.012	0.003	0.985
	10	0.011	0.002	0.987
	11	0.011	0.002	0.987
<hr/>				

Appendix C

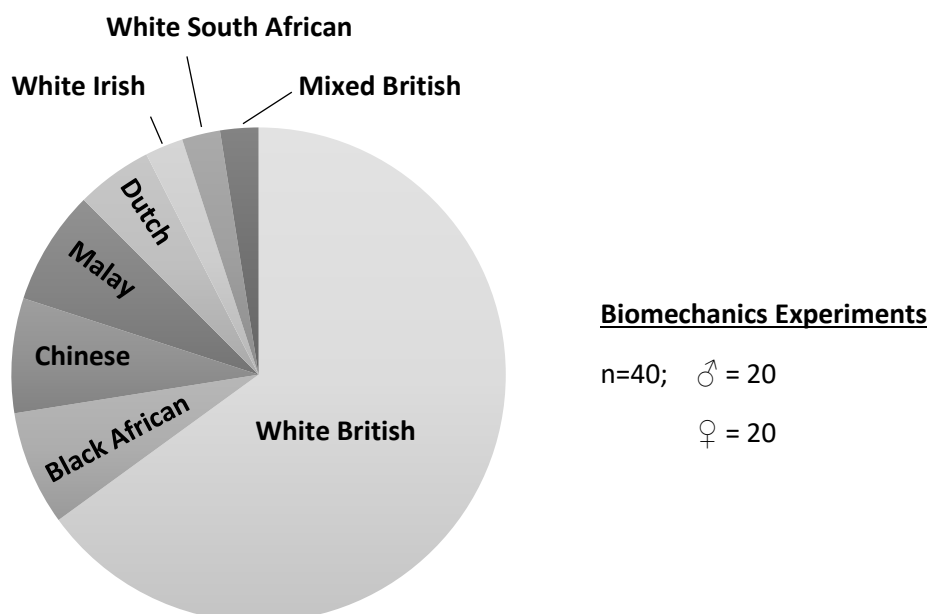
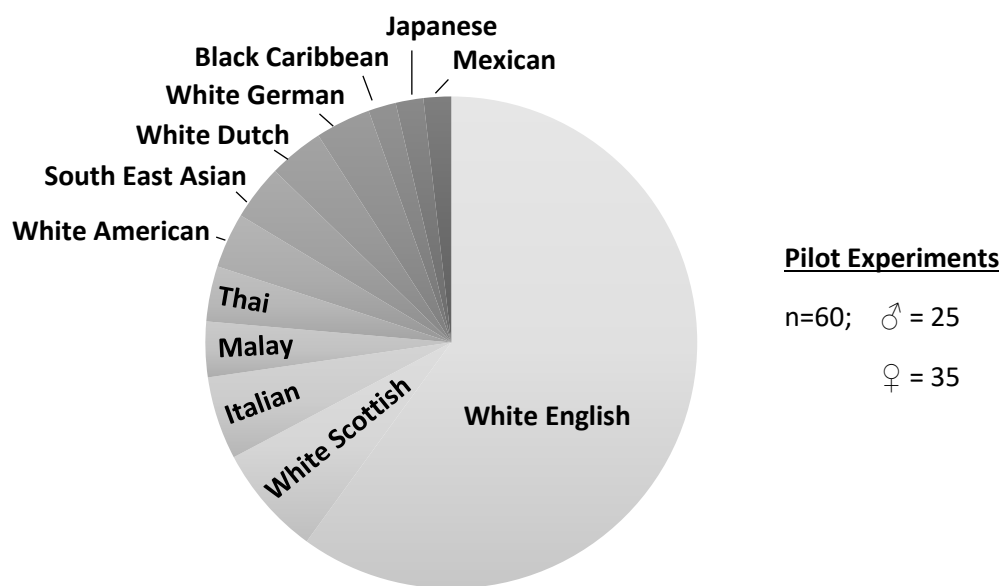
Measurements (cm) taken of the foot length and the predicted stature using Martin's 0.15 ratio (Martin 1914). Percentage change difference in track length values from the first day were calculated. Robbin's ratio of 0.14 was used for the experimental prints (EP), owing to the print maker being habitually shod. Model numbers correspond to the day that the model was made.

	Model no.	Foot length	% change in foot length	Predicted stature
<u>Formby print</u>	1	24.64	/	164.26
	2	24.64	0.01%	164.28
	3	25.75	4.42%	171.68
	4	23.11	6.47%	154.05
<u>EP left foot</u>	1	21.59	/	154.24
	2	21.46	0.62%	153.29
	3	21.37	1.06%	152.61
	4	20.64	4.40%	147.45
	5	20.56	4.78%	146.86
	6	20.99	2.80%	149.92
	7	20.54	4.87%	146.74
	8	20.30	6.02%	144.96
	9	20.79	3.74%	148.47
	10	20.98	2.86%	149.84
	11	21.21	1.76%	151.52
	12	21.32	1.26%	152.29
	13	21.62	-0.13%	154.44
	14	21.65	-0.25%	154.63
	15	21.59	0.01%	154.22
	16	22.96	-6.32%	163.99
	17	22.20	-2.79%	158.55
	18	22.07	-2.20%	157.63
	19	22.19	-2.76%	158.49
<u>EP right foot</u>	1	22.12	/	157.98
	2	21.84	1.26%	155.99
	3	21.35	3.46%	152.51
	4	21.32	3.58%	145.17
	5	20.84	5.77%	148.86
	6	20.97	5.20%	149.76
	7	21.06	4.77%	150.44
	8	21.70	1.89%	155.00
	9	22.60	-2.20%	161.45
	10	20.89	5.54%	149.22
	11	21.16	4.34%	151.13
	12	21.28	3.80%	151.97
	13	21.41	3.19%	152.94
	14	21.91	0.93%	156.51
	15	22.38	-1.19%	159.86
	16	22.94	-3.74%	163.89
	17	23.42	-5.89%	167.28
	18	22.15	-0.16%	158.23
	19	22.36	-1.08%	159.69

Appendix D

In total, 100 participants were recruited to participate in experiments for Chapter Three (no individual participated in both the preliminary trials and the biomechanical trials). Participants were actively sought from a variety of ethnic backgrounds, ages, sex, biometrics and activity levels. A breakdown of these details can be found in the following graphical displays.

D1: Ethnic background/population assessed:



D2: Ranks of activity:

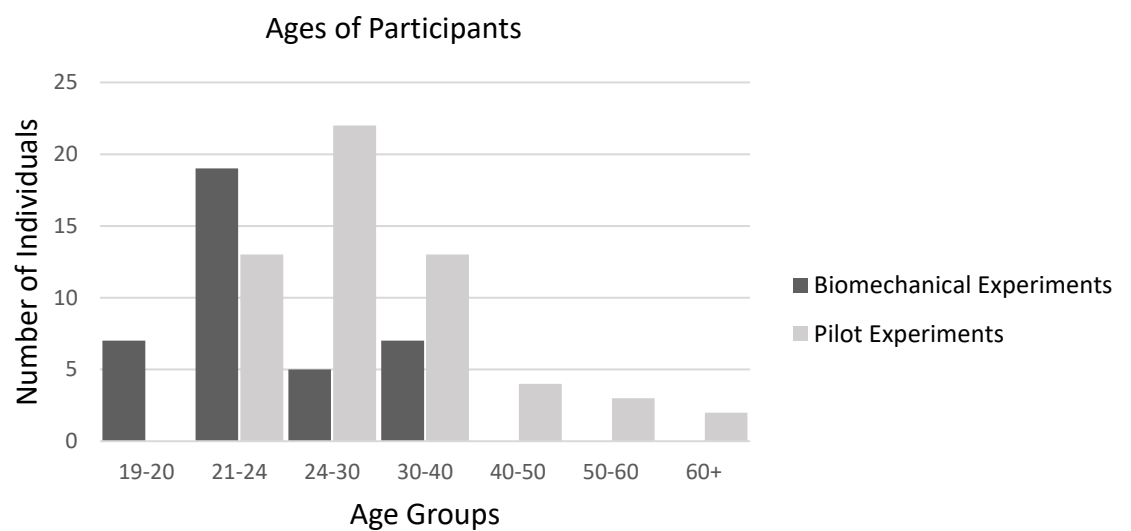


n=60; Rank One = Sedentary
Rank Two = Occasional activity
Rank Three = Intensive activity



n=40; Rank One = Sedentary
Rank Two = Occasional activity
Rank Three = Intensive activity

D3: Ranks of activity: ages of all participants



GAIT ANALYSIS STUDY

You are being invited to take part in a research study. Before you decide it is important that you understand why the research is being done and what it involves. Please take time to read the following information. Ask us if there is anything that is not clear or if you would like more information. Please take time to decide if you want to take part or not.

1. What is the purpose of the study?

The aim of the proposed study is to record a collection of modern and fossilised footprints to inform upon the functional morphology of the lower limbs and to determine if variables such as age, sex, mass, stature and speed can be calculated from footprint morphology. We are using modern populations to collect this data, but the overall aim of the study is to determine if these variables can be calculated from fossilised footprints in order to understand the evolutionary biomechanics of walking within early humans.

2. Am I eligible to take part?

All adults (18+) who are free from lower limb/spinal injuries and do not have a history of injury within this region are encouraged to take part.

3. Do I have to take part?

No, this study is completely voluntary. It is up to you to decide whether or not to take part. If you do you will be given this information sheet and asked to sign a consent form. You are still free to withdraw at any time (even during the experiments) and without giving a reason. A decision to withdraw will not affect your rights or any future services you receive.

4. What will happen to me if I take part?

1. You will be asked to sign a participant consent form.
2. The researcher will then measure your height, weight, foot length, age and ethnicity.
3. You will be asked to walk along two trackways filled with sand without socks or shoes on. One trackway will have wet sand, the other will be dry. You will be asked to walk along each trackway at a walking pace, then at fast-paced walking, and finally at a running pace.
4. You will have reflective markers attached to your leg with cameras recording your movement. Afterwards, a handheld DSLR camera will be used to record your footprints which will be made in the trackways.
5. Finally, you will be debriefed and thanked for participation.

5. Are there any risks / benefits involved?

There are no intended risks for taking part. All participants will receive a **£10 Amazon gift card** upon successful completion of the experiments. If a participant successfully completes the experiments/all trials and decides to withdraw their participation/use of their data afterwards, then they will not be required to return the Amazon gift card.

Taking part in this study will help to advance our understanding of the evolutionary biomechanics of walking within humans.

6. Will my taking part in the study be kept confidential?

All data provided by participants will be anonymised as participants will be provided with a Participant ID number (PID). This will be confidential, stored securely and separately from all other data. All other data will only be identified by the anonymised PID and cannot be linked back to you without the consent form.

This study has received ethical approval from LJMU's Research Ethics Committee
Contact Details of Researcher

Ashleigh Wiseman

Email: a.l.wiseman@2016.ljmu.ac.uk

Contact Details of Academic Supervisor

Dr. Isabelle De Groote

I.E.DeGroote@ljmu.ac.uk

If you any concerns regarding your involvement in this research, please discuss these with the researcher in the first instance. If you wish to make a complaint, please contact researchethics@ljmu.ac.uk and your communication will be re-directed to an independent person as appropriate.



QUESTIONNAIRE FOR PARTICIPANTS

Prior to commencing the experiments, we need to take a few measurements of your body, record biological data and keep a record of any lower limb/spinal pathologies that you may currently have, or have had in the past. If you have any queries/problems about this form we encourage you to speak to the researcher. You are free to withdraw from the study at any point without giving a reason. Your participation in the current study is completely voluntary.

N.B. One copy of this form will be retained by the researcher. One copy will be provided to the participant. A copy of your completed form will be scanned and emailed to you using the email address previously used for correspondence, unless otherwise stated by the participant.

All information in this form will be kept confidential.

Please tick this box if you were a participant involved in the pilot experiments of this study in August 2017 ☐

Name of participant:

Each participant will be assigned a unique participant number which will be used to identify them. These numbers will be assigned to a name. No participant names will be published.

Please fill in the following:

Sex:

D.O.B (in format of day/month/year):

Ethnicity/Ancestry (e.g., white British):

The following measurements of your body will be taken, in accordance with LJMU's code of ethical practise:

Height, hip height, foot length and body mass (weight).

Please tick to confirm that you are happy for these measurements to be taken:

I consent for the following measurements to be taken ☐

I do not consent for any measurements to be taken and wish to withdraw from the study

☐

Please leave this section blank. To be completed by a staff member.

Height:

Hip height:

Foot length:

Body mass (weight):

Are you currently free from any lower limb/spinal pathology? This includes any current breakages or disability that may affect lower limb mobility.

Yes ☐

No ☐

If you answered no, please provide more details. If you would prefer not to give details please answer "I prefer not to say". *All information will be kept confidential.*

Do you have a medical history of lower limb/spinal pathologies? *e.g., have you previously broken/fractured a bone or had any other impediment that affected your ability to walk?*

Please tick one:

Yes ☐

No ☐

If you answered yes, please provide more details. If you would prefer not to give details please answer "I prefer not to say". *All information will be kept confidential.*

Are you actively involved in any sports, activities or training? *e.g., football, running, training or ballet dancing.*

Please tick one:

Yes ☐

No ☐

If you answered yes, please provide more details including duration and how often you participate in your activity. If you would prefer not to give details please answer “I prefer not to say”. *All information will be kept confidential.*

Do you wear high-heeled shoes?

Please tick one:

Yes ☐

No ☐

If you answered yes, please provide more details including how often the shoes are worn and the typical height of the shoe. If you would prefer not to give details please answer “I prefer not to say”. *All information will be kept confidential.*

If we have any follow-up questions after your session has ended, can we contact you with questions? *If you are not willing to be contacted with follow-up questions, but wish to be informed of the results of the study please speak to the researcher.*

Yes ☐

No ☐

How would you like to be contacted?

By email ☐

By phone ☐

Contact details:



LIVERPOOL JOHN MOORES UNIVERSITY

CONSENT FORM

UAV Photogrammetry potential for the recording of prehistoric footprints: using 3D models to assess evolutionary biomechanics of walking.

Researcher: Ashleigh Wiseman.

School of Natural Sciences and Phycology

1. I confirm that I have read and understand the information provided for the above study. I have had the opportunity to consider the information, ask questions and have had these answered satisfactorily ☐
2. I understand that my participation is voluntary and that I am free to withdraw at any time, without giving a reason and that this will not affect my legal rights. ☐
3. I understand that any personal information collected during the study will be anonymised and remain confidential ☐
4. I agree to take part in the above study ☐

Name of Participant

Date

Signature

Name of Researcher

Date

Signature

Name of Person taking consent
(if different from researcher)

Date

Signature

Appendix F

Table on the following pages lists all fossil tracks used in Chapter Four. The data compiled here was kindly provided by collaborators. Where initials are used, data was collected by associated collaborator:

MRB – Matthew R. Bennett.

KGH – Kevin G. Hatala

IDG – Isabelle De Groote

CS – Christopher Stringer

NA – Nick Ashton

SD – Sarah Duffy

AW – Ashleigh L. A. Wiseman

All tracks from FwJj14E, Turkana Basin (provided by KGH) are from the Upper Footprint Layer.

3D data was collected from the following online repositories:

For access for Site G footprints see:

<http://footprints.bournemouth.ac.uk/archive/Laetoli/>

For access for Site S footprints see:

<https://www.morphosource.org/Search/Index?search=laetoli>

For access for Namibian footprints see:

<http://footprints.bournemouth.ac.uk/archive/Namibian%20Footprints/>

<u>FOSSIL LOCALITY</u>	SITE	TRACK NUMBER	TRACK ID	DATA BY:	DATA ONLINE?
<u>Laetoli</u>	Site G	G1	G1-35	MRB	Yes
	Site G	G1	G1-36	MRB	Yes
	Site G	G1	G1-37	MRB	Yes
	Site G	G1	G1-38	MRB	Yes
	Site G	G1	G1-39	MRB	Yes
	Site G	G1	G1-25	MRB	Yes
	Site G	G1	G1-26	MRB	Yes
	Site G	G1	G1-27	MRB	Yes
	Site G	G1	G1-28	MRB	Yes
	Site G	G1	G1-30	MRB	Yes
	Site G	G1	G1-31	MRB	Yes
	Site G	G1	G1-34	MRB	Yes
	Site S	L8	L8S11	Masao et al. 2016	Yes
	Site S	L8	L8S12	Masao et al. 2016	Yes
	Site S	L8	L8S13	Masao et al. 2016	Yes
	Site S	L8	L8S14	Masao et al. 2016	Yes
	Site S	M9	M9S12	Masao et al. 2016	Yes
	Site S	M9	M9S13	Masao et al. 2016	Yes
	Site S	TP2	TP2S2111	Masao et al. 2016	Yes
<u>Ileret</u>	FwJj14E	-	FU-A	KGH	No
	FwJj14E	-	FU-H	KGH	No
	FwJj14E	1	FUT1-6	KGH	No
	FwJj14E	1	FUT1-7A	KGH	No
	FwJj14E	-	FUT1-7B	KGH	No
	FwJj14E	1	FUT1-12	KGH	No
	FwJj14E	1	FUT1-13	KGH	No
	FwJj14E	1	FUT1-16	KGH	No
	FwJj14E	2	FUT2-1	KGH	No
	FwJj14E	2	FUT2-2	KGH	No
	FwJj14E	2	FUT2-4	KGH	No
	FwJj14E	-	FUT3-1	KGH	No
<u>Happisburgh</u>	-	-	Print 33	IDG&CS&NA&SD	No
	-	-	Print 39	IDG&CS&NA&SD	No
	-	-	Print 40	IDG&CS&NA&SD	No
	-	-	Print 49	IDG&CS&NA&SD	No
	-	-	Print 3	IDG&CS&NA&SD	No
	-	-	Print 4	IDG&CS&NA&SD	No
	-	-	Print 5	IDG&CS&NA&SD	No
	-	-	Print 6	IDG&CS&NA&SD	No
	-	-	Print 8	IDG&CS&NA&SD	No
	-	-	Print 9	IDG&CS&NA&SD	No
	-	-	Print 11	IDG&CS&NA&SD	No
	-	-	Print 12	IDG&CS&NA&SD	No
	-	-	Print 14	IDG&CS&NA&SD	No
	-	-	Print 18	IDG&CS&NA&SD	No
<u>Langebaan</u>	-	-	-	Iziko Museum	No
	-	-	-	Iziko Museum	No
<u>Terra Amata</u>	-	-	-	Terra Amata Museum	No
<u>Vârtop Cave</u>	-	-	-	Prof. Bogdan Onac	No
<u>Walvis Bay</u>	Site One	-	PATCH 7.1b	MRB	Yes
	Site One	-	PATCH 41 4	MRB	Yes
	Site One	-	PATCH 74 4	MRB	Yes
	Site One	-	H302	MRB	Yes

Site One	-	H305	MRB	Yes
Site One	-	H308	MRB	Yes
Site One	-	H309	MRB	Yes
Site One	-	H310	MRB	Yes
Site One	-	H311	MRB	Yes
Site One	-	H312	MRB	Yes
Site One	-	H313	MRB	Yes
Site One	-	H314	MRB	Yes
Site One	-	H315	MRB	Yes
Site One	-	H316	MRB	Yes
Site One	-	H141	MRB	Yes
Site One	-	H142	MRB	Yes
Site One	-	H143	MRB	Yes
Site One	-	H144	MRB	Yes
Site One	-	H145	MRB	Yes
Site One	-	H149	MRB	Yes
Site One	-	H155	MRB	Yes
Site One	-	H158	MRB	Yes
Site One	-	H159	MRB	Yes
Site One	-	H162	MRB	Yes
Site One	-	H318	MRB	Yes
Site One	-	H319	MRB	Yes
Site One	-	H321	MRB	Yes
Site One	-	H322	MRB	Yes
Site One	-	H323	MRB	Yes
Site One	-	H324	MRB	Yes
Site One	-	H59	MRB	Yes
Site One	-	H68	MRB	Yes
Site One	-	H65	MRB	Yes
Site One	-	H60	MRB	Yes
Site One	-	H66	MRB	Yes
Site One	-	H51	MRB	Yes
Site One	-	H55	MRB	Yes
Site One	-	H56	MRB	Yes
Site One	-	H57	MRB	Yes
Site One	-	H42	MRB	Yes
Site One	-	H45	MRB	Yes
Site One	-	H05	MRB	Yes
Site One	-	H06	MRB	Yes
Site One	-	H07	MRB	Yes
Site One	-	H13	MRB	Yes
Site One	-	H14	MRB	Yes
Site One	-	H70	MRB	Yes
Site One	-	H070A	MRB	Yes
Site One	-	H72	MRB	Yes
Site One	-	H74	MRB	Yes
Site One	-	H075	MRB	Yes
Site One	-	H14	MRB	Yes
Site One	-	H21	MRB	Yes
Site One	-	H42	MRB	Yes
Site One	-	H43	MRB	Yes
Site One	-	H45	MRB	Yes
Site One	-	H49	MRB	Yes
Site One	-	H47	MRB	Yes
Site One	-	301	MRB	Yes
Site One	-	317	MRB	Yes
Site One	-	H078	MRB	Yes
Site One	-	H079	MRB	Yes
Site One	-	H082	MRB	Yes

Site One	-	H086	MRB	Yes
Site One	-	H086	MRB	Yes
Site One	-	H087	MRB	Yes
Site One	-	H091	MRB	Yes
Site One	-	H097	MRB	Yes
Site One	-	H098	MRB	Yes
Site One	Trail One	H10	MRB	Yes
Site One	Trail One	H11	MRB	Yes
Site One	Trail One	H1	MRB	Yes
Site One	Trail One	H2	MRB	Yes
Site One	Trail One	H3	MRB	Yes
Site One	Trail One	H4	MRB	Yes
Site One	Trail One	H5	MRB	Yes
Site One	Trail One	H6	MRB	Yes
Site One	Trail One	H7	MRB	Yes
Site One	Trail One	H8	MRB	Yes
Site One	Trail One	H9	MRB	Yes
Site One	Trail One	H10	MRB	Yes
Site One	Trail One	H11	MRB	Yes
Site One	Trail One	H12	MRB	Yes
Site One	Trail One	H16	MRB	Yes
Site One	Trail One	H17	MRB	Yes
Site One	Trail One	H18	MRB	Yes
Site One	Trail One	H19	MRB	Yes
Site One	Trail One	H20	MRB	Yes
Site One	Trail One	H21	MRB	Yes
Site One	Trail One	H22	MRB	Yes
Site One	Trail One	H23	MRB	Yes
Site One	Trail One	H24	MRB	Yes
Site One	Trail One	h26	MRB	Yes
Site One	Trail One	H27	MRB	Yes
Site One	Trail One	H29	MRB	Yes
Site One	Trail One	H30	MRB	Yes
Site One	Trail One	H31	MRB	Yes
Site One	Trail One	H32	MRB	Yes
Site One	Trail One	H33	MRB	Yes
Site One	Trail One	H33	MRB	Yes
Site One	Trail One	H34	MRB	Yes
Site One	Trail One	H35	MRB	Yes
Site One	Trail One	H36	MRB	Yes
Site One	Trail One	H37	MRB	Yes
Site One	Trail One	H38	MRB	Yes
Site One	Trail One	H39	MRB	Yes
Site One	Trail One	H37	MRB	Yes
Site One	Trail One	H44	MRB	Yes
Site One	Trail One	H46	MRB	Yes
Site One	Trail One	H48	MRB	Yes
Site One	Trail One	H61	MRB	Yes
Site One	Trail One	H62	MRB	Yes
Site One	Trail One	H64	MRB	Yes
Site One	Trail One	H69	MRB	Yes
Site One	Trail One	H71	MRB	Yes
Site One	Trail One	H73	MRB	Yes
Site One	Trail Two	H77	MRB	Yes
Site One	Trail Two	HR20	MRB	Yes
Site One	Trail Two	HR21	MRB	Yes
Site One	Trail Two	HR29	MRB	Yes
Site One	Trail Two	HR31	MRB	Yes
Site One	Trail Two	HR36	MRB	Yes

	Site One	Trail Two	HR44	MRB	Yes
	Site One	Trail Two	HR51	MRB	Yes
	Site One	Trail Two	HR67	MRB	Yes
	Site One	Trail Two	HR86	MRB	Yes
	Site One	Trail Two	HR89	MRB	Yes
	Site One	Trail Two	HR91	MRB	Yes
	Site One	Trail Two	HR116	MRB	Yes
	Site One	Trail Two	HR130	MRB	Yes
	Site One	Trail Two	HARIETTE4	MRB	Yes
	Site One	Trail Two	HARRIETTE12	MRB	Yes
	Site One	Trail Two	HARRIETTE17	MRB	Yes
	Site One	Trail Two	HARRIETTE18	MRB	Yes
	Site One	Trail Two	HARRIETTE20	MRB	Yes
	Site One	Trail Two	HARRIETTE21	MRB	Yes
	Site One	Trail Two	HARRIETTE29	MRB	Yes
	Site One	Trail Two	HARRIETTE46	MRB	Yes
	Site One	Trail Two	HARRIETTE51	MRB	Yes
	Site One	Trail Two	HARRIETTE54	MRB	Yes
	Site One	Trail Two	HARRIETTE20	MRB	Yes
	Site One	Trail Two	HARRIETTE21	MRB	Yes
	Site One	Trail Two	HARRIETTE29	MRB	Yes
	Site One	Trail Two	HARRIETTE46	MRB	Yes
	Site One	Trail Two	HARRIETTE51	MRB	Yes
	Site One	Trail Two	HARRIETTE54	MRB	Yes
	Site One	Trail Two	HAR18239	MRB	Yes
<u>Formby Point</u>	Sefton Coast	-	PRINT A	MRB	Yes
	Sefton Coast	-	PRINT AA	MRB	Yes
	Sefton Coast	-	PRINT B	MRB	Yes
	Sefton Coast	-	PRINT F	MRB	Yes
	Sefton Coast	-	PRINT I	MRB	Yes
	Sefton Coast	-	PRINT J	MRB	Yes
	Sefton Coast	-	PRINT K	MRB	Yes
	Sefton Coast	-	PRINT L	MRB	Yes
	Sefton Coast	-	PRINT M	MRB	Yes
	Sefton Coast	-	PRINT N	MRB	Yes
	Sefton Coast	-	PRINT O	MRB	Yes
	Sefton Coast	-	PRINT P	MRB	Yes
	Sefton Coast	-	PRINT Q	MRB	Yes
	Sefton Coast	-	PRINT R	MRB	Yes
	Sefton Coast	-	PRINT S	MRB	Yes
	Sefton Coast	-	PRINT TT	MRB	Yes
	Sefton Coast	-	PRINT W	MRB	Yes
	Sefton Coast	-	PRINT X	MRB	Yes
	Sefton Coast	-	PRINT ZZ	MRB	Yes
	Sefton Coast	-	PRINT T5	MRB	Yes
	Cornerstone N	Track 13	285	AW	No
	Cornerstone N	Track 13	286	AW	No
	Cornerstone N	Track 13	289	AW	No
	Cornerstone N	Track 13	292	AW	No
	Cornerstone N	Track 11	231	AW	No
	Cornerstone N	Track 11	225	AW	No
	Cornerstone N	Track 11	219	AW	No
	Cornerstone N	Track 11	220	AW	No
	Cornerstone N	Track 7	202	AW	No
	Cornerstone N	Track 8	204	AW	No
	Cornerstone N	Track 8	205	AW	No
	Cornerstone N	Track 8	210	AW	No
	Cornerstone N	Track 9	212	AW	No
	Cornerstone N	Track 9	213	AW	No

Cornerstone N	Track 9	215	AW	No
Cornerstone N	Track 9	214	AW	No
Cornerstone N	Track 10	216	AW	No
Cornerstone N	Track 10	216-a	AW	No
Cornerstone N	Track 10	216-b	AW	No
Cornerstone N	Track 10	233	AW	No
Cornerstone N	Track 10	223	AW	No
Cornerstone N	Track 10	229	AW	No
Cornerstone N	-	202	AW	No
Blundell Path	1	1295	AW	No
Blundell Path	1	1296	AW	No
Blundell Path	1	1297	AW	No
Blundell Path	1	1298	AW	No
Blundell Path	1	1299	AW	No
Blundell Path	1	1300	AW	No
Blundell Path	1	1301	AW	No
Blundell Path	2	1303	AW	No
Blundell Path	2	1304	AW	No
Blundell Path	2	1305	AW	No
Blundell Path	3	1272	AW	No
Blundell Path	3	1365	AW	No
Blundell Path	3	1366	AW	No
Blundell Path	3	UNI	AW	No
Blundell Path	3	dpL	AW	No
Blundell Path	3	dpR	AW	No
Blundell Path	-	350	AW	No
Blundell Path	-	280	AW	No
Blundell Path	-	273	AW	No
Blundell Path	Track 5	309	AW	No
Blundell Path	Track 5	310	AW	No
Blundell Path	Track 18	348	AW	No
Blundell Path C	Track 18	349	AW	No
Blundell Path C		220	AW	No
Blundell Path C	-	316	AW	No
Blundell Path C	Track 4	261	AW	No
Blundell Path C	Track 4	262	AW	No
Blundell Path C	Track 4	263	AW	No
Blundell Path C	Track 4	264	AW	No
Blundell Path C	Track 4	265	AW	No
Gypsy Path	Track 15	print f101	AW	No
Gypsy Path	Track 15	print f110	AW	No
Gypsy Path	Track 15	print f8	AW	No
Gypsy Path	Track 15	print f31	AW	No
Gypsy Path	Track 15	print f113	AW	No
Gypsy Path	Track 15	print f40	AW	No

Appendix G

Effect sizes (ζ) (Cohen 1988) table displaying the significant shape variability between juvenile and adult fossil tracks, as produced from the MANOVA computed between-groups using the PC scores that represent 100% of shape variance and log-CS.

A shaded grey box indicates that the variability was non-significant between-groups ($P \geq 0.05$, within a 95% confidence interval). A shaded green box indicates that significant shape disparity was found between-groups ($P < 0.05$, within a 95% confidence interval). Boxes with a thick black outline indicate within-groups variability (e.g., the juvenile tracks differ in shape from the adult tracks within modern humans at Formby Point).

▲ – Juvenile Track

▼ – Sub-adult Track (these tracks were identified to belong to individuals which were borderline adult; i.e., age predictions were 17-19 years old)

▲ – Adult Track

		Formby Point			Happisburgh			Ileret	Laetoli	Walvis Bay		
		▲	Δ	▼	▲	Δ	▼	▲	▲	▲	Δ	▼
Formby Point	▲	0										
	Δ	6.238	0									
	▼	0.867	-0.413	0								
Happisburgh	▲	-0.465	-1.067	-0.311	0							
	Δ	-0.909	-0.867	-0.489	2.368	0						
	▼	-0.006	-0.878	-0.585	-0.481	-0.553	0					
Ileret	▲	-0.104	-1.421	-1.049	0.094	-0.583	-2.319	0				
Laetoli	▲	-0.103	-0.418	-1.107	-1.238	0.708	-0.316	-0.362	0			
Walvis Bay	▲	-0.219	1.318	0.774	-0.538	-0.522	-0.211	-0.474	-0.639	0		
	Δ	1.552	2.221	1.939	0.578	1.130	1.638	2.739	0.081	2.859	0	
	▼	-0.330	0.873	0.905	1.070	-0.633	0.357	0.217	2.551	5.336	3.251	0

